Goldilocks boronic esters: optimized properties through understanding hydrolysis kinetics

Reyner D. Vargas, Samantha S. Cox, James O. Larkin, Jingfei Dai, Yuecheng Jiang, Ivan Yuan, Margaret A. Hankins, Zachary T. Ball*

*zb1@rice.edu

Supporting Information

Contents

General Information

Chemicals

All chemicals were purchased from commercial suppliers and used without further purification. Bipyridine **S2** and palladium catalyst **S5** were prepared according to reported protocols.[1,2]

Buffers

Phosphate buffer solution (pH 7.4, 0.1 M), was purchased from Sigma-Aldrich, for pH 7.4 studies it was diluted and used without further modification. For pH 6.8 and 8.0 studies, the pH 7.4, 0.1 M solution was adjusted to the desired pH with 0.1 M NaOH or HCl. Piperazine (10 mM, pH 5.2) buffer was prepared by diluting piperazine (86.1 mg) with distilled water (950 mL). The pH was then adjusted to 5.2 using HCl (1 M) and the solution was then diluted to a final volume of 1000 mL.

Instrumentation

HPLC

Reverse-phase HPLC was performed on a Shimadzu SCL-40 with Phenomenex Jupiter 4µ Proteo 90A (250 x 4.6 mm analytical) and Phenomenex Jupiter 4µ Proteo 90A (240 x 15 mm preparative) columns. The flow rate was 1.0 mL/min for analytical and 6.0 mL/min for preparative. A gradient of acetonitrile/water with 0.1% trifluoroacetic acid was employed. Small molecules were detected using absorbance at 220 nm and 254 nm, peptides were detected using absorbance at 254 nm and 280 nm.

LC-MS and ESI-MS

The analyses were conducted on Agilent Quadrupole LC/MS spectrometer with an Agilent® ZORBAX Eclipse Plus C18 (5 cm × 2.1 mm, 1.8 um) or an Ascentis® Express Peptide ES-C18 column (15 cm × 2.1 mm, 2.7 um) at 35 °C. The flow rate was 0.8 mL/min. A gradient of acetonitrile/water with 0.1% formic acid was employed.

HRMS

The analysis was conducted on Agilent Quadrupole-TOF LC/MS spectrometer using electrospray ionization (ESI) at 35 °C. The flow rate was 0.4 mL/min, using acetonitrile/water with 0.1% formic acid.

NMR

Spectra were obtained on a Bruker AVANCE 6000 spectrometer.

Experimental Procedures

Small molecule boronic ester formation

In a 4 mL scintillation vial the corresponding boronic acid (0.025 mmol) and diol (0.025 mmol) were added and diluted in dry methanol (1 mL), the solvent was then removed under reduced pressure at 40 °C to afford the corresponding ester, usually in the form of an oil.

Small molecule boronic esters characterization

The formed boronic ester was re-dissolved in 1 mL of dry methanol, a 1 µL aliquot was then measured in the HPLC to confirm purity, another 1 µL was measured using the standard ESI-MS procedure to confirm the mass of the formed product.

For UV-active compounds, a TLC analysis was also performed, where the boronic ester was eluted in a TLC using ethyl acetate in hexanes as the eluent.

Small molecule boronic ester hydrolysis procedures

The re-dissolved solution of the corresponding boronic ester (25 mM) was diluted either 10-fold (2.5 mM) or 100-fold (0.25 mM) in the corresponding buffer. For esters with low aqueous solubility, the 100-fold (0.25 mM) dilution was prepared using a mixture of 10% dimethyl sulfoxide (DMSO) in buffer, to a final volume of 1 mL.

For the 2.5 mM and 0.25 mM solutions, 10 µL and 70 µL aliquots, respectively, were analyzed using the standard HPLC methodology at different time points.

For small molecules not detected by HPLC (**14-20**), 0.025 mM solutions were prepared, and 10 µL aliquots were analyzed using the standard LC-MS methodology at different time points.

The corresponding boronic ester peak area was integrated (using the total ion chromatogram (TIC) for LC-MS) and monitored over time. Data were fitted to a pseudo-first order decay model by plotting ln[boronic ester peak area] versus elapsed time.

Peptide synthesis

Peptides were synthesized using standard solid phase peptide synthesis protocols[3] using rink amide resin (P3Biosystems, 52001) and Fmoc-amino acids purchased from NovaBiochem and used without further purification. Peptides were purified by reverse-phase HPLC and characterized by ESI-MS, before being borylated using the peptide borylation procedure (page S16).

Peptide boronic ester formation

In a 4 mL vial, peptide boronic acid (0.2 µmol) and diol (2 µmol) were diluted with 400 µL of dry methanol. The mixture was stirred overnight under air at 55 °C and the crude was purified by reverse-phase HPLC and characterized by ESI-MS before being used.

Peptide boronic ester hydrolysis

The formed peptide boronic ester was redissolved in buffer (400 µL) and 15 µL aliquots were analyzed using the standard peptide HPLC methodology.

Organic synthesis procedures

Synthesis of Gpin

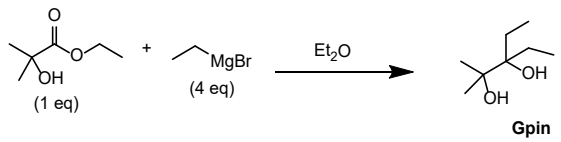

Gpin

Ethyl 2-hydroxyisobutyrate (6.32 g, 50.8 mmol) was dissolved in anhydrous diethyl ether (50 mL) in a round bottom flask equipped with a stir bar. Under nitrogen atmosphere, ethylmagnesium bromide (50 mL, 150 mmol, 3.0 M soln in diethyl ether) was added at 0 °C, the mixture was allowed to come to room temperature and was stirred overnight. The soln was then quenched with the addition of an excess of water, filtered through celite to remove the magnesium salts, and dried over sodium sulfate to afford **Gpin** (7.06 g, 48.4 mmol, 95%) as a colorless oil. The compound was found to be sufficiently pure without additional purification

^{1}H NMR (600 MHz, $CDCl_3$) δ 2.25 (s, 1H), 2.02 (s, 1H), 1.68 – 1.50 (m, 4H), 1.21 (s, 6H), 0.91 (t, J = 7.6 Hz, 6H).

^{13}C NMR (151 MHz, $CDCl_3$) δ 77.9, 75.9, 26.6, 25.6, 8.9.

MS (ESI-TOF) *m/z* calcd. for $C_8H_{19}O_2^+$ ($[M+H]^+$) 147.2374, found 147.2371.

Synthesis of ester S1

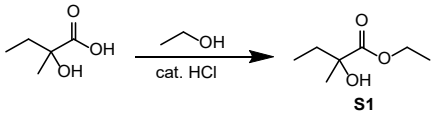

S1

2-hydroxy-2-methylbutyric acid (4.98 g, 42.3 mmol) was added to a round bottom flask equipped with a stir bar and dissolved in dry ethanol (100 mL), one drop of conc. aq. HCl was added, and the reaction was refluxed for 96 h. The crude was then dried over Na_2SO_4. Finally, the solvent was removed under reduced pressure to afford ester **S1** (5.51 g, 37.7 mmol, 89 %) as a yellowish oil. The compound was found to be sufficiently pure without additional purification

^{1}H NMR (600 MHz, $CDCl_3$) δ 4.28 – 4.03 (m, 2H), 3.23 (s, 1H), 1.76 – 1.67 (m, 1H), 1.63 – 1.55 (m, 1H), 1.32 (s, 3H), 1.23 (t, J = 7.2 Hz, 3H), 0.81 (t, J = 7.4 Hz, 3H).

^{13}C NMR (151 MHz, $CDCl_3$) δ 177.2, 74.8, 61.7, 33.1, 25.7, 14.2, 7.9.

MS (ESI-TOF) *m/z* calcd. for $C_6H_{13}O_3^+$ ($[M+H]^+$) 133.1664, found 133.1682.

Synthesis of 3pin

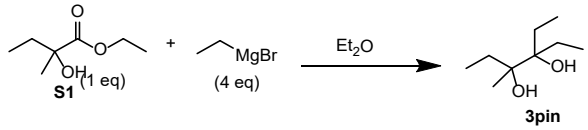

Ester **S1** (2.01 g, 13.7 mmol) was dissolved in anhydrous diethyl ether (25 mL) in a round bottom flask equipped with a stir bar. Under nitrogen atmosphere, ethylmagnesium bromide (18.3 mL, 54.8 mmol, 3.0 M soln in diethyl ether) was added at 0 °C, the mixture was allowed to come to room temperature and was stirred overnight. The soln was then quenched with the addition of an excess of water, filtered through celite to remove the magnesium salts, and dried over Na_2SO_4. The was solvent removed under reduced pressure, and the crude material was purified via silica gel chromatography. Product-containing fractions were concentrated under reduced pressure to afford **3pin** (1.4 g, 8.7 mmol, 64 %) as a yellowish oil.

1H NMR (600 MHz, $CDCl_3$) δ 2.04 (s, 1H), 2.01 (s, 1H), 1.71 – 1.52 (m, 5H), 1.46 – 1.38 (m, 1H), 1.12 (s, 3H), 0.95 – 0.89 (m, 9H).

13C NMR (151 MHz, $CDCl_3$) δ 78.4, 77.6, 28.9, 26.7, 26.6, 21.0, 9.2, 9.0, 8.0.

MS (ESI-TOF) *m/z* calcd. for $C_9H_{21}O_2^+$ ($[M+H]^+$) 161.2644, found 161.2637.

Synthesis of B_2Gpin_2

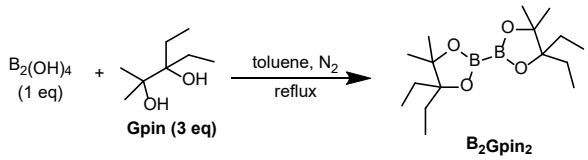

To a 50 mL round bottom flask equipped with a stir bar and molecular sieves (powdered, 3Å, ~50 mg) tetrahydroxydiboron (500 mg, 5.60 mmol, 1 equiv) and **Gpin** (2.42 g, 16.7 mmol, 3 equiv) were added and the mixture was diluted with 20 mL of toluene. The flask was heated to reflux for 12 h under N_2 atmosphere. The reaction was cooled to room temperature, filtered, extracted with methylene chloride, and concentrated under reduced pressure to obtain **B_2Gpin_2** as a white paste (1.6 g, 5.2 mmol, 92%).

^{1}H NMR (600 MHz, $CDCl_3$) δ 1.67 (ddt, J = 35.9, 14.3, 7.4 Hz, 8H), 1.29 (s, 12H), 0.88 (t, J = 7.5 Hz, 12H).

^{13}C NMR (151 MHz, $CDCl_3$) δ 87.5, 83.9, 26.3, 25.6, 8.5.

^{11}B NMR (192 MHz, $CDCl_3$) δ 30.64.

MS (ESI-TOF) *m/z* calcd. for $C_9H_{21}O_2^+$ ($[M+H]^+$) 311.2565, found 311.2571.

Synthesis of amine S4

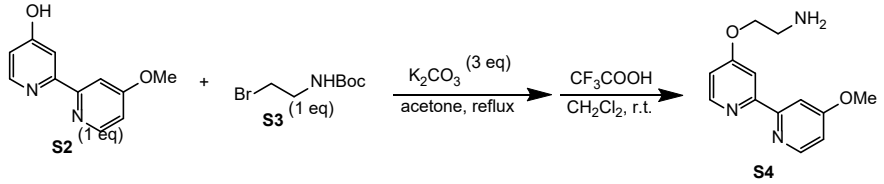

To a 100 mL round bottom flask equipped with a stir bar, bipyridine **S2** (1.0 g, 4.9 mmol, 1.0 equiv), bromide **S3** (1.1 g, 4.9 mmol, 1 equiv) and K_2CO_3 (2 g, 14.8 mmol, 3 equiv) were added and diluted with 50 mL of dry acetone, the reaction was allowed to reflux overnight, the crude was then cooled to room temperature, filtered with celite and evaporated under reduced pressure. The formed oil was then treated, without any further purification, with trifluoroacetic acid in methylene chloride (5 mL, 20% CF_3COOH in dichloromethane) for two hours at room temperature. The crude was then evaporated under reduced pressure and purified via silica gel chromatography (eluent: 97:2:1 dichloromethane/methanol/triethylamine). Product-containing fractions were concentrated under reduced pressure to afford **S4** (1.05 g, 4.3 mmol, 88 %) as an oil.

^{1}H NMR (600 MHz, CD_3OD) δ 8.69 (d, *J* = 6.0 Hz, 1H), 8.65 (d, *J* = 6.5 Hz, 1H), 8.14 (d, *J* = 2.5 Hz, 1H), 8.09 (d, *J* = 2.4 Hz, 1H), 7.47 (dd, *J* = 6.6, 2.6 Hz, 1H), 7.37 (dd, *J* = 6.0, 2.4 Hz, 1H), 4.60 – 4.53 (m, 2H), 4.18 (s, 3H), 3.49 (t, *J* = 5.4, 4.4 Hz, 2H).

^{13}C NMR (151 MHz, CD_3OD) δ 173.1, 168.9, 150.9, 150.6, 150.5, 146.8, 114.3, 113.5, 111.0, 110.6, 66.8, 58.2, 39.8.

MS (ESI-TOF) *m/z* calcd. for $C_{13}H_{16}N_3O_2^+$ ($[M+H]^+$) 246.1242, found 246.1240.

Synthesis of 12-Gpin

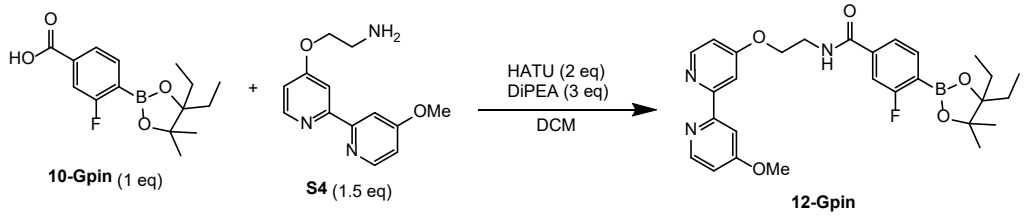

Boronate ester **10-Gpin** (29.1 mg, 0.0989 mmol, 1.00 equiv) was prepared according to the small molecule general boronic ester formation procedure in a 20 mL vial and carried to the next step without purification. A stir bar and HATU (76.0 mg, 0.200 mmol, 2.02 equiv) were added to the vial, and the mixture was diluted with dichloromethane (5 mL). Next, *N,N*-diisopropylethylamine (52.0 µL, 0.299 mmol, 3.02 equiv) was added and the solution was let stirring for 5 min followed by the addition of amine **S4** (37 mg, 0.15 mmol, 1.5 equiv, soln in 5 mL dichloromethane). The mixture was stirred for 1 h, and then the solvents evaporated under reduced pressure. The crude was then purified via silica gel chromatography (eluent: 97:2:1 dichloromethane/methanol/triethylamine). Product-containing fractions were concentrated under reduced pressure to afford **12-Gpin** (44.3 mg, 0.0805 mmol, 85 %) as an oil.

^{1}H NMR (600 MHz, $CDCl_3$) δ 8.70 (d, *J* = 6.5 Hz, 1H), 8.59 (d, *J* = 6.0 Hz, 1H), 8.15 (d, *J* = 2.4 Hz, 1H), 8.09 (d, *J* = 2.6 Hz, 1H), 7.72 (dd, *J* = 7.7, 5.8 Hz, 1H), 7.53 (dd, *J* = 7.7, 1.5 Hz, 1H), 7.48 (t, *J* = 5.9 Hz, 1H), 7.43 (dd, *J* = 9.7, 1.5 Hz, 1H), 7.16 (dd, *J* = 6.5, 2.6 Hz, 1H), 7.08 (dd, *J* = 6.0, 2.4 Hz, 1H), 4.47 (t, *J* = 5.6 Hz, 2H), 4.12 (s, 3H), 3.92 (q, *J* = 5.7 Hz, 2H), 1.75 (dh, *J* = 29.0, 7.3 Hz, 4H), 1.39 (s, 6H), 0.93 (t, *J* = 7.5 Hz, 6H).

^{13}C NMR (151 MHz, $CDCl_3$) δ 170.9, 168.1, 167.9, 166.99, 166.98, 166.2, 151.2, 149.4, 149.2, 145.6, 138.6, 137.3, 122.0, 114.4, 114.2, 114.0, 113.3, 109.3, 109.1, 88.2, 84.8, 67.6, 57.3, 39.2, 26.1, 25.4, 8.41, 8.36.

MS (ESI-TOF) *m/z* calcd. for $C_{28}H_{34}FN_3O_5^+$ ($[M+H]^+$) 522.4044, found 522.4037.

Synthesis of 12-3pin

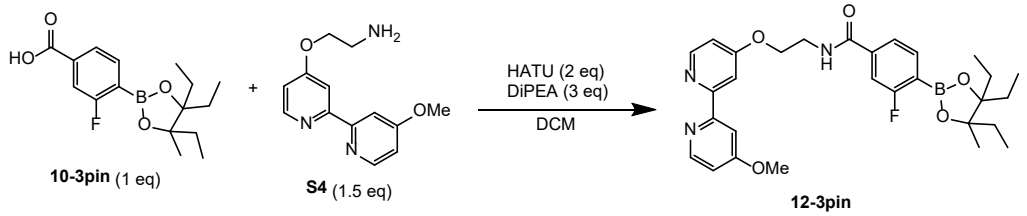

Boronate ester **10-3pin** (30.7 mg, 0.0997 mmol, 1.00 equiv) was prepared according to the small molecule general boronic ester formation procedure in a 20 mL vial and carried to the next step without purification. A stir bar and HATU (76.0 mg, 0.200 mmol, 2.01 equiv) were added and the mixture was diluted with dichloromethane (5 mL). Then *N,N*-diisopropylethylamine (52.0 µL, 0.302 mmol, 3.03 equiv) was added and the solution was stirred for 5 min followed by the addition of amine **S4** (37 mg, 0.15 mmol, 1.5 equiv, soln in 5 mL dichloromethane). The mixture was stirred for 1 h, and then the solvents evaporated under reduced pressure. The crude was then purified via silica gel chromatography (eluent: 97:2:1 dichloromethane/methanol/triethylamine). Product-containing fractions were concentrated under reduced pressure to afford **12-3pin** (49.2 mg, 0.092 mmol, 92%) as a colorless oil.

^{1}H NMR (600 MHz, $CDCl_3$) δ 8.60 (d, *J* = 6.5 Hz, 1H), 8.49 (d, *J* = 6.0 Hz, 1H), 8.05 (d, *J* = 2.4 Hz, 1H), 7.98 (d, *J* = 2.6 Hz, 1H), 7.64 (dd, *J* = 7.7, 5.8 Hz, 1H), 7.55 (t, *J* = 5.9 Hz, 1H), 7.47 (dd, *J* = 7.7, 1.5 Hz, 1H), 7.37 (dd, *J* = 9.6, 1.5 Hz, 1H), 7.07 (dd, *J* = 6.4, 2.6 Hz, 1H), 7.00 (dd, *J* = 6.0, 2.4 Hz, 1H), 4.38 (t, *J* = 5.6 Hz, 2H), 4.03 (s, 3H), 3.83 (q, *J* = 5.7 Hz, 2H), 1.82 – 1.56 (m, 6H), 1.42 (dq, *J* = 14.5, 7.4 Hz, 1H), 1.24 (s, 3H), 0.97 (t, *J* = 7.3 Hz, 3H), 0.85 (dt, *J* = 11.3, 7.5 Hz, 6H).

^{13}C NMR (151 MHz, $CDCl_3$) δ 170.7, 168.0, 166.8, 166.2, 151.6, 149.8, 149.2, 145.7, 138.8, 137.2, 122.1, 114.4, 114.2, 114.1, 113.2, 109.1, 109.0, 88.9, 86.7, 67.6, 57.2, 39.2, 29.9, 26.6, 25.3, 20.8, 8.9, 8.6, 8.3.

MS (ESI-TOF) *m/z* calcd. for $C_{29}H_{36}FN_3O_5^+$ ($[M+H]^+$) 536.2732, found 536.2736.

Synthesis of 12-Epin

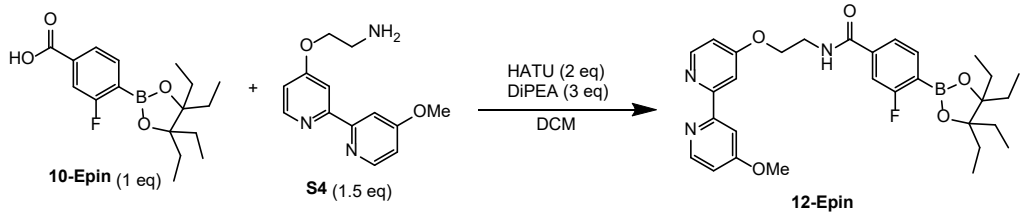

Boronate ester **10-Epin** (32.3 mg, 0.101 mmol, 1.00 equiv) was prepared according to the small molecule general boronic ester formation procedure in a 20 mL vial and carried to the next step without purification. A stir bar and HATU (76.0 mg, 0.200 mmol, 0.198 equiv) were added and diluted with dichloromethane (5 mL), then neat *N,N*-diisopropylethylamine (52.0 µL, 0.302 mmol, 3.04 equiv) was added and the solution was let stirring for 5 minutes, followed by the addition of amine **S4** (37 mg, 0.15 mmol, 1.5 equiv, soln in 5 mL dichloromethane). The mixture was stirred for 1 h, and then the solvents evaporated under reduced pressure. The crude was then purified via silica gel chromatography (eluent: 97:2:1 dichloromethane/methanol/triethylamine). Product-containing fractions were concentrated under reduced pressure to afford **12-Epin** (51.2 mg, 0.093 mmol, 93%) as an oil.

^{1}H NMR (600 MHz, $CDCl_3$) δ 8.73 (d, *J* = 6.5 Hz, 1H), 8.59 (d, *J* = 5.9 Hz, 1H), 8.26 (d, *J* = 2.4 Hz, 1H), 8.16 (d, *J* = 2.6 Hz, 1H), 7.71 (dd, *J* = 7.7, 5.8 Hz, 1H), 7.52 (dd, *J* = 7.7, 1.5 Hz, 1H), 7.47 (t, *J* = 6.1 Hz, 1H), 7.41 (dd, *J* = 9.6, 1.5 Hz, 1H), 7.14 (dd, *J* = 6.5, 2.6 Hz, 1H), 7.06 (dd, *J* = 6.0, 2.4 Hz, 1H), 4.50 (t, *J* = 5.6 Hz, 2H), 4.12 (s, 3H), 3.93 (d, *J* = 5.7 Hz, 2H), 1.86 – 1.61 (m, 8H), 1.02 – 0.87 (m, 12H).

^{13}C NMR (151 MHz, $CDCl_3$) δ 170.8, 167.9, 167.7, 166.8, 166.2, 152.0, 149.8, 149.6, 145.4, 138.7, 137.2, 122.0, 114.3, 114.2, 113.3, 109.0, 89.4, 77.4, 77.2, 77.0, 67.5, 57.2, 39.2, 26.5, 9.0.

MS (ESI-TOF) *m/z* calcd. for $C_{30}H_{38}FN_3O_5^+$ ($[M+H]^+$) 550.2888, found 550.2890.

Boronic acid – alkyne probes

Synthesis of 24-3pin

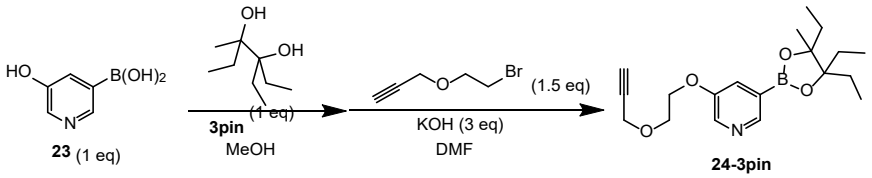

Boronic acid **23** (69.5 mg, 0.501 mmol, 1.00 equiv) and **3pin** (81.2 mg, 0.506 mmol, 1.01 equiv) were added to a 20 m: vial and diluted with dry methanol (10 mL), the solvent was evaporated under reduced pressure to afford the corresponding boronic ester and was carried to the next step without purification. A stir bar, 2-Bromoethyl(2-propynyl) ether (85.8 µL, 0.751 mmol, 1.50 equiv) and potassium hydroxide (83.4 mg, 1.49 mmol, 2.98 equiv) were added to the vial and the mixture was diluted with dimethylformamide (10 mL). The mixture was stirred overnight and then the solvents were evaporated under reduced pressure. The crude was then purified via silica gel chromatography (eluent 49:49:2 hexanes/ethyl acetate/triethyl amine). Product containing fractions were concentrated under reduced pressure to afford **24-3pin** (116 mg, 0.336 mmol, 67%) as a colorless oil.

^{1}H NMR (600 MHz, CD_3OD) δ 8.39 (s, 1H), 8.32 (s, 1H), 7.67 (s, 1H), 4.24 (q, *J* = 3.4 Hz, 4H), 3.97 – 3.83 (m, 2H), 2.87 (t, *J* = 2.4 Hz, 1H), 1.88 (dt, *J* = 14.3, 7.4 Hz, 1H), 1.84 – 1.70 (m, 4H), 1.60 – 1.51 (m, 1H), 1.34 (d, *J* = 2.3 Hz, 3H), 1.10 – 1.02 (m, 3H), 0.95 (td, *J* = 7.6, 3.5 Hz, 6H).

^{13}C NMR (151 MHz, CD_3OD) δ 156.6, 147.5, 140.9, 128.3, 90.3, 88.2, 80.4, 76.2, 69.2, 68.9, 59.2, 30.8, 27.5, 26.4, 21.2, 8.80, 8.76, 8.64.

MS (ESI-TOF) *m/z* calcd. for $C_{19}H_{29}BNO_4^+$ ($[M+H]^+$) 346.2184, found 346.2187.

Synthesis of 24-Epin

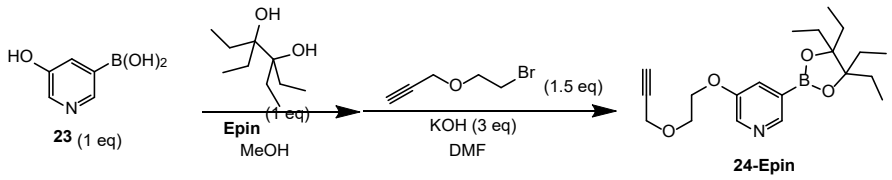

Boronic acid **23** (69.1 mg, 0.498 mmol, 1.00 equiv) and **Epin** (88.0 mg, 0.505 mmol, 1.01 equiv) were added to a 20 mL vial and diluted with dry methanol (10 mL), the solvent was evaporated under reduced pressure to afford the corresponding boronic ester and was carried to the next step without purification. A stir bar, 2-Bromoethyl(2-propynyl) ether (85.3 µL, 0.747 mmol, 1.50 equiv and potassium hydroxide (83.6 mg, 1.49 mmol, 3.00 equiv) were added to the vial and the mixture was diluted with dimethylformamide (10 mL). The mixture was stirred overnight and then the solvents were evaporated under reduced pressure. The crude was then purified via silica gel chromatography (eluent 49:49:2 hexanes/ethyl acetate/triethyl amine). Product containing fractions were concentrated under reduced pressure to afford **24-Epin** (114 mg, 0.319 mmol, 64 %) as a colorless oil.

^{1}H NMR (600 MHz, CD_3OD) δ 8.39 (d, *J* = 41.4 Hz, 2H), 7.67 (d, *J* = 2.8 Hz, 1H), 4.25 (q, *J* = 3.0 Hz, 4H), 3.91 (dq, *J* = 4.3, 2.2 Hz, 2H), 2.87 (q, *J* = 2.3 Hz, 1H), 1.89 – 1.74 (m, 8H), 1.06 – 0.96 (m, 12H).

^{13}C NMR (151 MHz, CD_3OD) δ 156.7, 147.6, 141.0, 128.2, 90.9, 80.4, 76.1, 69.2, 69.0, 59.2, 27.6, 9.2.

MS (ESI-TOF) *m/z* calcd. for $C_{20}H_{30}BNO_4^+$ ($[M+H]^+$) 360.2341, found 360.2340.

Iridium catalyst synthesis

Synthesis of 25-Gpin

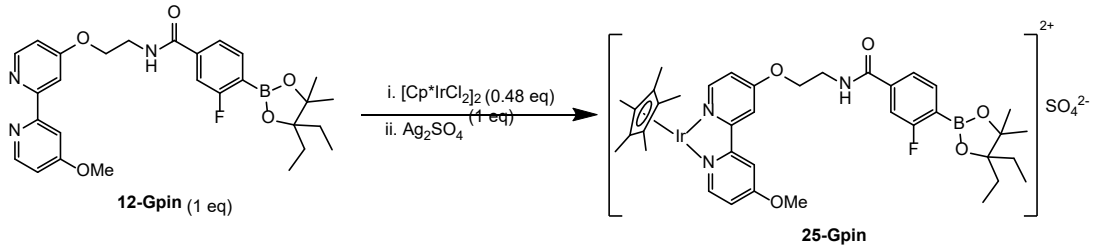

To a 4 mL vial equipped with a stir bar, bipyridine **12-Gpin** (26.1 mg, 0.0500 mmol, 1.00 equiv) and pentamethylcyclopentadienyl iridium dichloride dimer (19.1 mg, 0.0243 mmol, 0.486 equiv) were added and diluted with methanol (1 mL), the mixture was allowed to stir until homogeneous (approximately 10 minutes). To the crude solution, silver sulfate (15.6 mg, 0.0500 mmol, 1.00 equiv) was added, the mixture was stirred for 1h. The mixture was centrifuged and the supernatant was collected to remove the formed salts. The collected solution was then added dropwise to cold pentane (30 mL), precipitating the desired complex. The mixture was centrifuged again. The solvent was decanted, and the resulting solid washed with cold pentanes (2×15 mL) and dried under vacuum to afford iridium complex **25-Gpin** as an orange oil (44.6 mg, 0.046 mmol 93%).

^{1}H NMR (600 MHz, CD_3OD) δ 8.69 (dd, *J* = 6.6, 2.5 Hz, 2H), 8.25 (t, *J* = 2.5 Hz, 1H), 8.15 (dd, *J* = 5.2, 2.7 Hz, 1H), 7.76 (dd, *J* = 7.7, 5.8 Hz, 1H), 7.61 (dd, *J* = 7.7, 1.5 Hz, 1H), 7.50 (dd, *J* = 9.8, 1.5 Hz, 1H), 7.37 (ddd, *J* = 21.0, 6.6, 2.7 Hz, 2H), 4.55 (t, *J* = 5.7 Hz, 2H), 4.12 (s, 3H), 3.86 (t, *J* = 5.6 Hz, 2H), 1.86 – 1.74 (m, 4H), 1.67 (s, 15H), 1.40 (s, 6H), 0.96 (t, *J* = 7.5 Hz, 6H).

^{13}C NMR (151 MHz, CD_3OD) δ 168.6, 167.8, 167.7, 167.5, 166.0, 157.1, 156.9, 152.2, 138.9, 136.8, 122.1, 122.0, 115.3, 114.6, 113.8, 113.7, 110.1, 110.0, 88.6, 88.0, 84.6, 67.5, 56.3, 38.7, 33.9, 25.7, 24.3, 22.0, 13.0, 7.24, 7.19.

MS (ESI-TOF) *m/z* calcd. for $C_{38}H_{48}BFIrN_3O_5^+$ ($[M]^{2+}$) 424.6650, found 424.6649.

Synthesis of 25-Epin

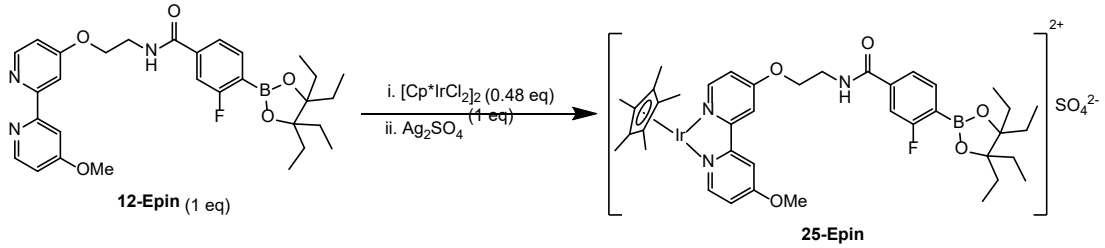

To a 4-mL vial equipped with a stir bar, bipyridine **12-Epin** (27.5 mg, 0.0500 mmol, 1.00 equiv) and pentamethylcyclopentadienyl iridium dichloride dimer (19.1 mg, 0.0243 mmol, 0.486 equiv) were added and diluted with methanol (1 mL), the mixture was allowed to stir until homogeneous (approximately 10 minutes). To the crude solution, silver sulfate (15.6 mg, 0.0500 mmol, 1.00 equiv) was added, the mixture was stirred for 1h. The mixture was centrifuged and the supernatant was collected to remove the formed salts. The collected solution was then added dropwise to cold pentane (30 mL), precipitating the desired complex. The mixture was centrifuged again. The solvent was decanted, and the resulting solid washed with cold pentanes (2×15 mL) and dried under vacuum to afford iridium complex **25-Epin** as an orange oil (43.0 mg, 0.44 mmol 87%).

^{1}H NMR (600 MHz, CD_3OD) δ 8.97 (dd, *J* = 6.6, 1.6 Hz, 2H), 8.26 (d, *J* = 2.7 Hz, 1H), 8.16 (d, *J* = 2.8 Hz, 1H), 7.76 (dd, *J* = 7.7, 5.8 Hz, 1H), 7.61 (dd, *J* = 7.7, 1.5 Hz, 1H), 7.50 (dd, *J* = 9.7, 1.5 Hz, 1H), 7.43 (dd, *J* = 6.6, 2.7 Hz, 1H), 7.39 (dd, *J* = 6.6, 2.7 Hz, 1H), 4.57 (h, *J* = 4.9 Hz, 2H), 4.13 (s, 3H), 3.87 (t, *J* = 5.7 Hz, 2H), 1.80 (hept, *J* = 7.4 Hz, 8H), 1.68 (s, 15H), 1.02 – 0.92 (m, 12H).

^{13}C NMR (151 MHz, CD_3OD) δ 169.1, 168.2, 167.73, 167.68, 167.58, 166.1, 162.6, 162.3, 157.6, 157.4, 152.8, 136.8, 136.7, 122.0, 122.0, 114.8, 114.1, 113.8, 113.6, 110.1, 110.09, 110.06, 89.2, 87.8, 67.6, 56.4, 26.1, 26.0, 7.8, 7.3.

MS (ESI-TOF) *m/z* calcd. for $C_{40}H_{52}BFIrN_3O_5^+$ ($[M]^{2+}$) 438.6807, found 438.6804.

Miyaura borylation reactions

Synthesis of 5-pin

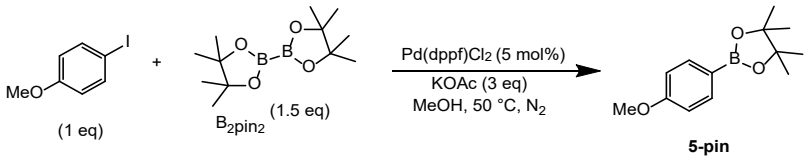

To a 4-mL vial equipped with a stir bar, 1-iodo-4-methoxybenzene (5.8 mg, 0.025 mmol, 1 equiv), **B_2pin_2** (9.6 mg, 0.038 mmol, 1.5 equiv), [1,1'-bis(diphenylphosphino)ferrocene]palladium(II) dichloride (0.9 mg, 0.0012 mmol, 0.05 equiv) and potassium acetate (7.4 mg, 0.075 mmol, 3 equiv) were added and diluted with dry methanol (1 mL). The mixture was then sparged with nitrogen for 5 min and let stirring overnight at 50 °C. The solvent was then removed under reduced pressure, and the crude was purified via silica gel chromatography (eluent: 98:2 hexanes/ethyl acetate). Product-containing fractions were concentrated under reduced pressure to afford the pinacol ester **5-pin** (4.2 mg, 0.093 mmol, 72%) as a white solid.

^{1}H NMR (600 MHz, $CDCl_3$) δ 7.78 – 7.73 (m, 2H), 6.91 – 6.86 (m, 2H), 3.83 (s, 3H), 1.33 (s, 12H).

^{13}C NMR (151 MHz, $CDCl_3$) δ 162.29, 136.65, 113.45, 83.70, 77.37, 77.16, 76.95, 55.24, 25.00.

MS (ESI-TOF) *m/z* calcd. for $C_{13}H_{20}BO_3^+$ ($[M+H]^+$) 235.1506, found 235.1501.

Synthesis of 5-Gpin

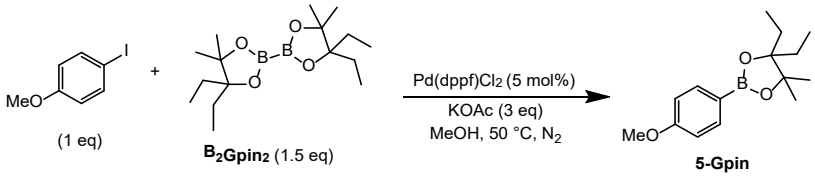

To a 4 mL vial equipped with a stir bar 1-iodo-4-methoxybenzene (6.0 mg, 0.026 mmol, 1 equiv), **B_2Gpin_2** (12.1 mg, 0.039 mmol, 1.5 equiv), [1,1'-bis(diphenylphosphino)ferrocene]palladium(II) dichloride (0.9 mg, 0.0012 mmol, 0.05 equiv) and potassium acetate (7.7 mg, 0.078 mmol, 3 equiv) were added and diluted with dry methanol (1 mL). The mixture was then sparged with nitrogen for 5 min and let stirring overnight at 50 °C. The solvent was then removed under reduced pressure, and the crude was purified via silica gel chromatography (eluent: 98:2 hexanes/ethyl acetate). Product-containing fractions were concentrated under reduced pressure to afford the pinacol ester **5-Gpin** (6.6 mg, 0.093 mmol, 97%) as a white solid.

^{1}H NMR (600 MHz, $CDCl_3$) δ 7.83 – 7.67 (m, 2H), 6.99 – 6.81 (m, 2H), 3.83 (s, 3H), 1.83 – 1.68 (m, 4H), 1.38 (s, 6H), 0.93 (d, J = 7.5 Hz, 6H).

^{13}C NMR (151 MHz, $CDCl_3$) δ 162.12, 136.54, 113.31, 83.99, 77.25, 77.03, 76.82, 55.09, 31.61, 26.01, 25.39, 14.14, 8.34.

MS (ESI-TOF) *m/z* calcd. for $C_{15}H_{24}BO_3^+$ ($[M+H]^+$) 263.1818 found 263.1825.

Peptide borylation procedure

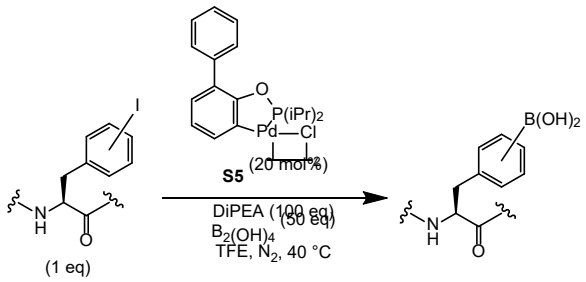

To a 4 mL vial equipped with a stir bar, palladacyclic phosphinite catalyst **S5** (0.4 µmol, 20 mol%, 26.7 µL of a 15 mM solution in chloroform) and aryl-iodide peptide (2 µmol, 1 equiv, 66.7 µL of a 30 mM solution in dimethyl sulfoxide) were diluted in 650 µL of 2,2,2-trifluoroethanol and sparged with nitrogen for 5 minutes. In a separate vial, tetrahydroxydiboron (9.0 mg, 100 µmol, 50 equiv) and neat *N,N*-diisopropylethylamine (35 µL, 200 µmol, 100 equiv) were added under nitrogen and sonicated for 15 minutes before being transferred dropwise into the vial containing the catalyst and the peptide. The reaction mixture was stirred at 40 °C for 16-18 h. The product was separated from the reaction mixture via preparative HPLC and lyophilized.

Supplementary data

For figure 2

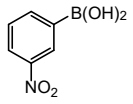

8

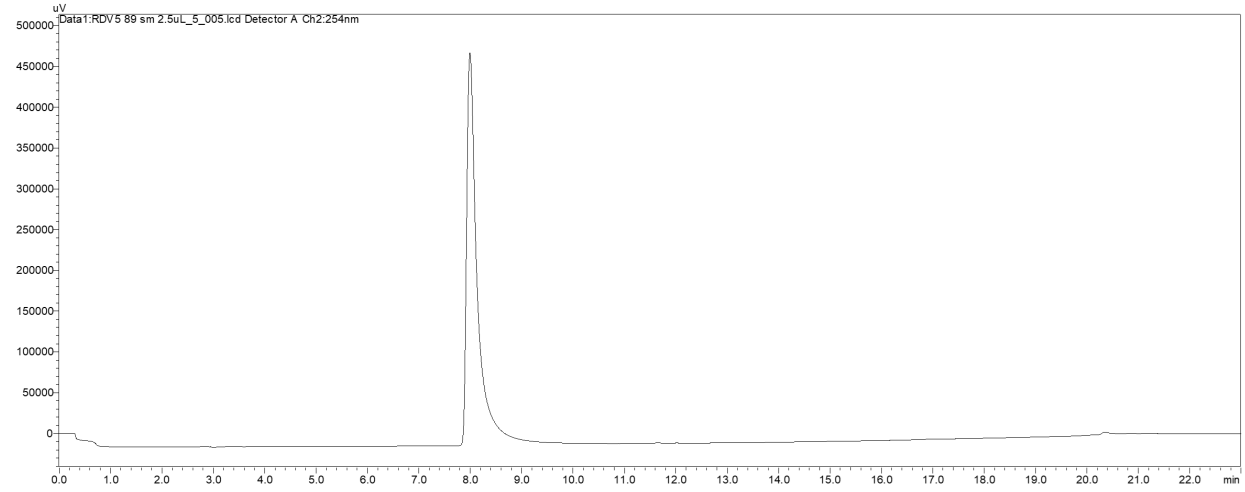

Figure S1. RP-HPLC trace at 254 nm (30-70% MeCN over 23 min) of free boronic acid **8**.

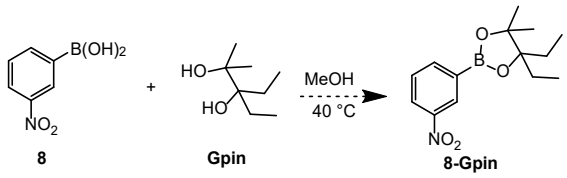

8 **Gpin** **8-Gpin**

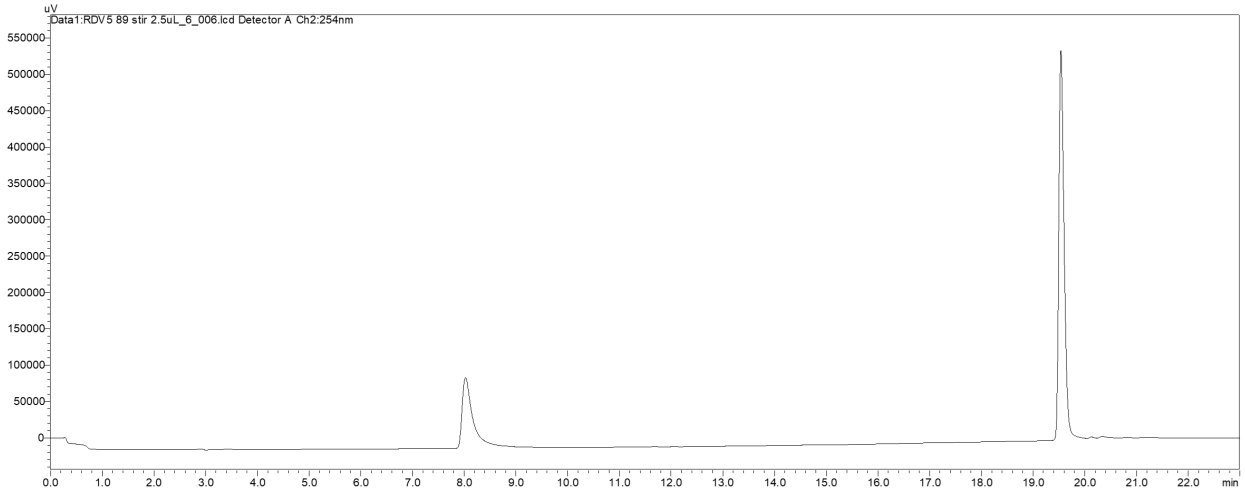

Figure S2. RP-HPLC trace at 254 nm (30-70% MeCN over 23 min) of free boronic acid **8** and **Gpin** mixture before rotovaping.

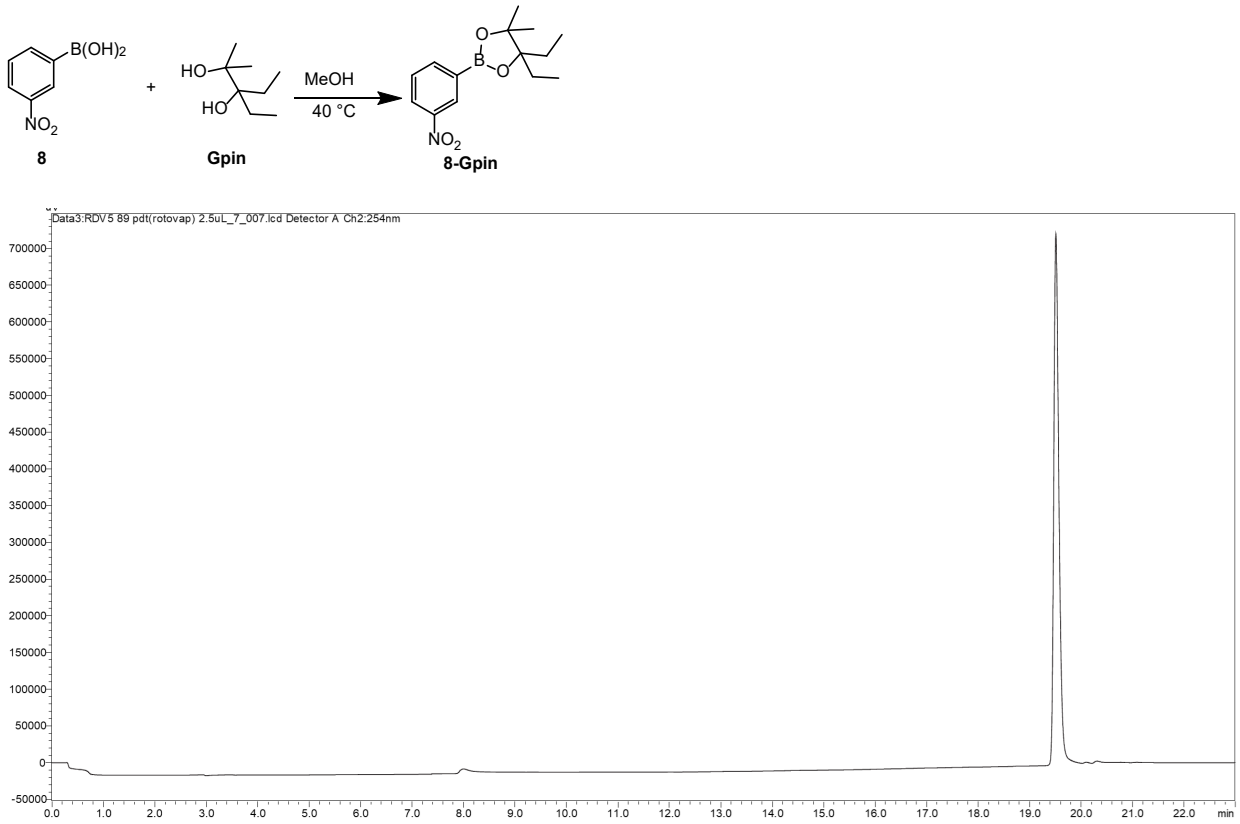

Figure S3. RP-HPLC trace at 254 nm (30-70% MeCN over 23 min) of 8-Gpin made after concentration on a rotary evaporator.

For figure 3

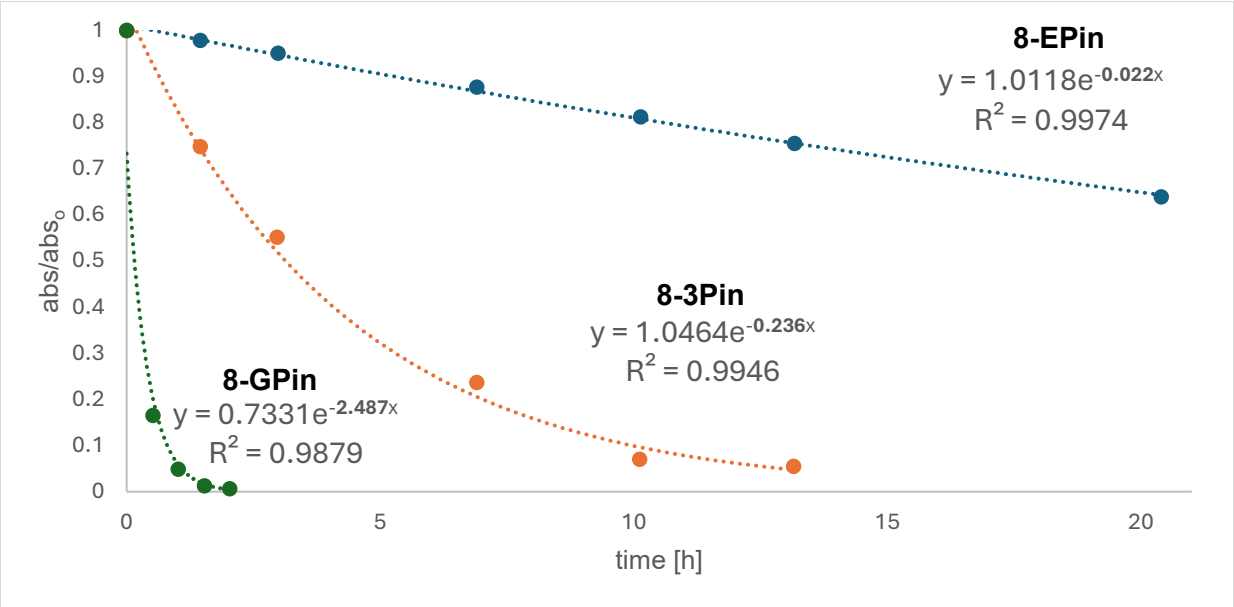

Figure S4. Overlay plot of the hydrolysis data for**8-Gpin**, **8-3pin** and **8-Epin** in pH 6.8 PBS, using normalized absorbance (abs/abs_o). Each dataset was fitted to a single-exponential decay model, and the extracted rate hydrolysis constant (k) corresponds to the exponential coefficient in the fitted function, representing the pseudo-first-order hydrolysis rate for each ester.

For figure 4

Table S1. All the hydrolysis half-life measured at PBS pH 7.4 for all the boronic esters in figure 4.

molecule	pin	Gpin	3pin	Epin
		Hydrolysis half-life at pH 7.4 (h)		
1		5.4	14.4	18.9
2	0.1	7.8	19.5	25.1
3	0.1	5.6	15.3	20.2
4	0.4	13.9	75.3	117.5
5	0.2	10.9	60.8	99.0
6		7.5	12.6	21.3
7		0.2	1.5	18.2
8		0.3	1.2	24.2
9		0.4	10.4	16.1
10		0.4	2.7	24.8
11		1.6	8.2	34.1
12		0.4	2	50
13			0.6	2.6
14		1.2	3.3	
15		2.1	3.6	10.2
16		0.7	4.1	24.2
17			2.3	13.6
18		0.3	12	
19		4.6	18.4	
20		5.7	21.8	
21		1.7		
22		16.6		

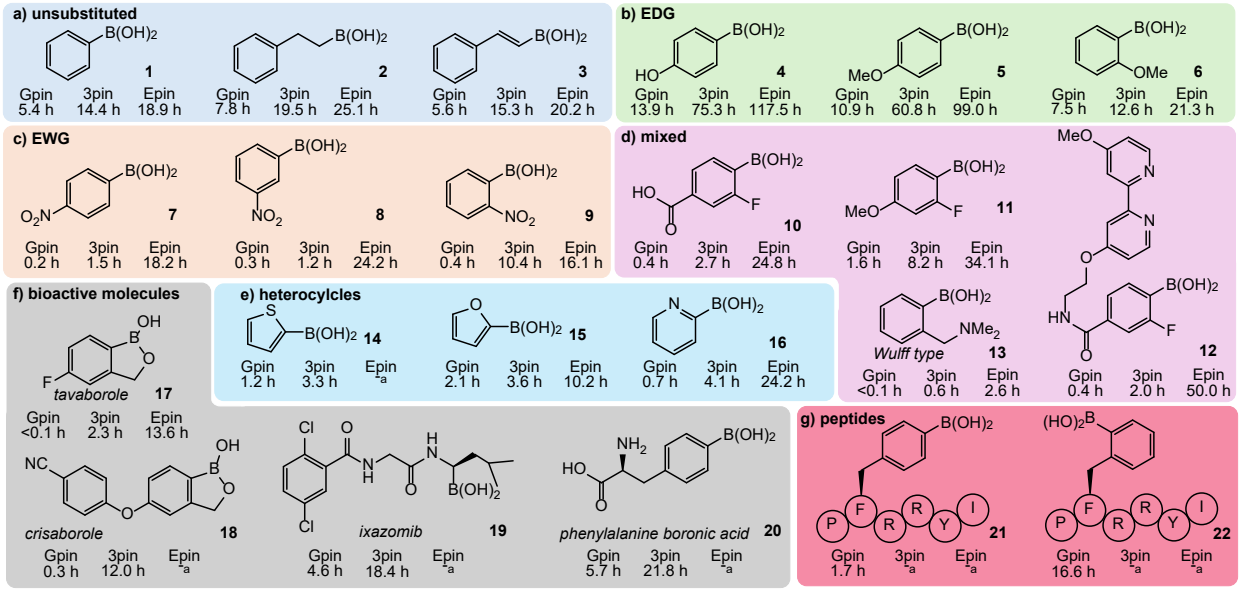

Figure S5. Alternative version of figure 4 reporting the hydrolysis half-life at pH 7.4 of the measured Gpin, 3pin and Epin esters.

Table S2. All the $k_{hydrolysis}$ measured at PBS pH 7.4 for all the boronic esters in figure 4.

molecule	**pin**	***repl.***	**Gpin**	***repl.***	**3pin**	***repl.***	**Epin**	***repl.***
					$k_{hydrolysis}$ at pH 7.4 (h^{-1})			
1			0.128	*0.131*	0.048	*0.047*	0.037	*0.037*
2	7.638		0.089	*0.088*	0.036	*0.035*	0.028	*0.030*
3	6.266	*6.062*	0.124	*0.122*	0.045	*0.045*	0.034	*0.034*
4	1.732		0.050	*0.049*	0.0092	*0.0091*	0.0059	*0.0058*
5	3.118		0.064	*0.063*	0.011	*0.012*	0.0072	*0.0067*
6			0.092		0.055		0.034	*0.033*
7			3.060		0.466	*0.462*	0.038	
8			2.817		0.578		0.029	*0.028*
9			1.852	*1.890*	0.067		0.043	*0.042*
10			1.743		0.257		0.028	*0.026*
11			0.428		0.085		0.020	*0.020*
12			1.856	*1.905*	0.347		0.014	
13			>7		1.155	*1.137*	0.267	*0.279*
14			0.576	*0.559*	0.209		-[a]	
15			0.331		0.133		0.067	*0.067*
16			0.986		0.168		0.029	*0.027*
17			>7		0.301		0.051	
18			2.568		0.575		-[a]	
19			0.149		0.038		-[a]	
20			0.122		0.032	*0.033*	-[a]	
21			0.408		-[a]		-[a]	
22			0.042		-[a]		-[a]	

a. Ester insoluble in buffer

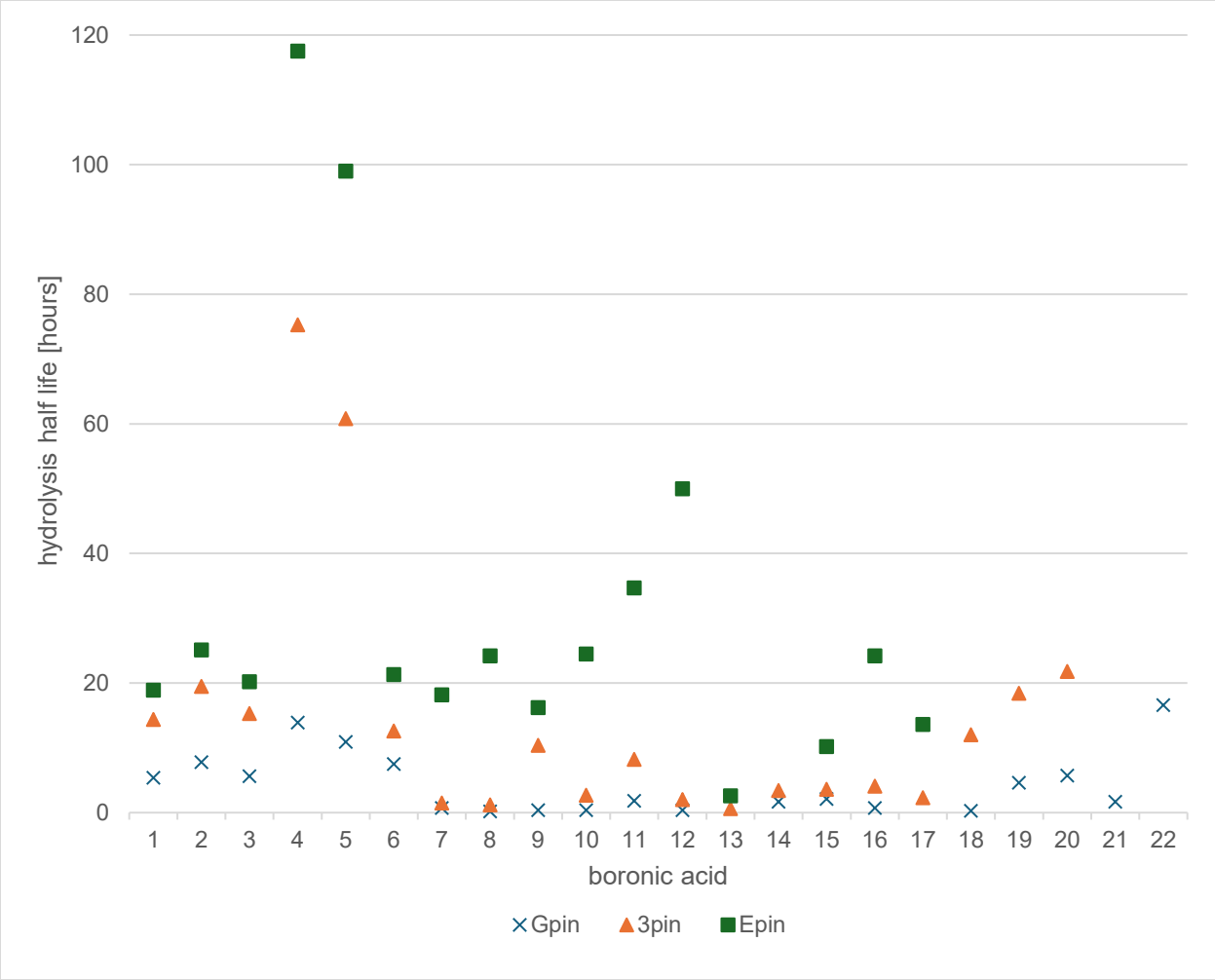

Figure S6. Plotted graph displaying all the hydrolysis half-life at pH 7.4 for all the boronic esters studied in figure 4 (original plot without structures).

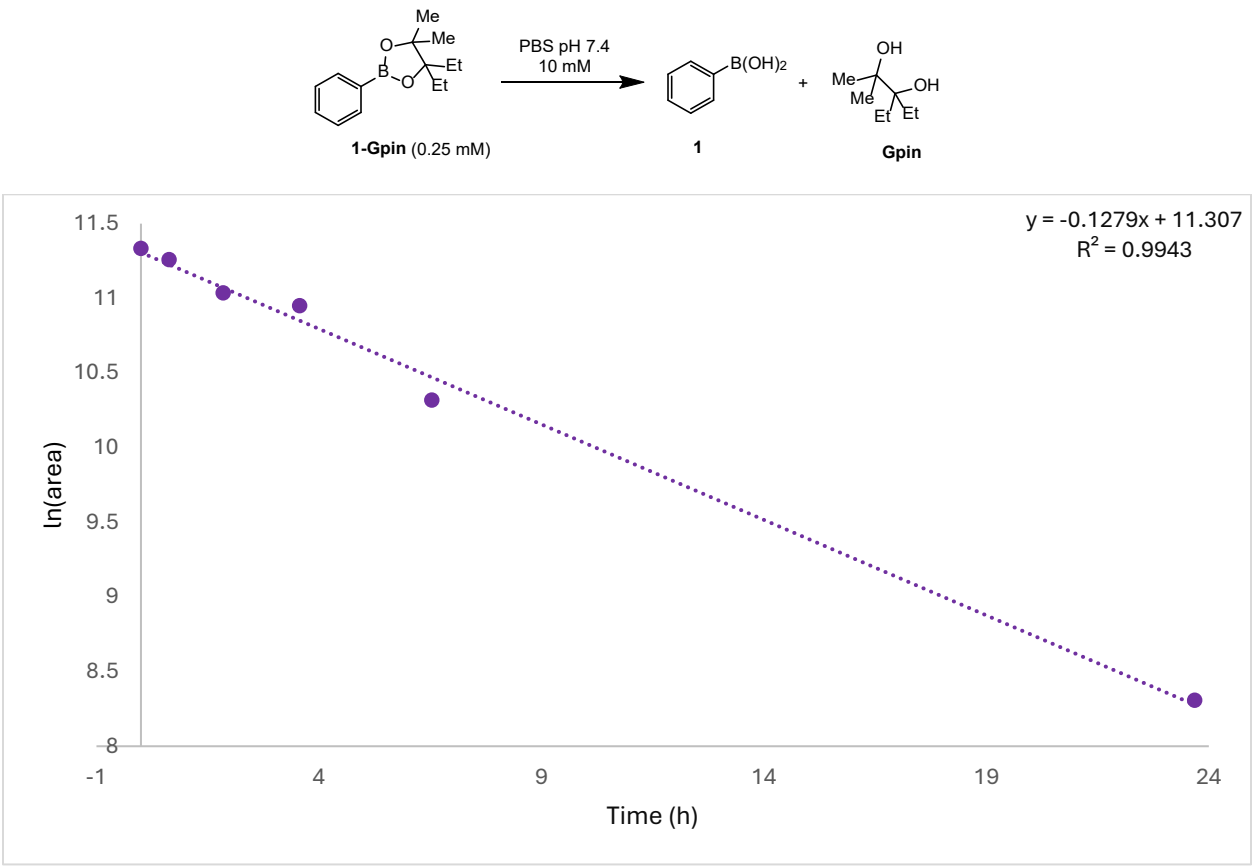

Figure S7. Plot of ln[boronic ester peak area] versus time for boronic ester **1-Gpin**. Data were fitted to a first order decay model using linear regression. The slope of the best-fit line corresponds to the pseudo-first order rate constant (k), from which the hydrolysis half-life ($t_{1/2}$) of 5.4 h was calculated**.**

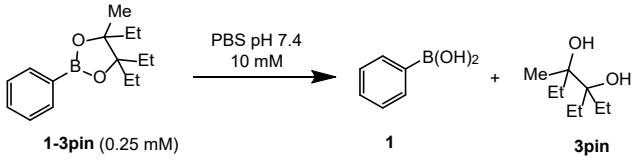

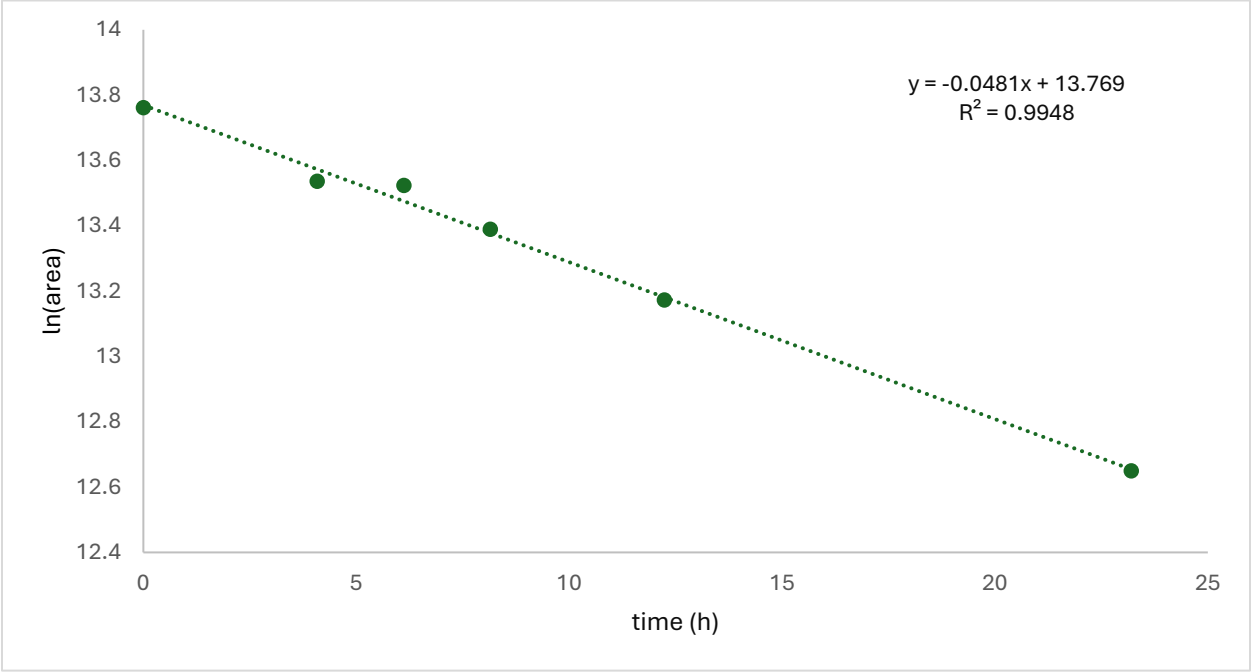

Figure S8. Plot of ln[boronic ester peak area] versus time for boronic ester **1-3pin**. Data were fitted to a first order decay model using linear regression. The slope of the best-fit line corresponds to the pseudo-first order rate constant (k), from which the hydrolysis half-life ($t_{1/2}$) of 14.4 h was calculated.

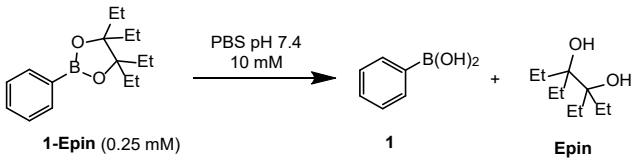

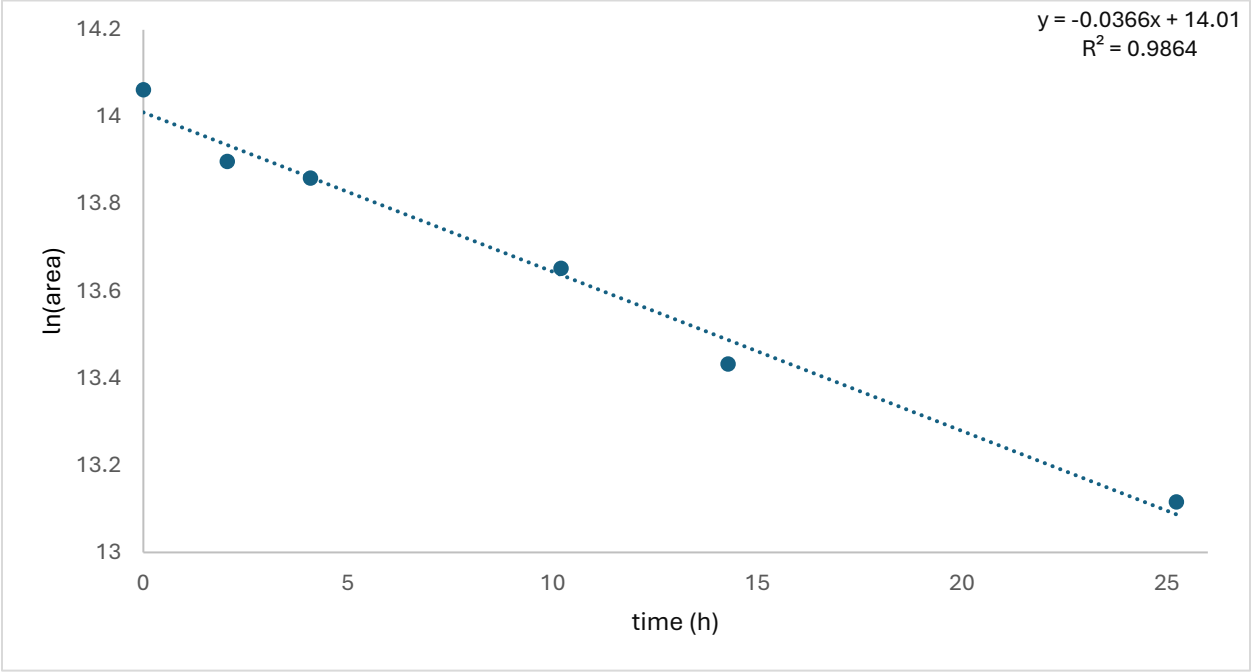

Figure S9. Plot of ln[boronic ester peak area] versus time for boronic ester **1-Epin.** Data were fitted to a first order decay model using linear regression. The slope of the best-fit line corresponds to the pseudo-first order rate constant (k), from which the hydrolysis half-life ($t_{1/2}$) of 18.9 h was calculated.

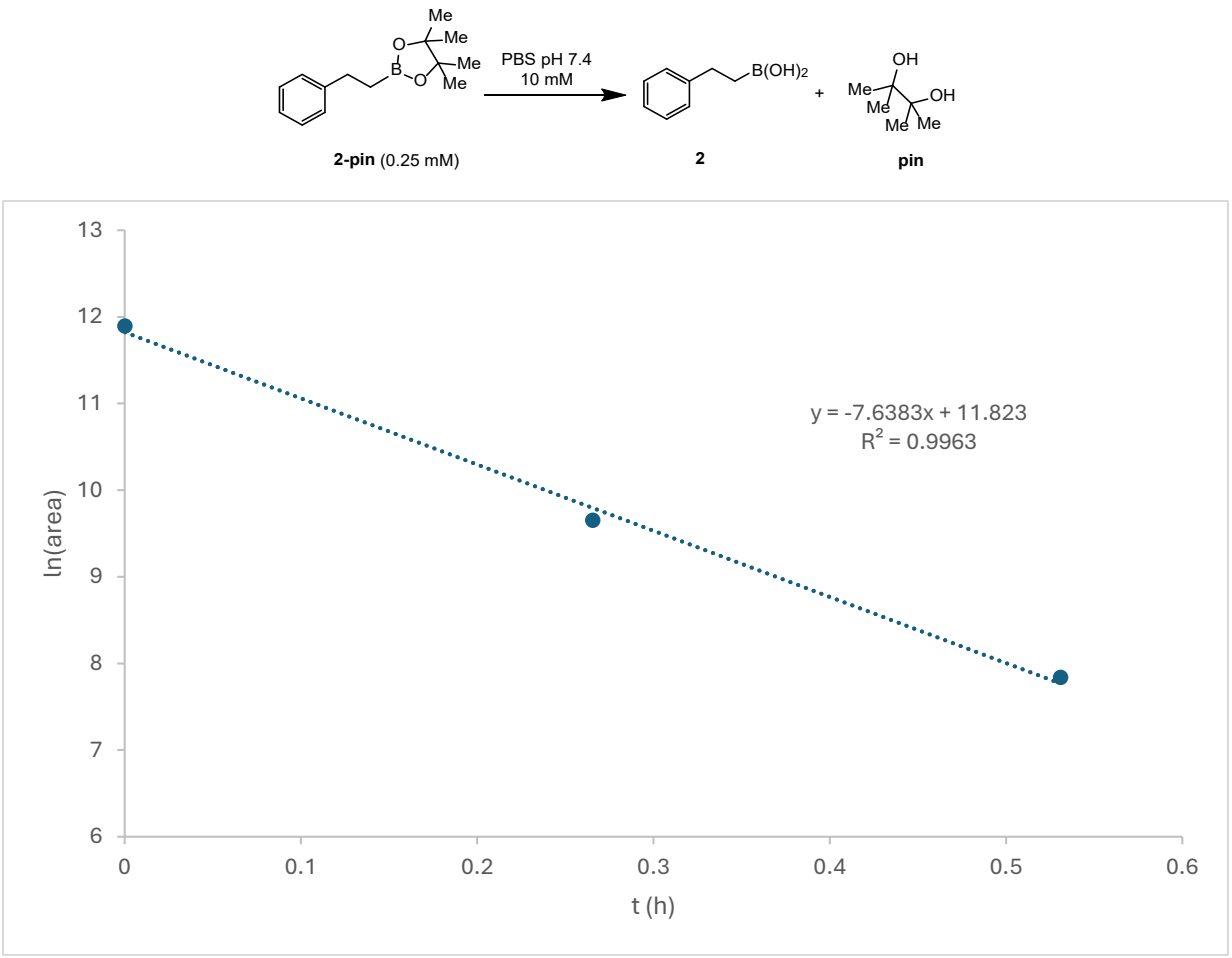

Figure S10. Plot of ln[boronic ester peak area] versus time for boronic ester **2-pin.** Data were fitted to a first order decay model using linear regression. The slope of the best-fit line corresponds to the pseudo-first order rate constant (k), from which the hydrolysis half-life ($t_{1/2}$) of 0.1 h was calculated.

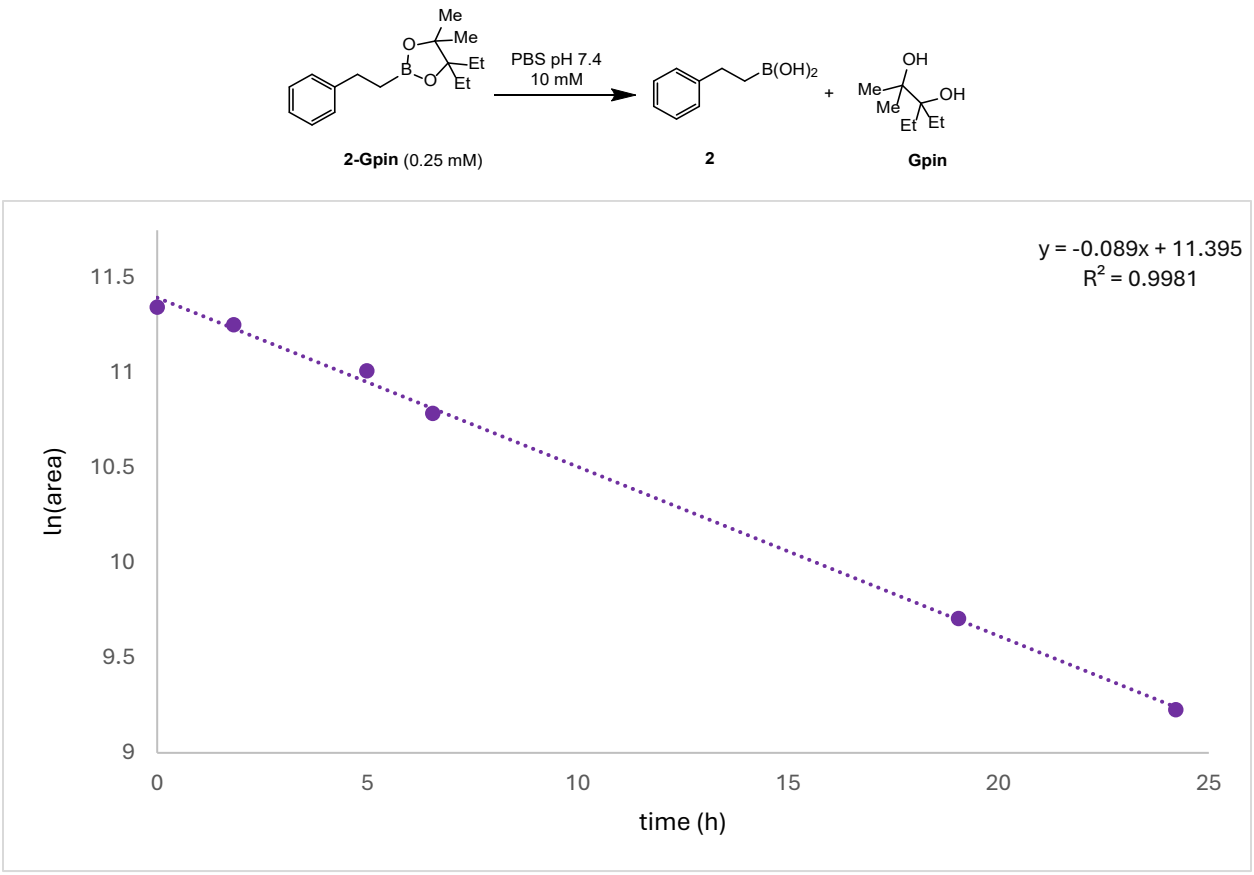

Figure S11. Plot of ln[boronic ester peak area] versus time for boronic ester **2-Gpin**. Data were fitted to a first order decay model using linear regression. The slope of the best-fit line corresponds to the pseudo-first order rate constant (k), from which the hydrolysis half-life ($t_{1/2}$) of 7.8 h was calculated.

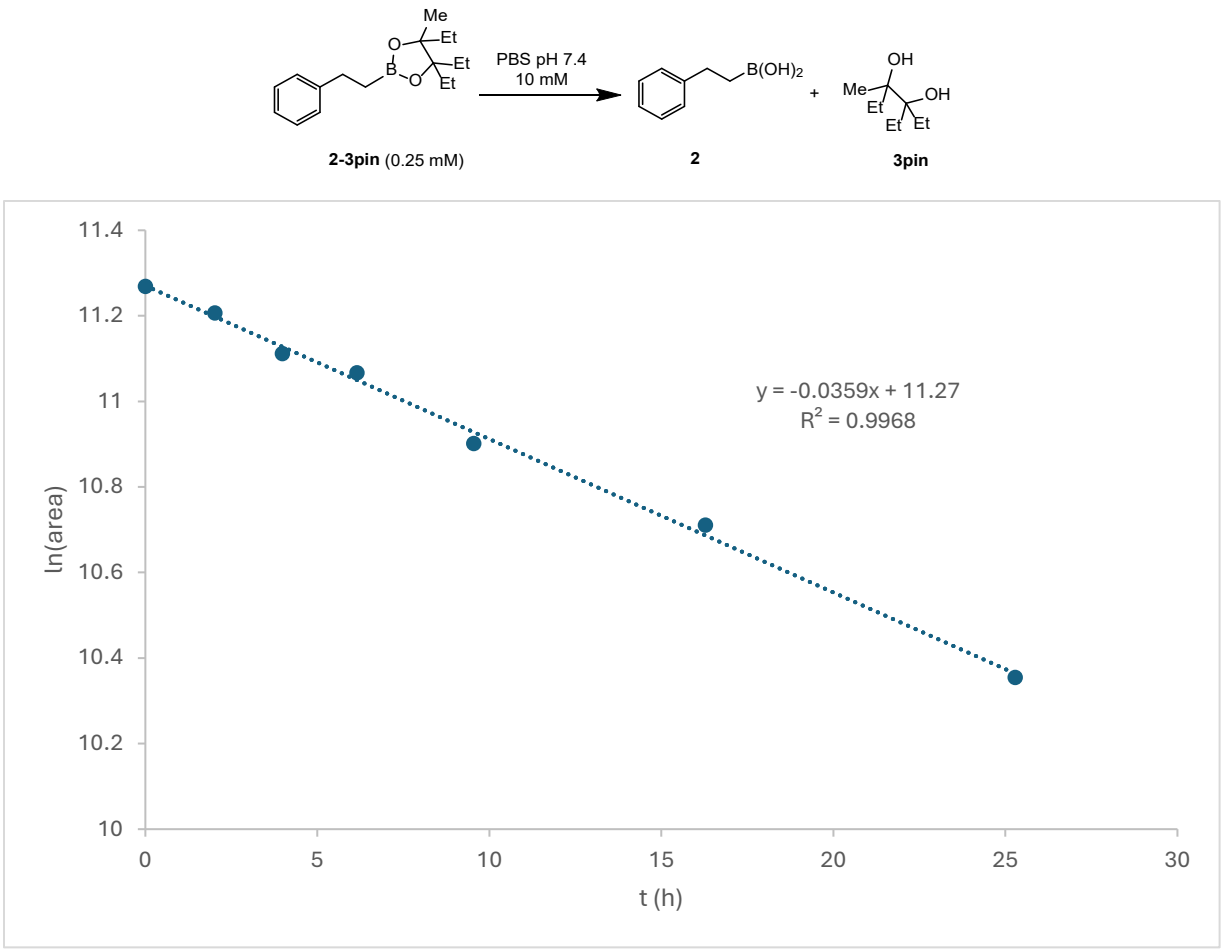

Figure S12. Plot of ln[boronic ester peak area] versus time for boronic ester **2-3pin**. Data were fitted to a first order decay model using linear regression. The slope of the best-fit line corresponds to the pseudo-first order rate constant (k), from which the hydrolysis half-life ($t_{1/2}$) of 19.5 h was calculated.

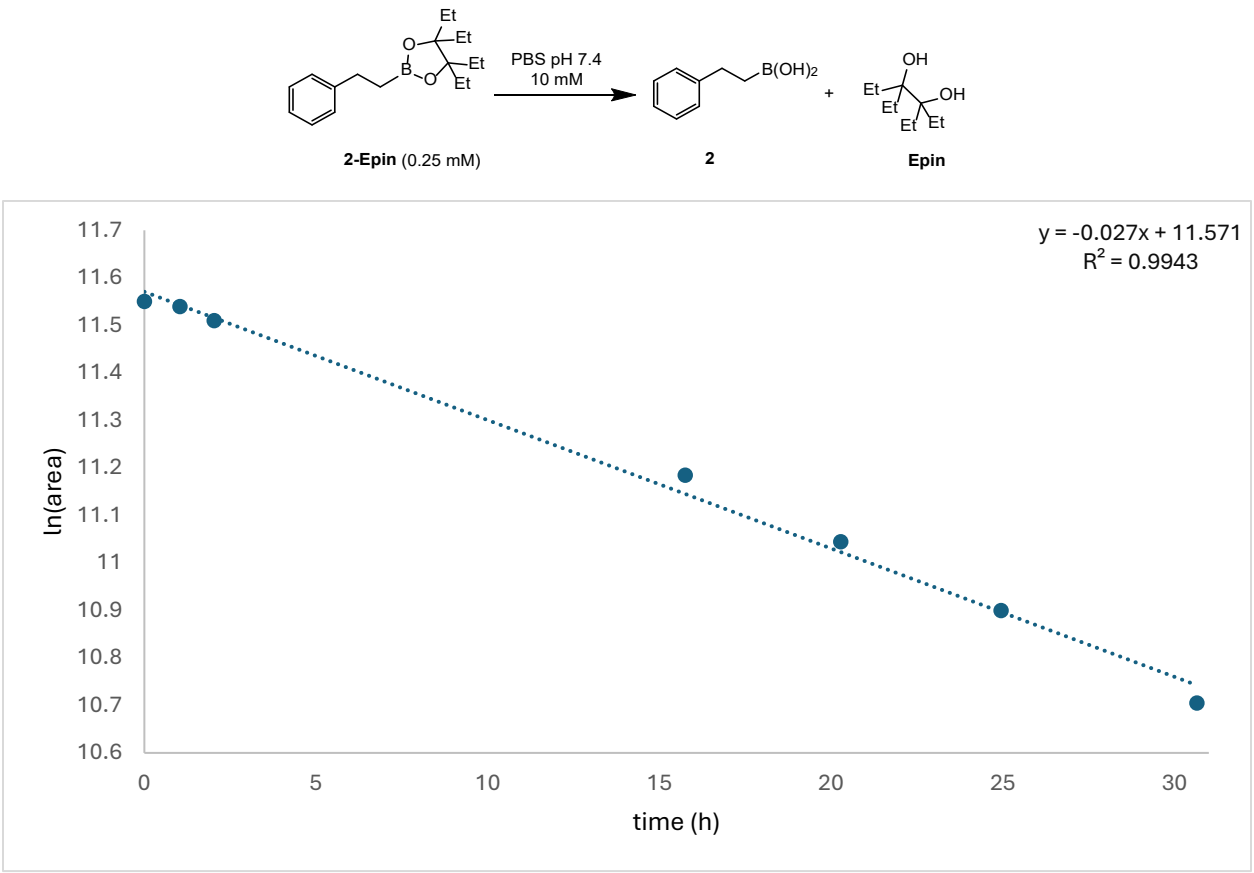

Figure S13. Plot of ln[boronic ester peak area] versus time for boronic ester **2-Epin.** Data were fitted to a first order decay model using linear regression. The slope of the best-fit line corresponds to the pseudo-first order rate constant (k), from which the hydrolysis half-life ($t_{1/2}$) of 25.1 h was calculated.

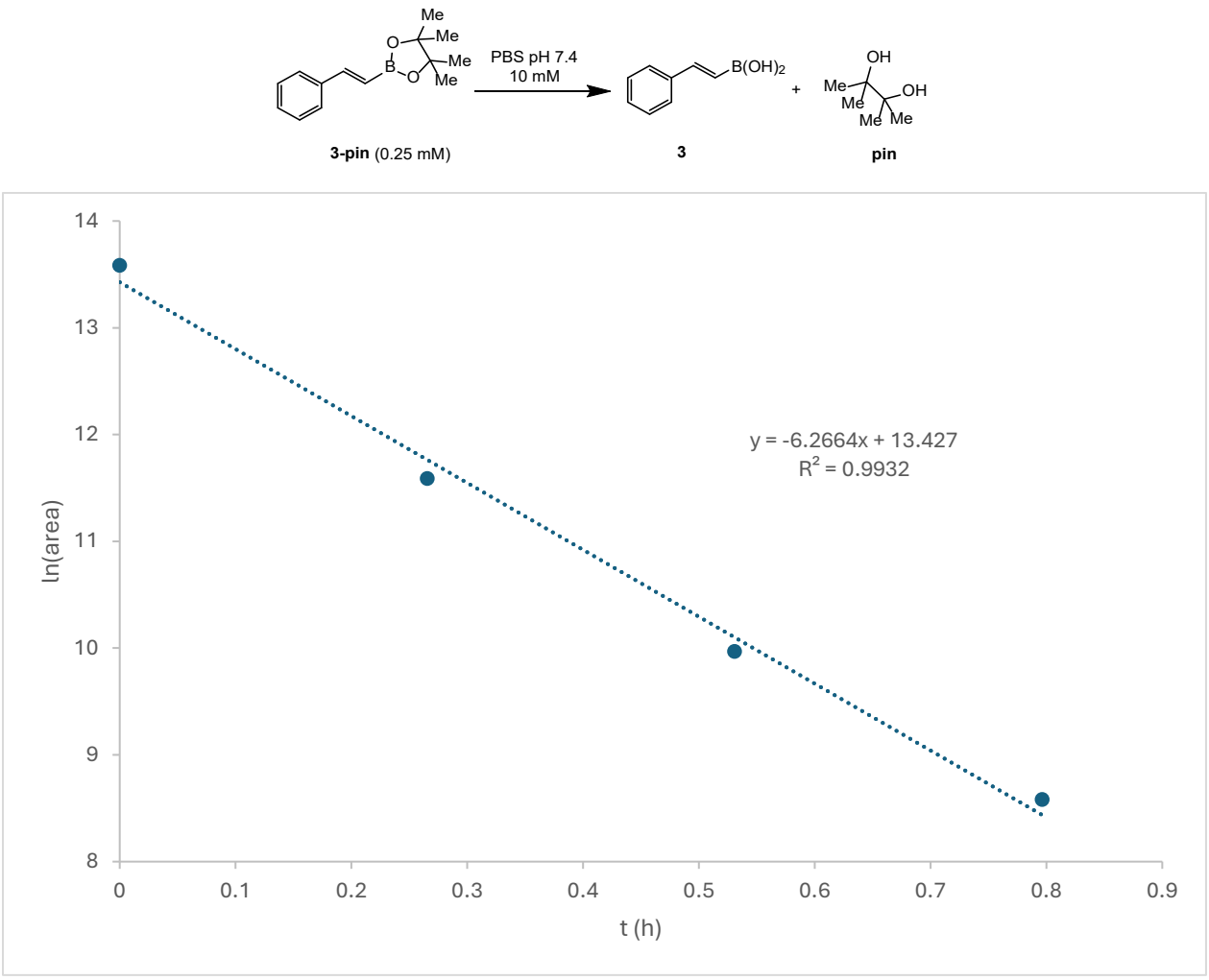

Figure S14. Plot of ln[boronic ester peak area] versus time for boronic ester **3-pin**. Data were fitted to a first order decay model using linear regression. The slope of the best-fit line corresponds to the pseudo-first order rate constant (k), from which the hydrolysis half-life ($t_{1/2}$) of 0.1 h was calculated.

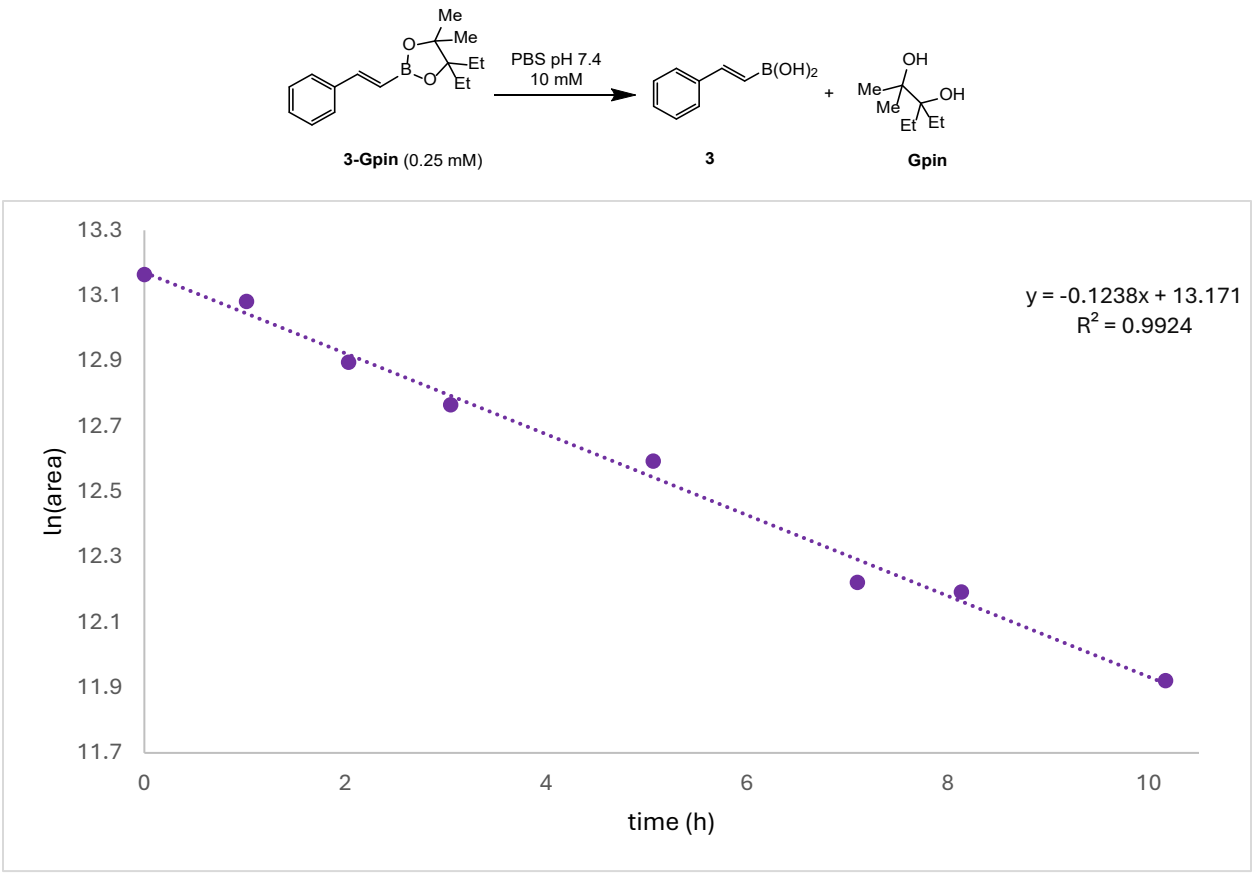

Figure S15. Plot of ln[boronic ester peak area] versus time for boronic ester **3-Gpin**. Data were fitted to a first order decay model using linear regression. The slope of the best-fit line corresponds to the pseudo-first order rate constant (k), from which the hydrolysis half-life ($t_{1/2}$) of 5.6 h was calculated.

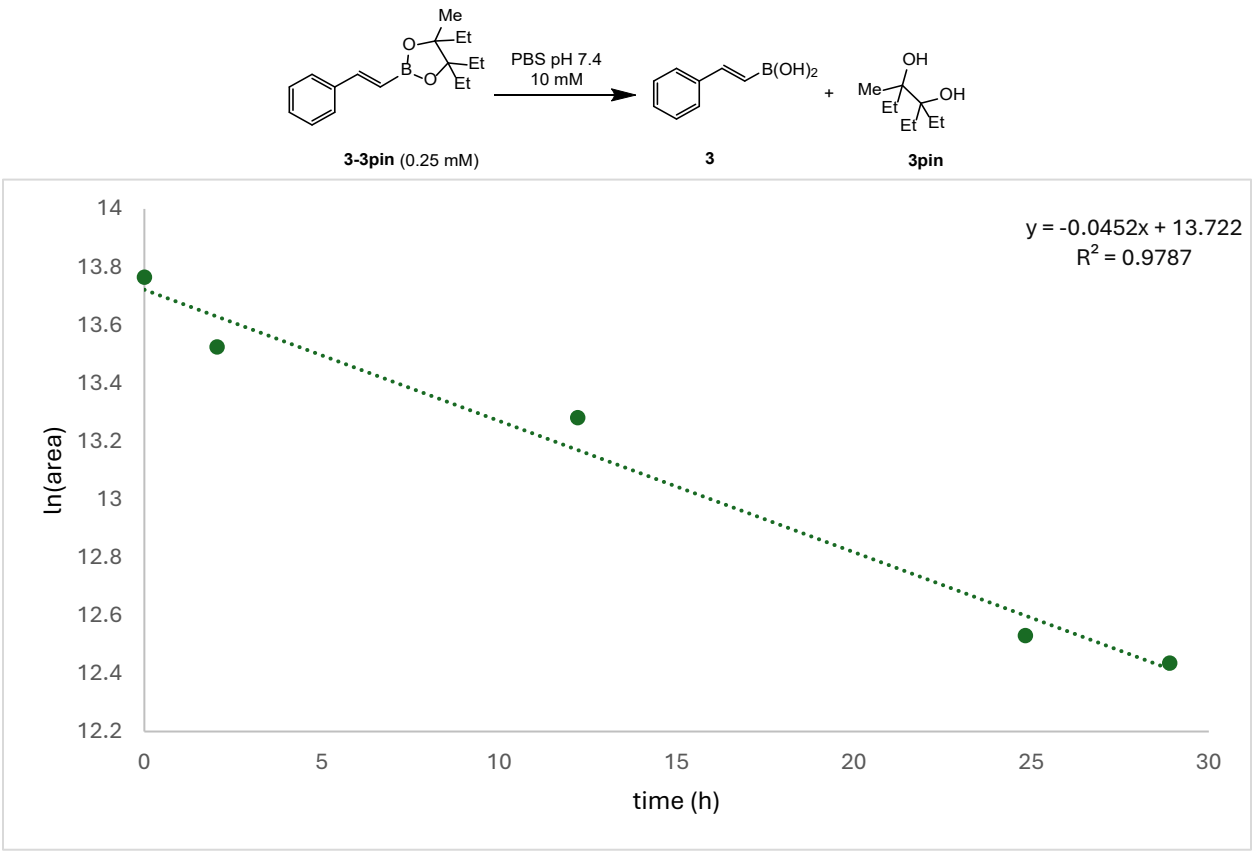

Figure S16. Plot of ln[boronic ester peak area] versus time for boronic ester **3-3pin**. Data were fitted to a first order decay model using linear regression. The slope of the best-fit line corresponds to the pseudo-first order rate constant (k), from which the hydrolysis half-life ($t_{1/2}$) of 15.3 h was calculated**.**

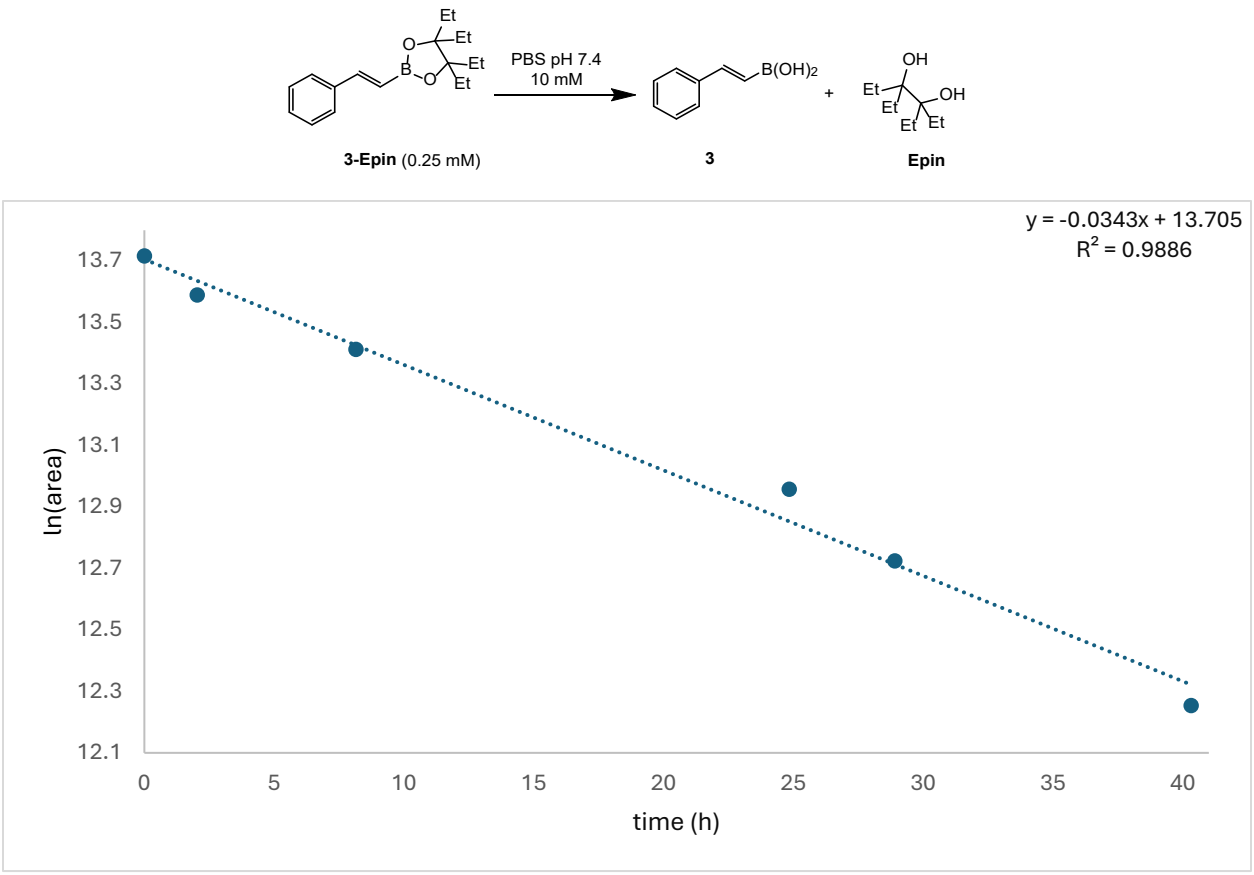

Figure S17. Plot of ln[boronic ester peak area] versus time for boronic ester **3-Epin**. Data were fitted to a first order decay model using linear regression. The slope of the best-fit line corresponds to the pseudo-first order rate constant (k), from which the hydrolysis half-life ($t_{1/2}$) of 20.2 h was calculated.

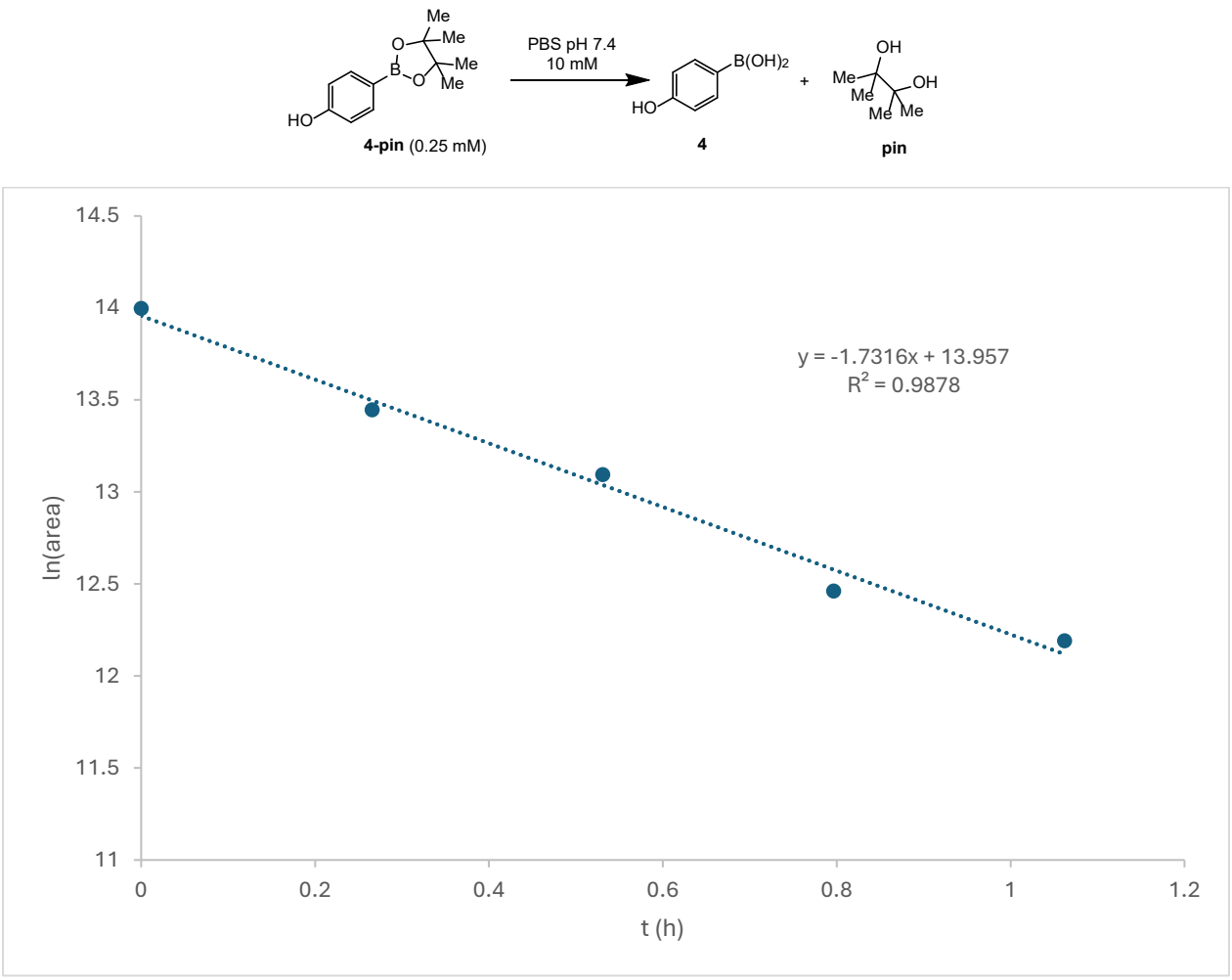

Figure S18. Plot of ln[boronic ester peak area] versus time for boronic ester **4-pin**. Data were fitted to a first order decay model using linear regression. The slope of the best-fit line corresponds to the pseudo-first order rate constant (k), from which the hydrolysis half-life ($t_{1/2}$) of 0.4 h was calculated.

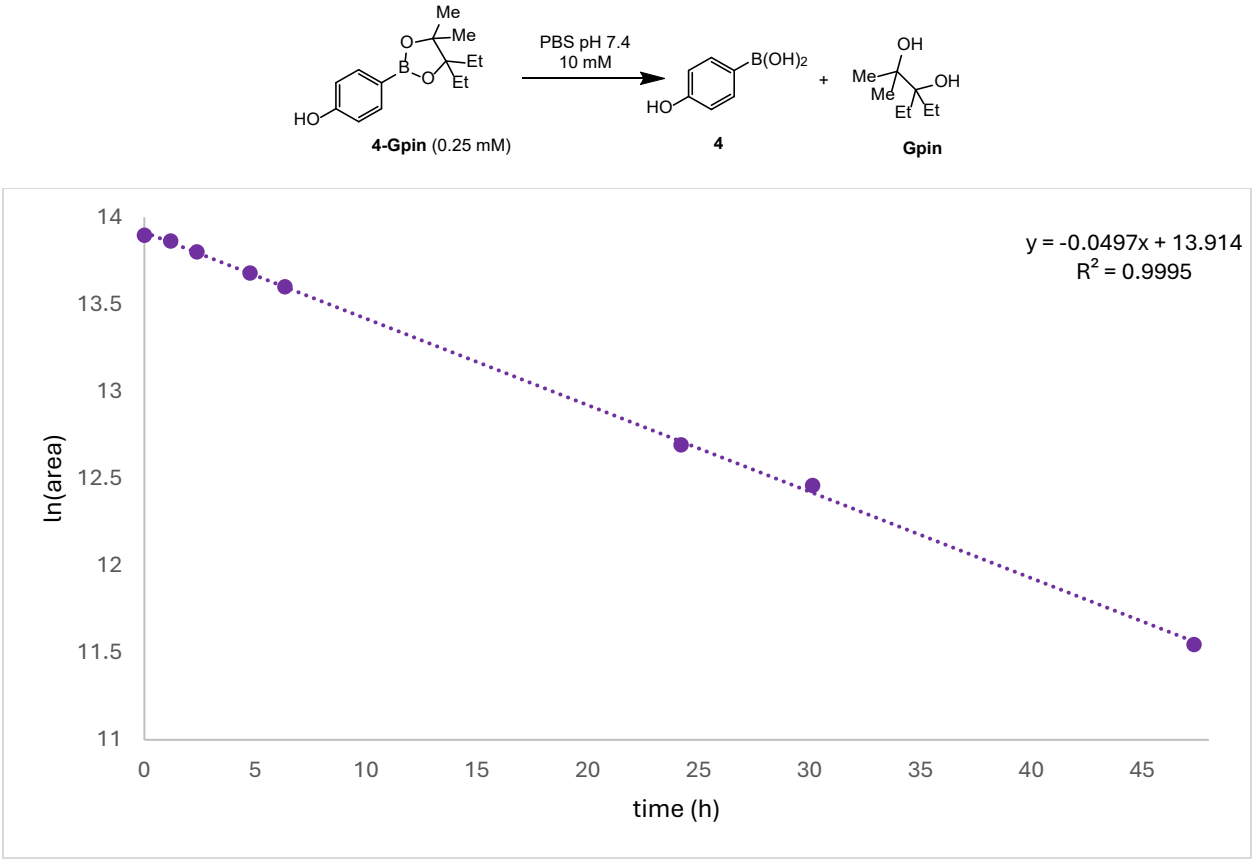

Figure S19. Plot of ln[boronic ester peak area] versus time for boronic ester **4-Gpin**. Data were fitted to a first order decay model using linear regression. The slope of the best-fit line corresponds to the pseudo-first order rate constant (k), from which the hydrolysis half-life ($t_{1/2}$) of 13.9 h was calculated.

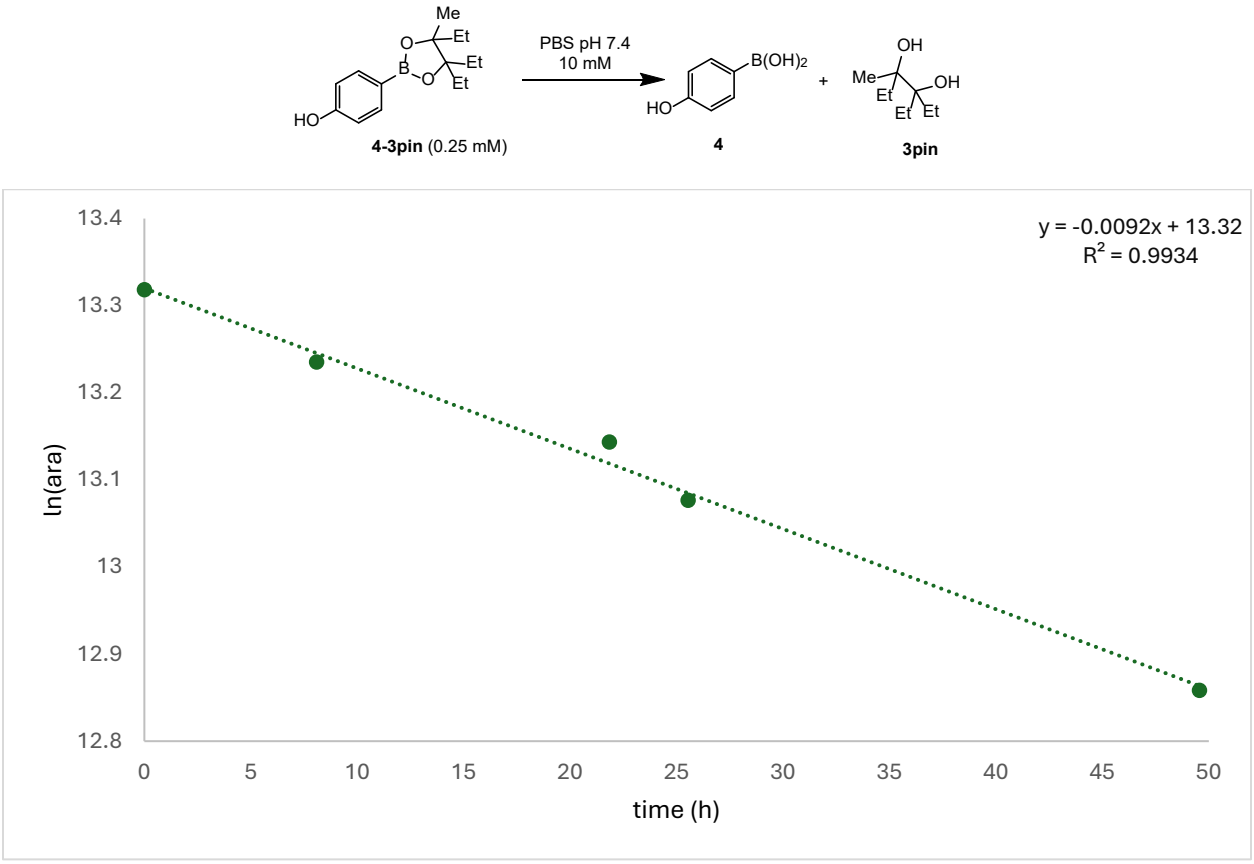

Figure S20. Plot of ln[boronic ester peak area] versus time for boronic ester **4-3pin**. Data were fitted to a first order decay model using linear regression. The slope of the best-fit line corresponds to the pseudo-first order rate constant (k), from which the hydrolysis half-life ($t_{1/2}$) of 75.3 h was calculated.

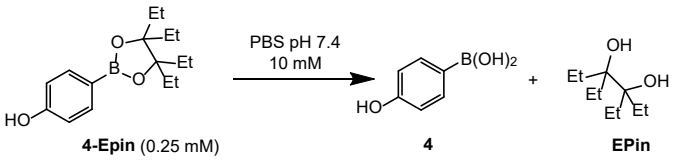

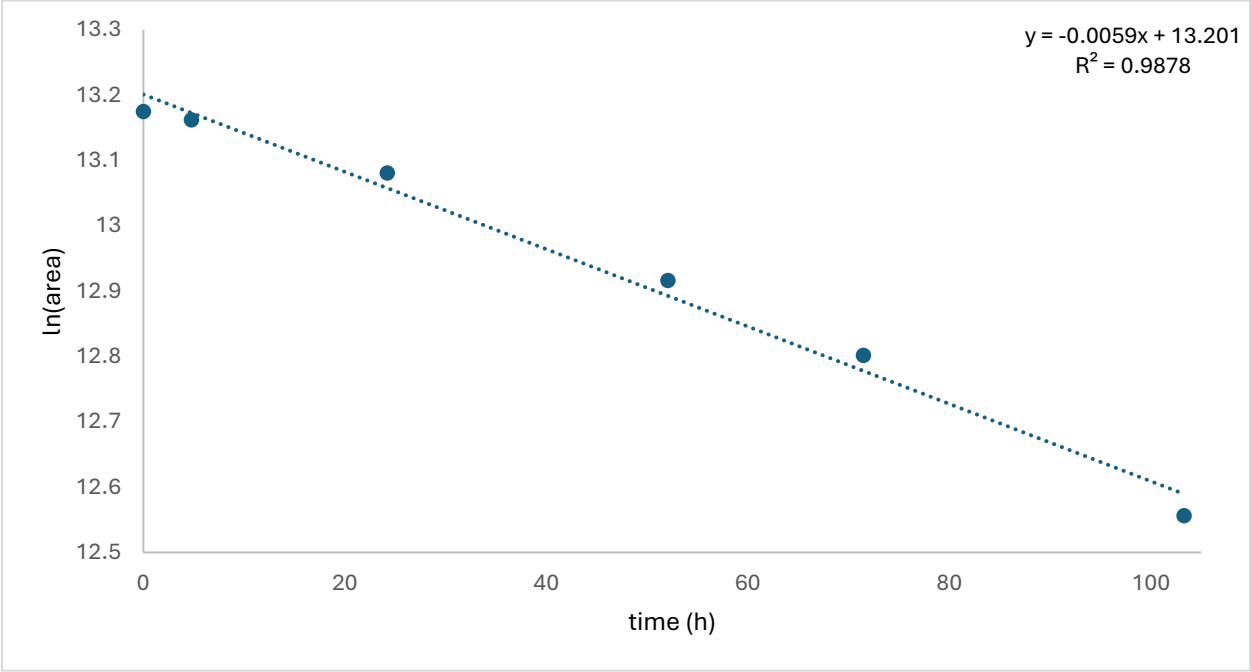

Figure S21. Plot of ln[boronic ester peak area] versus time for boronic ester **4-Epin**. Data were fitted to a first order decay model using linear regression. The slope of the best-fit line corresponds to the pseudo-first order rate constant (k), from which the hydrolysis half-life ($t_{1/2}$) of 117.5 h was calculated.

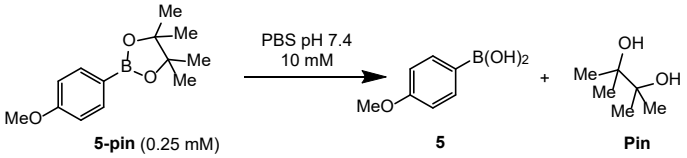

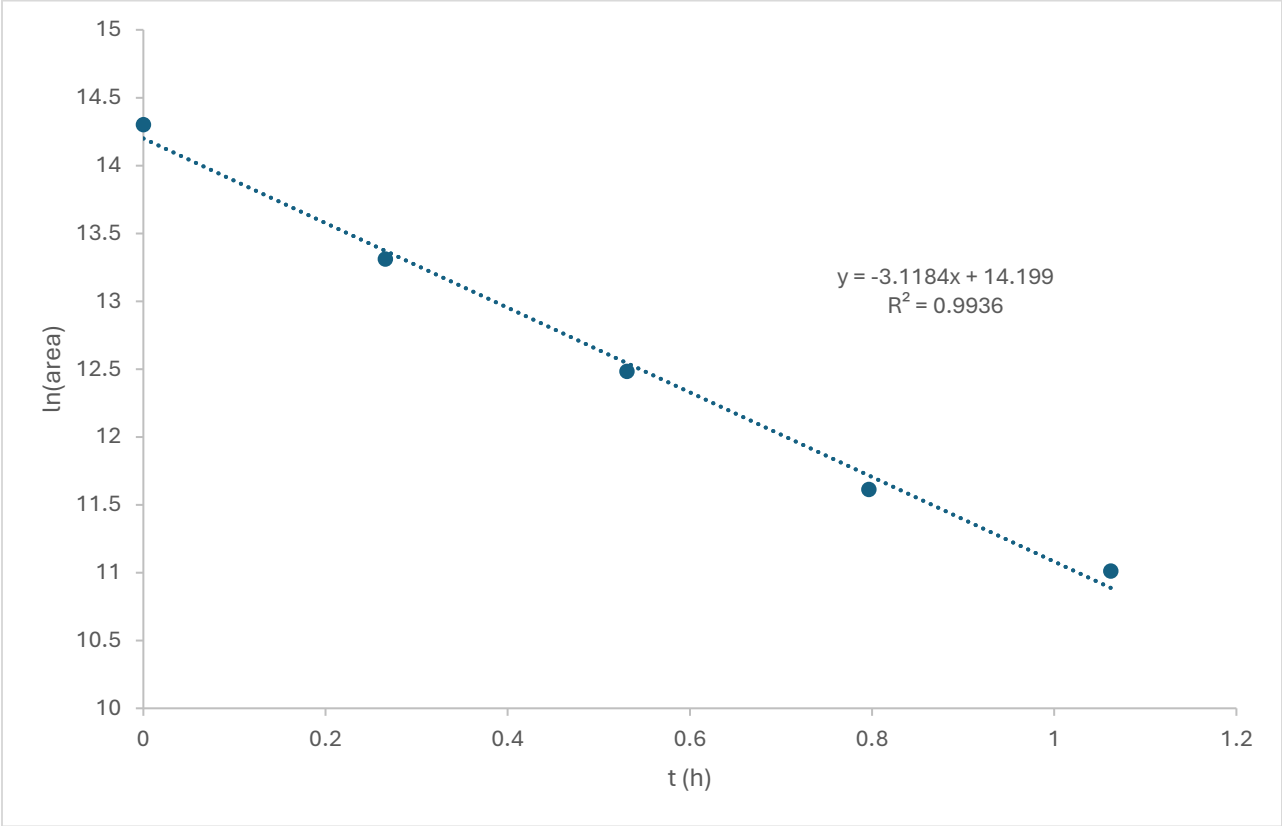

Figure S22. Plot of ln[boronic ester peak area] versus time for boronic ester **5-pin**. Data were fitted to a first order decay model using linear regression. The slope of the best-fit line corresponds to the pseudo-first order rate constant (k), from which the hydrolysis half-life ($t_{1/2}$) of 0.2 h was calculated.

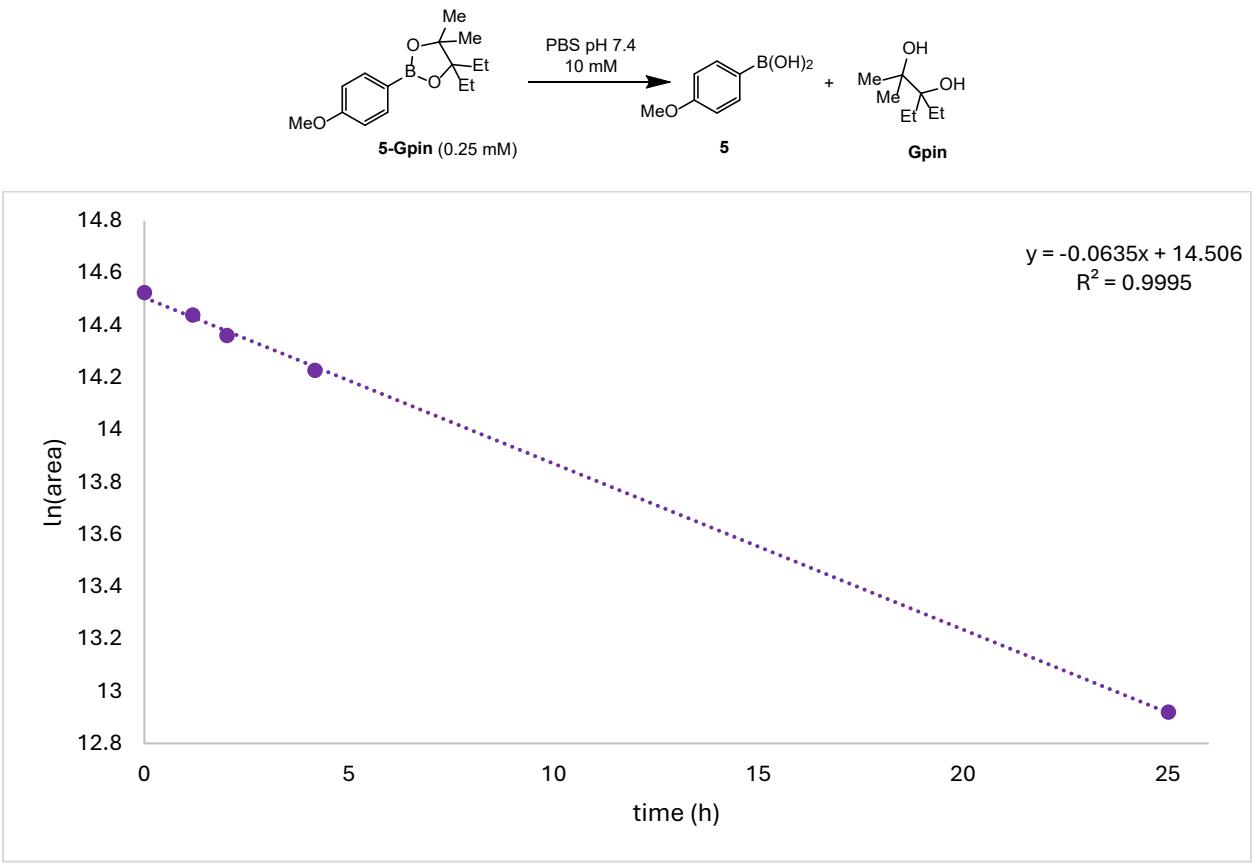

Figure S23. Plot of ln[boronic ester peak area] versus time for boronic ester **5-Gpin**. Data were fitted to a first order decay model using linear regression. The slope of the best-fit line corresponds to the pseudo-first order rate constant (k), from which the hydrolysis half-life ($t_{1/2}$) of 10.9 h was calculated.

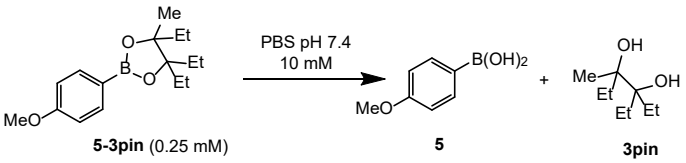

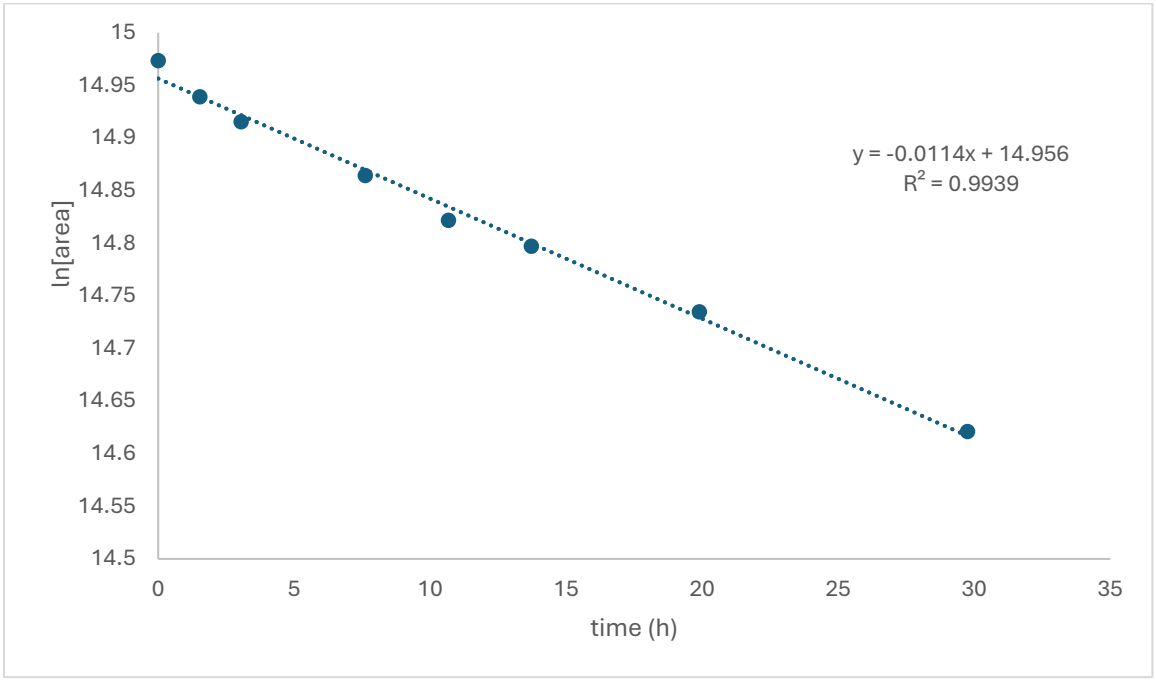

Figure S24. Plot of ln[boronic ester peak area] versus time for boronic ester **5-3pin**. Data were fitted to a first order decay model using linear regression. The slope of the best-fit line corresponds to the pseudo-first order rate constant (k), from which the hydrolysis half-life ($t_{1/2}$) of 60.8 h was calculated.

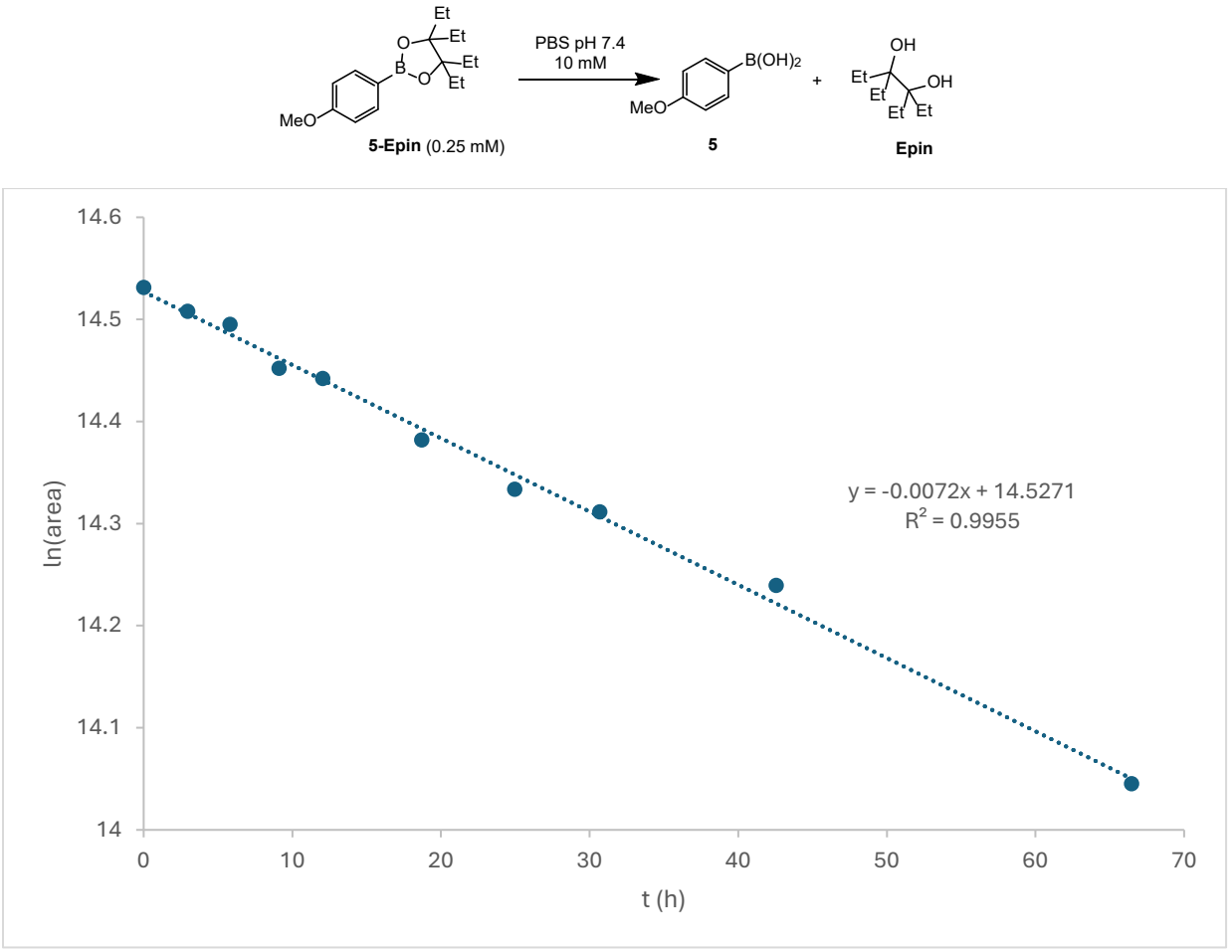

Figure S25. Plot of ln[boronic ester peak area] versus time for boronic ester **5-Epin**. Data were fitted to a first order decay model using linear regression. The slope of the best-fit line corresponds to the pseudo-first order rate constant (k), from which the hydrolysis half-life ($t_{1/2}$) of 99.0 h was calculated.

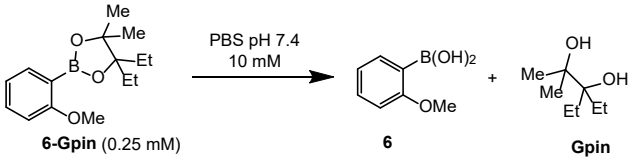

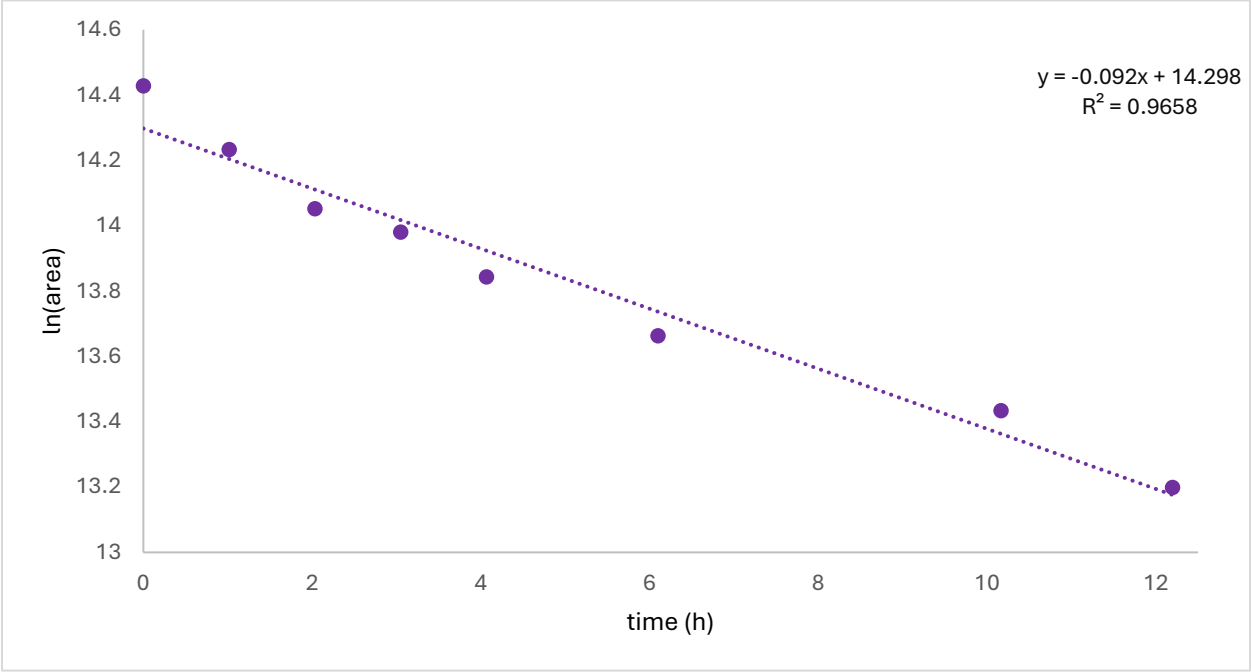

Figure S26. Plot of ln[boronic ester peak area] versus time for boronic ester **6-Gpin**. Data were fitted to a first order decay model using linear regression. The slope of the best-fit line corresponds to the pseudo-first order rate constant (k), from which the hydrolysis half-life ($t_{1/2}$) of 7.5 h was calculated.

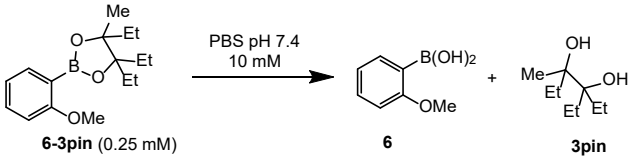

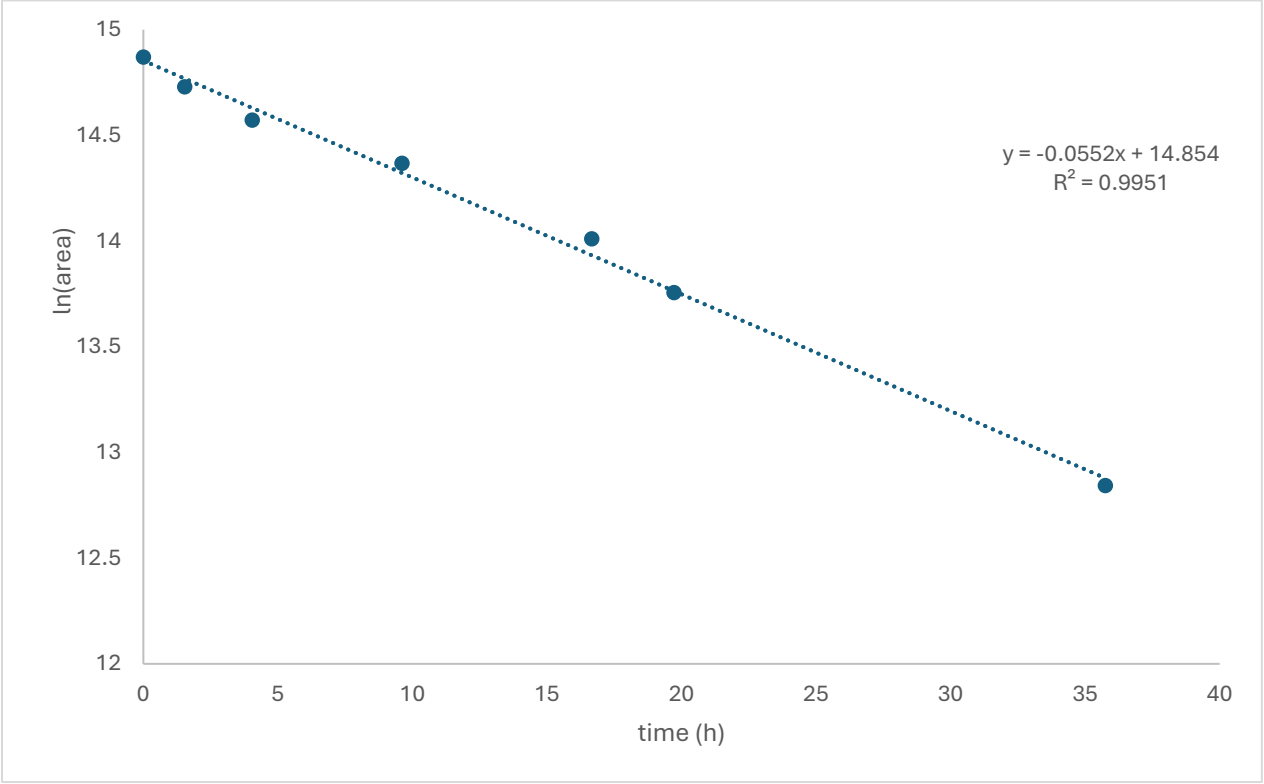

Figure S27. Plot of ln[boronic ester peak area] versus time for boronic ester **6-3pin**. Data were fitted to a first order decay model using linear regression. The slope of the best-fit line corresponds to the pseudo-first order rate constant (k), from which the hydrolysis half-life ($t_{1/2}$) of 12.6 h was calculated.

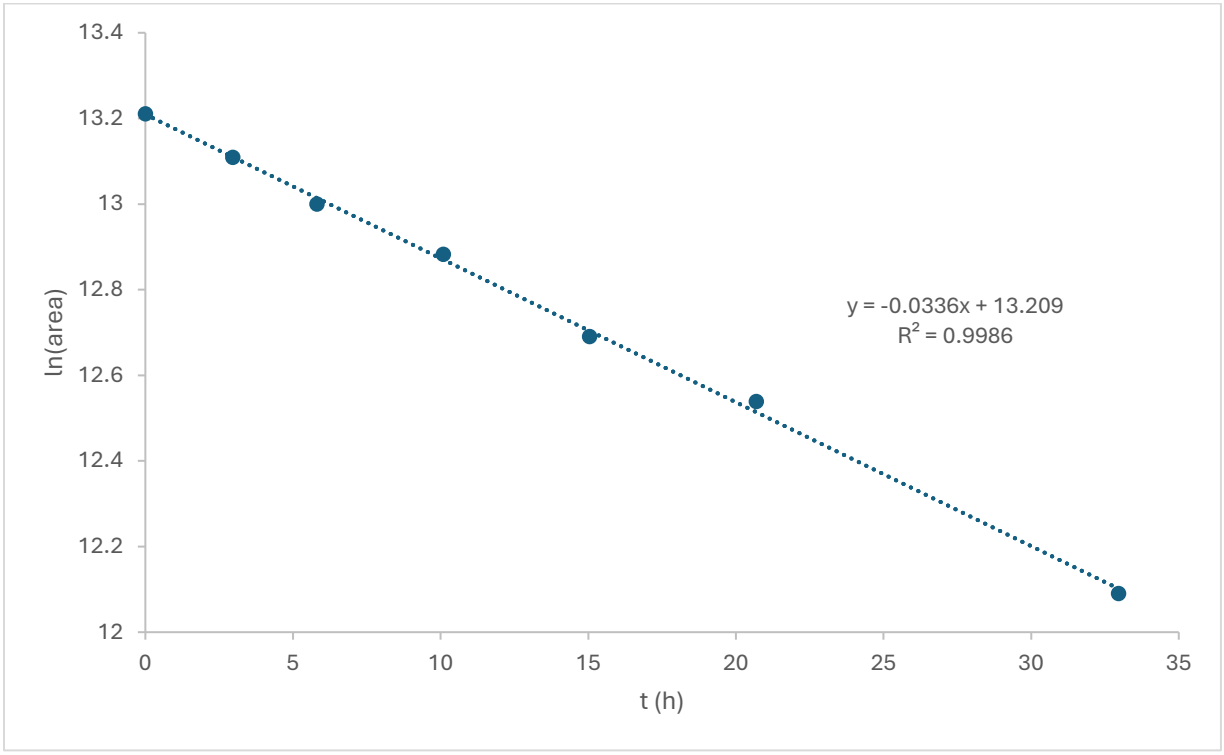

Figure S28. Plot of ln[boronic ester peak area] versus time for boronic ester **6-Epin**. Data were fitted to a first order decay model using linear regression. The slope of the best-fit line corresponds to the pseudo-first order rate constant (k), from which the hydrolysis half-life ($t_{1/2}$) of 21.3 h was calculated.

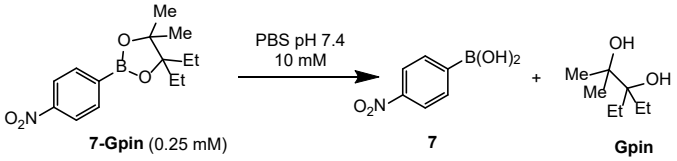

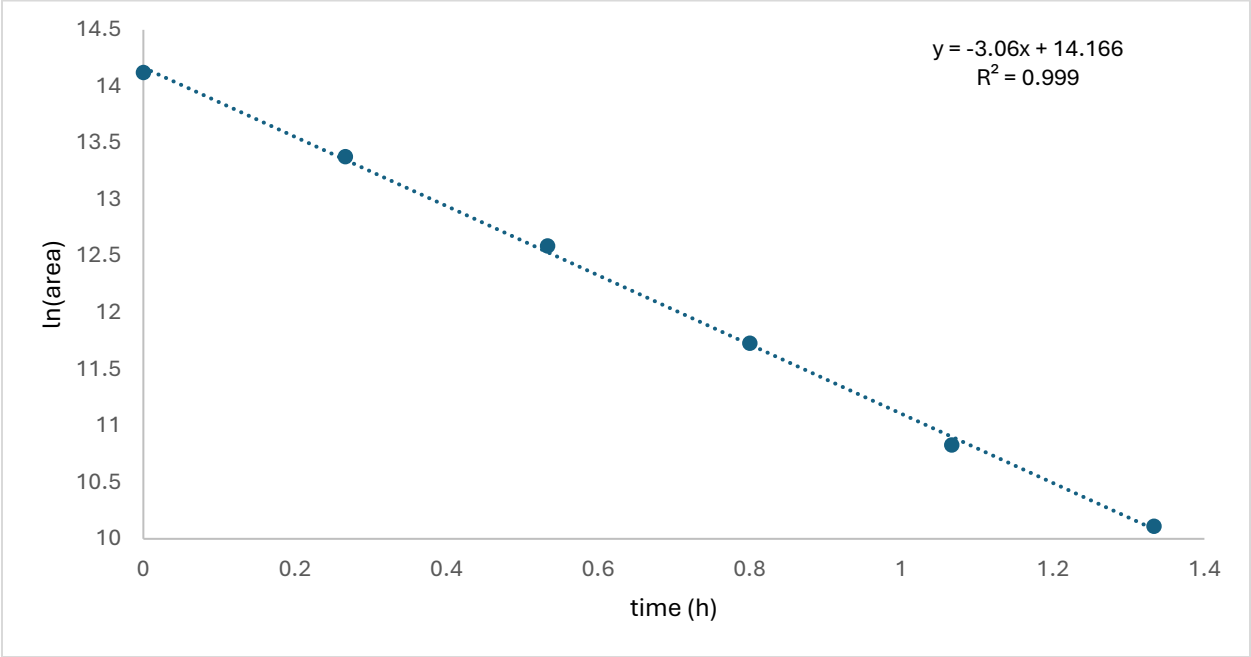

Figure S29. Plot of ln[boronic ester peak area] versus time for boronic ester **7-Gpin**. Data were fitted to a first order decay model using linear regression. The slope of the best-fit line corresponds to the pseudo-first order rate constant (k), from which the hydrolysis half-life ($t_{1/2}$) of 0.2 h was calculated.

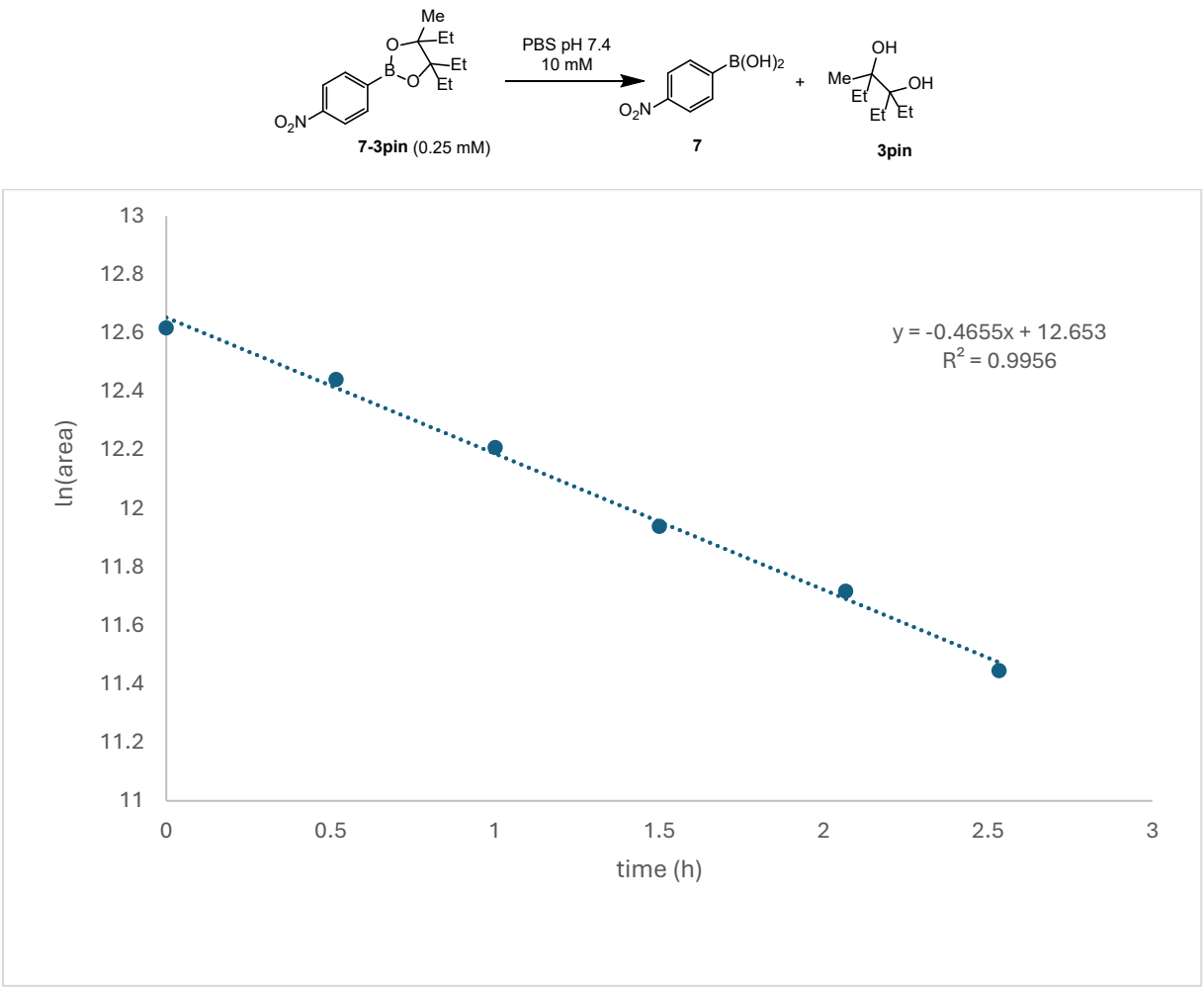

Figure S30. Plot of ln[boronic ester peak area] versus time for boronic ester **7-3pin**. Data were fitted to a first order decay model using linear regression. The slope of the best-fit line corresponds to the pseudo-first order rate constant (k), from which the hydrolysis half-life ($t_{1/2}$) of 1.5 h was calculated.

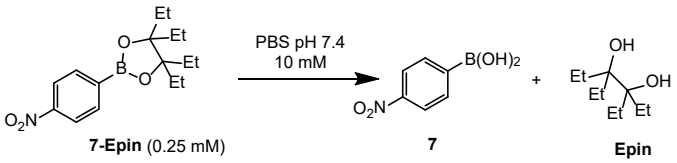

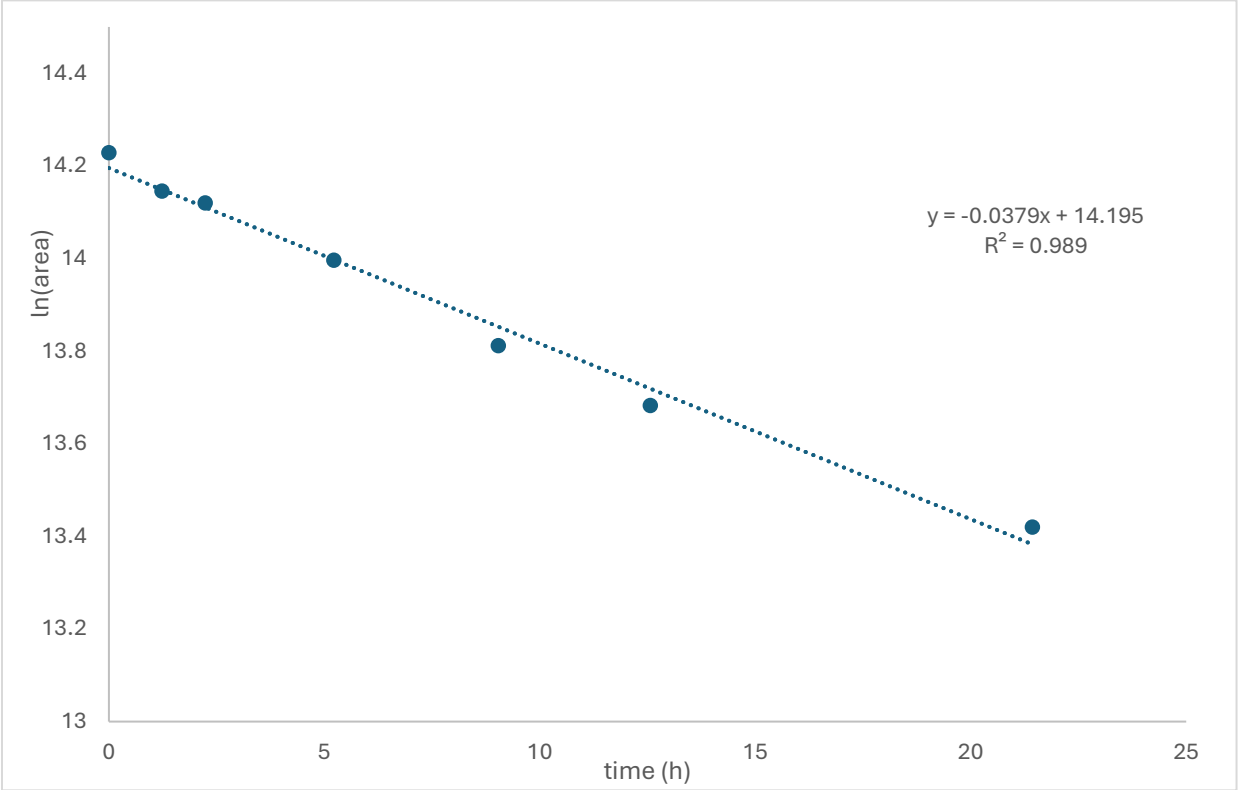

Figure S31. Plot of ln[boronic ester peak area] versus time for boronic ester **7-Epin**. Data were fitted to a first order decay model using linear regression. The slope of the best-fit line corresponds to the pseudo-first order rate constant (k), from which the hydrolysis half-life ($t_{1/2}$) of 18.2 h was calculated.

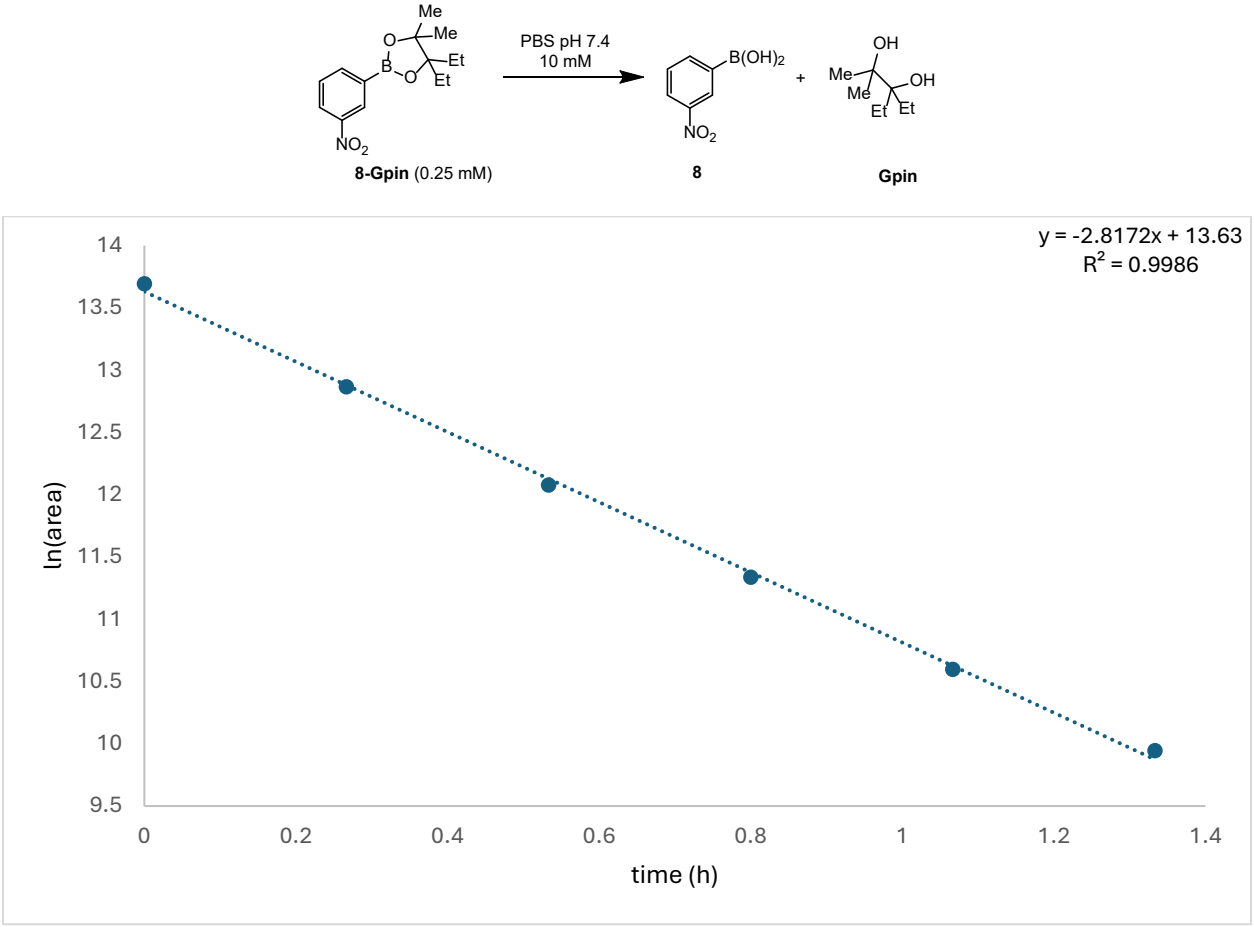

Figure S32. Plot of ln[boronic ester peak area] versus time for boronic ester **8-Gpin**. Data were fitted to a first order decay model using linear regression. The slope of the best-fit line corresponds to the pseudo-first order rate constant (k), from which the hydrolysis half-life ($t_{1/2}$) of 0.3 h was calculated.

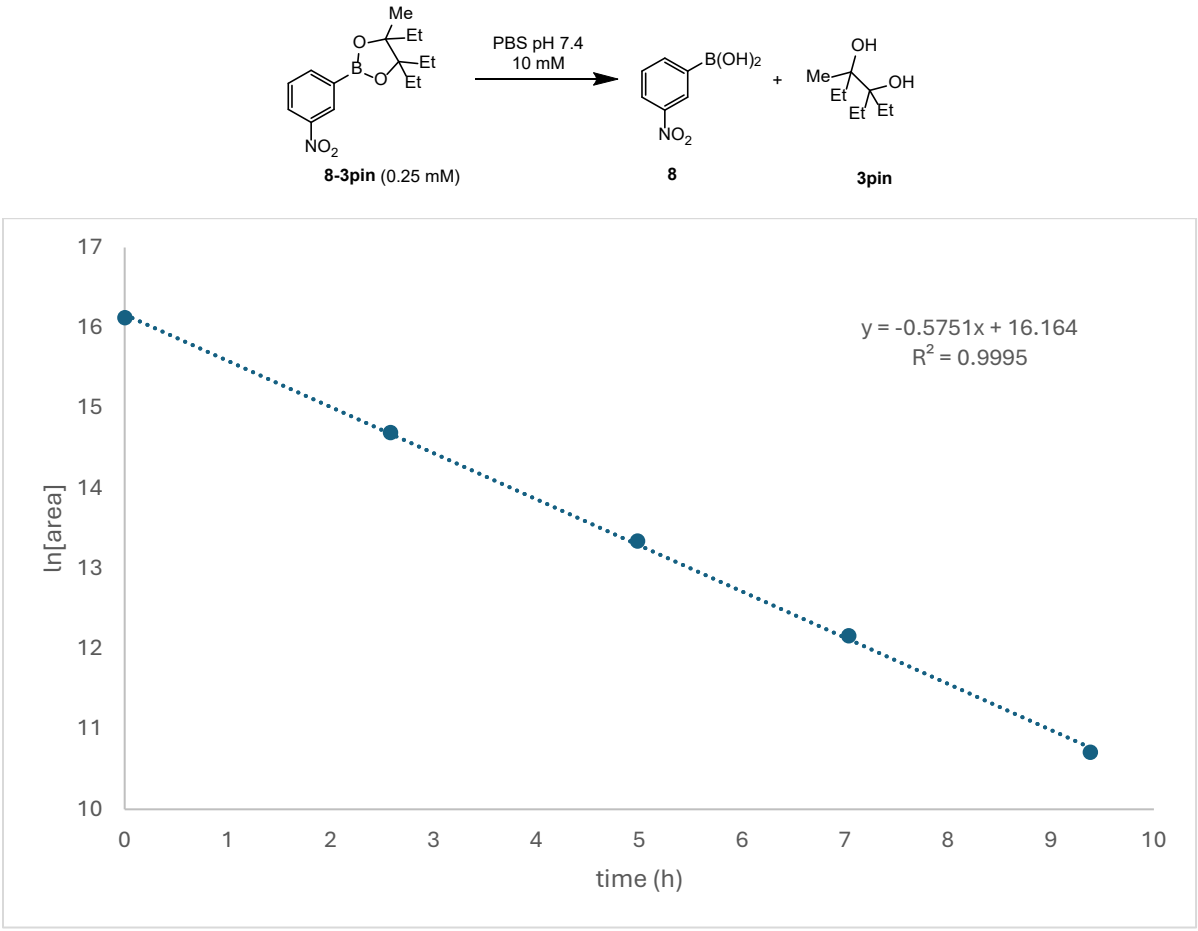

Figure S33. Plot of ln[boronic ester peak area] versus time for boronic ester **8-3pin**. Data were fitted to a first order decay model using linear regression. The slope of the best-fit line corresponds to the pseudo-first order rate constant (k), from which the hydrolysis half-life ($t_{1/2}$) of 1.2 h was calculated.

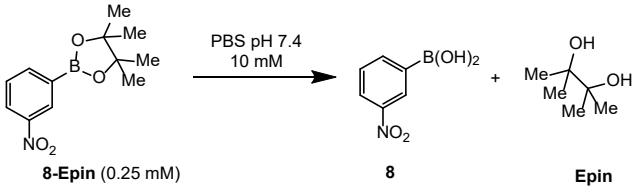

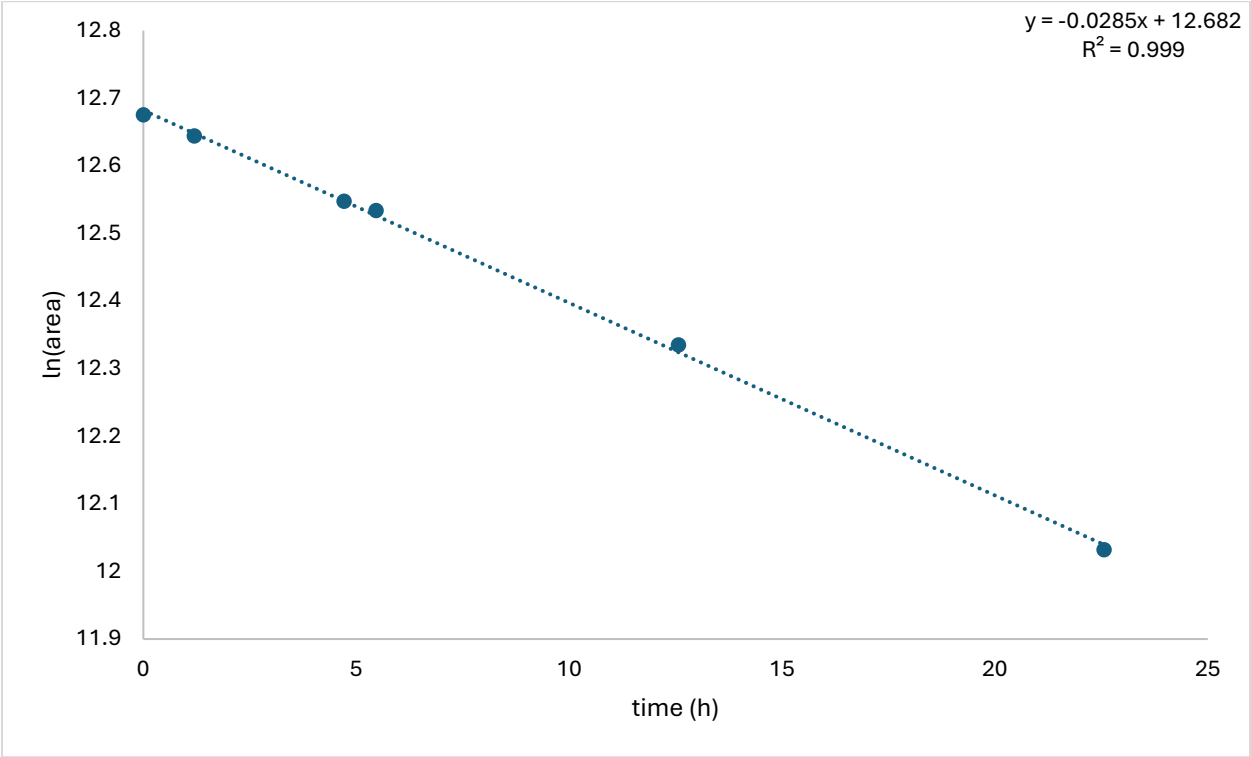

Figure S34. Plot of ln[boronic ester peak area] versus time for boronic ester **8-Epin**. Data were fitted to a first order decay model using linear regression. The slope of the best-fit line corresponds to the pseudo-first order rate constant (k), from which the hydrolysis half-life ($t_{1/2}$) of 24.3 h was calculated.

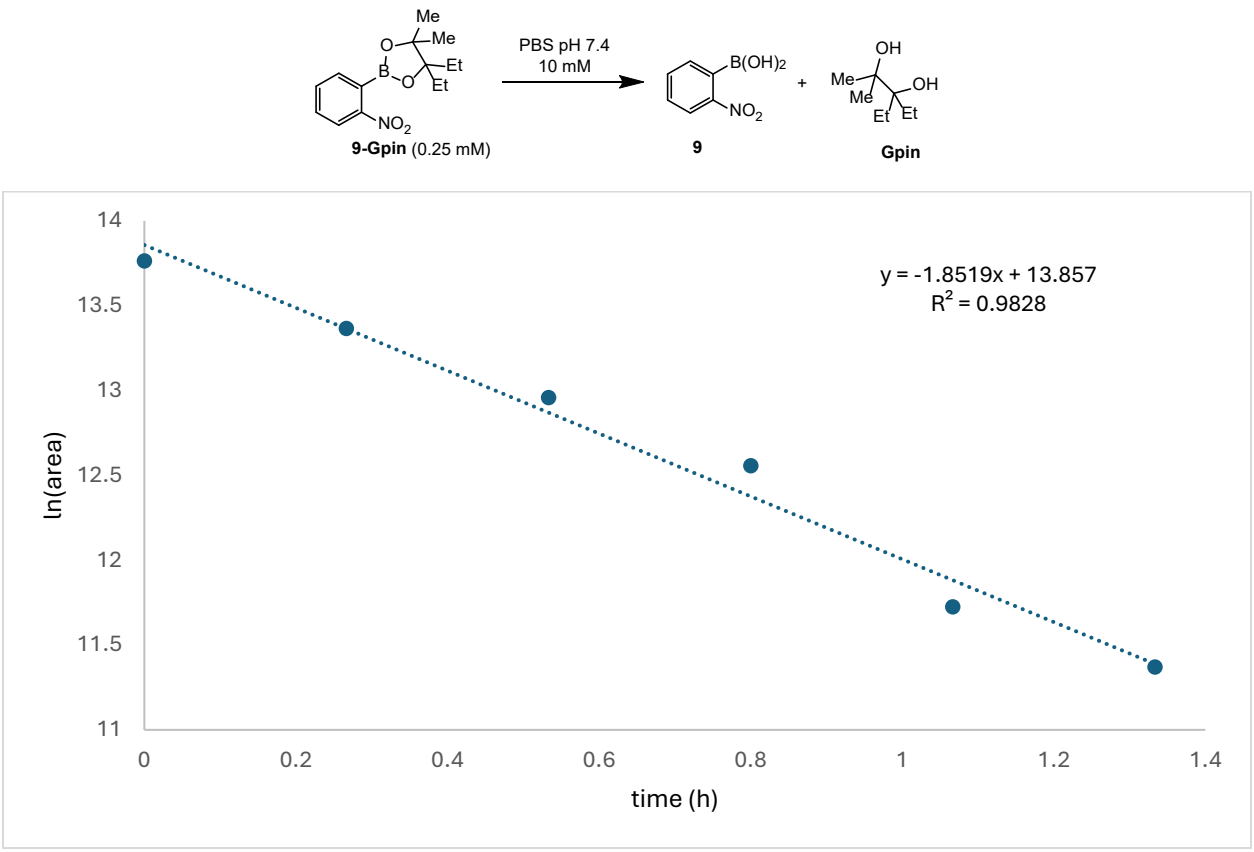

Figure S35. Plot of ln[boronic ester peak area] versus time for boronic ester **9-Gpin**. Data were fitted to a first order decay model using linear regression. The slope of the best-fit line corresponds to the pseudo-first order rate constant (k), from which the hydrolysis half-life ($t_{1/2}$) of 0.4 h was calculated.

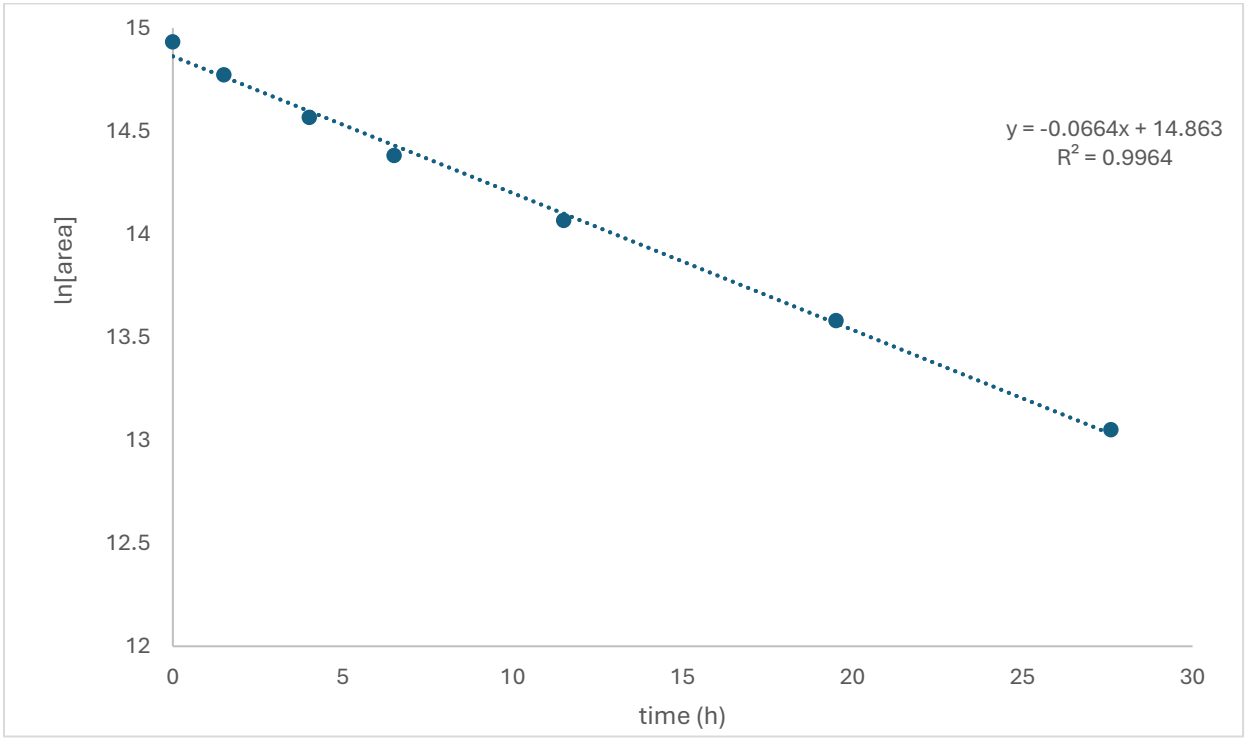

Figure S36. Plot of ln[boronic ester peak area] versus time for boronic ester **9-3pin**. Data were fitted to a first order decay model using linear regression. The slope of the best-fit line corresponds to the pseudo-first order rate constant (k), from which the hydrolysis half-life ($t_{1/2}$) of 10.4 h was calculated.

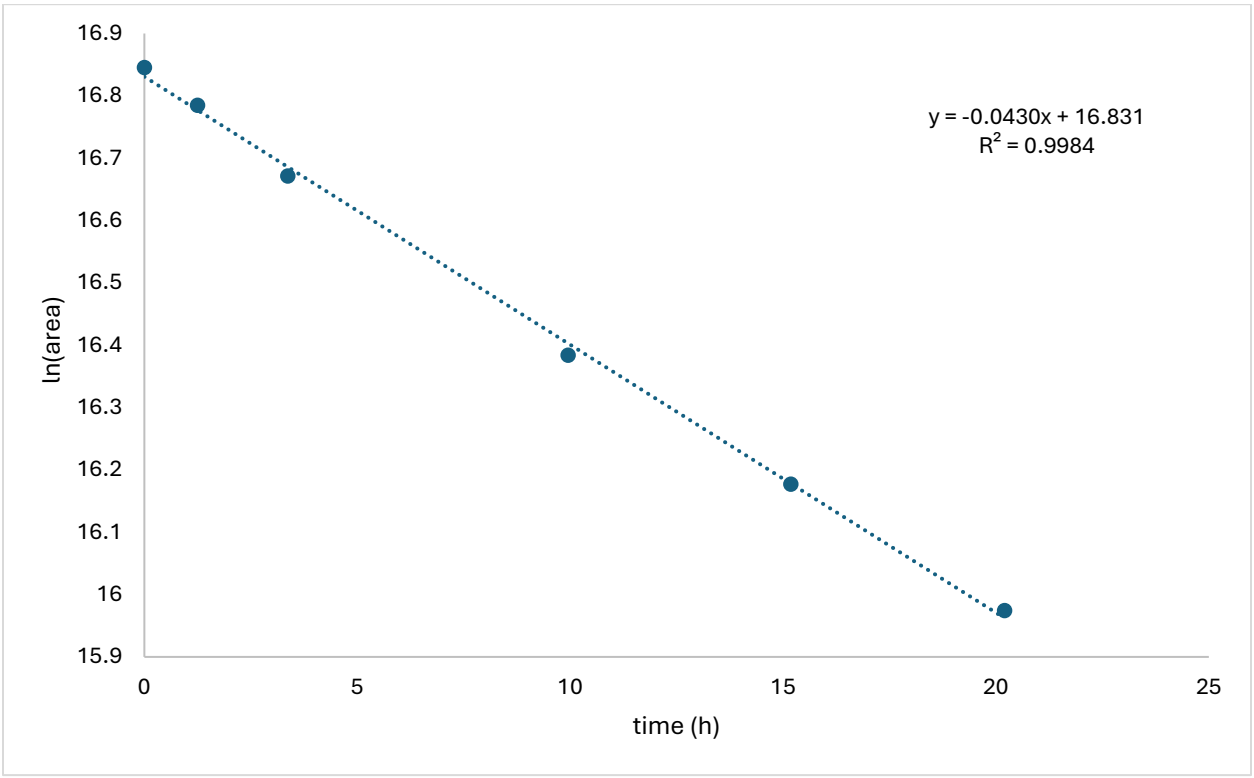

Figure S37. Plot of ln[boronic ester peak area] versus time for boronic ester **9-Epin**. Data were fitted to a first order decay model using linear regression. The slope of the best-fit line corresponds to the pseudo-first order rate constant (k), from which the hydrolysis half-life ($t_{1/2}$) of 16.1 h was calculated.

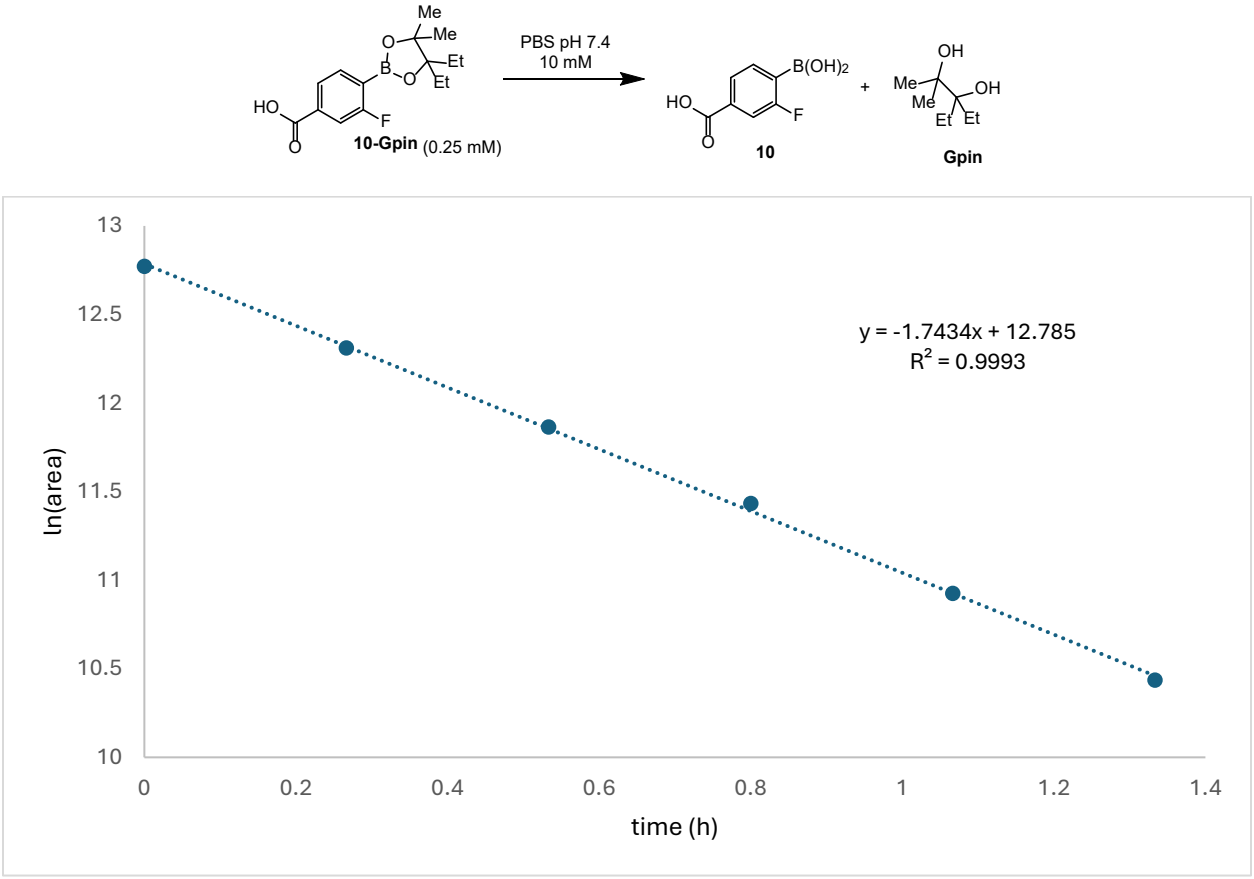

Figure S38. Plot of ln[boronic ester peak area] versus time for boronic ester **10-Gpin**. Data were fitted to a first order decay model using linear regression. The slope of the best-fit line corresponds to the pseudo-first order rate constant (k), from which the hydrolysis half-life ($t_{1/2}$) of 0.4 h was calculated.

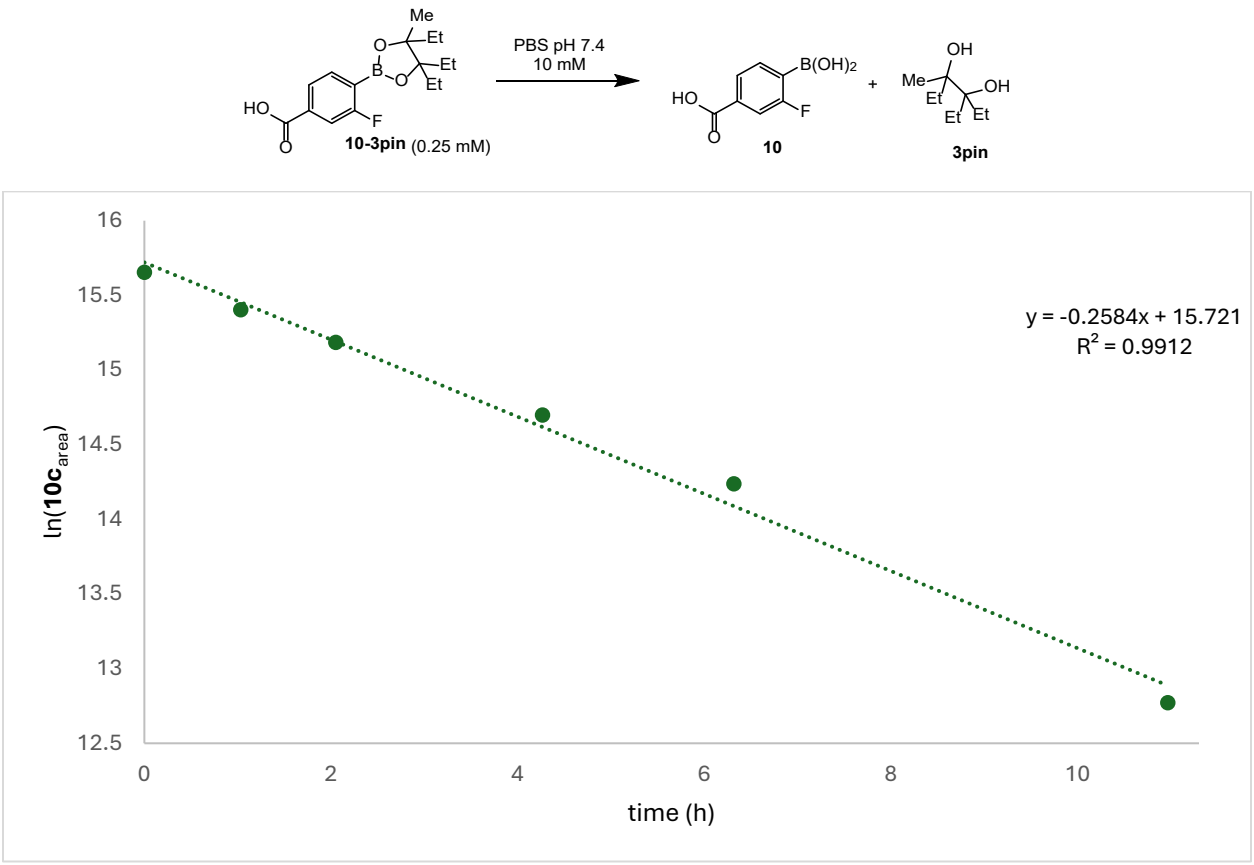

Figure S39. Plot of ln[boronic ester peak area] versus time for boronic ester **10-3pin**. Data were fitted to a first order decay model using linear regression. The slope of the best-fit line corresponds to the pseudo-first order rate constant (k), from which the hydrolysis half-life ($t_{1/2}$) of 2.7 h was calculated.

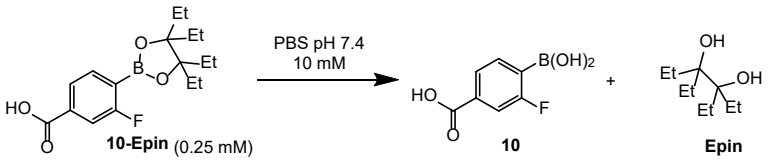

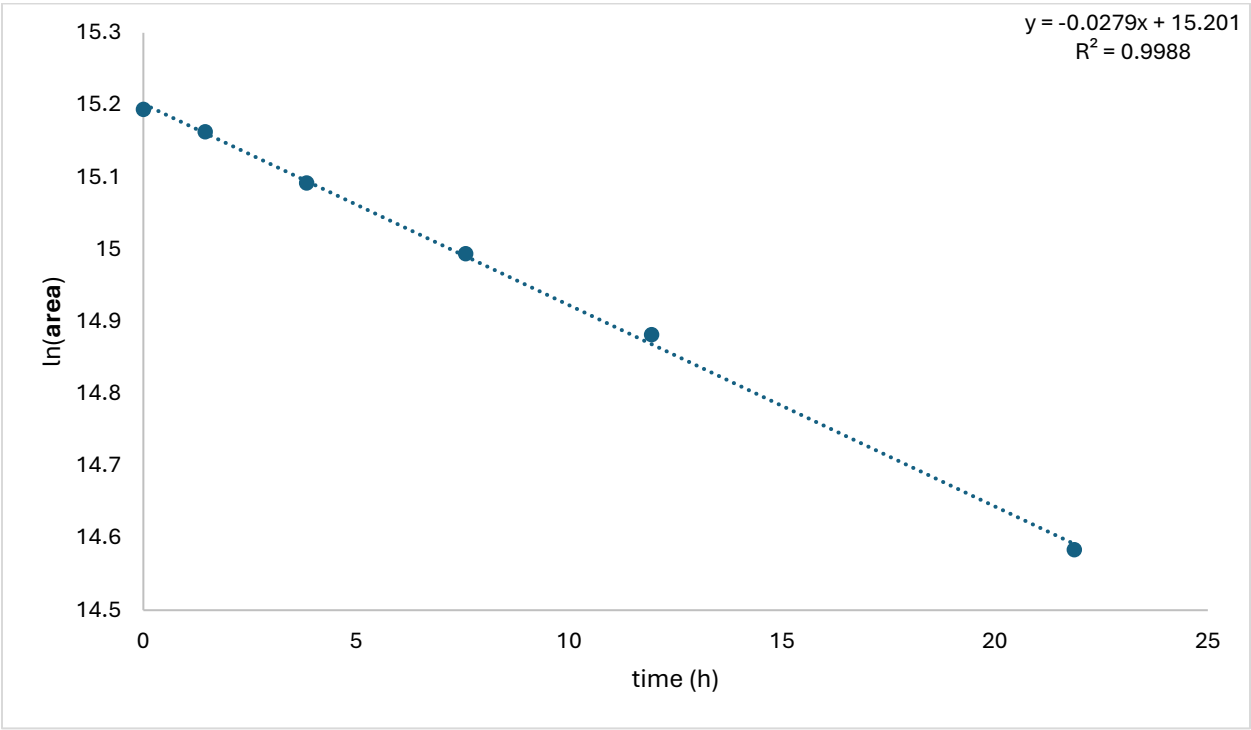

Figure S40. Plot of ln[boronic ester peak area] versus time for boronic ester **10-Epin**. Data were fitted to a first order decay model using linear regression. The slope of the best-fit line corresponds to the pseudo-first order rate constant (k), from which the hydrolysis half-life ($t_{1/2}$) of 24.8 h was calculated.

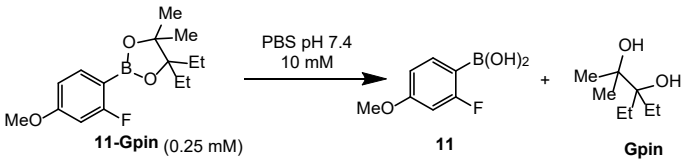

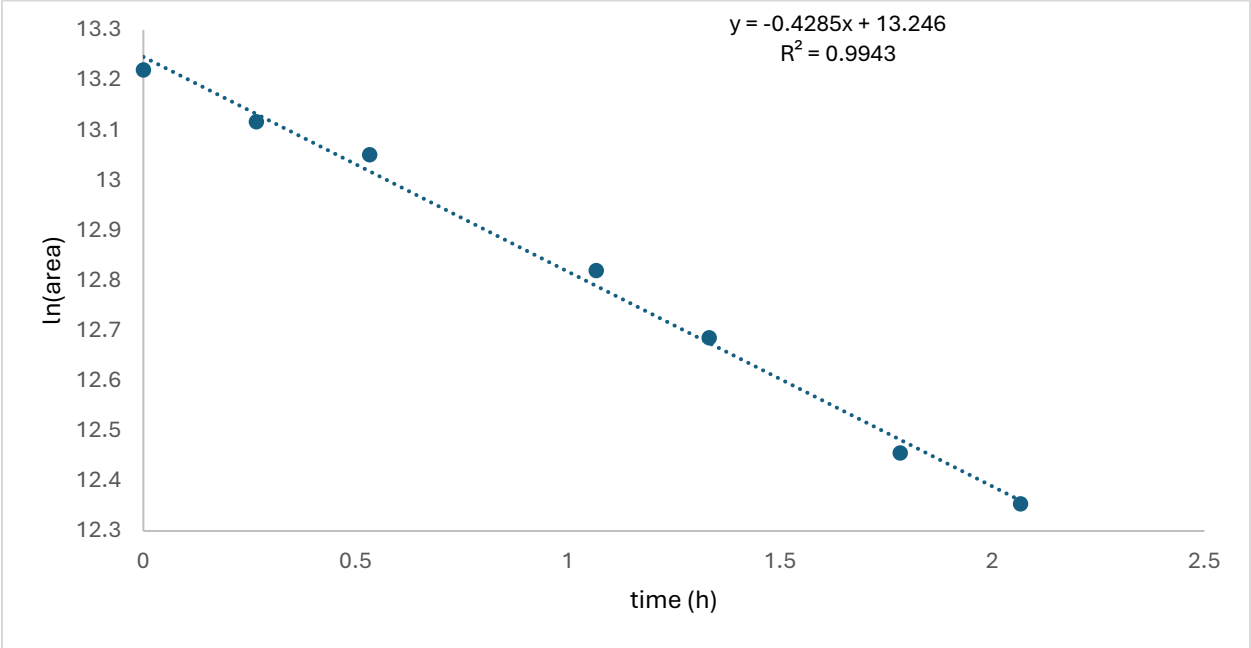

Figure S41. Plot of ln[boronic ester peak area] versus time for boronic ester **11-Gpin**. Data were fitted to a first order decay model using linear regression. The slope of the best-fit line corresponds to the pseudo-first order rate constant (k), from which the hydrolysis half-life ($t_{1/2}$) of 1.6 h was calculated.

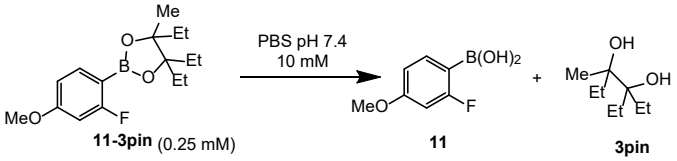

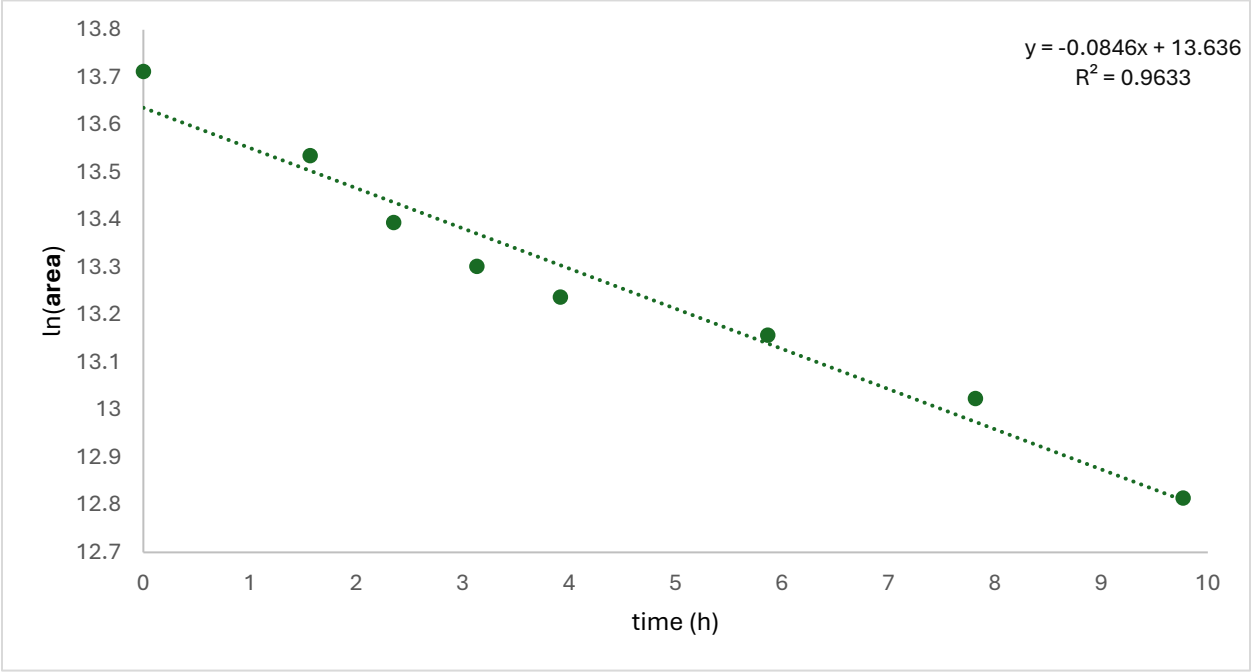

Figure S42. Plot of ln[boronic ester peak area] versus time for boronic ester **11-3pin**. Data were fitted to a first order decay model using linear regression. The slope of the best-fit line corresponds to the pseudo-first order rate constant (k), from which the hydrolysis half-life ($t_{1/2}$) of 8.2 h was calculated.

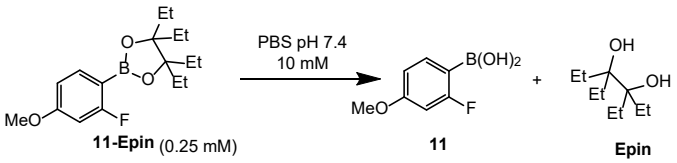

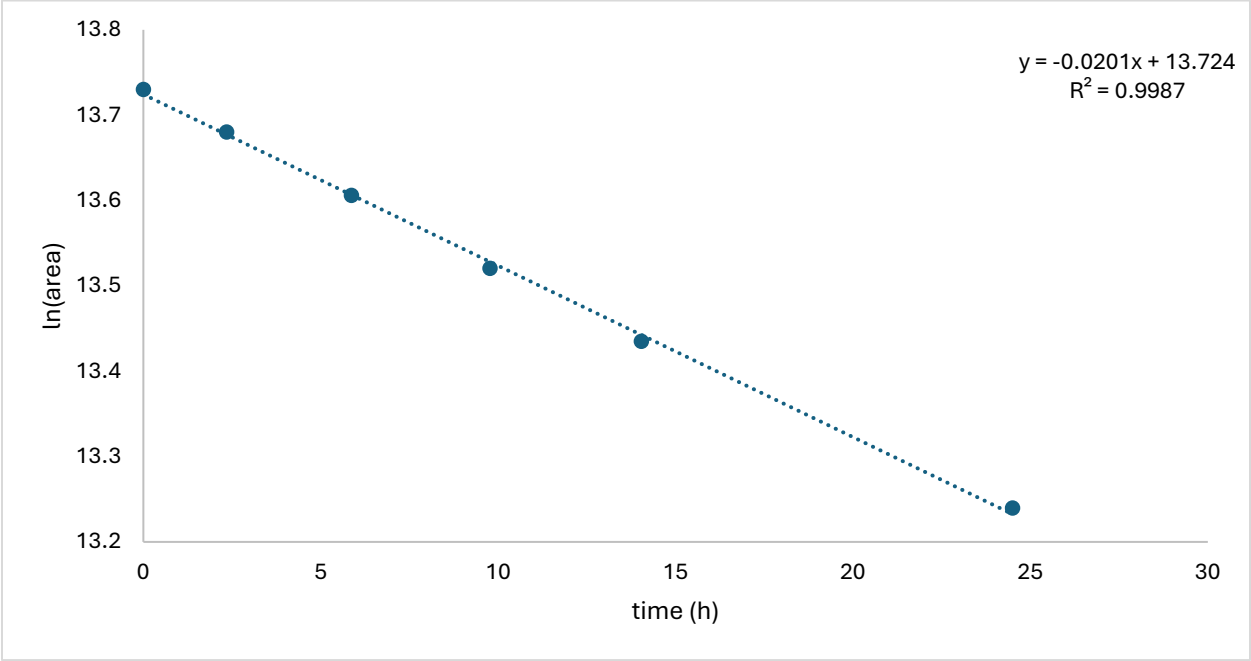

Figure S43. Plot of ln[boronic ester peak area] versus time for boronic ester **11-Epin**. Data were fitted to a first order decay model using linear regression. The slope of the best-fit line corresponds to the pseudo-first order rate constant (k), from which the hydrolysis half-life ($t_{1/2}$) of 34.5 h was calculated.

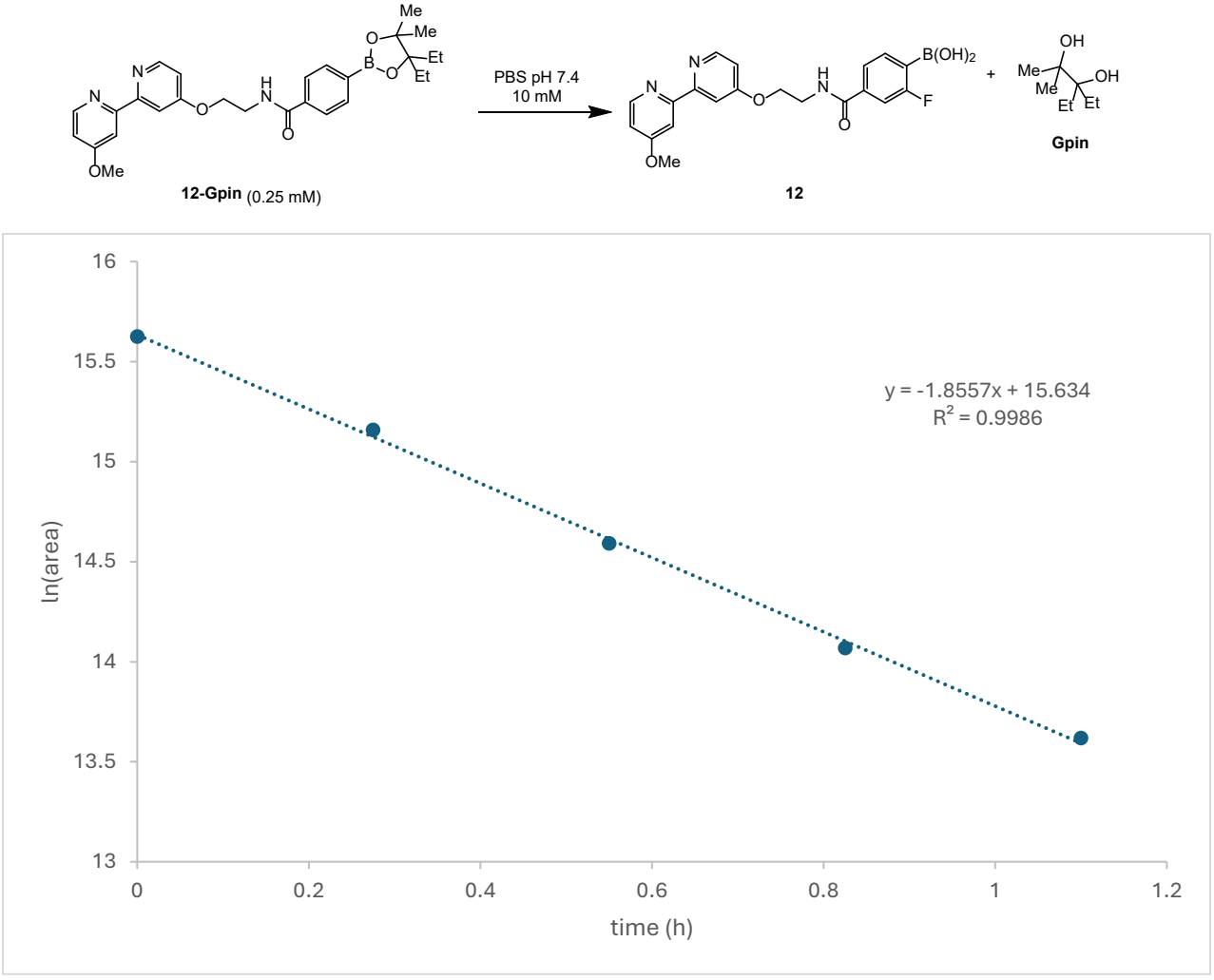

Figure S44. Plot of ln[boronic ester peak area] versus time for boronic ester **12-Gpin**. Data were fitted to a first order decay model using linear regression. The slope of the best-fit line corresponds to the pseudo-first order rate constant (k), from which the hydrolysis half-life ($t_{1/2}$) of 0.4 h was calculated.

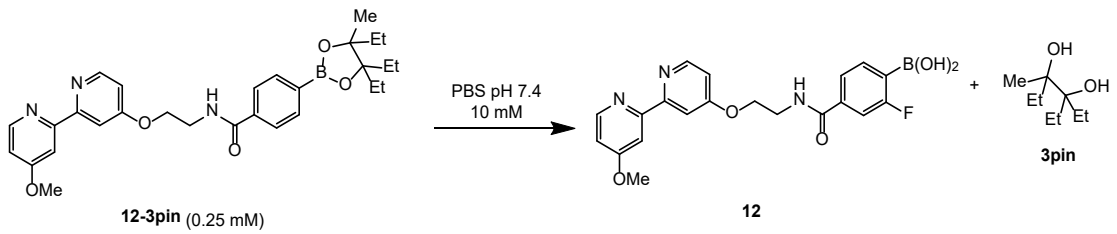

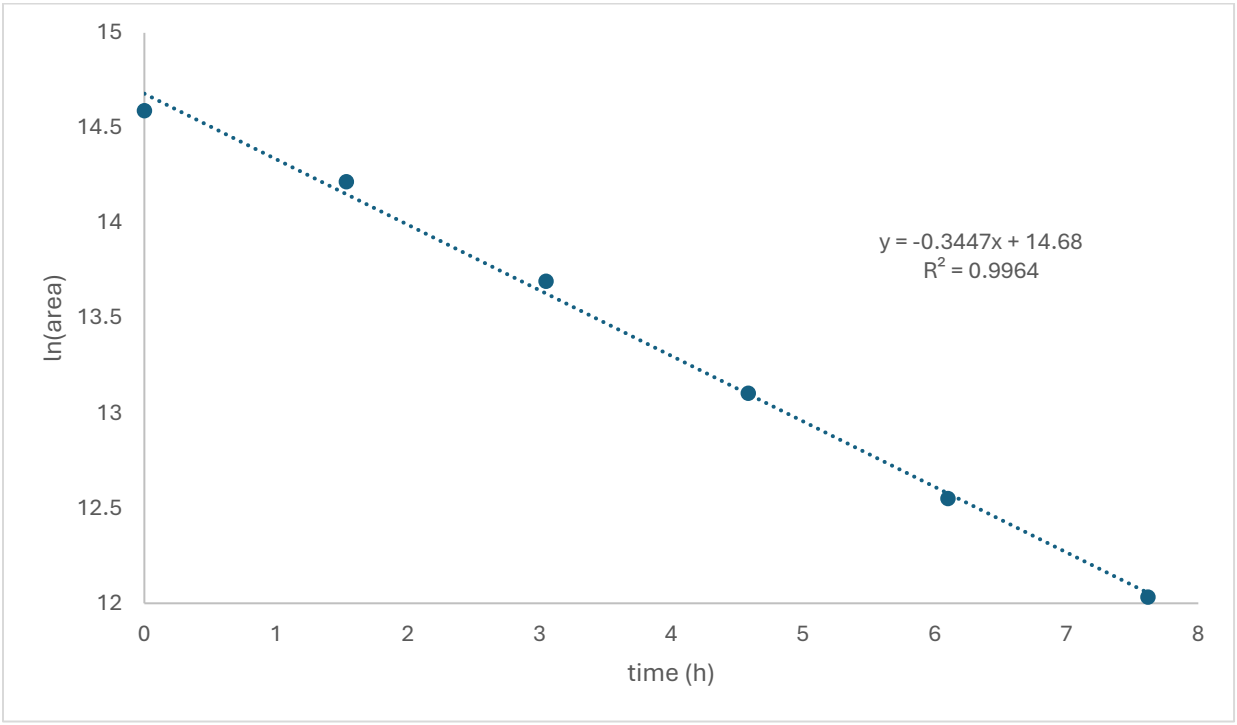

Figure S45. Plot of ln[boronic ester peak area] versus time for boronic ester **12-3pin**. Data were fitted to a first order decay model using linear regression. The slope of the best-fit line corresponds to the pseudo-first order rate constant (k), from which the hydrolysis half-life ($t_{1/2}$) of 2.0 h was calculated.

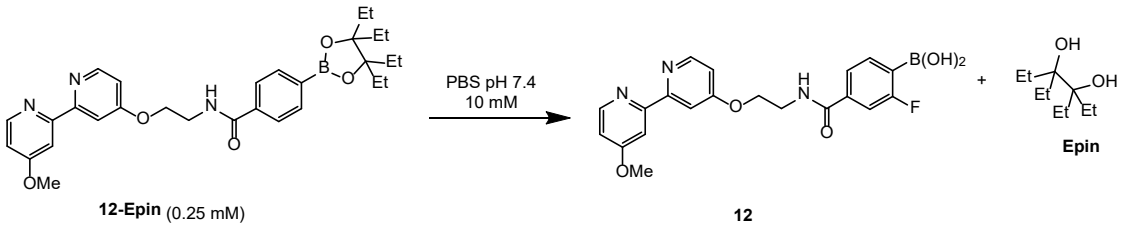

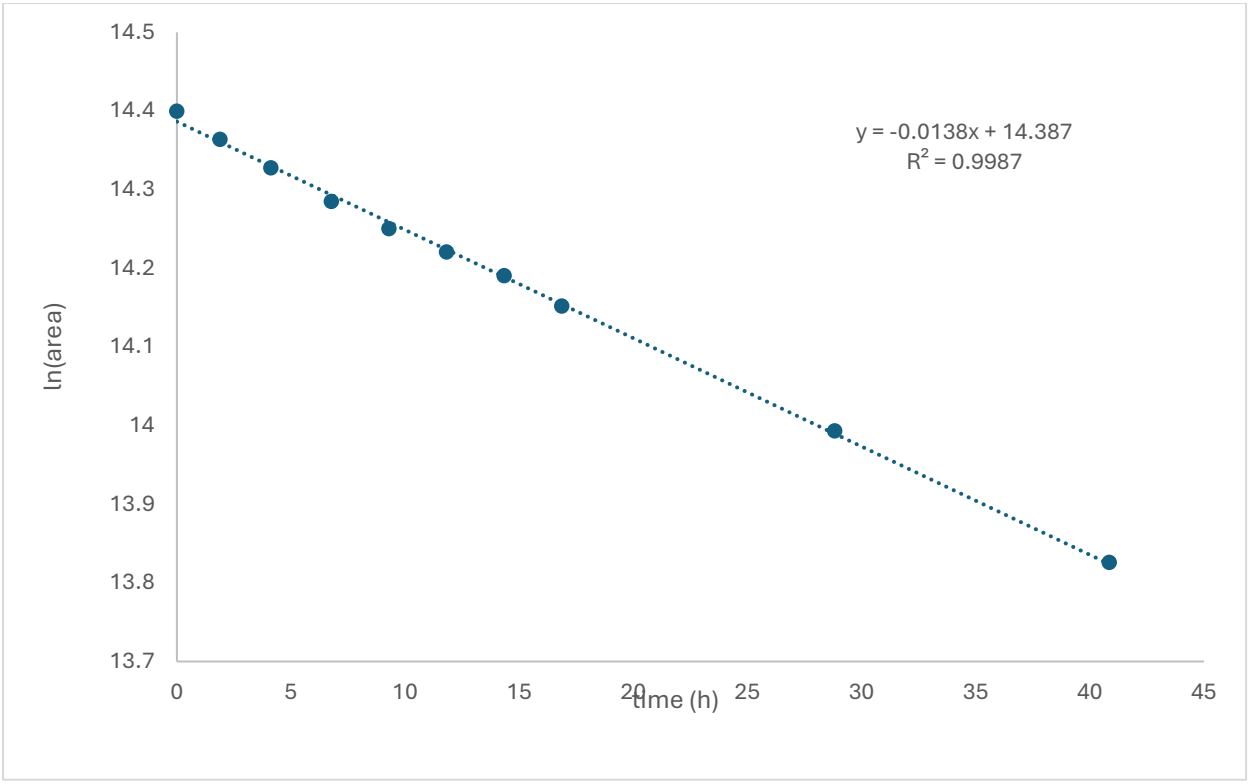

Figure S46. Plot of ln[boronic ester peak area] versus time for boronic ester **12-Epin**. Data were fitted to a first order decay model using linear regression. The slope of the best-fit line corresponds to the pseudo-first order rate constant (k), from which the hydrolysis half-life ($t_{1/2}$) of 50.0 h was calculated.

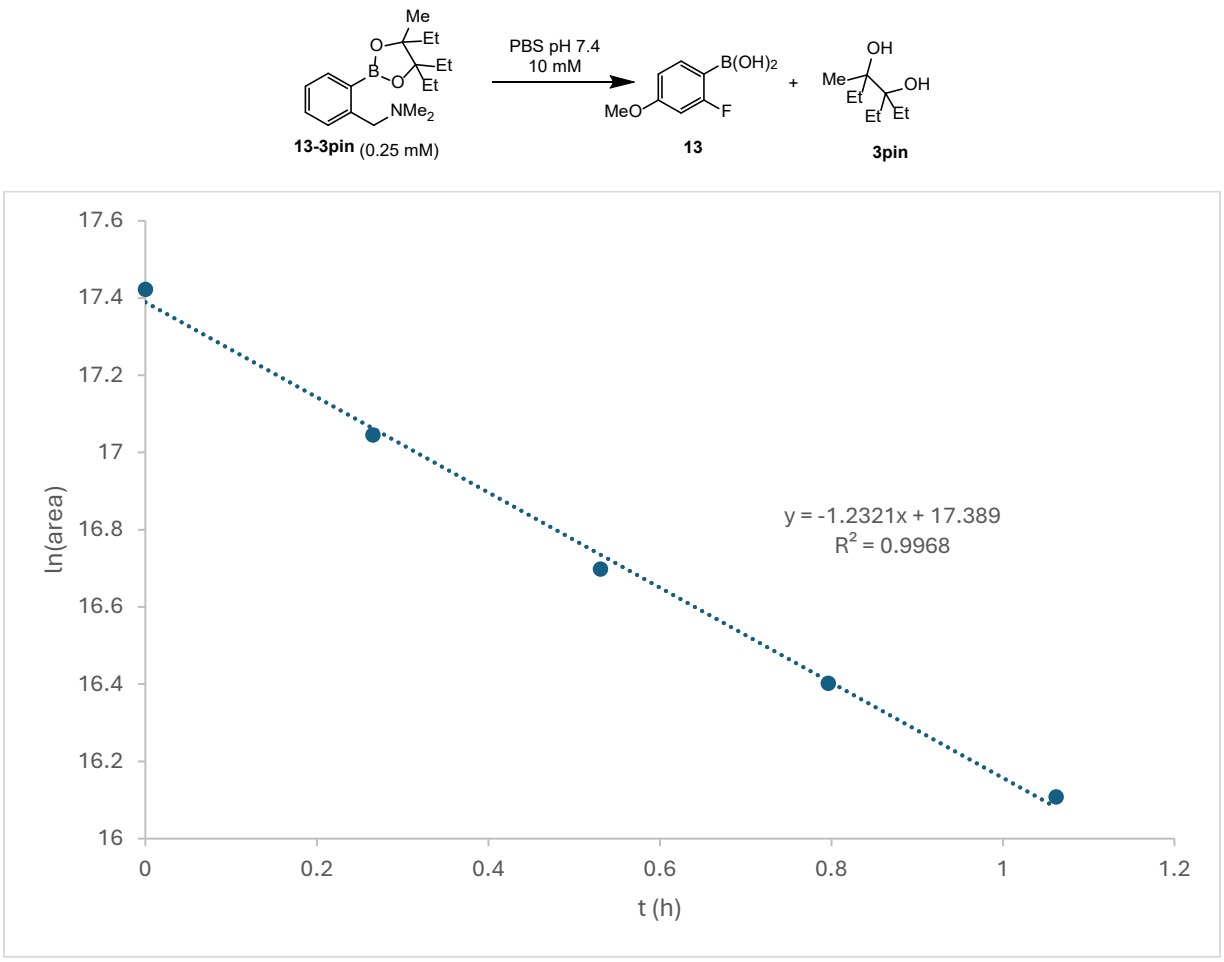

Figure S47. Plot of ln[boronic ester peak area] versus time for boronic ester **13-3pin**. Data were fitted to a first order decay model using linear regression. The slope of the best-fit line corresponds to the pseudo-first order rate constant (k), from which the hydrolysis half-life ($t_{1/2}$) of 0.6 h was calculated.

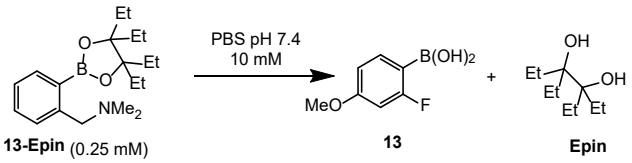

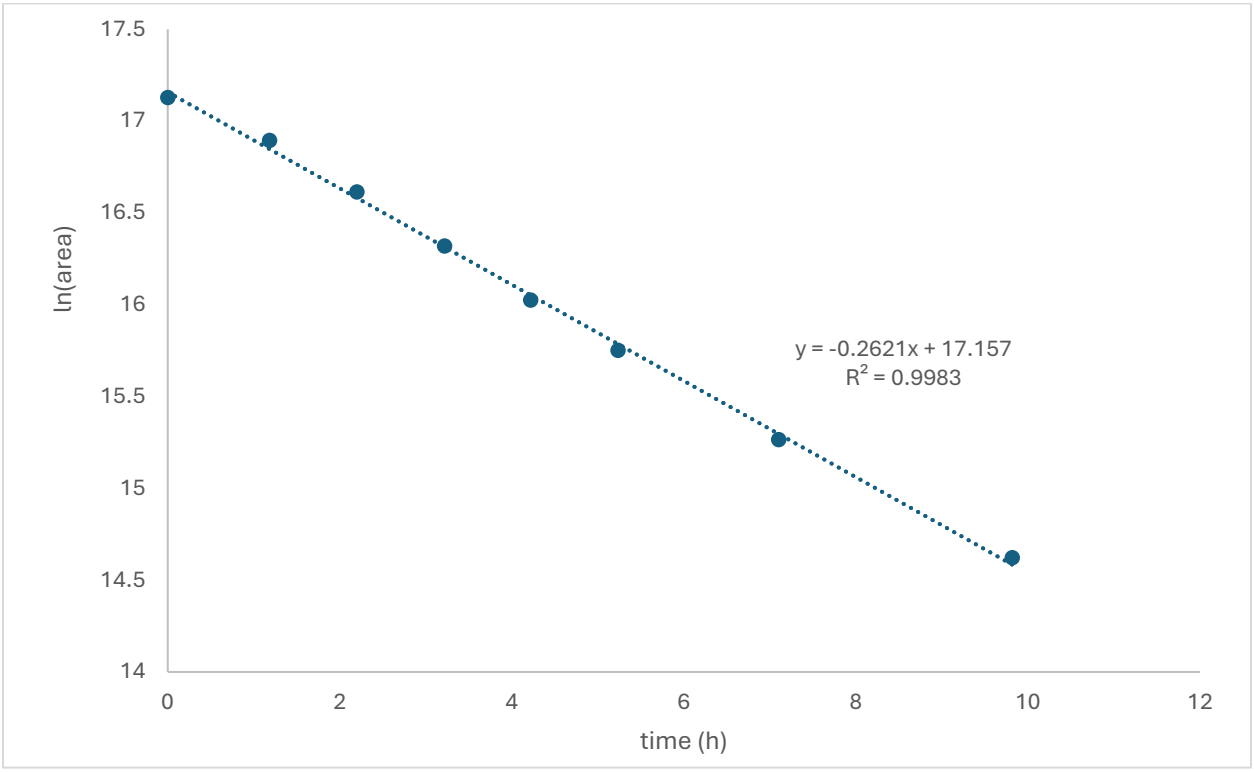

Figure S48. Plot of ln[boronic ester peak area] versus time for boronic ester **13-Epin**. Data were fitted to a first order decay model using linear regression. The slope of the best-fit line corresponds to the pseudo-first order rate constant (k), from which the hydrolysis half-life ($t_{1/2}$) of 2.6 h was calculated.

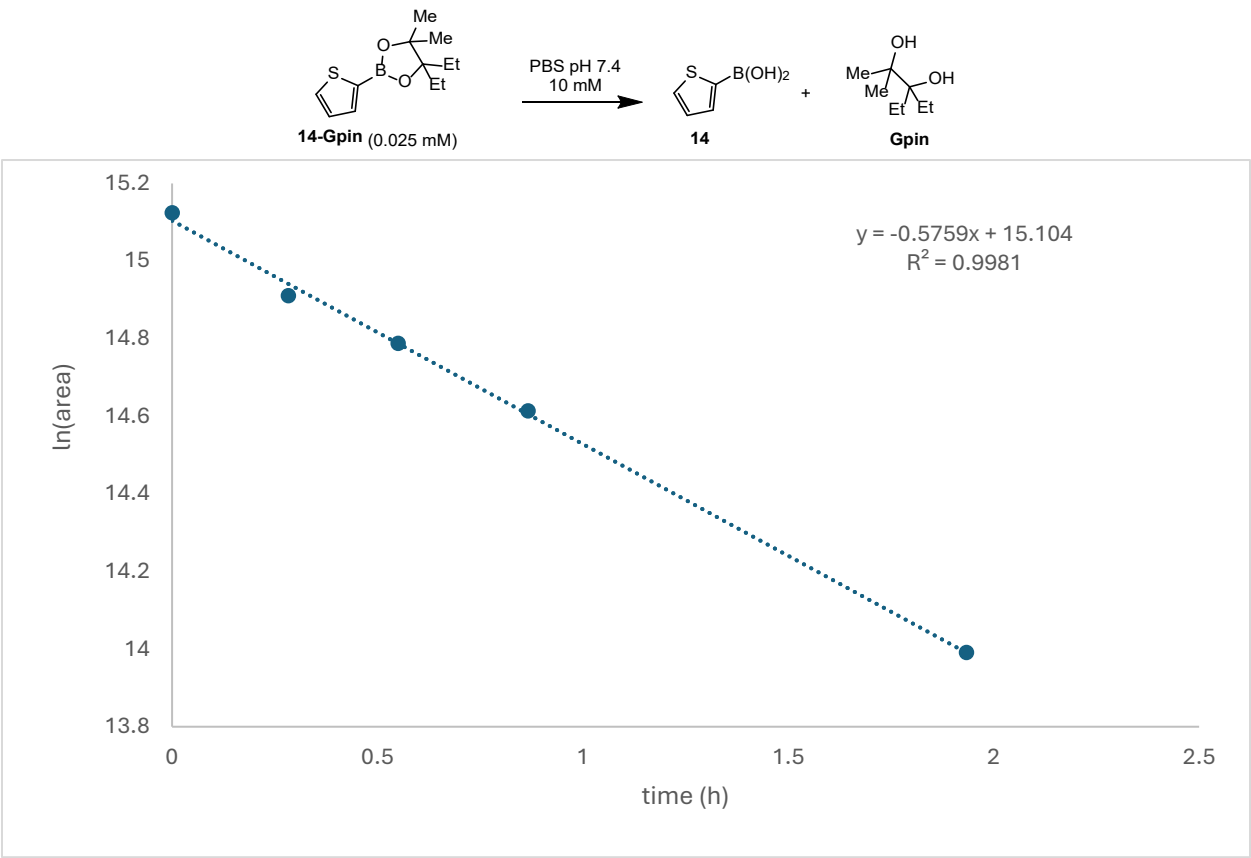

Figure S49. Plot of ln[boronic ester peak area] versus time for boronic ester **14-Gpin**. Data were fitted to a first order decay model using linear regression. The slope of the best-fit line corresponds to the pseudo-first order rate constant (k), from which the hydrolysis half-life ($t_{1/2}$) of 1.2 h was calculated.

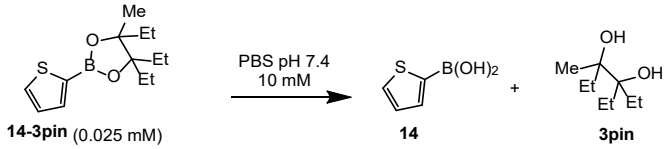

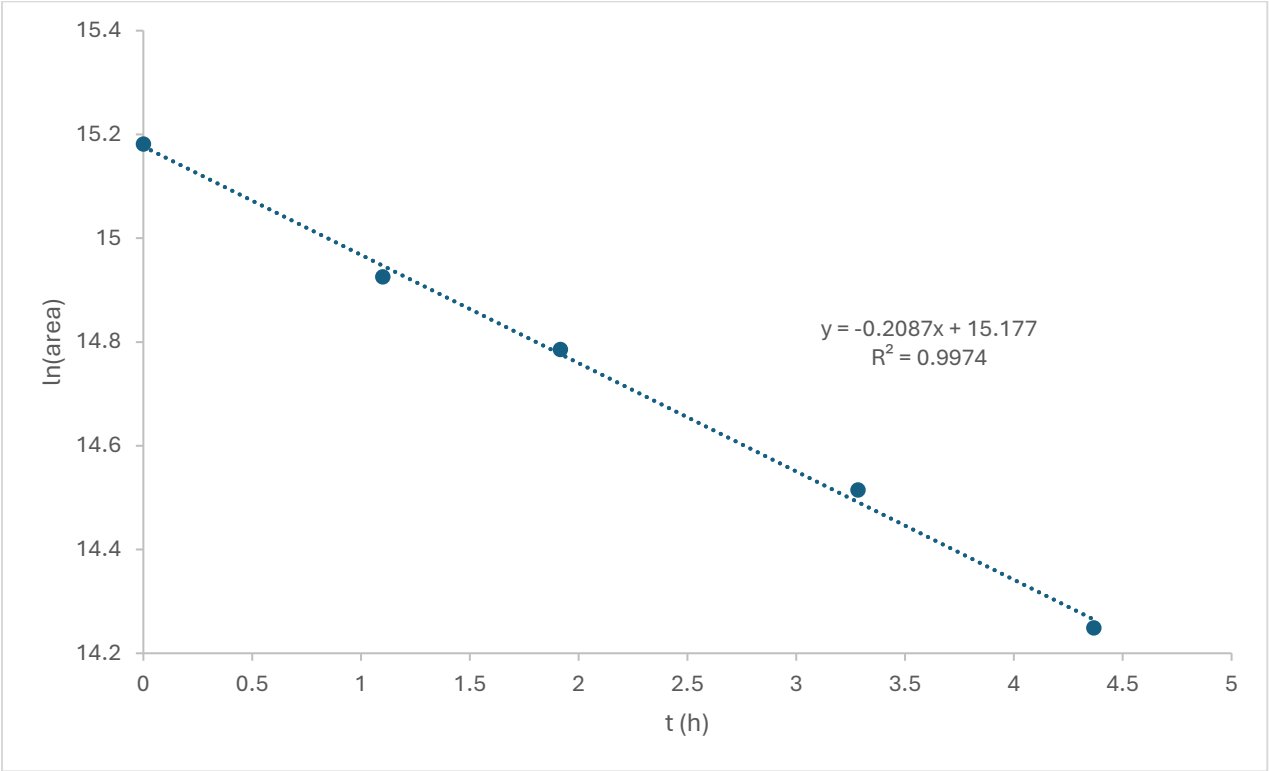

Figure S50. Plot of ln[boronic ester peak area] versus time for boronic ester **14-3pin**. Data were fitted to a first order decay model using linear regression. The slope of the best-fit line corresponds to the pseudo-first order rate constant (k), from which the hydrolysis half-life ($t_{1/2}$) of 3.3 h was calculated.

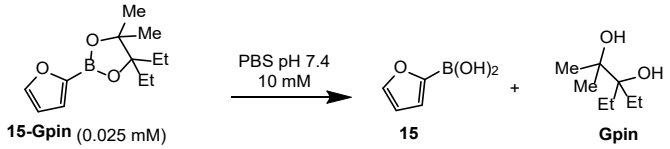

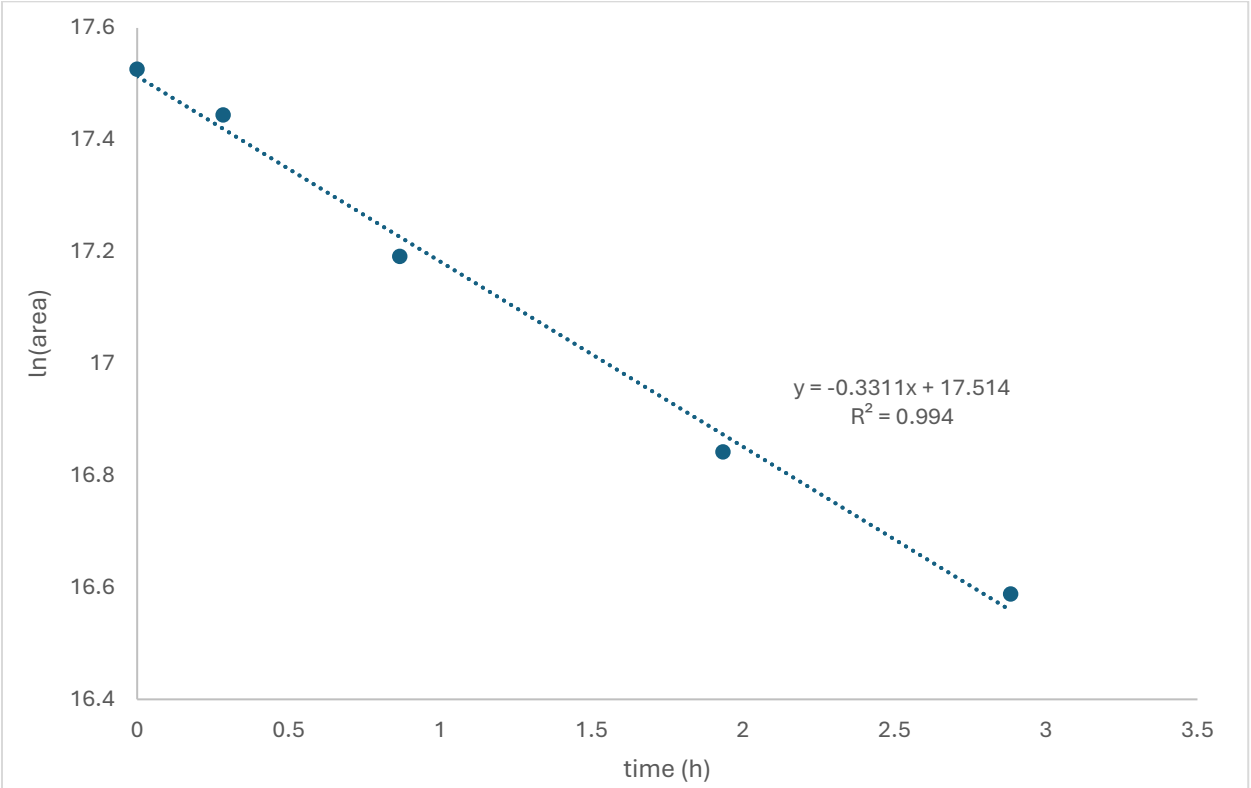

Figure S51. Plot of ln[boronic ester peak area] versus time for boronic ester **15-Gpin**. Data were fitted to a first order decay model using linear regression. The slope of the best-fit line corresponds to the pseudo-first order rate constant (k), from which the hydrolysis half-life ($t_{1/2}$) of 2.1h was calculated.

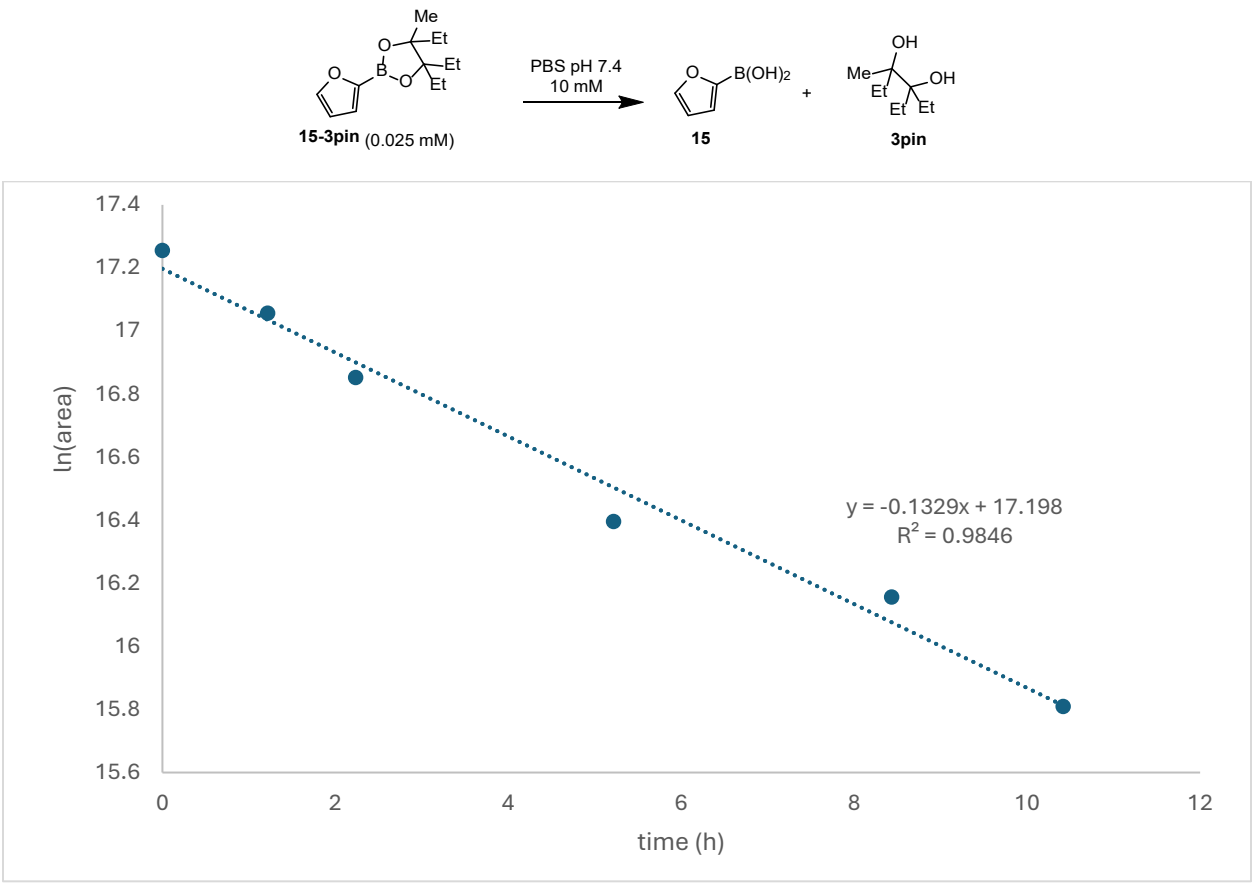

Figure S52. Plot of ln[boronic ester peak area] versus time for boronic ester **15-3pin**. Data were fitted to a first order decay model using linear regression. The slope of the best-fit line corresponds to the pseudo-first order rate constant (k), from which the hydrolysis half-life ($t_{1/2}$) of 5.0 h was calculated.

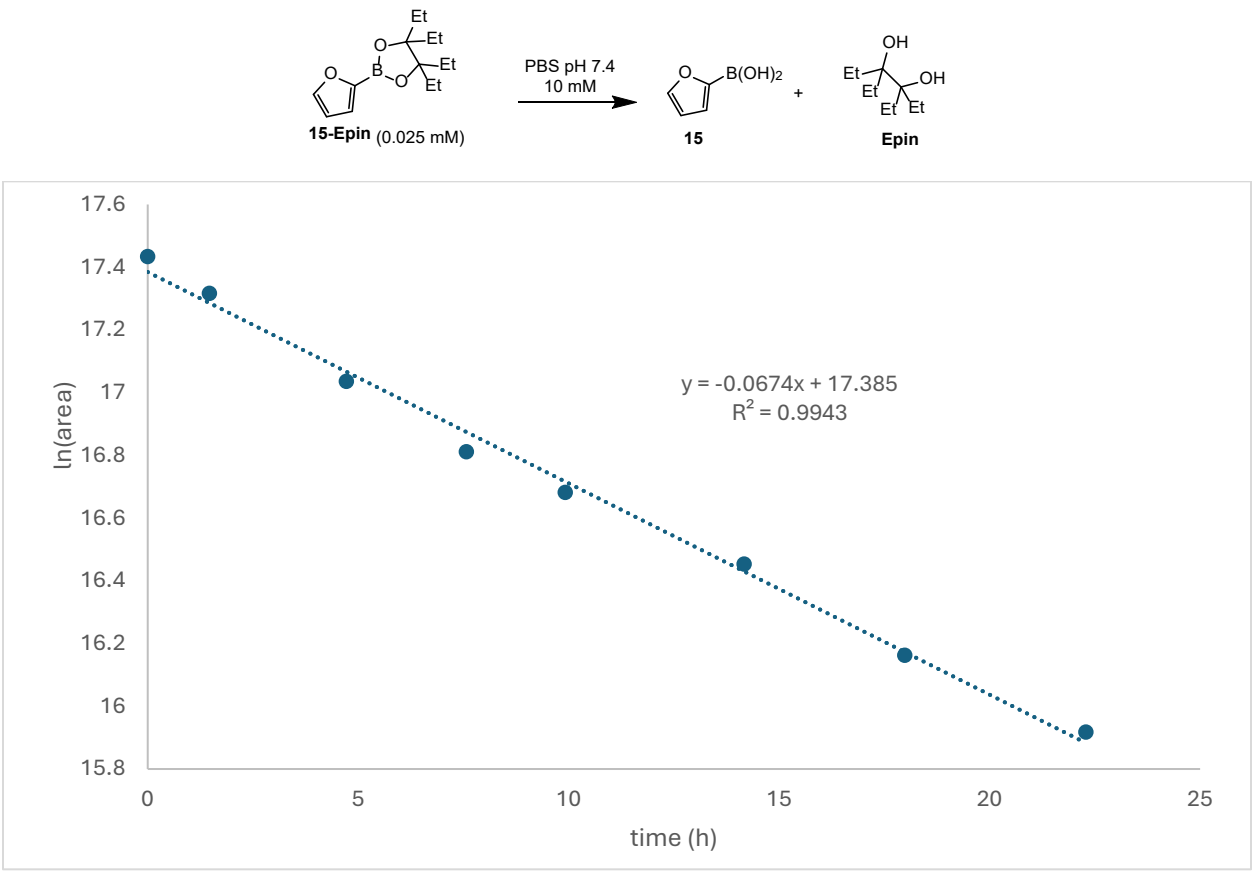

Figure S53. Plot of ln[boronic ester peak area] versus time for boronic ester **15-Epin**. Data were fitted to a first order decay model using linear regression. The slope of the best-fit line corresponds to the pseudo-first order rate constant (k), from which the hydrolysis half-life ($t_{1/2}$) of 10.2 h was calculated.

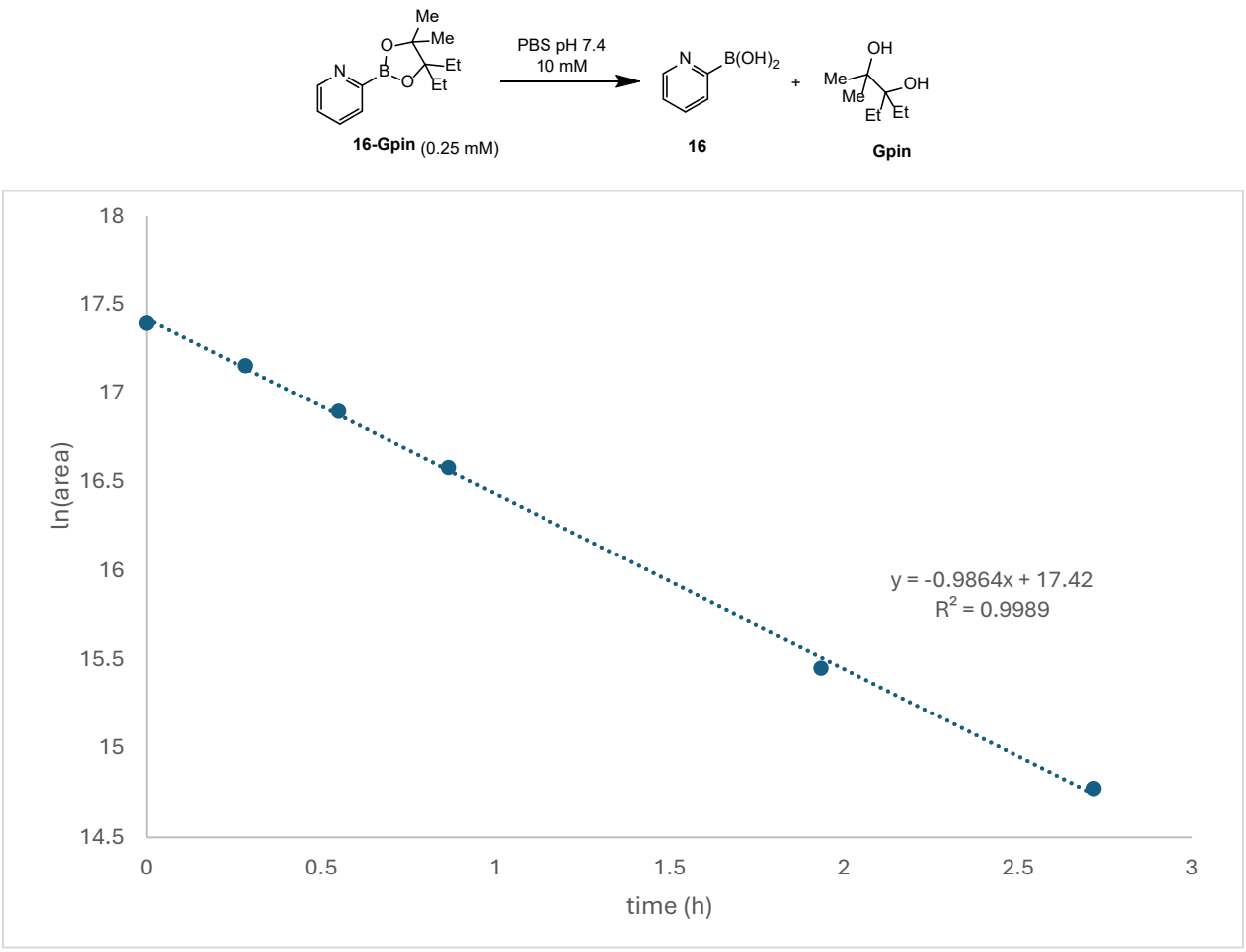

Figure S54. Plot of ln[boronic ester peak area] versus time for boronic ester **16-Gpin**. Data were fitted to a first order decay model using linear regression. The slope of the best-fit line corresponds to the pseudo-first order rate constant (k), from which the hydrolysis half-life ($t_{1/2}$) of 0.7 h was calculated.

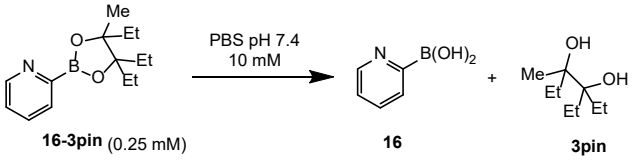

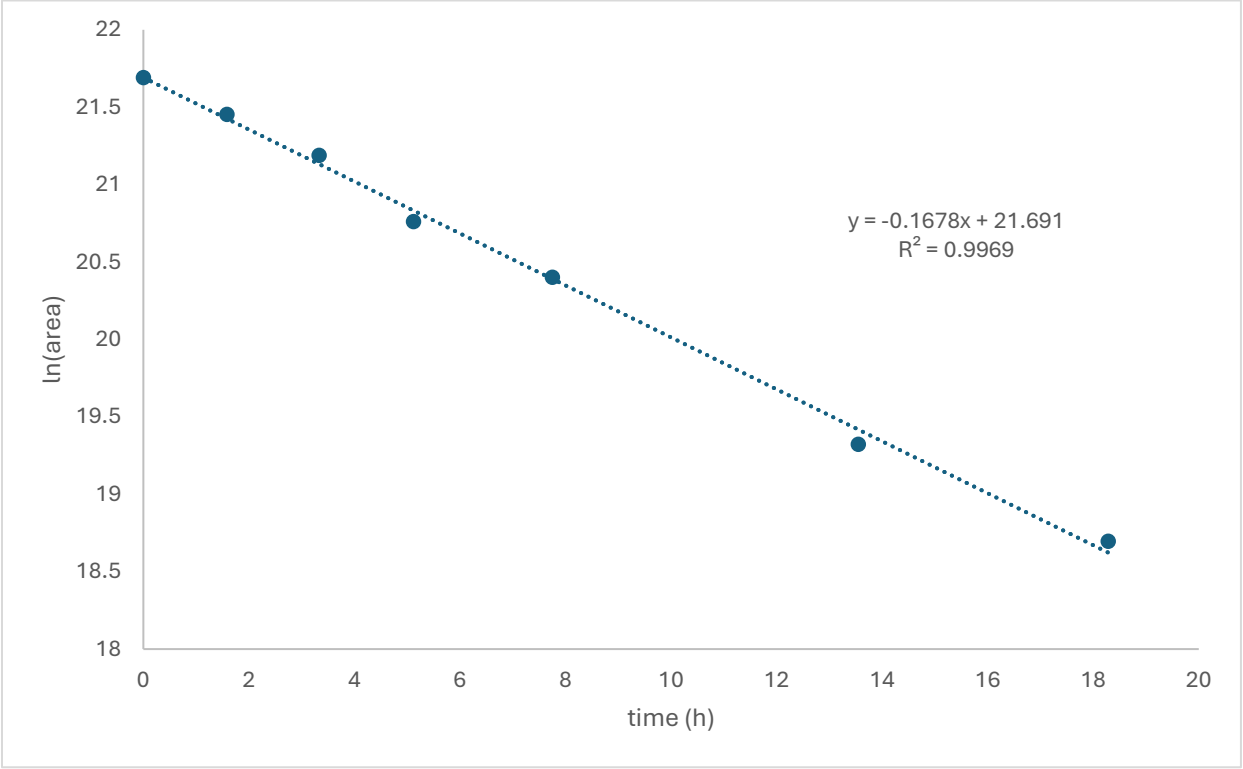

Figure S55. Plot of ln[boronic ester peak area] versus time for boronic ester **15-3pin**. Data were fitted to a first order decay model using linear regression. The slope of the best-fit line corresponds to the pseudo-first order rate constant (k), from which the hydrolysis half-life ($t_{1/2}$) of 4.1 h was calculated.

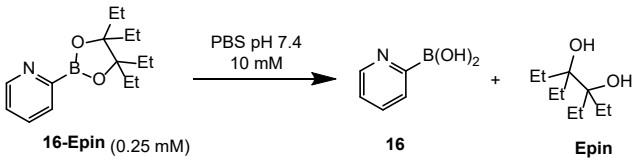

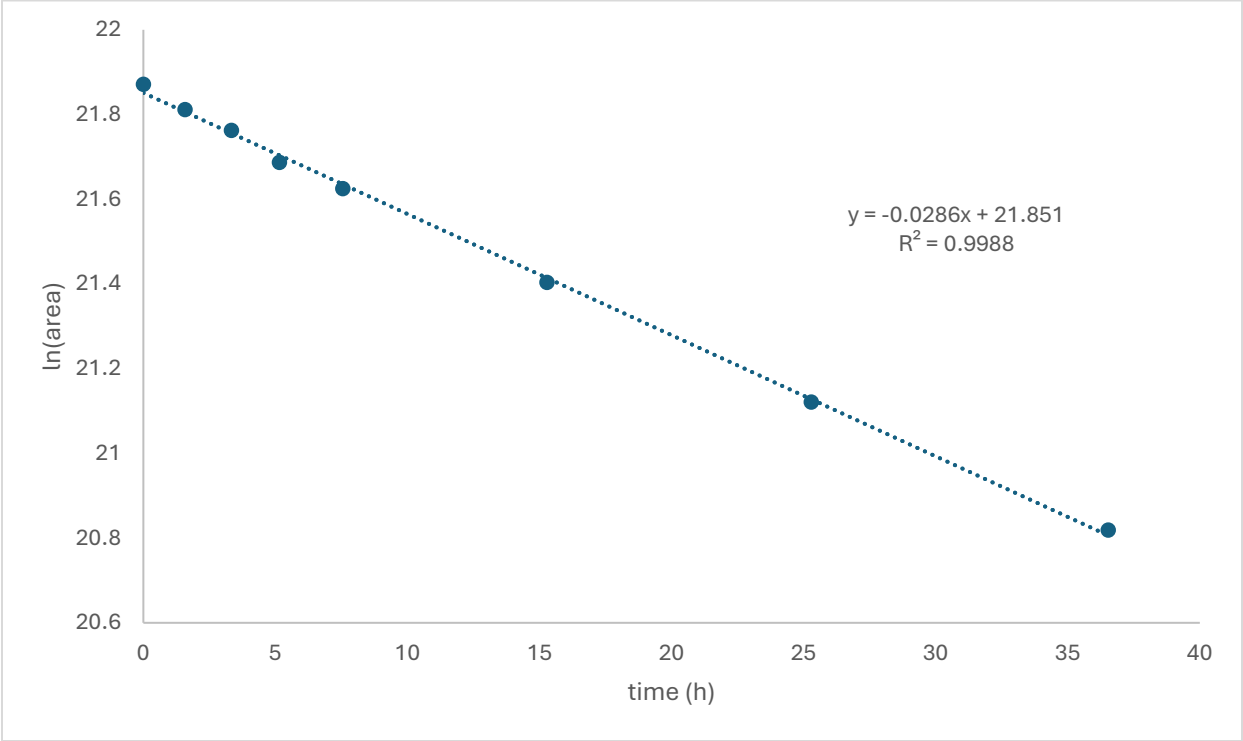

Figure S56. Plot of ln[boronic ester peak area] versus time for boronic ester **15-Epin**. Data were fitted to a first order decay model using linear regression. The slope of the best-fit line corresponds to the pseudo-first order rate constant (k), from which the hydrolysis half-life ($t_{1/2}$) of 24.2 h was calculated.

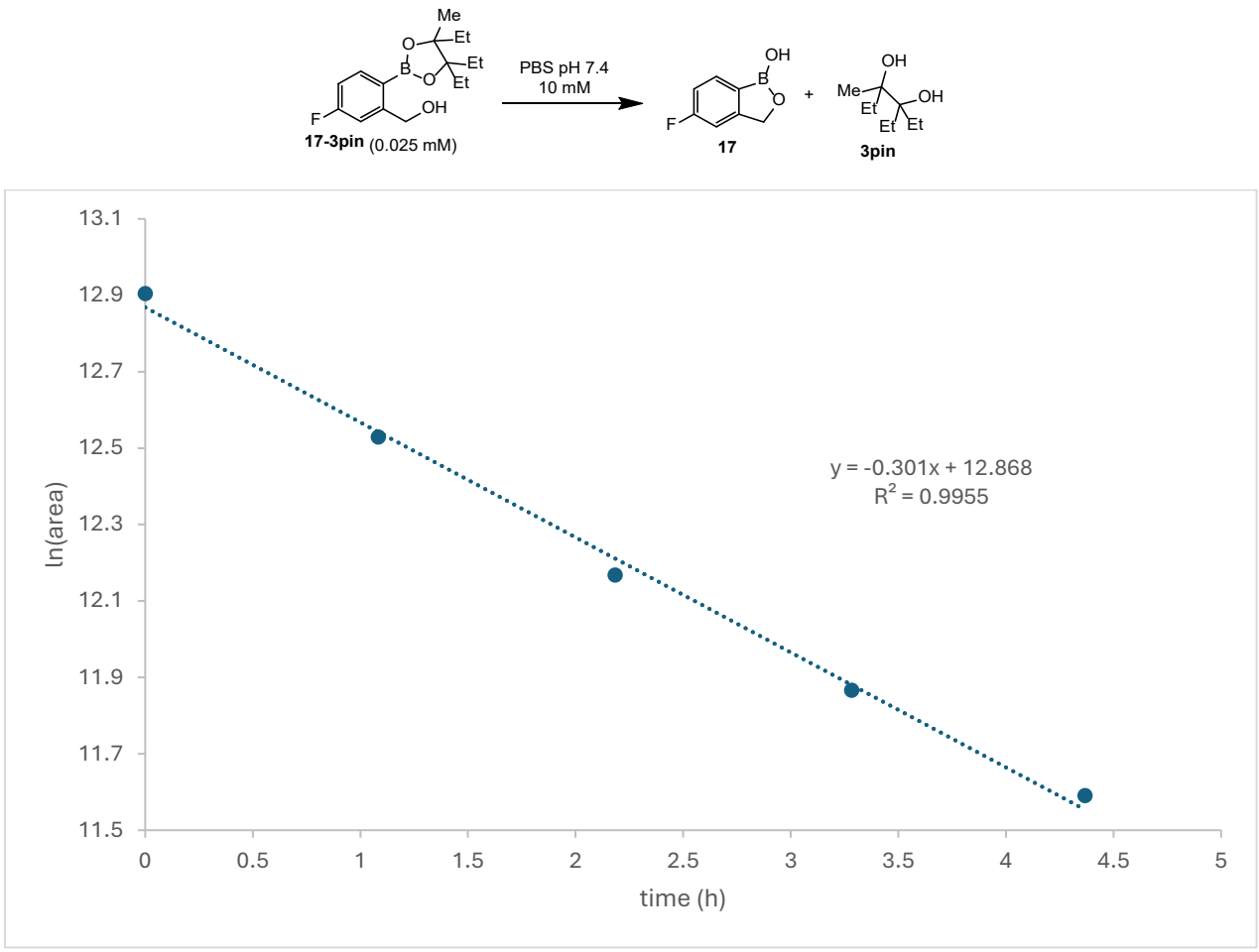

Figure S57. Plot of ln[boronic ester peak area] versus time for boronic ester **17-3pin**. Data were fitted to a first order decay model using linear regression. The slope of the best-fit line corresponds to the pseudo-first order rate constant (k), from which the hydrolysis half-life ($t_{1/2}$) of 2.3 h was calculated.

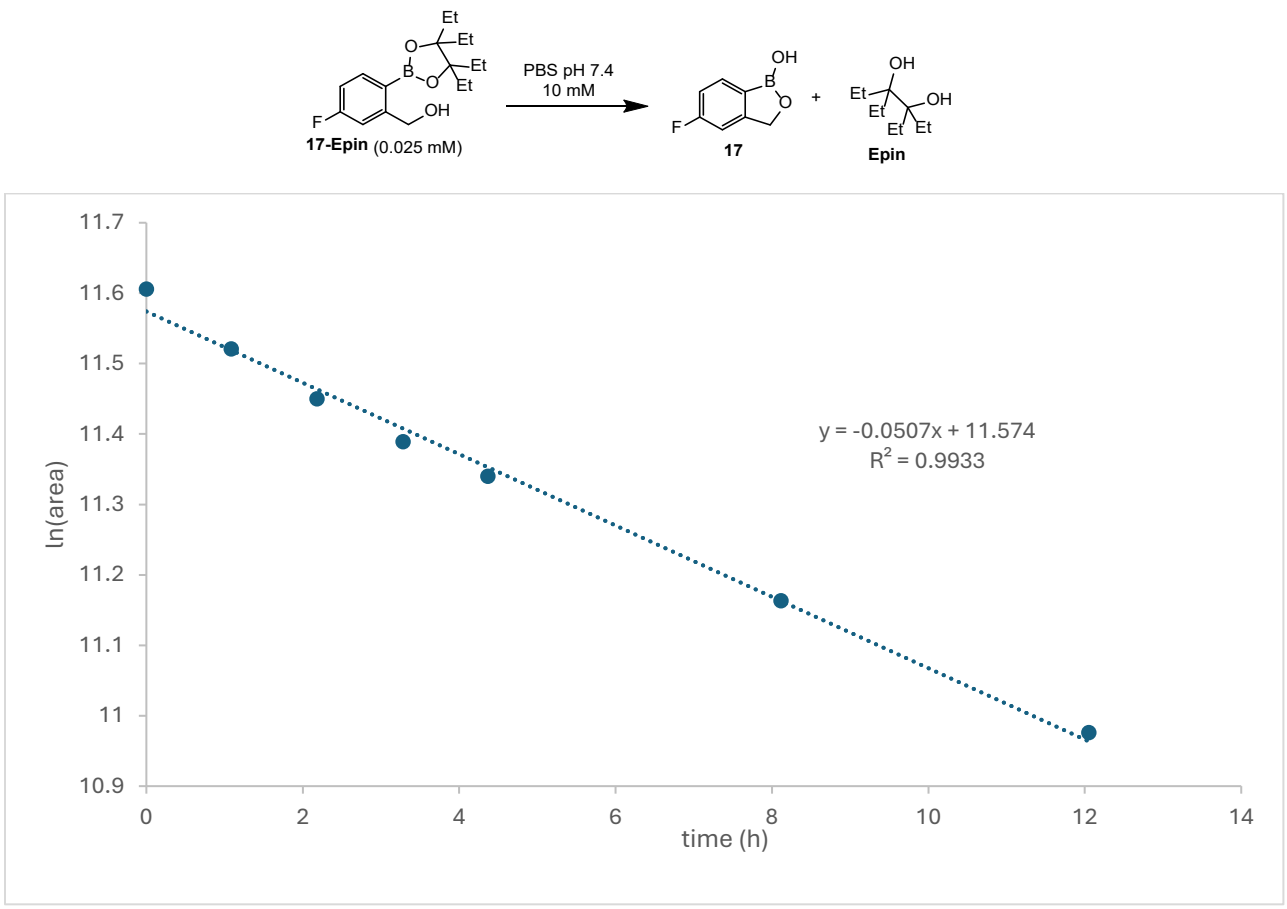

Figure S58. Plot of ln[boronic ester peak area] versus time for boronic ester **17-Epin**. Data were fitted to a first order decay model using linear regression. The slope of the best-fit line corresponds to the pseudo-first order rate constant (k), from which the hydrolysis half-life ($t_{1/2}$) of 13.6 h was calculated.

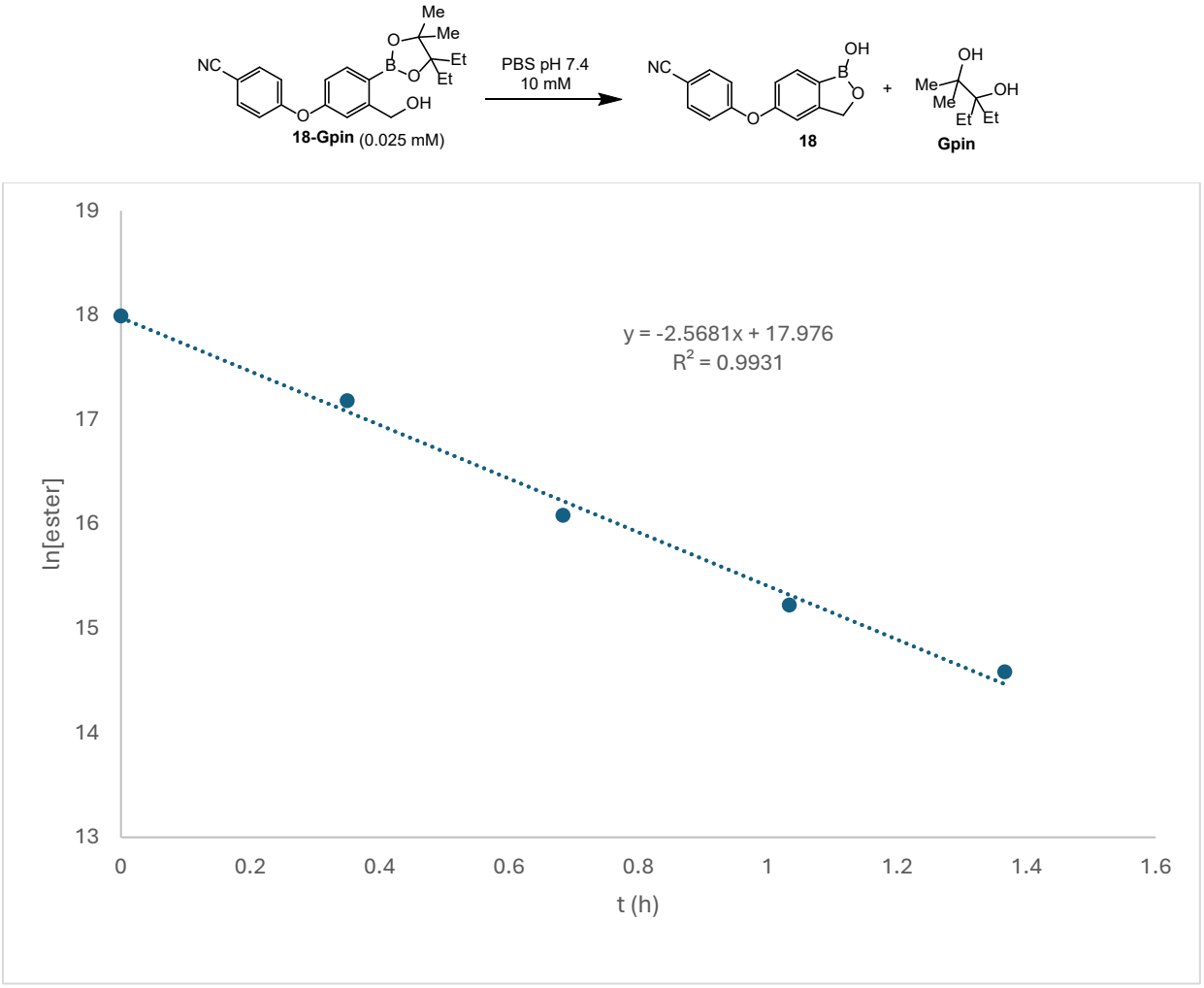

Figure S59. Plot of ln[boronic ester peak area] versus time for boronic ester **18-Gpin**. Data were fitted to a first order decay model using linear regression. The slope of the best-fit line corresponds to the pseudo-first order rate constant (k), from which the hydrolysis half-life ($t_{1/2}$) of 0.3 h was calculated.

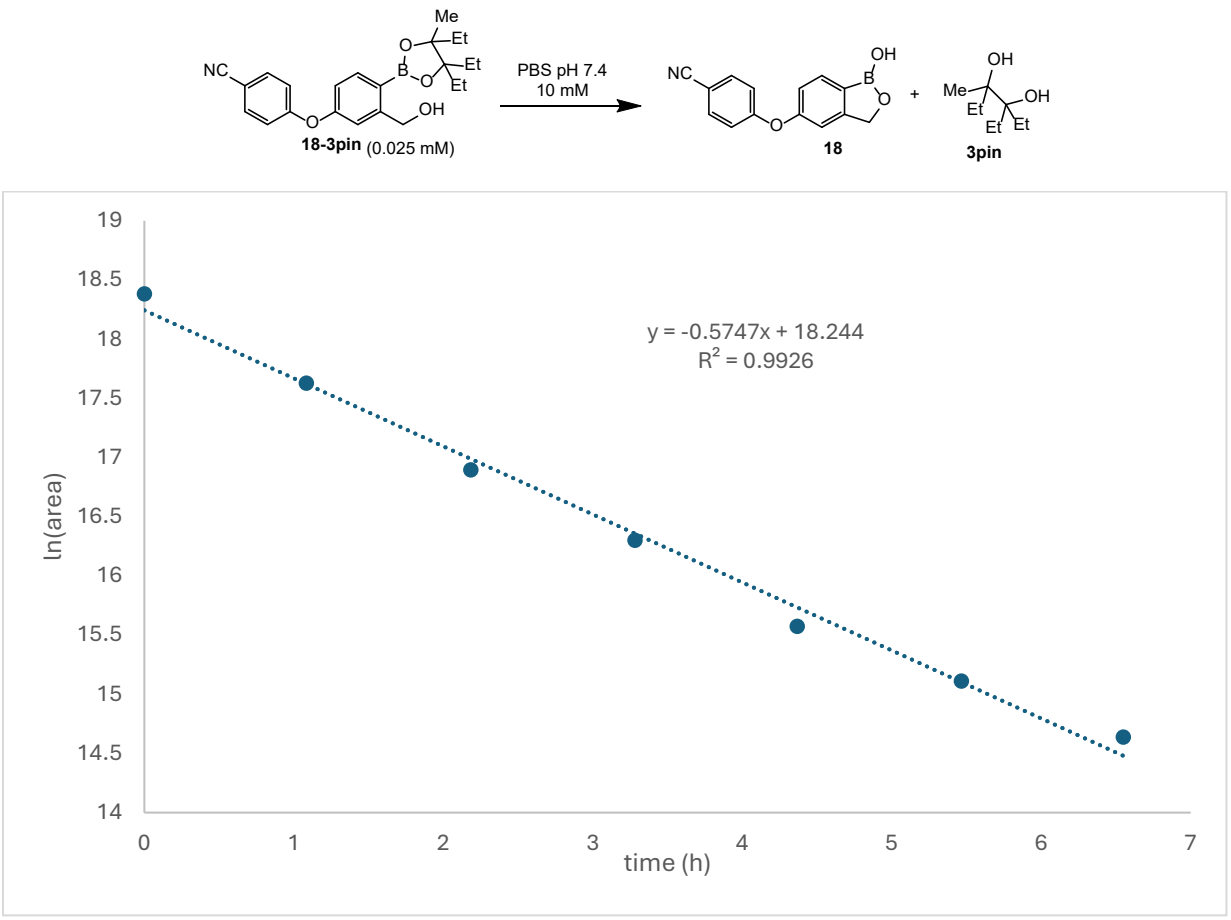

Figure S60. Plot of ln[boronic ester peak area] versus time for boronic ester **18-3pin**. Data were fitted to a first order decay model using linear regression. The slope of the best-fit line corresponds to the pseudo-first order rate constant (k), from which the hydrolysis half-life ($t_{1/2}$) of 1.2 h was calculated.

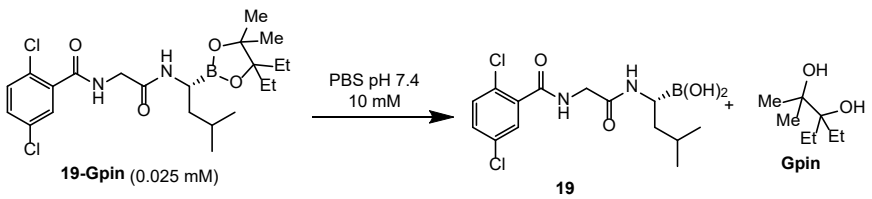

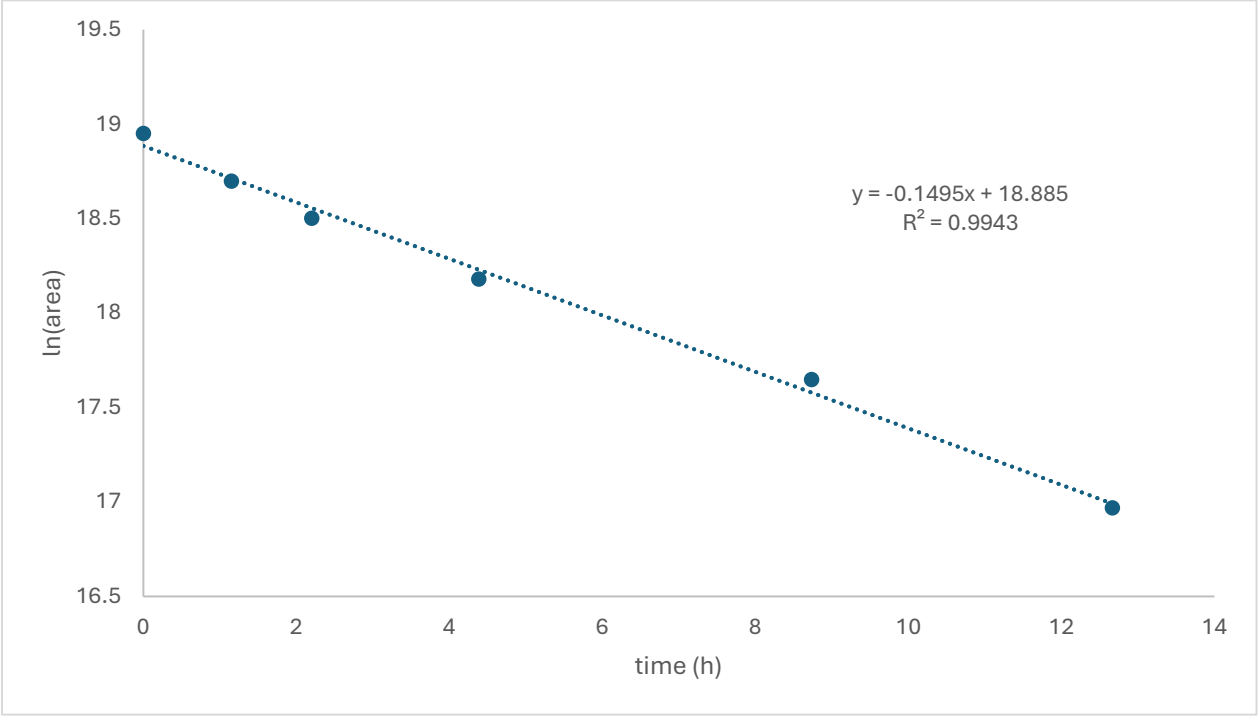

Figure S61. Plot of ln[boronic ester peak area] versus time for boronic ester **19-Gpin**. Data were fitted to a first order decay model using linear regression. The slope of the best-fit line corresponds to the pseudo-first order rate constant (k), from which the hydrolysis half-life ($t_{1/2}$) of 4.6 h was calculated.

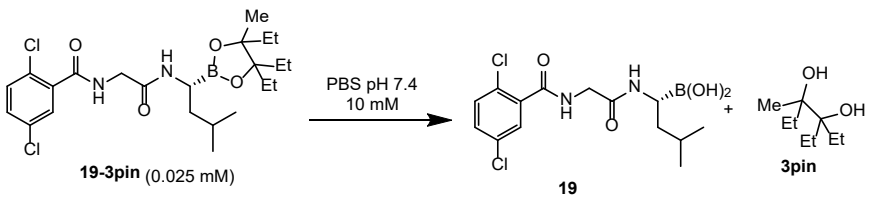

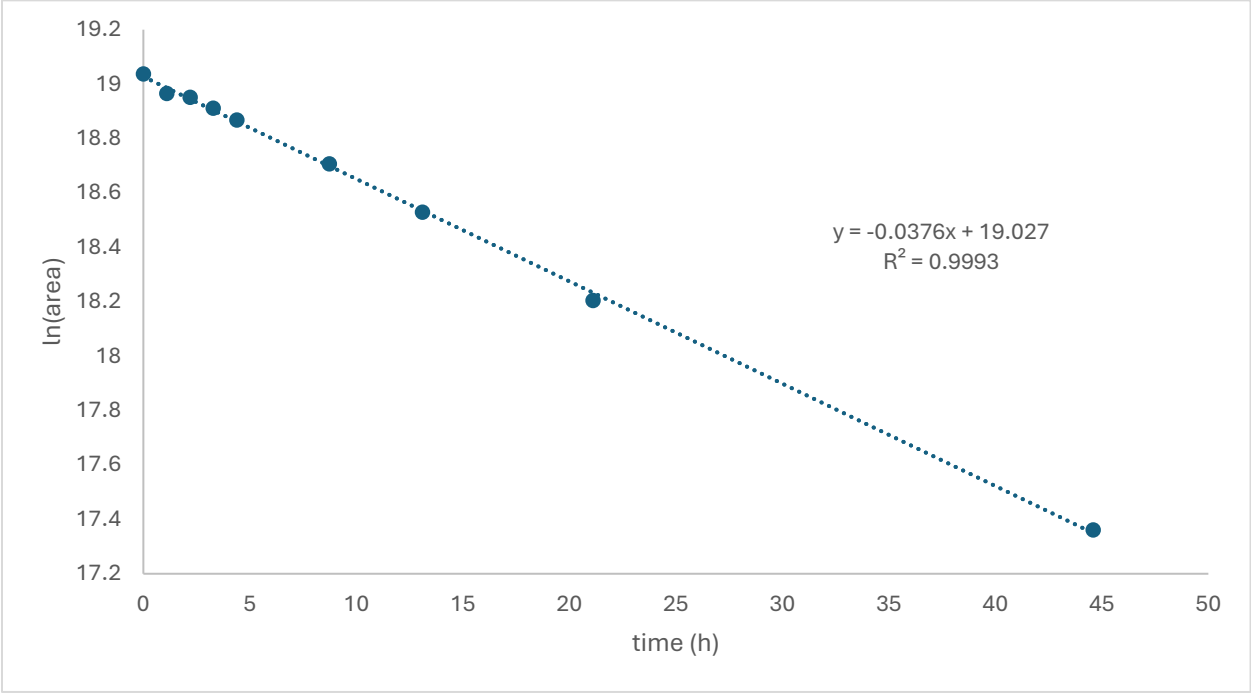

Figure S62. Plot of ln[boronic ester peak area] versus time for boronic ester **19-3pin**. Data were fitted to a first order decay model using linear regression. The slope of the best-fit line corresponds to the pseudo-first order rate constant (k), from which the hydrolysis half-life ($t_{1/2}$) of 18.4 h was calculated.

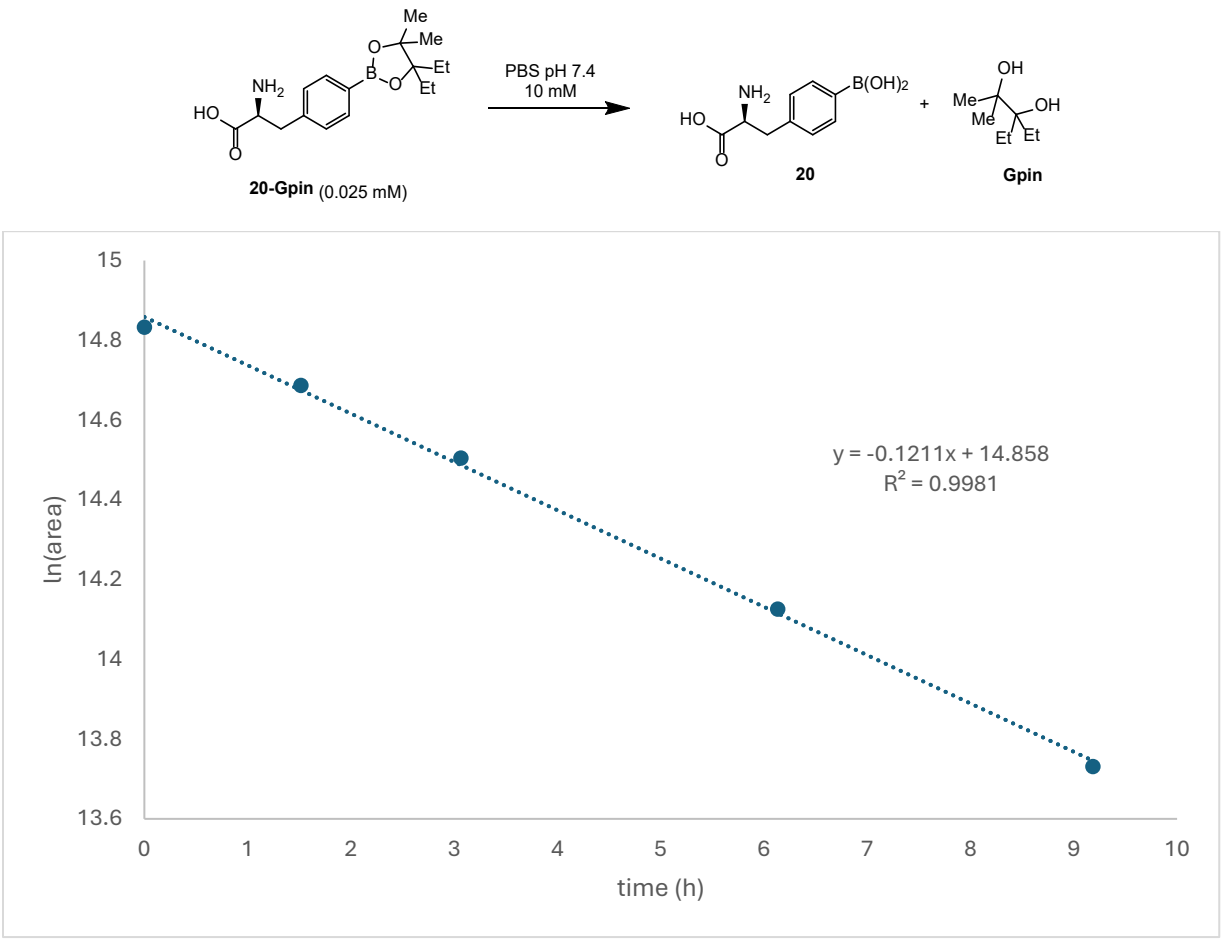

Figure S63. Plot of ln[boronic ester peak area] versus time for boronic ester **20-Gpin**. Data were fitted to a first order decay model using linear regression. The slope of the best-fit line corresponds to the pseudo-first order rate constant (k), from which the hydrolysis half-life ($t_{1/2}$) of 5.7 h was calculated.

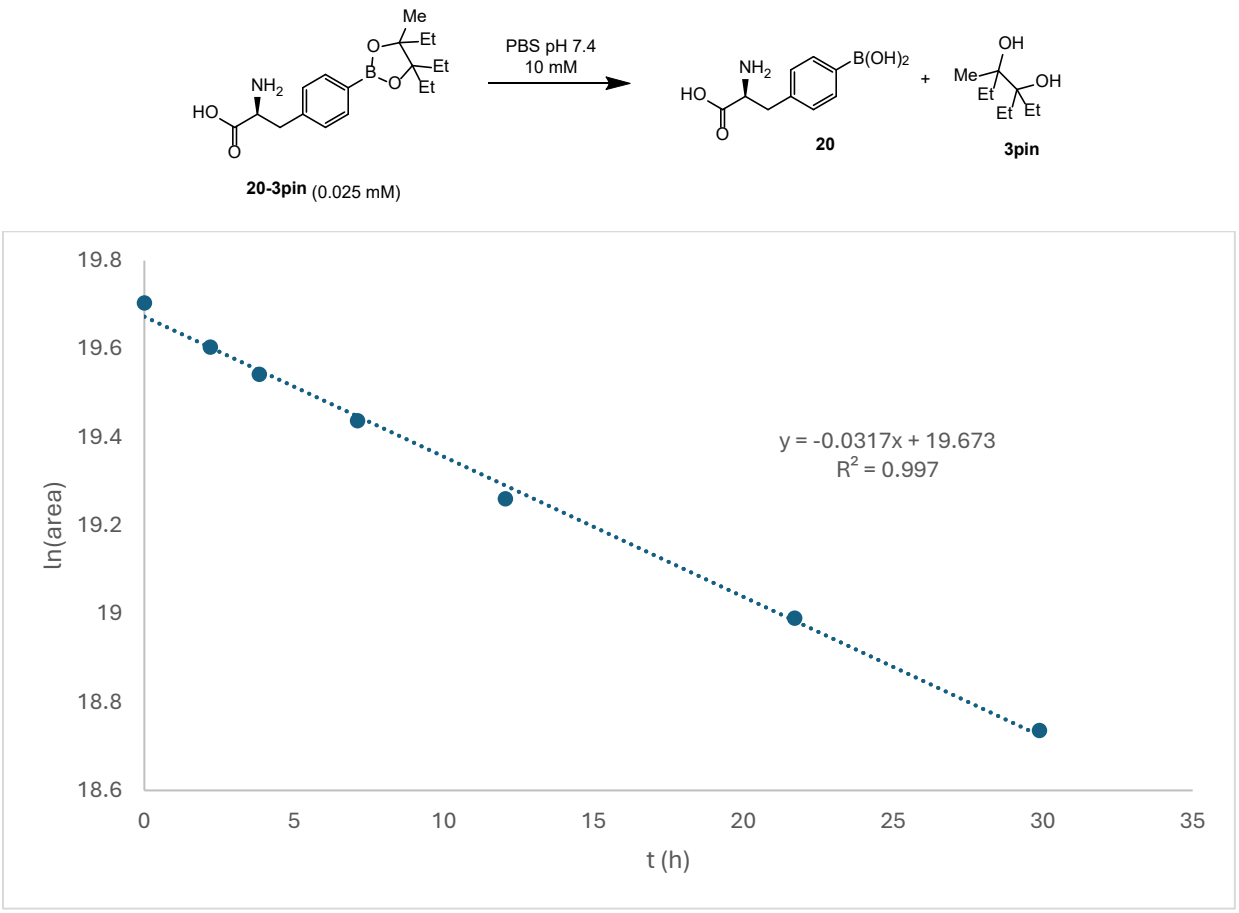

Figure S64. Plot of ln[boronic ester peak area] versus time for boronic ester **20-3pin**. Data were fitted to a first order decay model using linear regression. The slope of the best-fit line corresponds to the pseudo-first order rate constant (k), from which the hydrolysis half-life ($t_{1/2}$) of 21.8 h was calculated.

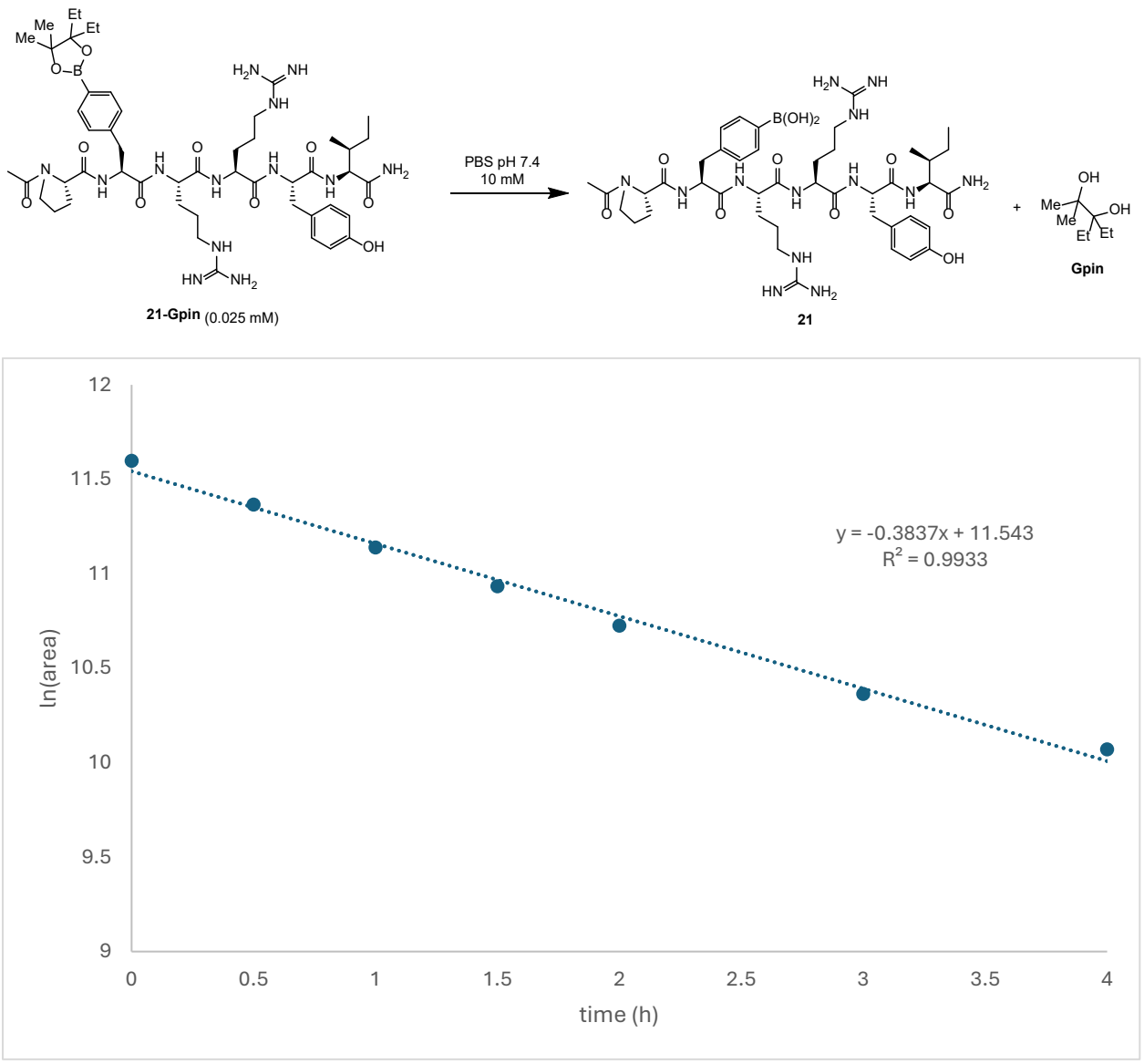

Figure S65. Plot of ln[boronic ester peak area] versus time for boronic ester **21-Gpin**. Data were fitted to a first order decay model using linear regression. The slope of the best-fit line corresponds to the pseudo-first order rate constant (k), from which the hydrolysis half-life ($t_{1/2}$) of 1.7 h was calculated.

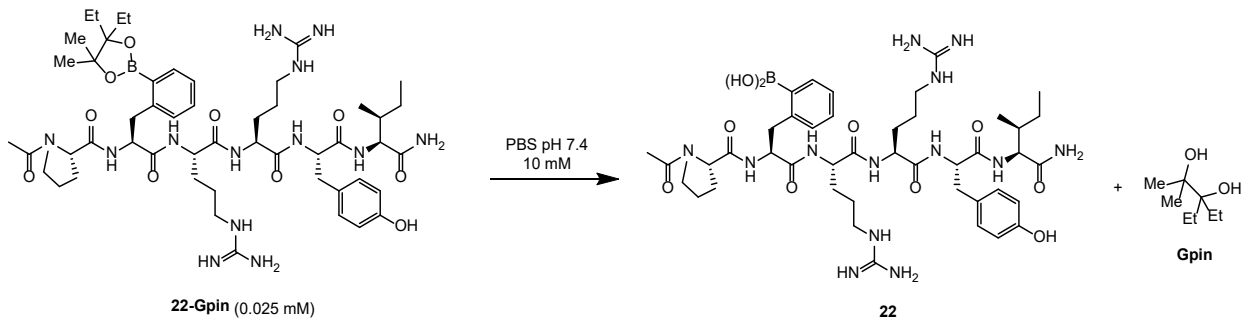

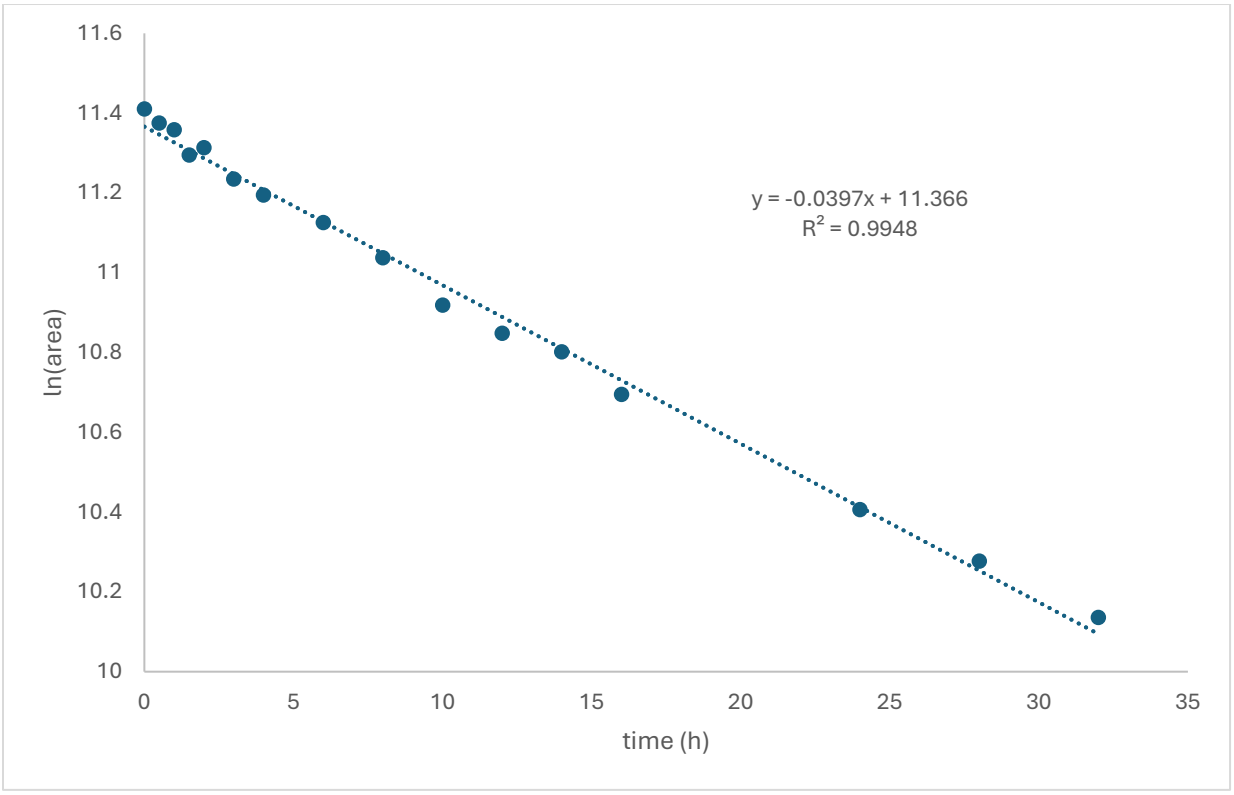

Figure S66. Plot of ln[boronic ester peak area] versus time for boronic ester **22-Gpin**. Data were fitted to a first order decay model using linear regression. The slope of the best-fit line corresponds to the pseudo-first order rate constant (k), from which the hydrolysis half-life ($t_{1/2}$) of 16.6 h was calculated.

For figure 5

Table S3. Summarized data used for the determination of the Hammett plots at pH 7.4 and 5.2 of Gpin *p*-phenylboronic esters.

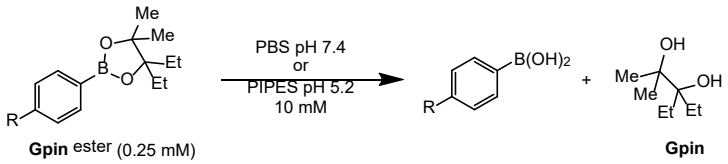

molecule	R group	σ_{para}	pH 5.2			pH 7.4		
			$k_{hydrolysis}$	$k_{hydrolysis}/k_H$	log(k/kh)	$k_{hydrolysis}$	$k_{hydrolysis}/k_H$	log(k/kh)
7-Gpin	-NO2	0.78	1.2306	22.37455	1.349754	0.9582	7.464908	0.873024
S6-Gpin	-COOH	0.45	0.4236	7.701818	0.886593	0.3460	2.695531	0.430644
1-Gpin	-H	0	0.0550	1	0	0.1284	1	0
S7-Gpin	-CH2CH2COOH	-0.07	0.0510	0.927273	-0.03279	0.1220	0.950447	-0.02207
5-Gpin	-OMe	-0.27	0.0118	0.214545	-0.66848	0.0817	0.636488	-0.19621
4-Gpin	-OH	-0.37	0.0087	0.158182	-0.80084	0.0497	0.38719	-0.41208

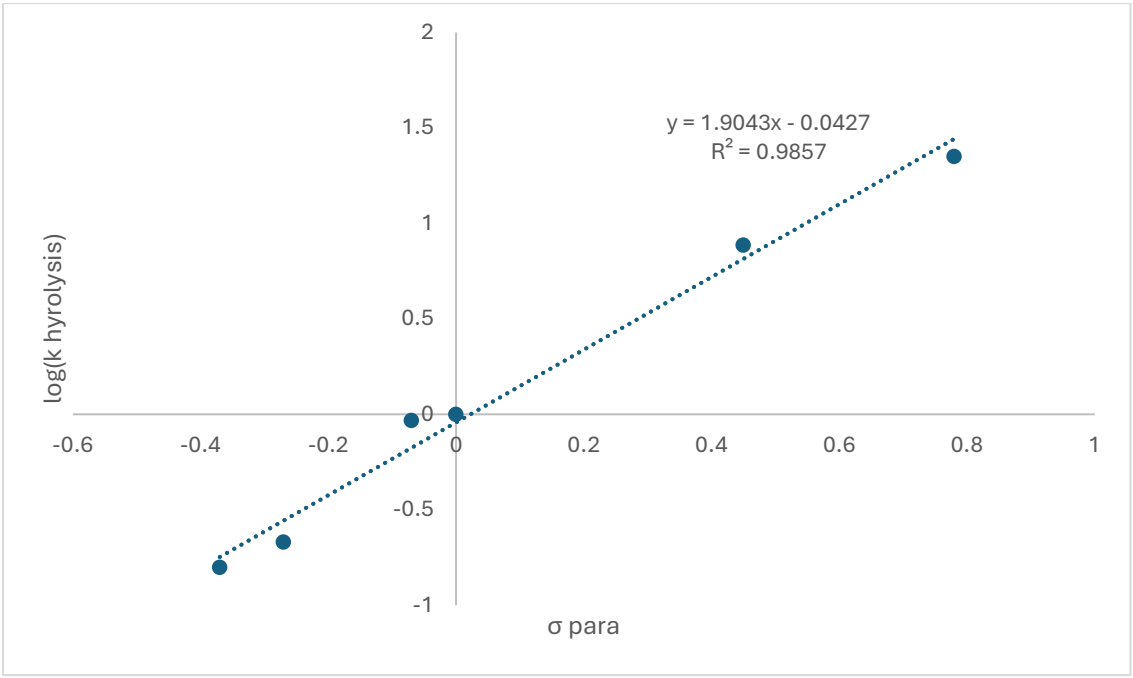

Figure S67. Hammet plot for the hydrolysis of Gpin *p*-phenylboronic esters at pH 5.2.

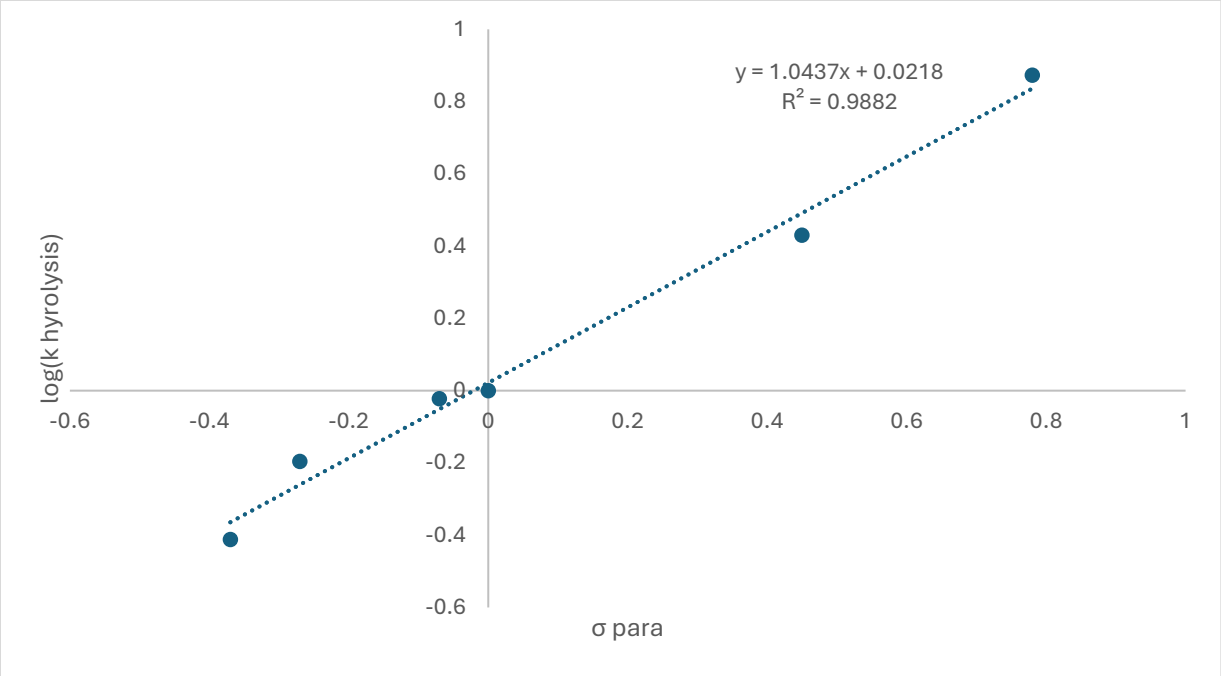

Figure S68. Hammet plot for the hydrolysis of Gpin *p*-phenylboronic esters at pH 7.4.

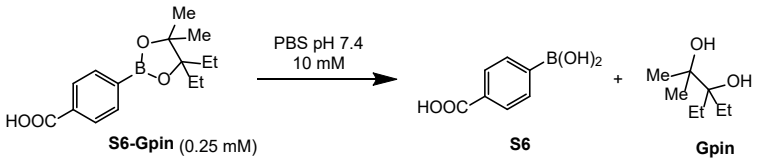

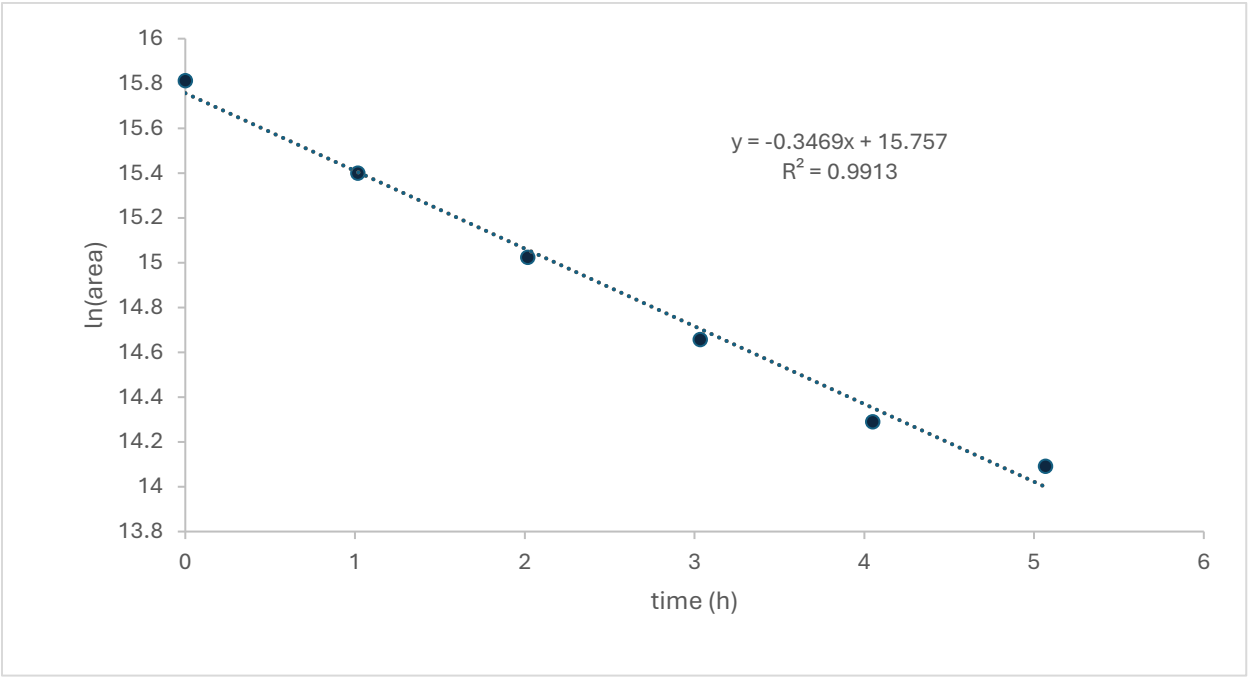

Figure S69. Plot of ln[boronic ester peak area] versus time at pH 7.4 for boronic ester **S6-Gpin**. Data were fitted to a first order decay model using linear regression. The slope of the best-fit line corresponds to the pseudo-first order rate constant (k), from which the hydrolysis half-life ($t_{1/2}$) of 2.0 h was calculated.

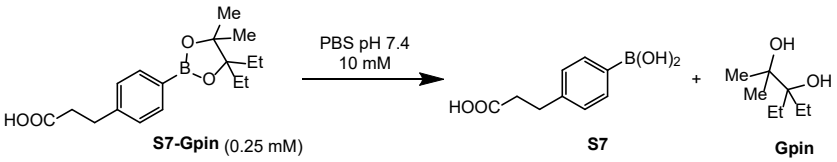

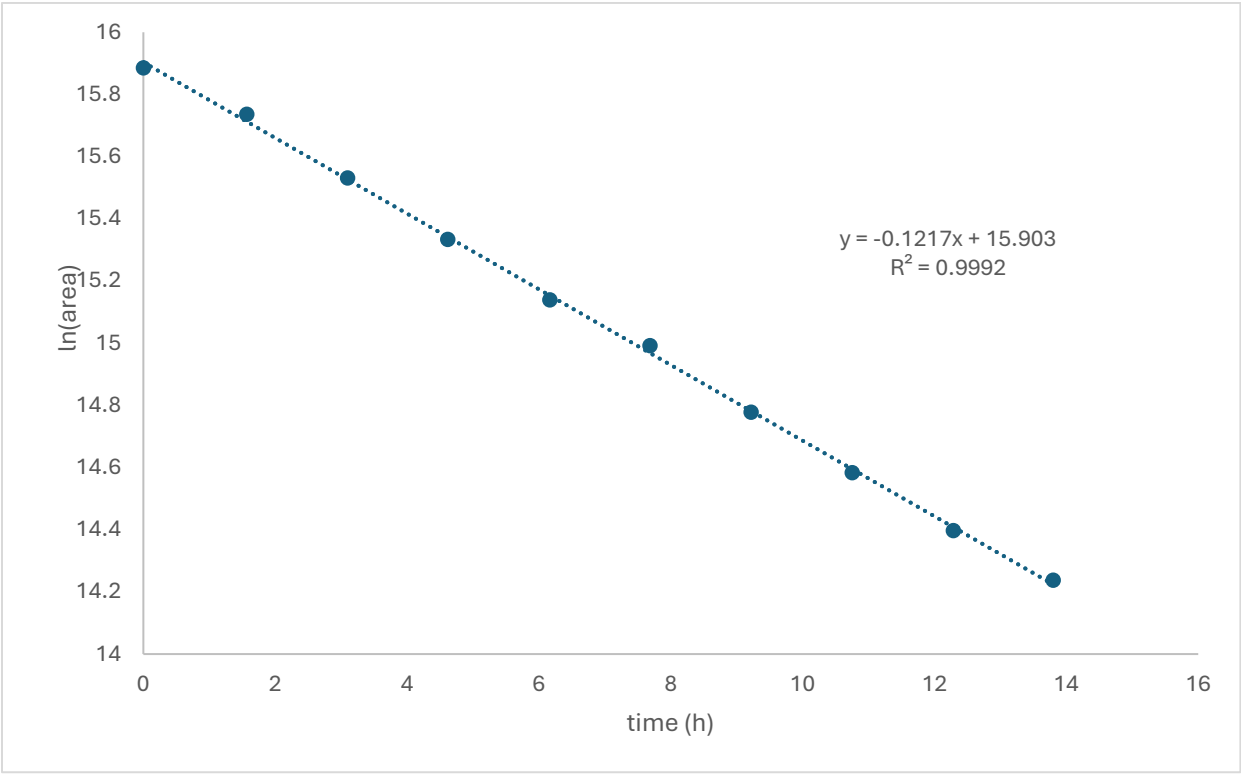

Figure S70. Plot of ln[boronic ester peak area] versus time at pH 7.4 for boronic ester **S7-Gpin**. Data were fitted to a first order decay model using linear regression. The slope of the best-fit line corresponds to the pseudo-first order rate constant (k), from which the hydrolysis half-life ($t_{1/2}$) of 5.7 h was calculated.

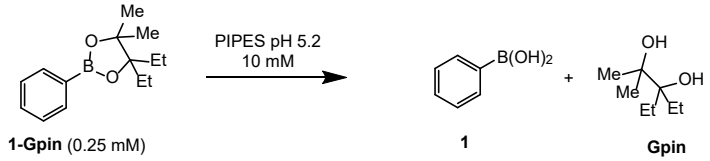

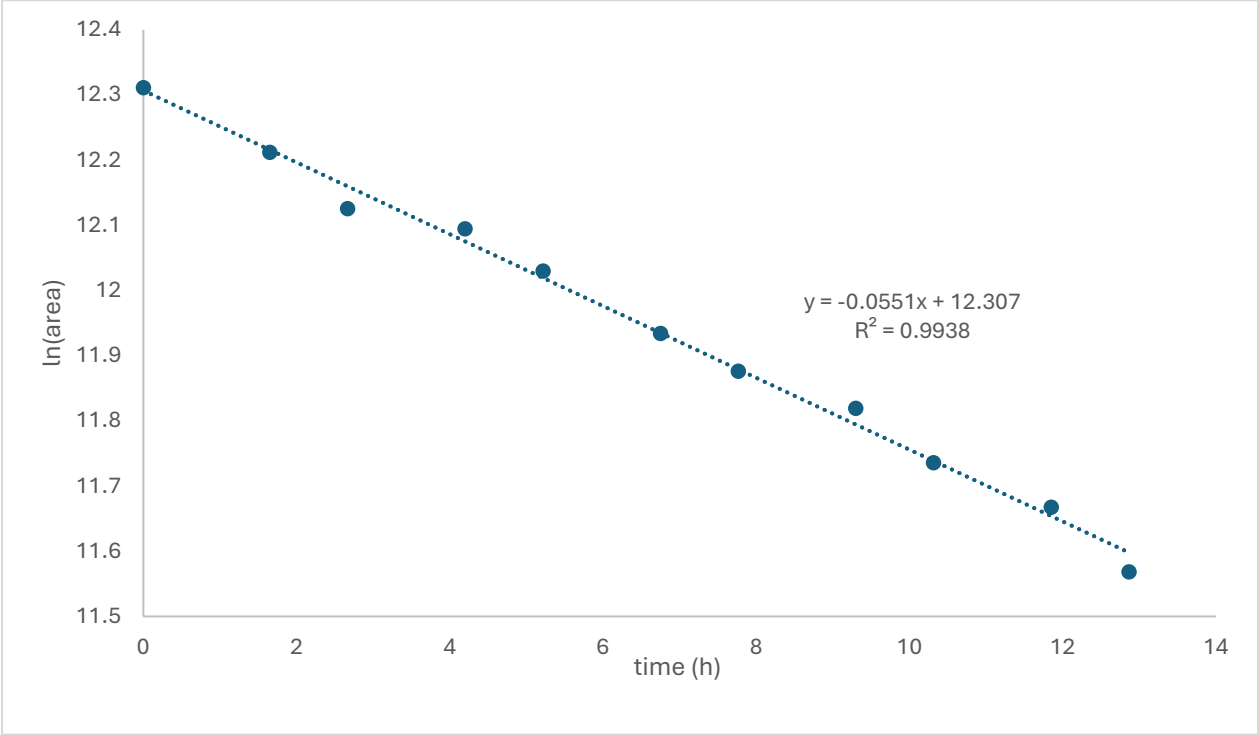

Figure S71. Plot of ln[boronic ester peak area] versus time at pH 5.2 for boronic ester **1-Gpin**. Data were fitted to a first order decay model using linear regression. The slope of the best-fit line corresponds to the pseudo-first order rate constant (k), from which the hydrolysis half-life ($t_{1/2}$) of 12.6 h was calculated.

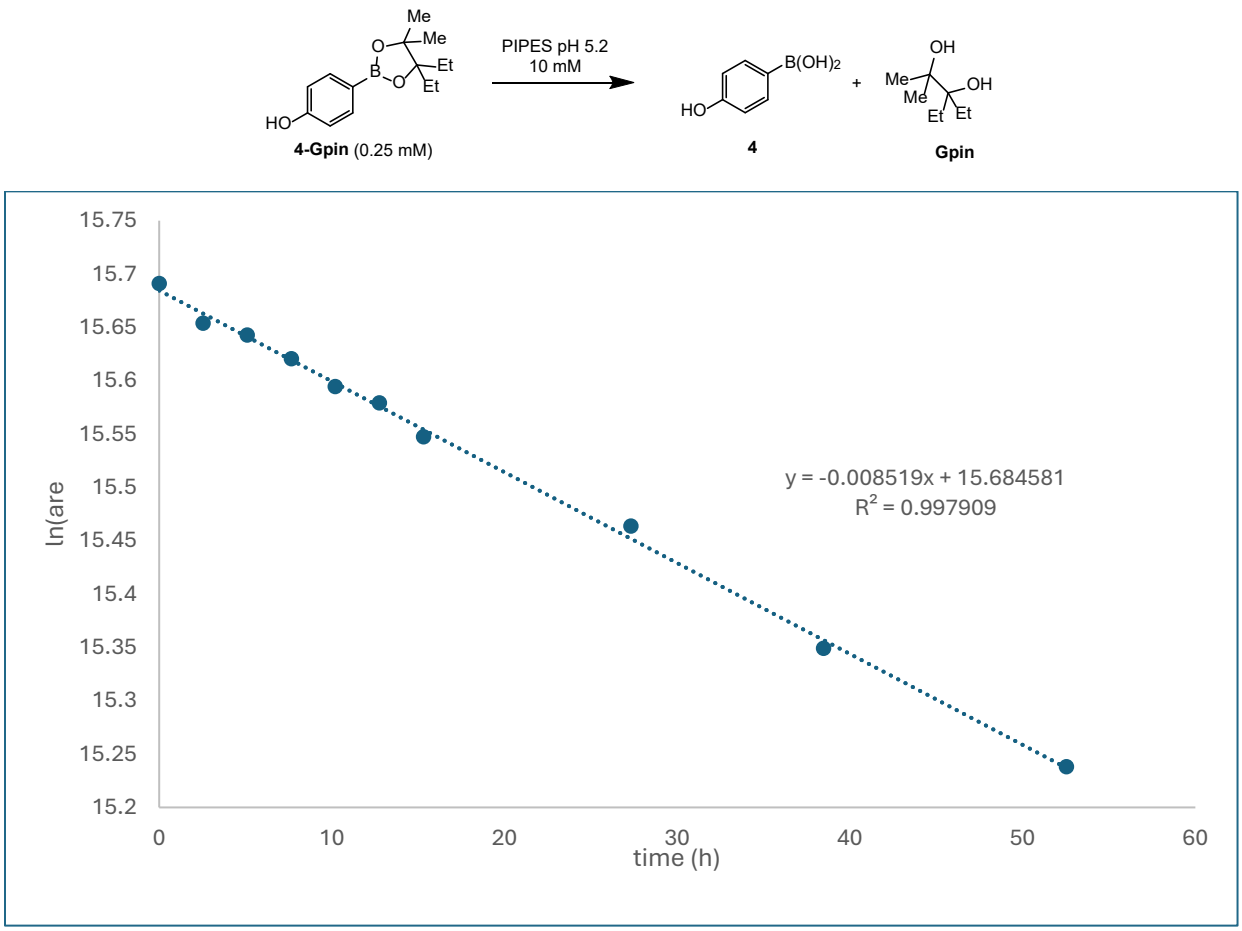

Figure S72. Plot of ln[boronic ester peak area] versus time at pH 5.2 for boronic ester **4-Gpin**. Data were fitted to a first order decay model using linear regression. The slope of the best-fit line corresponds to the pseudo-first order rate constant (k), from which the hydrolysis half-life ($t_{1/2}$) of 79.7 h was calculated.

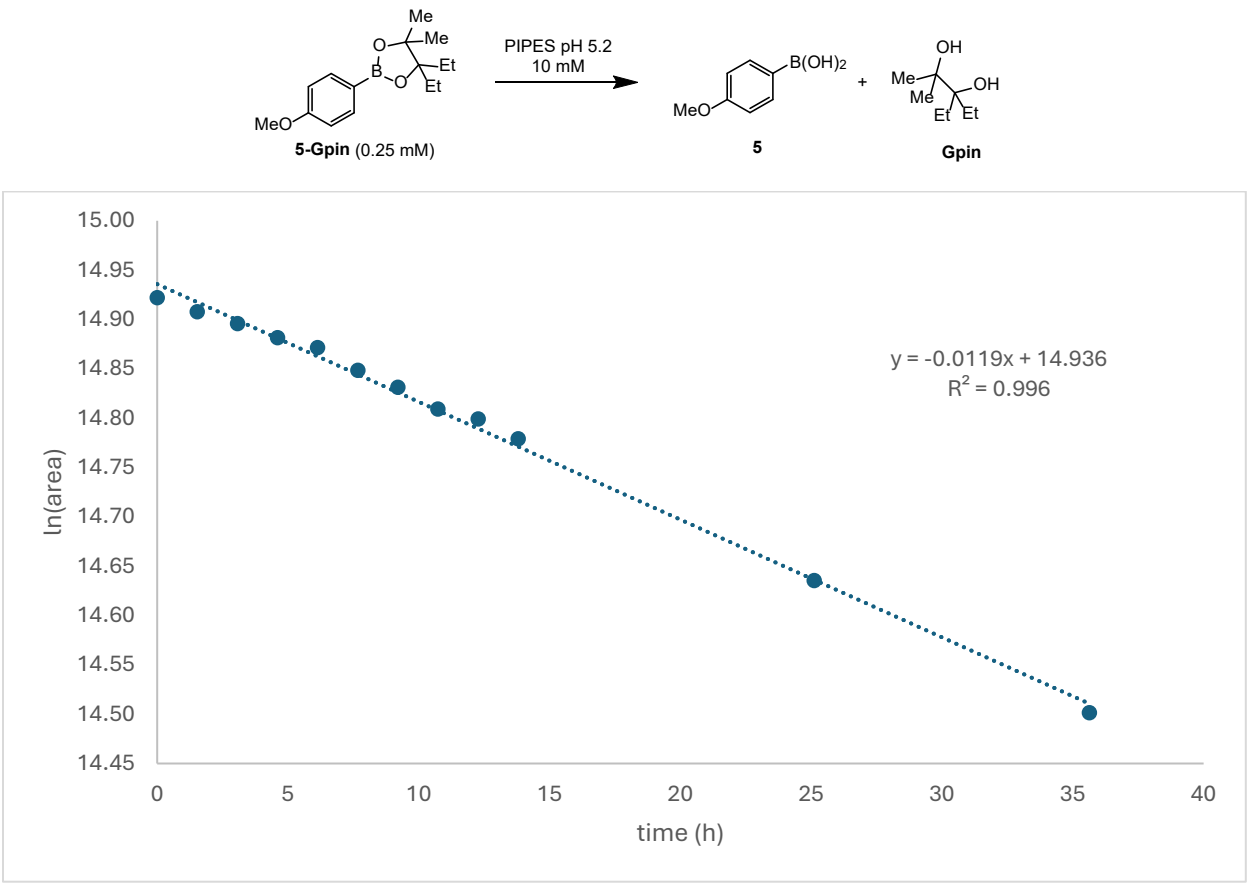

Figure S73. Plot of ln[boronic ester peak area] versus time at pH 5.2 for boronic ester **5-Gpin**. Data were fitted to a first order decay model using linear regression. The slope of the best-fit line corresponds to the pseudo-first order rate constant (k), from which the hydrolysis half-life ($t_{1/2}$) of 58.7 h was calculated.

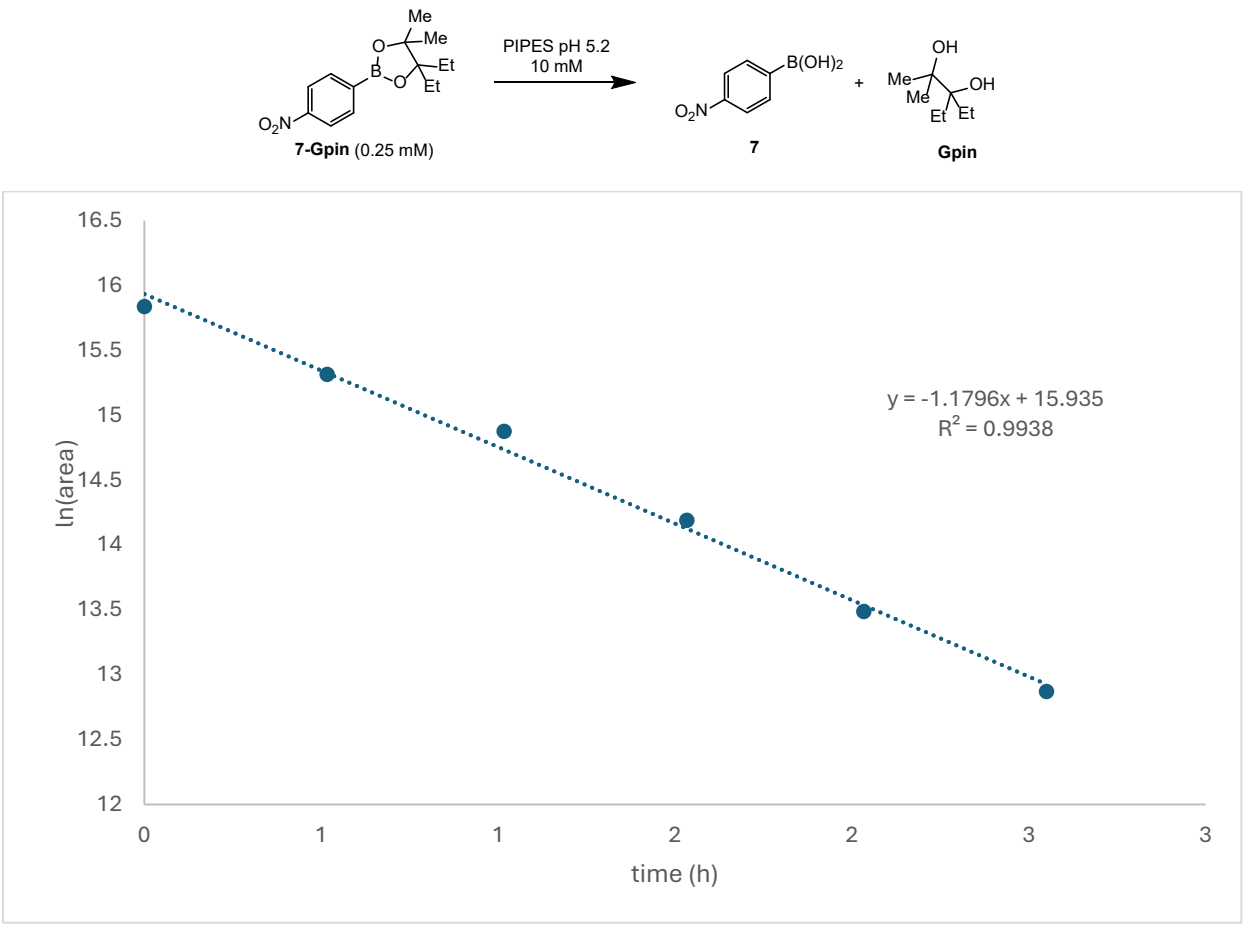

Figure S74. Plot of ln[boronic ester peak area] versus time at pH 5.2 for boronic ester **7-Gpin**. Data were fitted to a first order decay model using linear regression. The slope of the best-fit line corresponds to the pseudo-first order rate constant (k), from which the hydrolysis half-life ($t_{1/2}$) of 0.6 h was calculated.

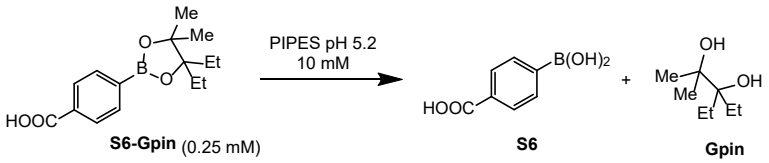

S6-Gpin (0.25 mM) **S6** **Gpin**

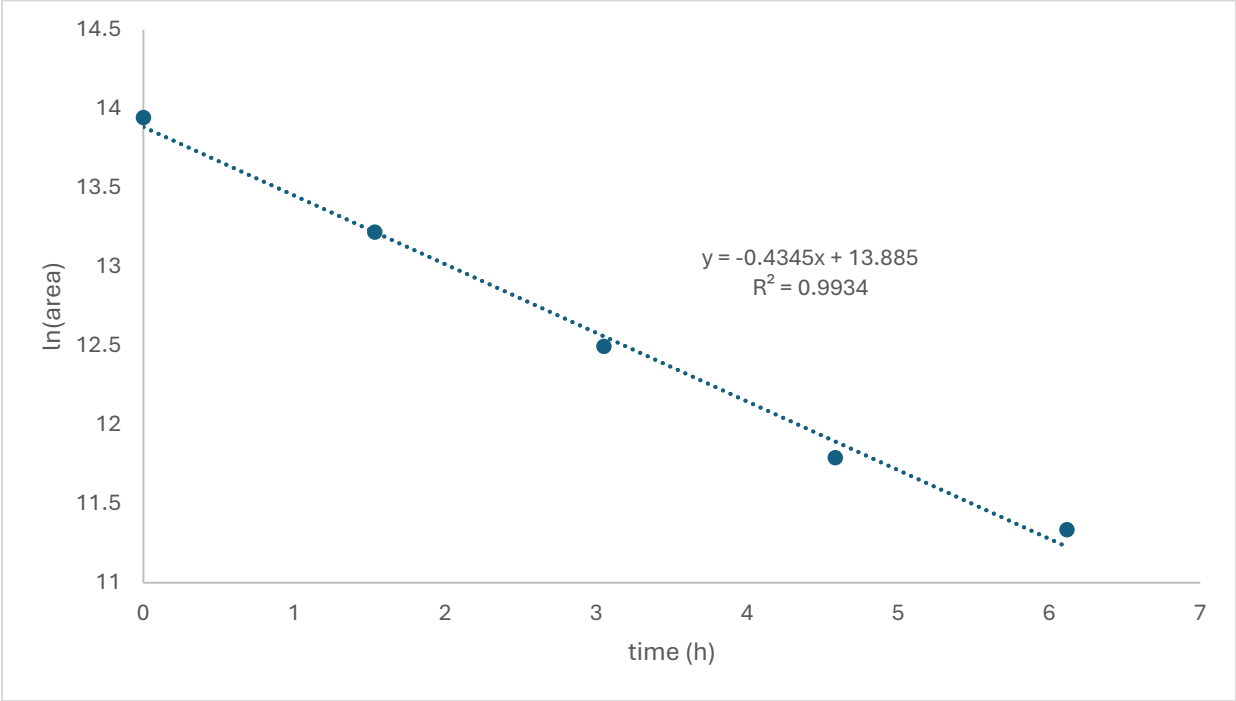

Figure S75. Plot of ln[boronic ester peak area] versus time at pH 5.2 for boronic ester **S6-Gpin**. Data were fitted to a first order decay model using linear regression. The slope of the best-fit line corresponds to the pseudo-first order rate constant (k), from which the hydrolysis half-life ($t_{1/2}$) of 1.6 h was calculated.

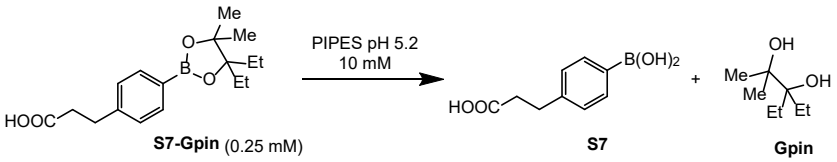

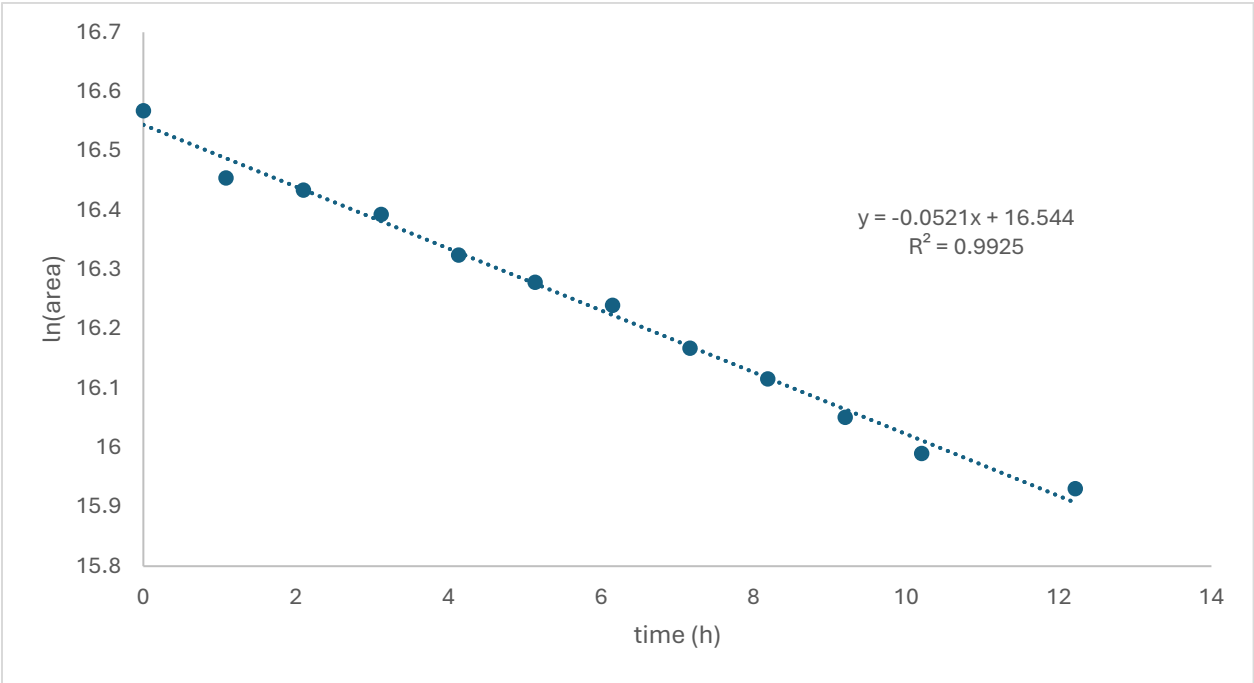

Figure S76. Plot of ln[boronic ester peak area] versus time at pH 5.2 for boronic ester **S7-Gpin**. Data were fitted to a first order decay model using linear regression. The slope of the best-fit line corresponds to the pseudo-first order rate constant (k), from which the hydrolysis half-life ($t_{1/2}$) of 13.6 h was calculated.

For figure 6

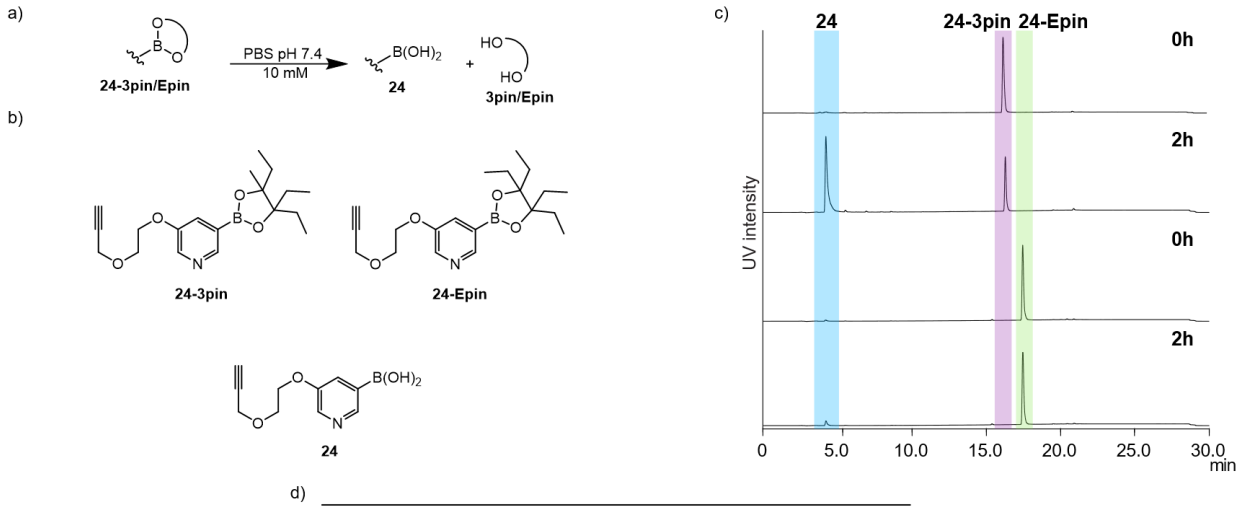

d)

	24-3pin (2 h)		24-Epin (2 h)	
	24-3Pin	24	24-EPin	24
Area	2361381	7419298	6768754	145192
%	**21.0**	**79.0**	**97.9**	**2.1**

Figure S77. Hydrolysis studies of esters **24-3pin** and **24-Epin**. a) Hydrolysis conditions. b) Structures of the esters and the free boronic acid. c) Overlay of the chromatograms used at 0 h and 2 h for the measurement of the hydrolysis of **24-3pin** and **24-Epin**. d) Integrated area of the corresponding esters and free-boronic acid probes used to determine the hydrolysis percentage.

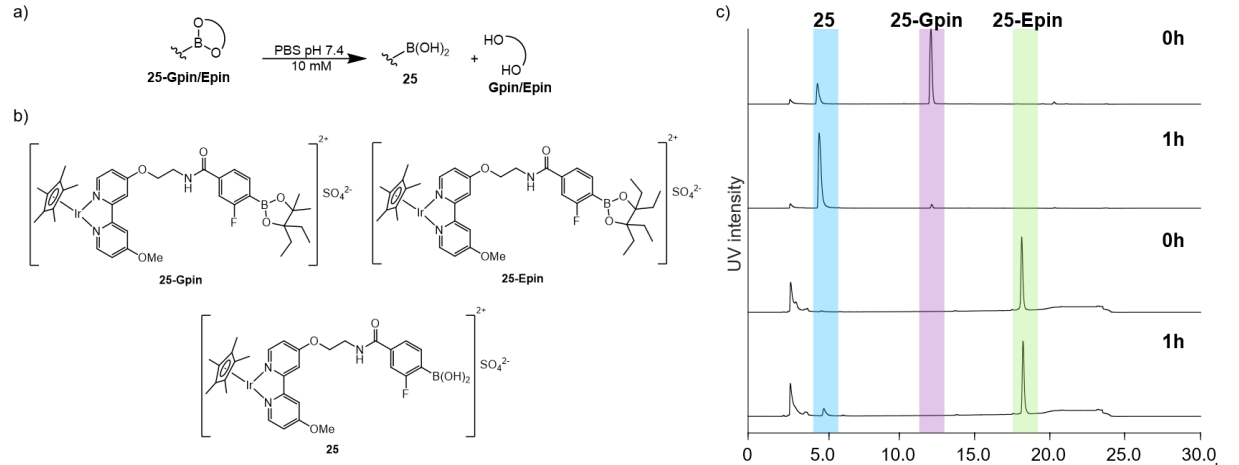

d)

	25-Gpin (1 h)		25-Epin (1 h)	
	25-GPin	25	25-EPin	25
Area	328771	7302400	1633800	24425
%	**4.3**	**95.7**	**98.5**	**1.5**

Figure S78. Hydrolysis studies of esters **25-Gpin** and **25-Epin**. a) Hydrolysis conditions. b) Structures of the esters and the free boronic acid. c) Overlay of the chromatograms used at 0 h and 1 h for the measurement of the hydrolysis of **25-Gpin** and **25-Epin**. d) Integrated area of the corresponding esters and free-boronic acid probes used to determine the hydrolysis percentage.

For figure 7

Figure S79. B_2pin_2 (B) and B_2Gpin_2 (G) TLC curcumin stain analysis using 10% ethyl acetate in hexanes as an eluent.

For table 1

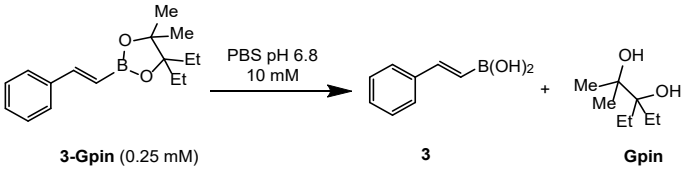

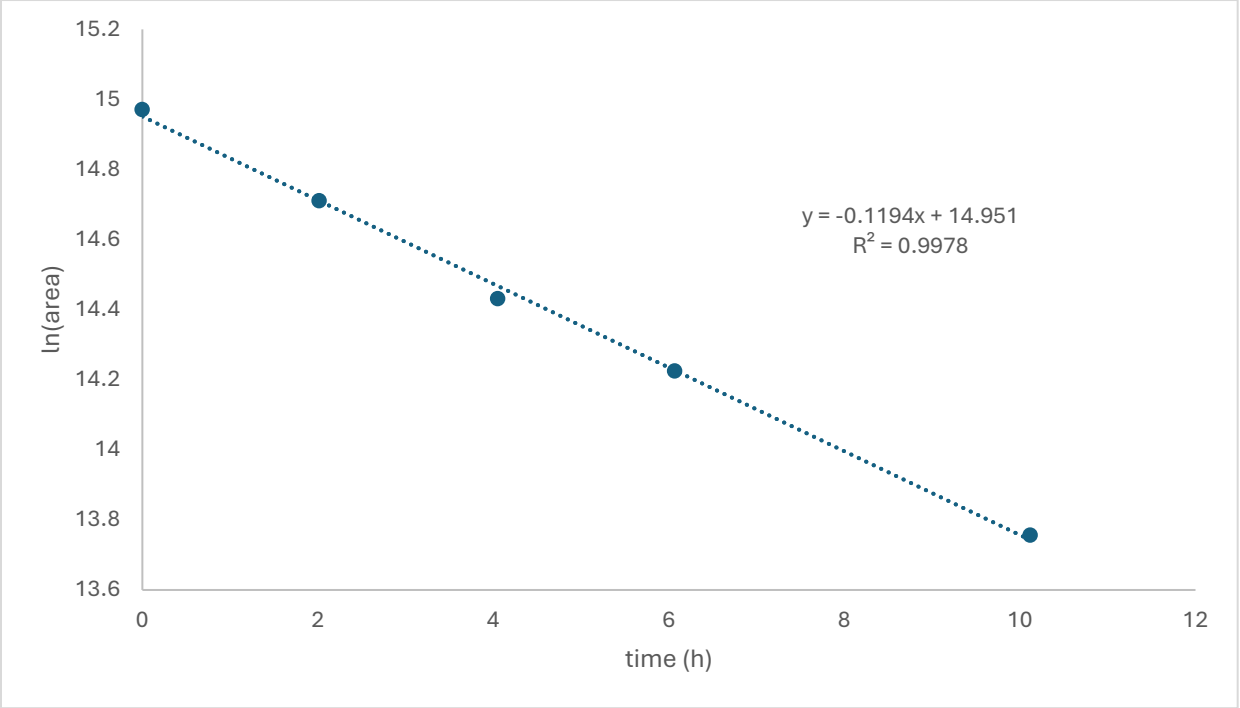

Figure S80. Plot of ln[boronic ester peak area] versus time at pH 6.8 for boronic ester **3-Gpin**. Data were fitted to a first order decay model using linear regression. The slope of the best-fit line corresponds to the pseudo-first order rate constant (k), from which the hydrolysis half-life ($t_{1/2}$) of 5.8 h was calculated.

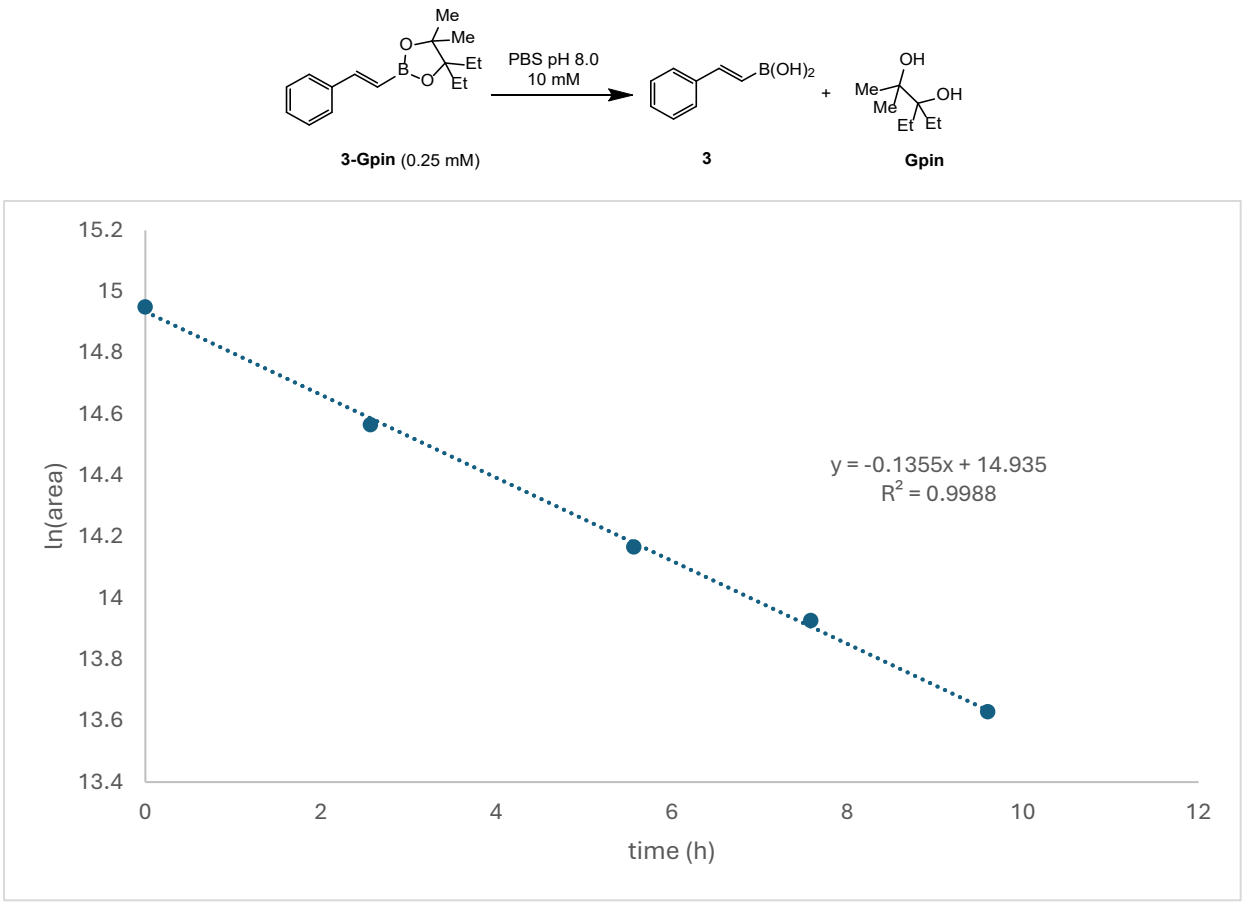

Figure S81. Plot of ln[boronic ester peak area] versus time at pH 8.0 for boronic ester **3-Gpin**. Data were fitted to a first order decay model using linear regression. The slope of the best-fit line corresponds to the pseudo-first order rate constant (k), from which the hydrolysis half-life ($t_{1/2}$) of 5.1 h was calculated.

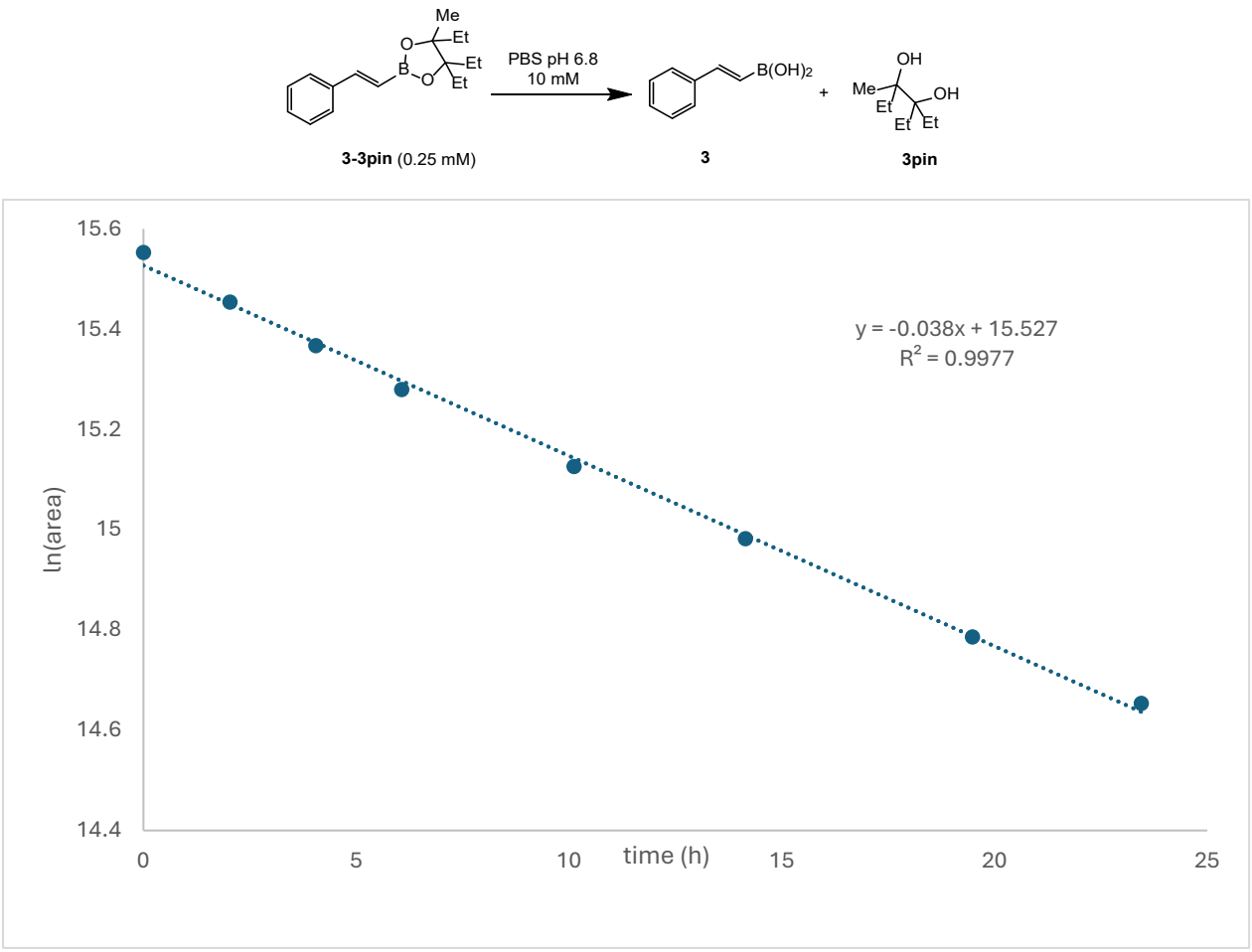

Figure S82. Plot of ln[boronic ester peak area] versus time at pH 6.8 for boronic ester **3-3pin**. Data were fitted to a first order decay model using linear regression. The slope of the best-fit line corresponds to the pseudo-first order rate constant (k), from which the hydrolysis half-life ($t_{1/2}$) of 18.1 h was calculated.

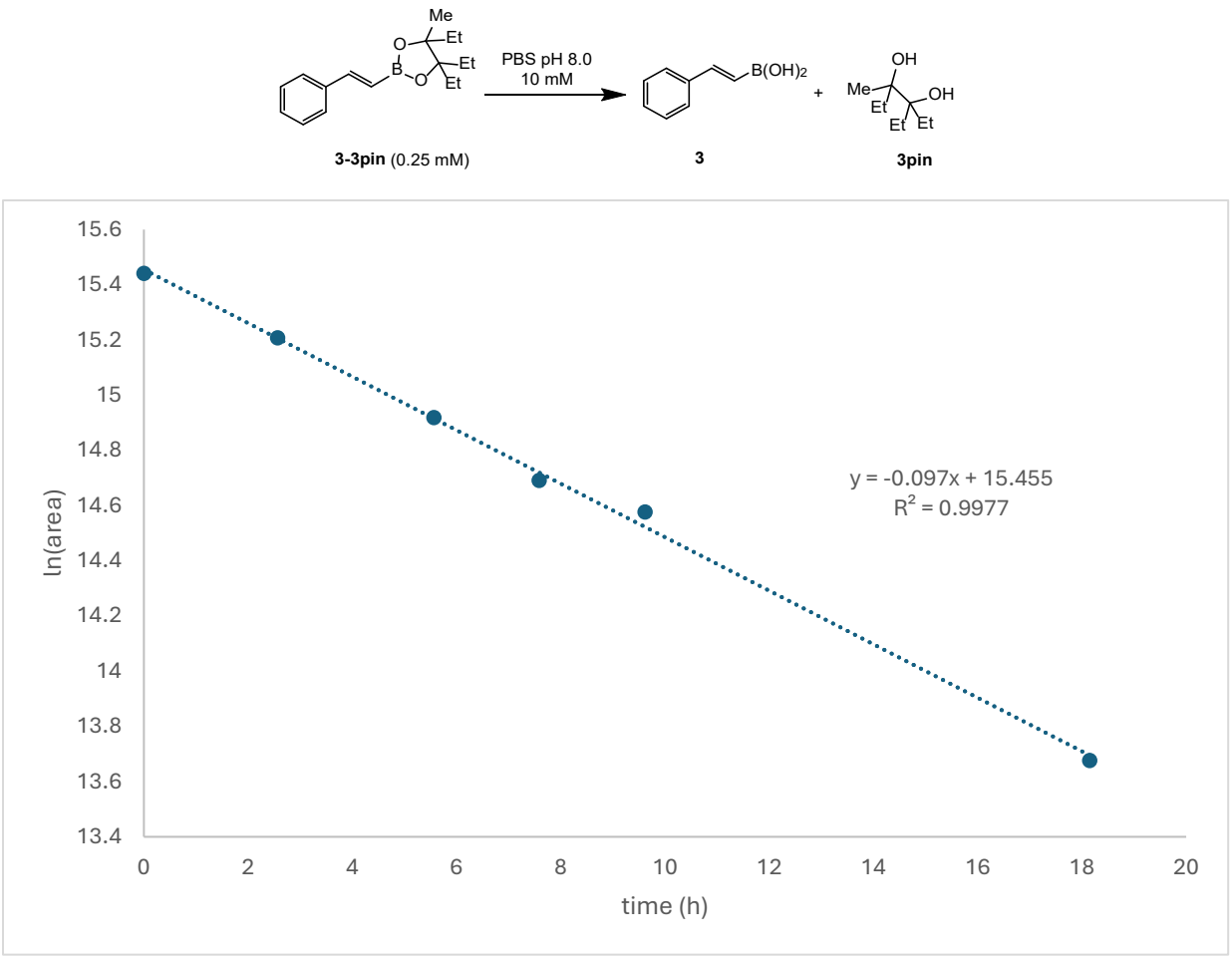

Figure S83. Plot of ln[boronic ester peak area] versus time at pH 8.0 for boronic ester **3-3pin**. Data were fitted to a first order decay model using linear regression. The slope of the best-fit line corresponds to the pseudo-first order rate constant (k), from which the hydrolysis half-life ($t_{1/2}$) of 7.2 h was calculated.

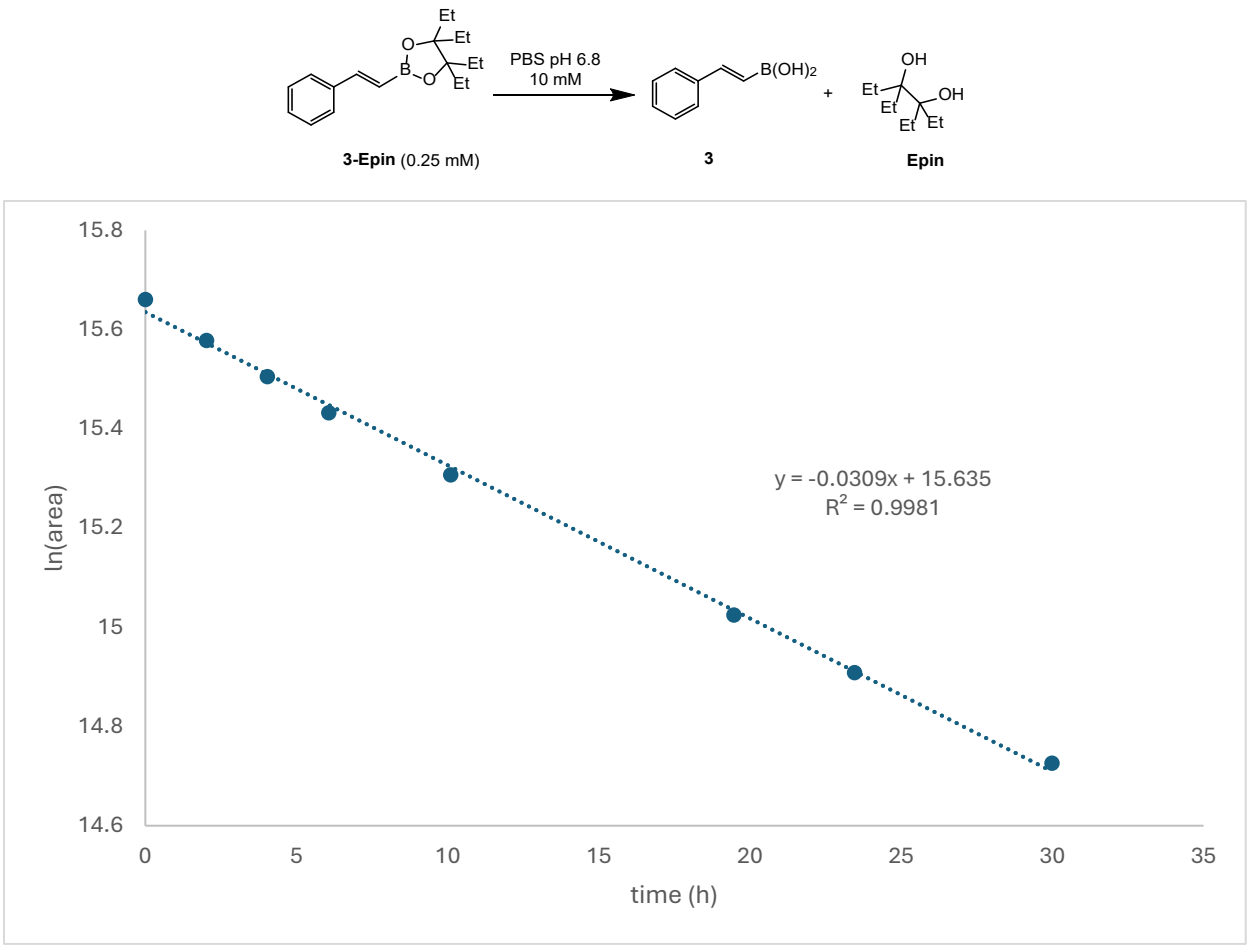

Figure S84. Plot of ln[boronic ester peak area] versus time at pH 6.8 for boronic ester **3-Epin**. Data were fitted to a first order decay model using linear regression. The slope of the best-fit line corresponds to the pseudo-first order rate constant (k), from which the hydrolysis half-life ($t_{1/2}$) of 22.3 h was calculated.

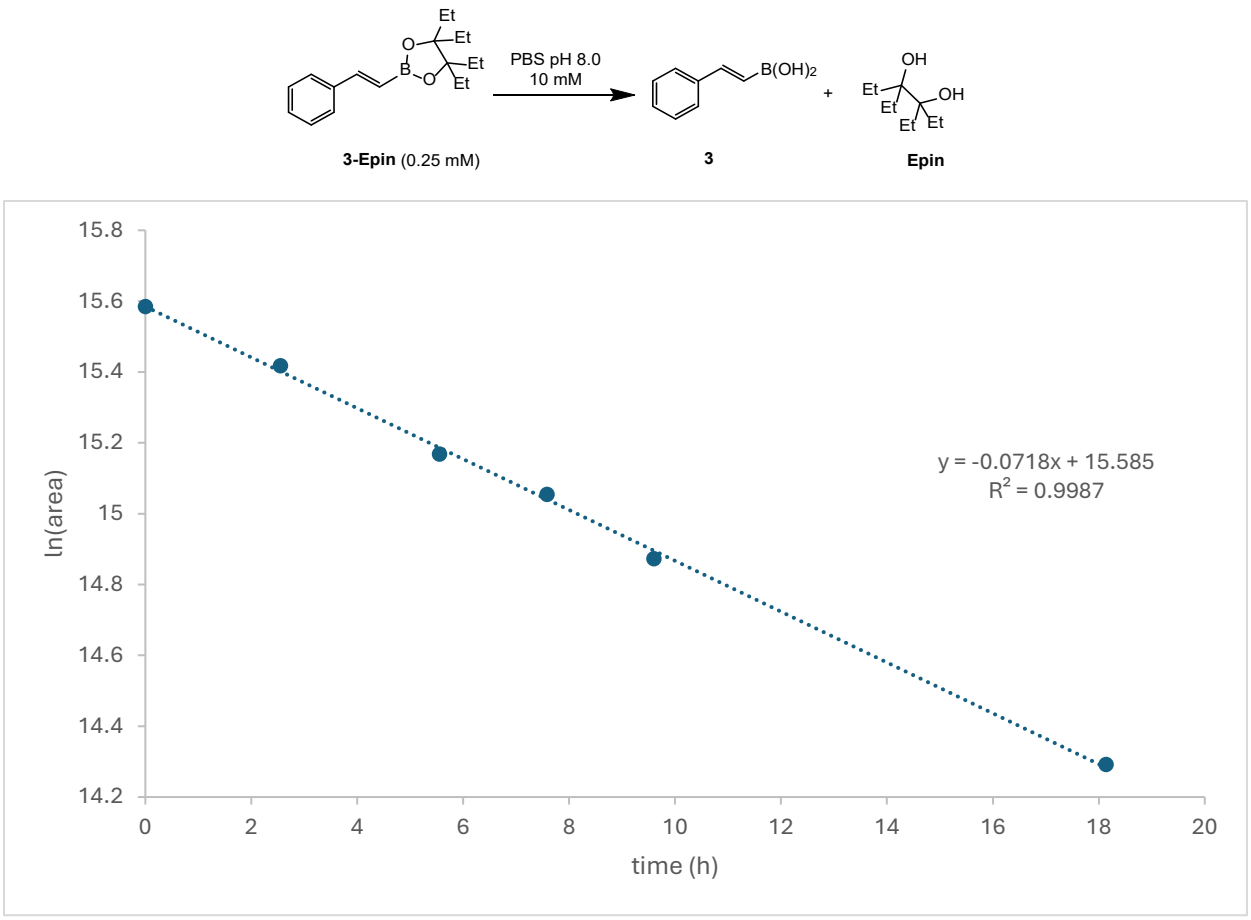

Figure S85. Plot of ln[boronic ester peak area] versus time at pH 8.0 for boronic ester **5-Epin**. Data were fitted to a first order decay model using linear regression. The slope of the best-fit line corresponds to the pseudo-first order rate constant (k), from which the hydrolysis half-life ($t_{1/2}$) of 9.6 h was calculated.

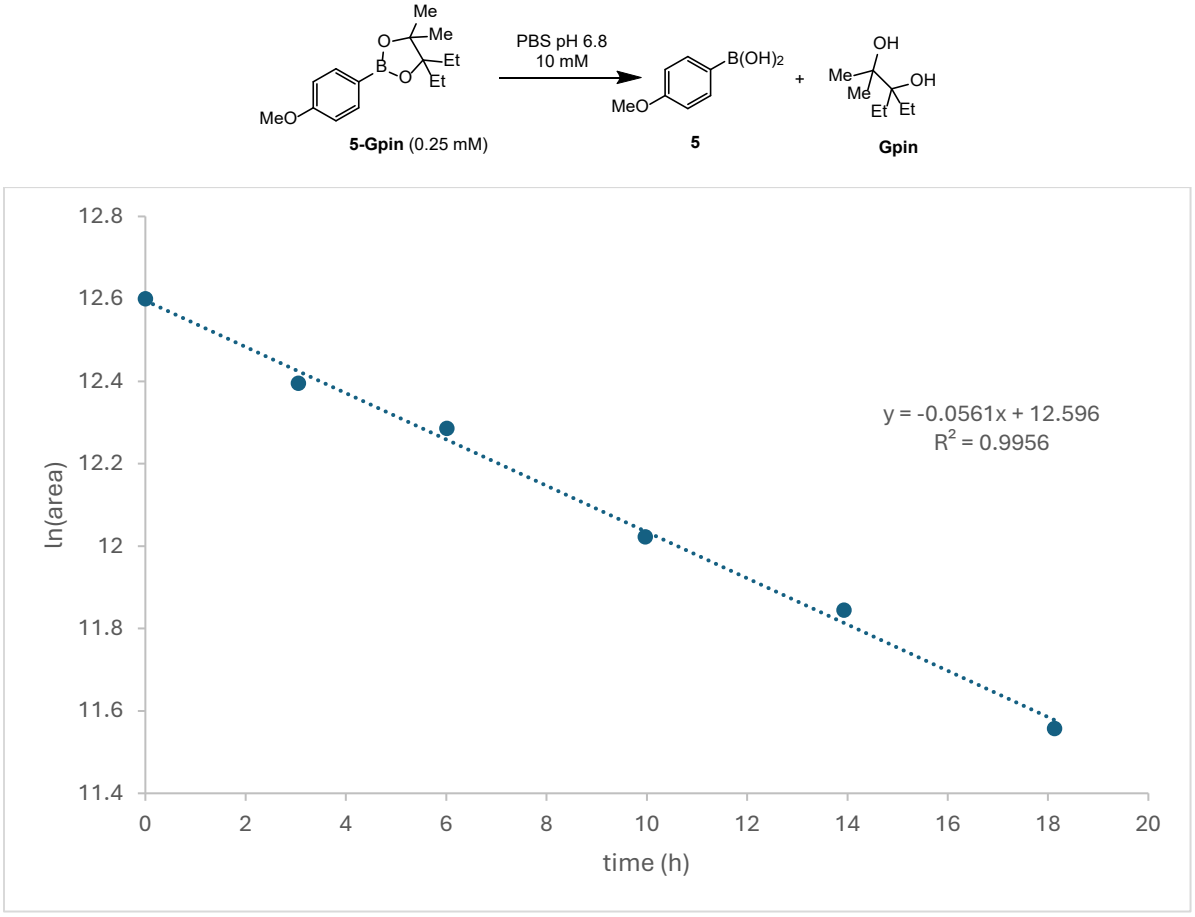

Figure S86. Plot of ln[boronic ester peak area] versus time at pH 6.8 for boronic ester **5-Gpin**. Data were fitted to a first order decay model using linear regression. The slope of the best-fit line corresponds to the pseudo-first order rate constant (k), from which the hydrolysis half-life ($t_{1/2}$) of 12.4 h was calculated.

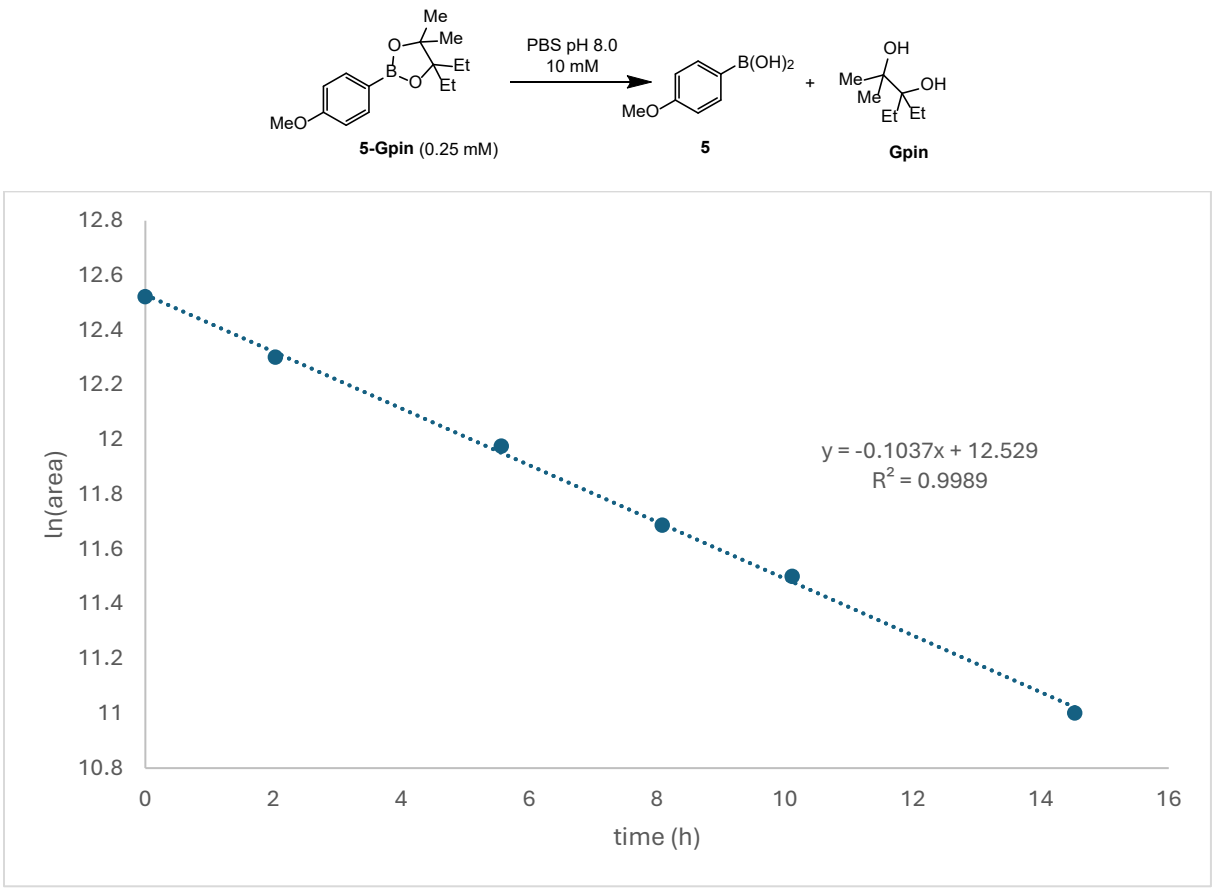

Figure S87. Plot of ln[boronic ester peak area] versus time at pH 8.0 for boronic ester **5-Gpin**. Data were fitted to a first order decay model using linear regression. The slope of the best-fit line corresponds to the pseudo-first order rate constant (k), from which the hydrolysis half-life ($t_{1/2}$) of 6.7 h was calculated.

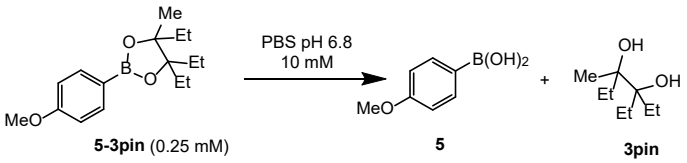

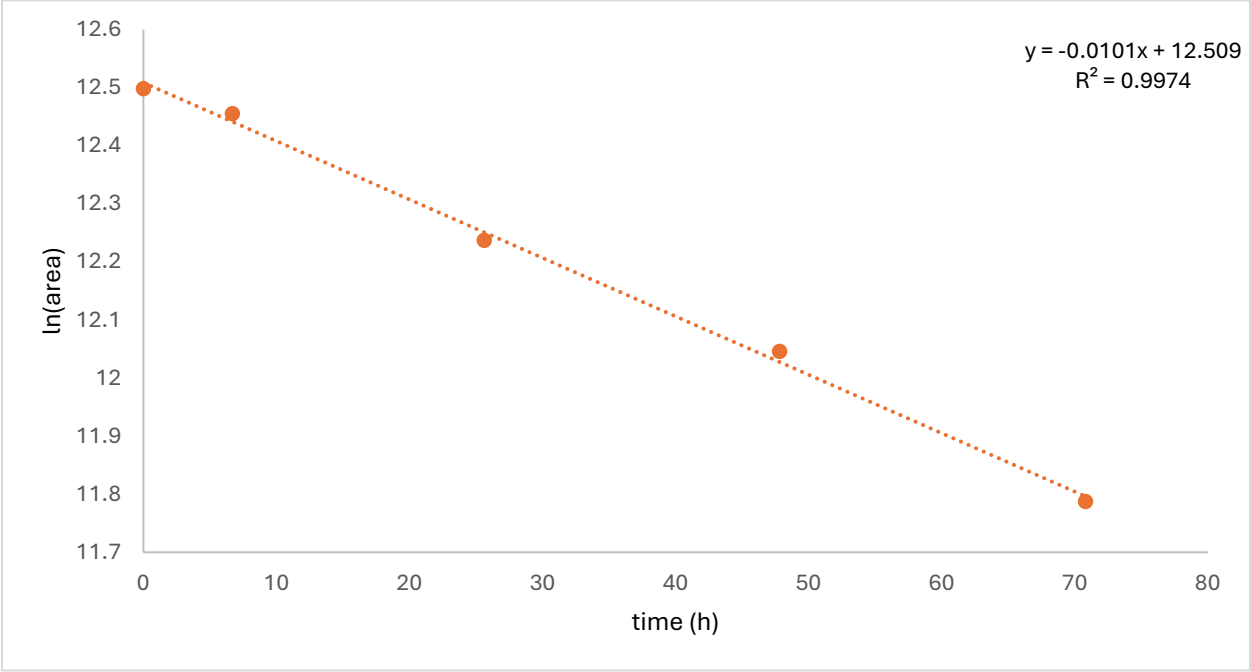

Figure S88. Plot of ln[boronic ester peak area] versus time at pH 6.8 for boronic ester **5-3pin**. Data were fitted to a first order decay model using linear regression. The slope of the best-fit line corresponds to the pseudo-first order rate constant (k), from which the hydrolysis half-life ($t_{1/2}$) of 68.6 h was calculated.

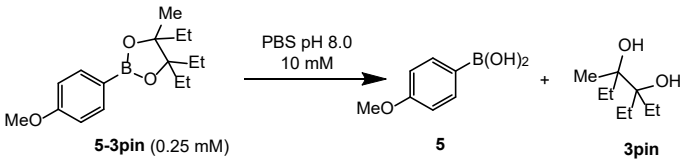

5-3pin (0.25 mM) **5** **3pin**

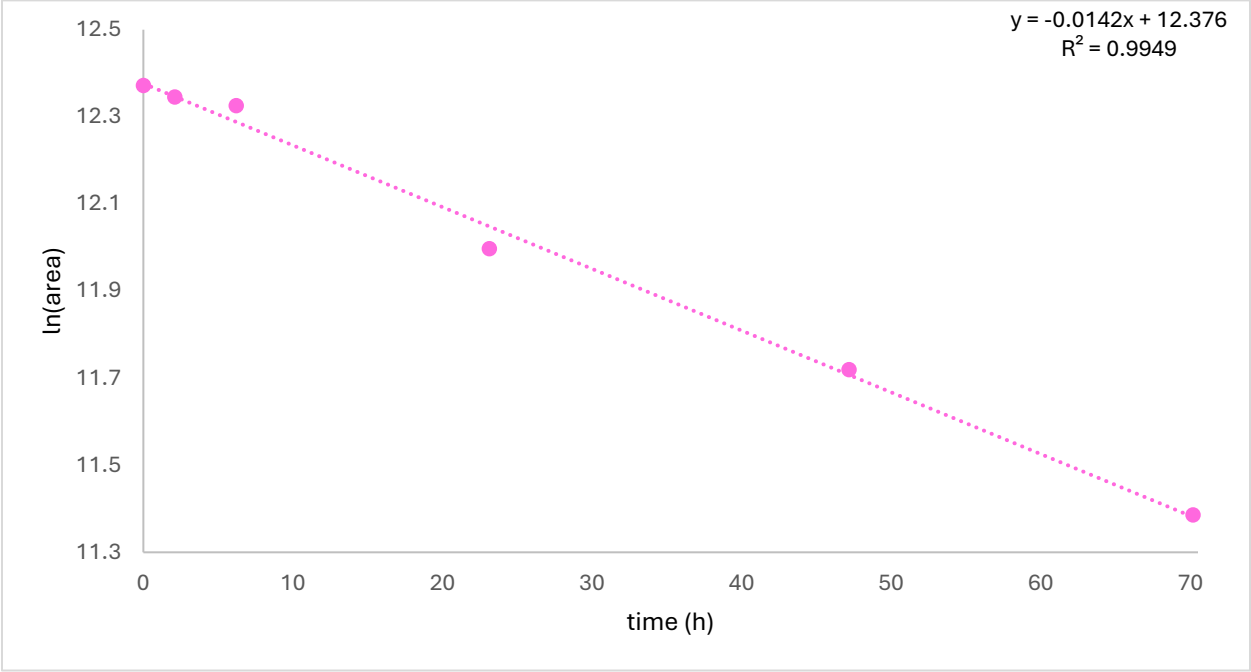

Figure S89. Plot of ln[boronic ester peak area] versus time at pH 8.0 for boronic ester **5-3pin**. Data were fitted to a first order decay model using linear regression. The slope of the best-fit line corresponds to the pseudo-first order rate constant (k), from which the hydrolysis half-life ($t_{1/2}$) of 48.8 h was calculated.

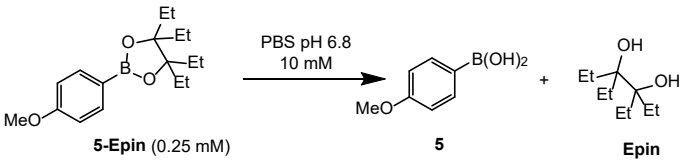

5-Epin (0.25 mM) **5** **Epin**

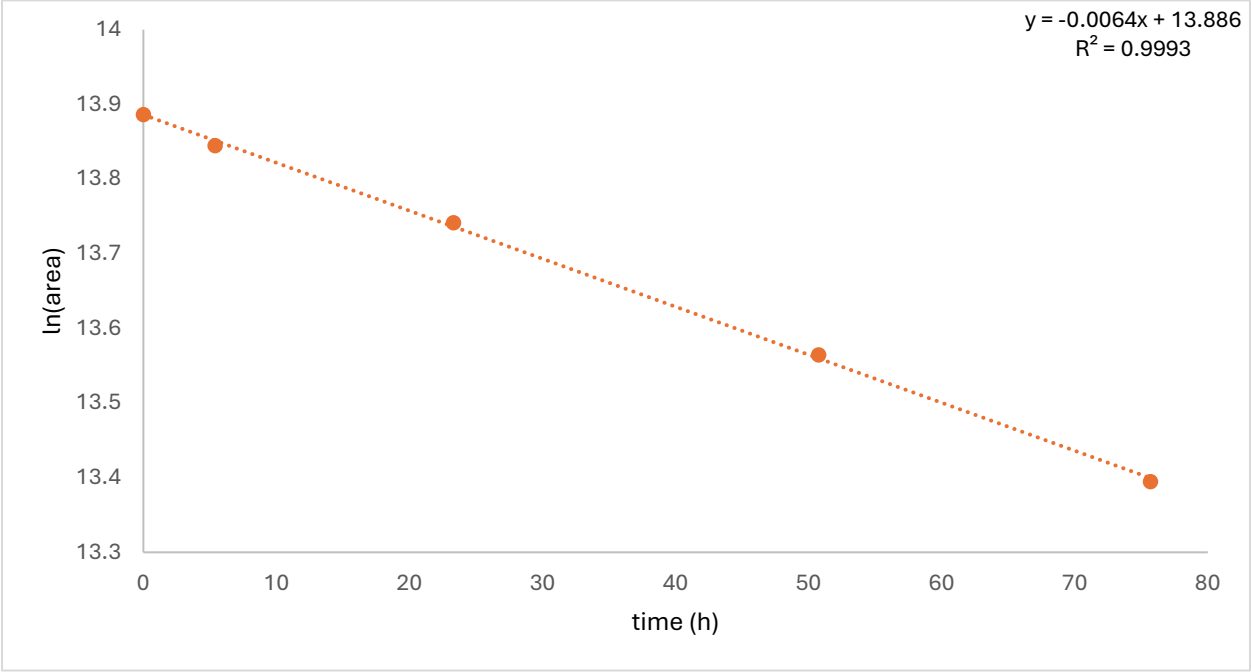

Figure S90. Plot of ln[boronic ester peak area] versus time at pH 6.8 for boronic ester **5-Epin**. Data were fitted to a first order decay model using linear regression. The slope of the best-fit line corresponds to the pseudo-first order rate constant (k), from which the hydrolysis half-life ($t_{1/2}$) of 111.8 h was calculated.

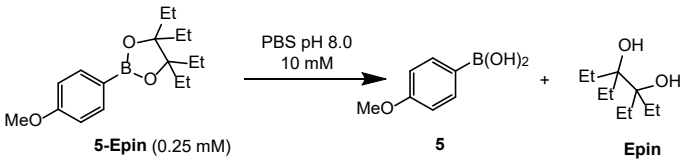

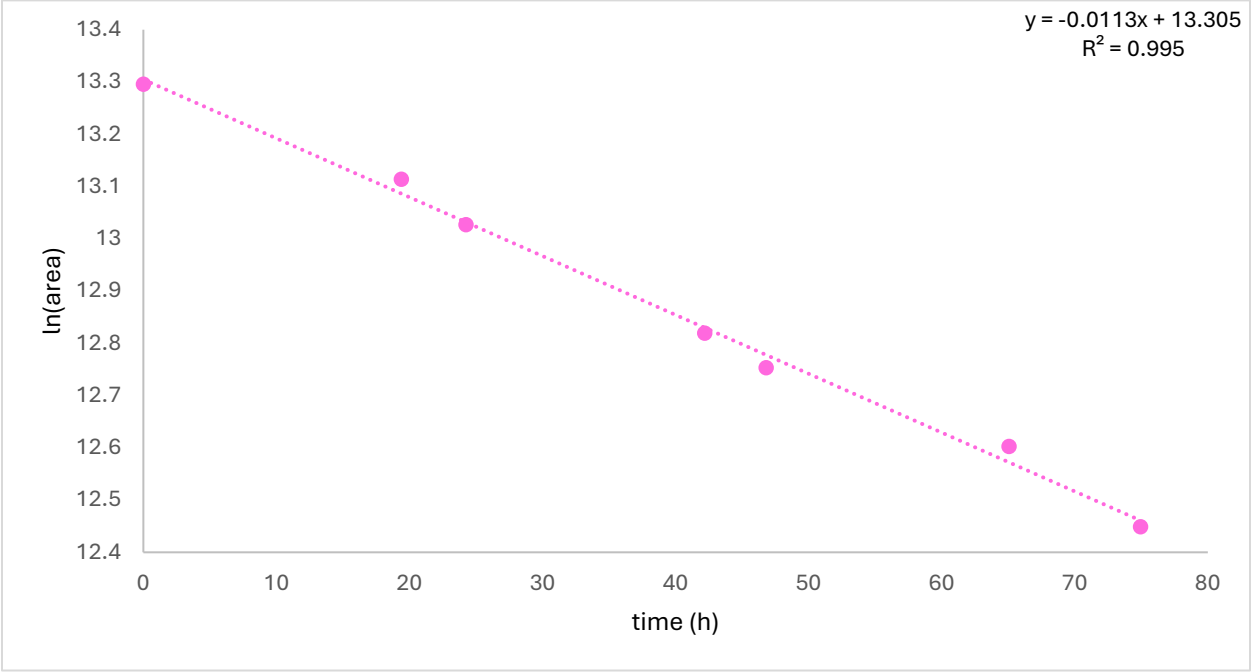

Figure S91. Plot of ln[boronic ester peak area] versus time at pH 8.0 for boronic ester 5-Epin. Data were fitted to a first order decay model using linear regression. The slope of the best-fit line corresponds to the pseudo-first order rate constant (k), from which the hydrolysis half-life ($t_{1/2}$) of 61.3 h was calculated.

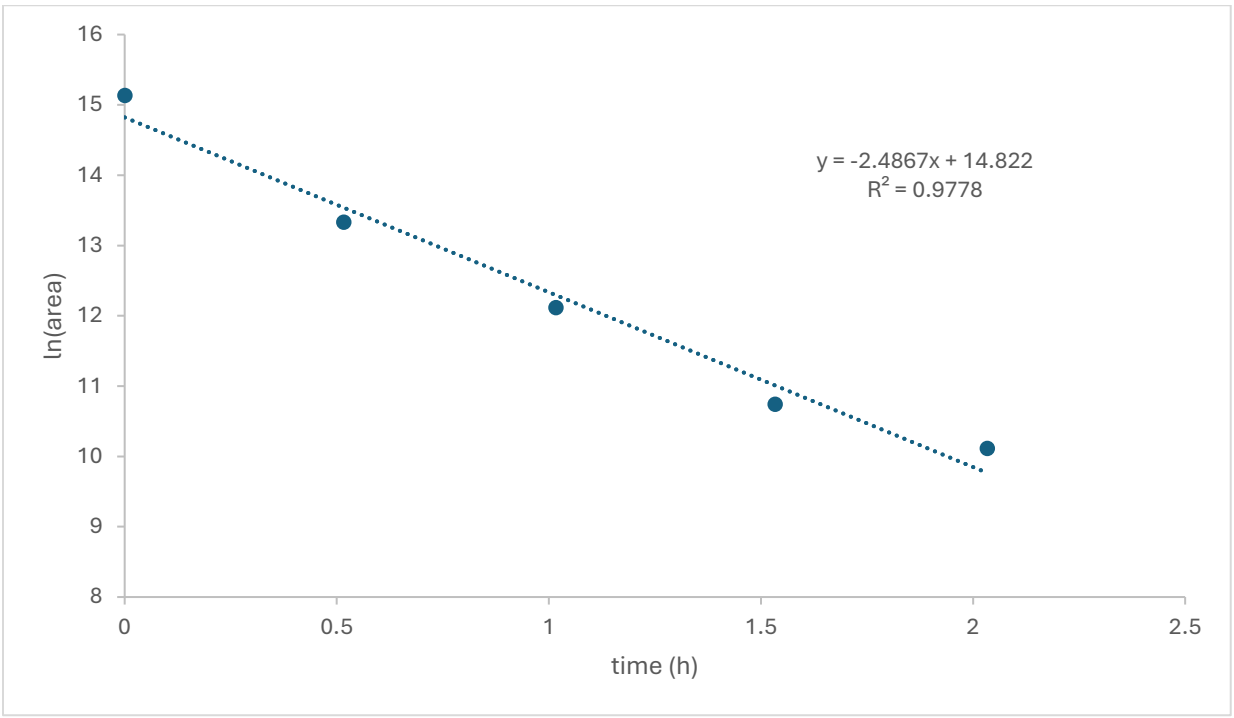

Figure S92. Plot of ln[boronic ester peak area] versus time at pH 6.8 for boronic ester **8-Gpin**. Data were fitted to a first order decay model using linear regression. The slope of the best-fit line corresponds to the pseudo-first order rate constant (k), from which the hydrolysis half-life ($t_{1/2}$) of 0.3 h was calculated.

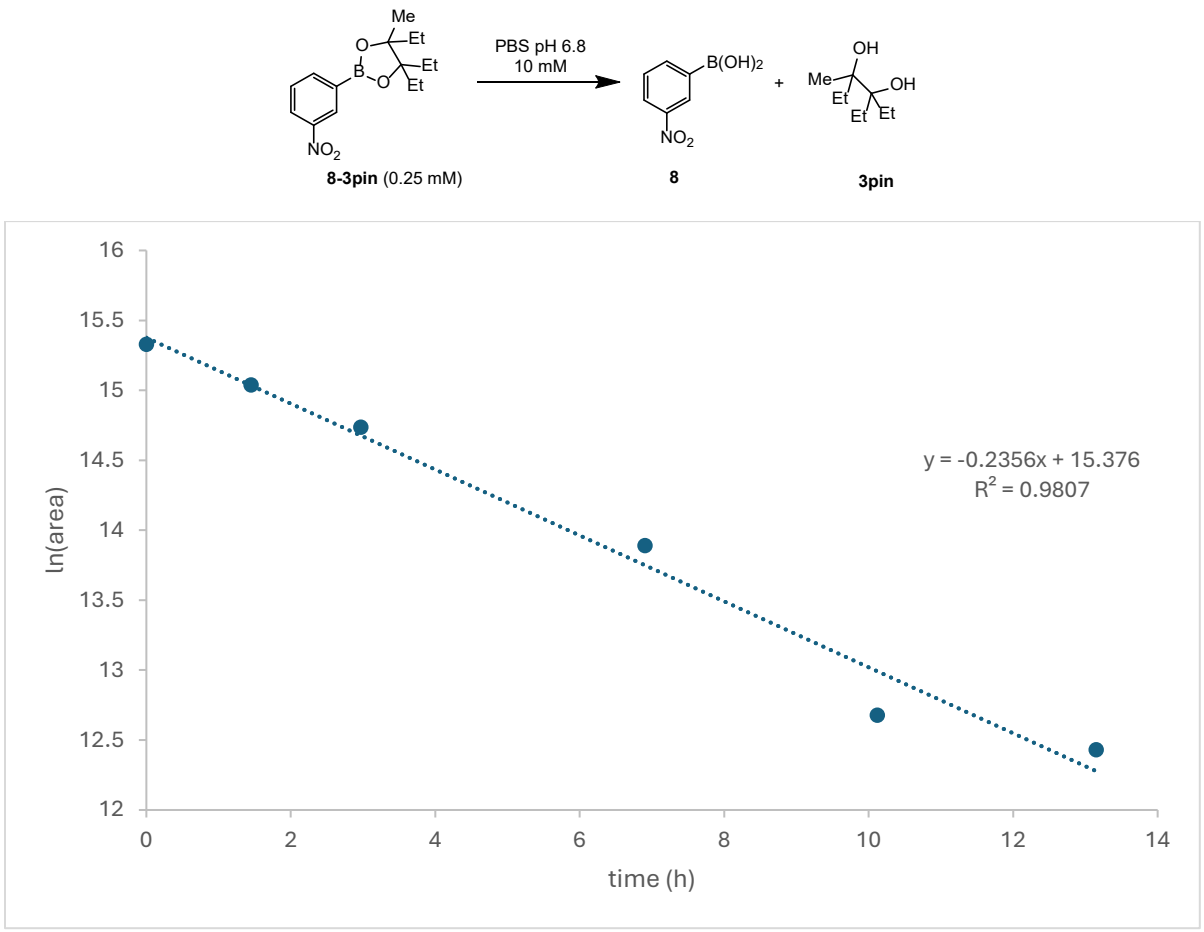

Figure S93. Plot of ln[boronic ester peak area] versus time at pH 6.8 for boronic ester **8-3pin**. Data were fitted to a first order decay model using linear regression. The slope of the best-fit line corresponds to the pseudo-first order rate constant (k), from which the hydrolysis half-life ($t_{1/2}$) of 2.9 h was calculated.

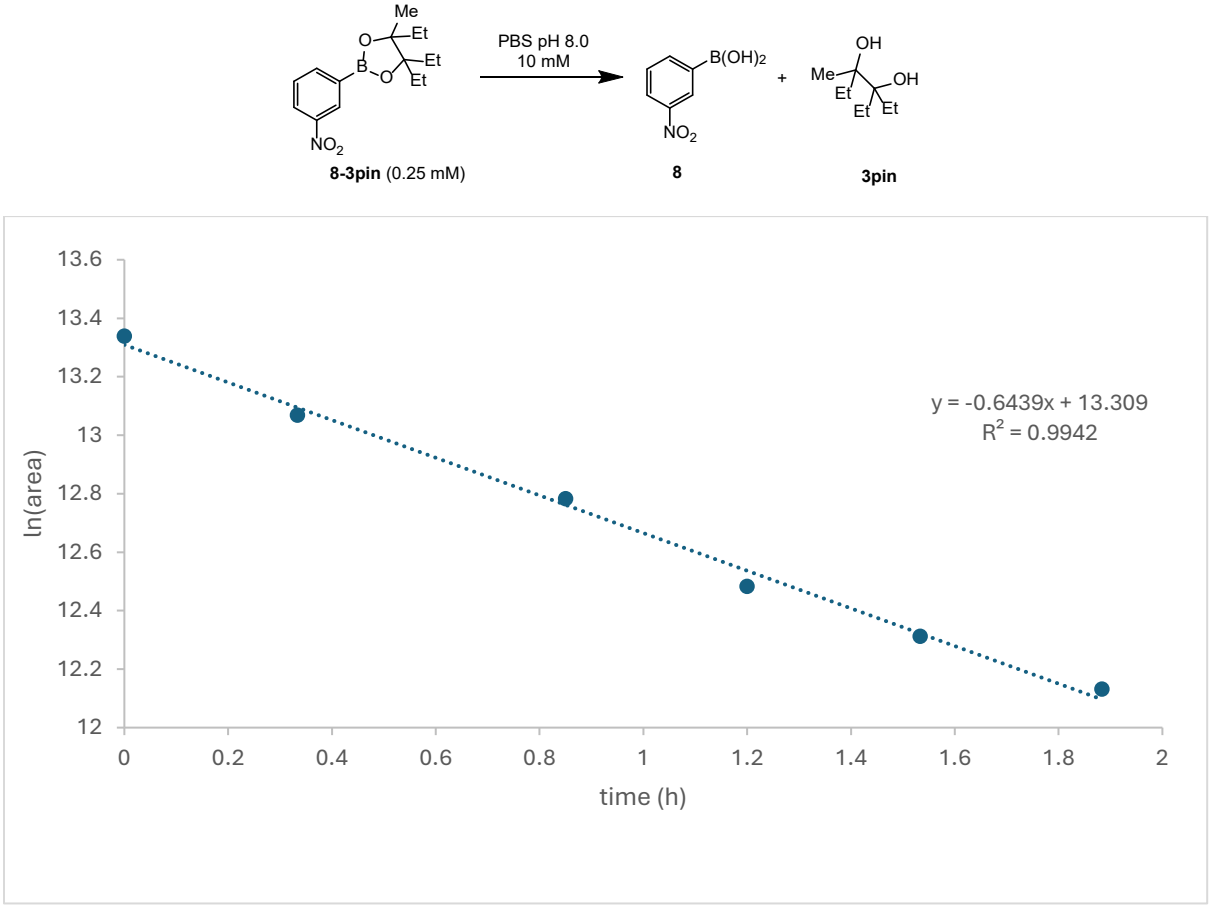

Figure S94. Plot of ln[boronic ester peak area] versus time at pH 8.0 for boronic ester **8-3pin**. Data were fitted to a first order decay model using linear regression. The slope of the best-fit line corresponds to the pseudo-first order rate constant (k), from which the hydrolysis half-life ($t_{1/2}$) of 1.1 h was calculated.

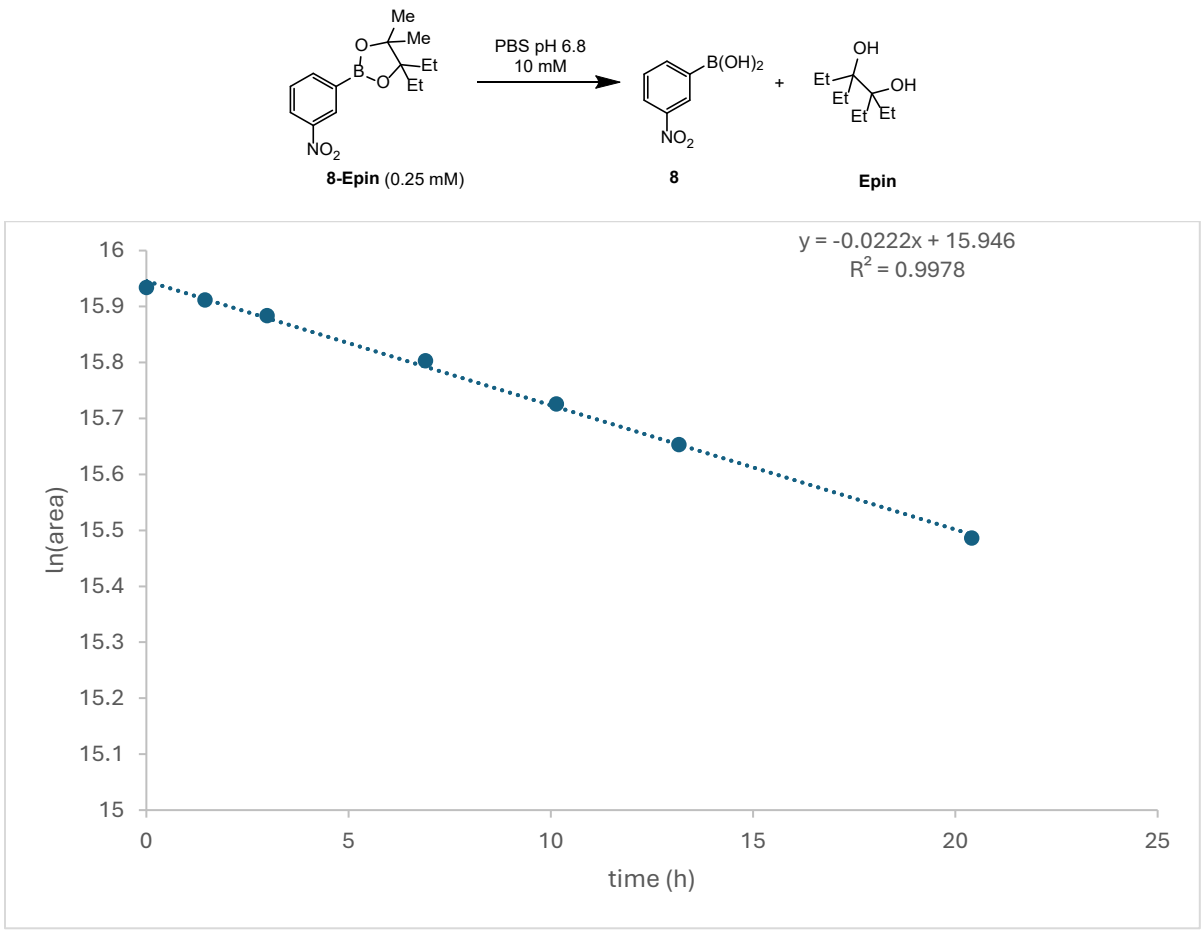

Figure S95. Plot of ln[boronic ester peak area] versus time at pH 6.8 for boronic ester **8-Epin**. Data were fitted to a first order decay model using linear regression. The slope of the best-fit line corresponds to the pseudo-first order rate constant (k), from which the hydrolysis half-life ($t_{1/2}$) of 31.5 h was calculated.

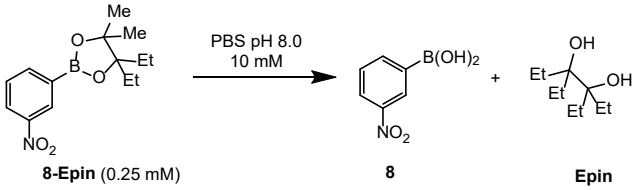

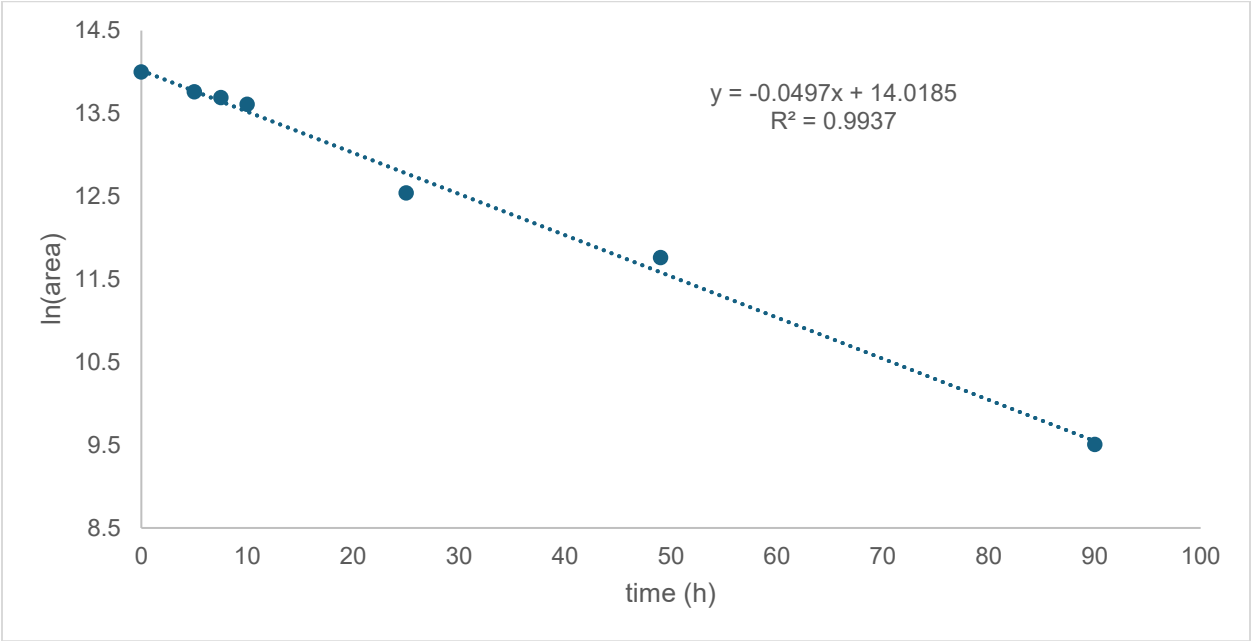

Figure S96. Plot of ln[boronic ester peak area] versus time at pH 8.0 for boronic ester **8-Epin**. Data were fitted to a first order decay model using linear regression. The slope of the best-fit line corresponds to the pseudo-first order rate constant (k), from which the hydrolysis half-life ($t_{1/2}$) of 13.8 h was calculated.

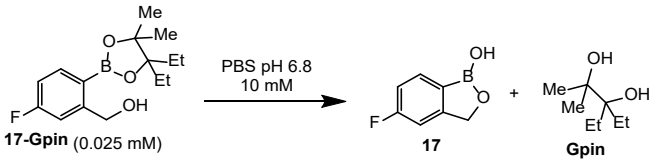

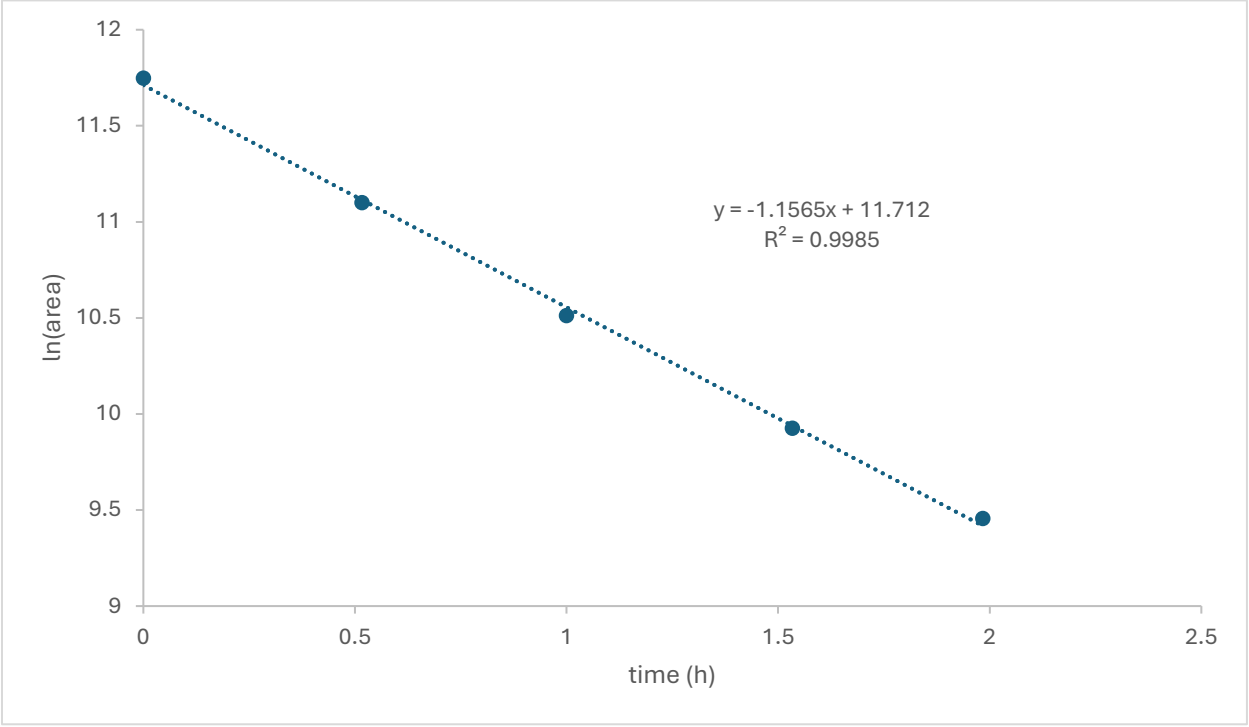

Figure S97. Plot of ln[boronic ester peak area] versus time for boronic ester **17-Gpin**. Data were fitted to a first order decay model using linear regression. The slope of the best-fit line corresponds to the pseudo-first order rate constant (k), from which the hydrolysis half-life ($t_{1/2}$) of 0.7 h was calculated.

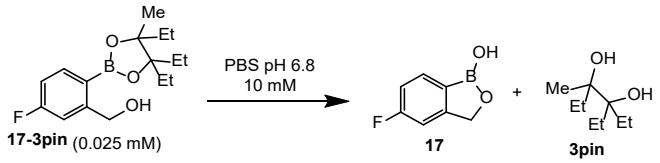

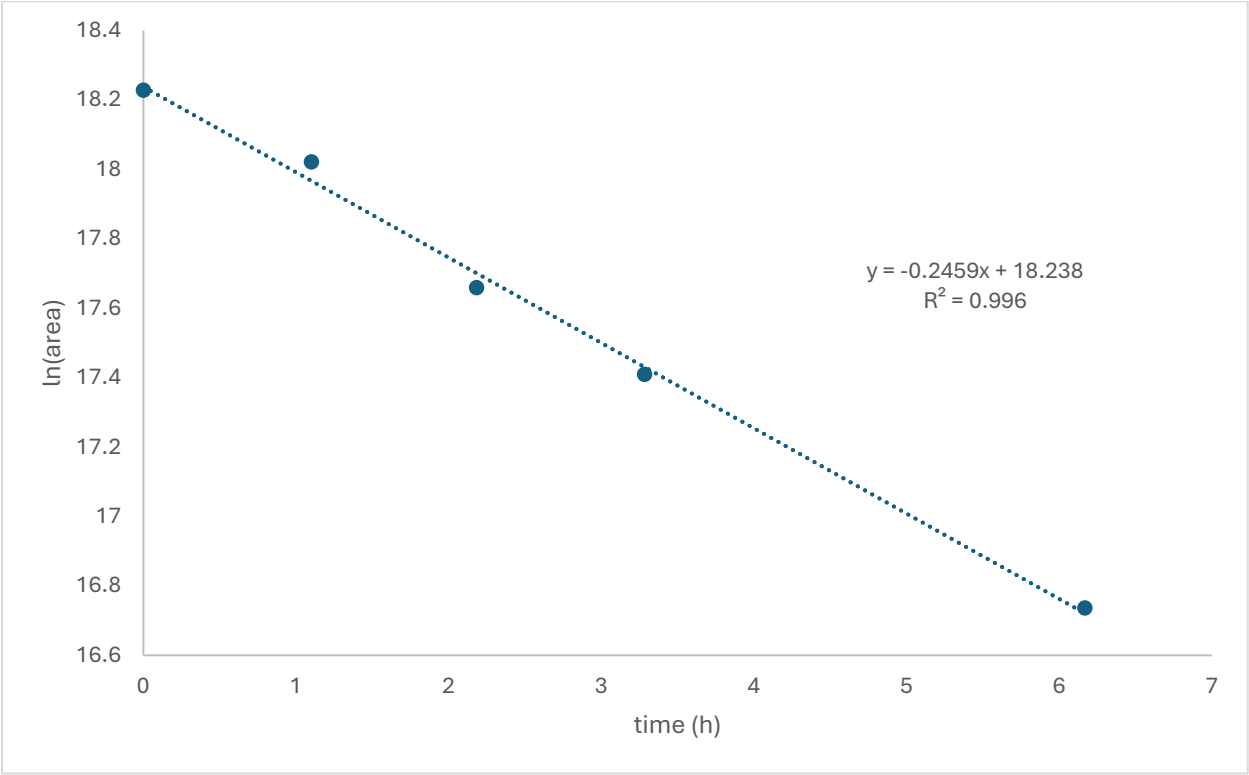

Figure S98. Plot of ln[boronic ester peak area] versus time at pH 6.8 for boronic ester **17-3pin**. Data were fitted to a first order decay model using linear regression. The slope of the best-fit line corresponds to the pseudo-first order rate constant (k), from which the hydrolysis half-life ($t_{1/2}$) of 2.8 h was calculated.

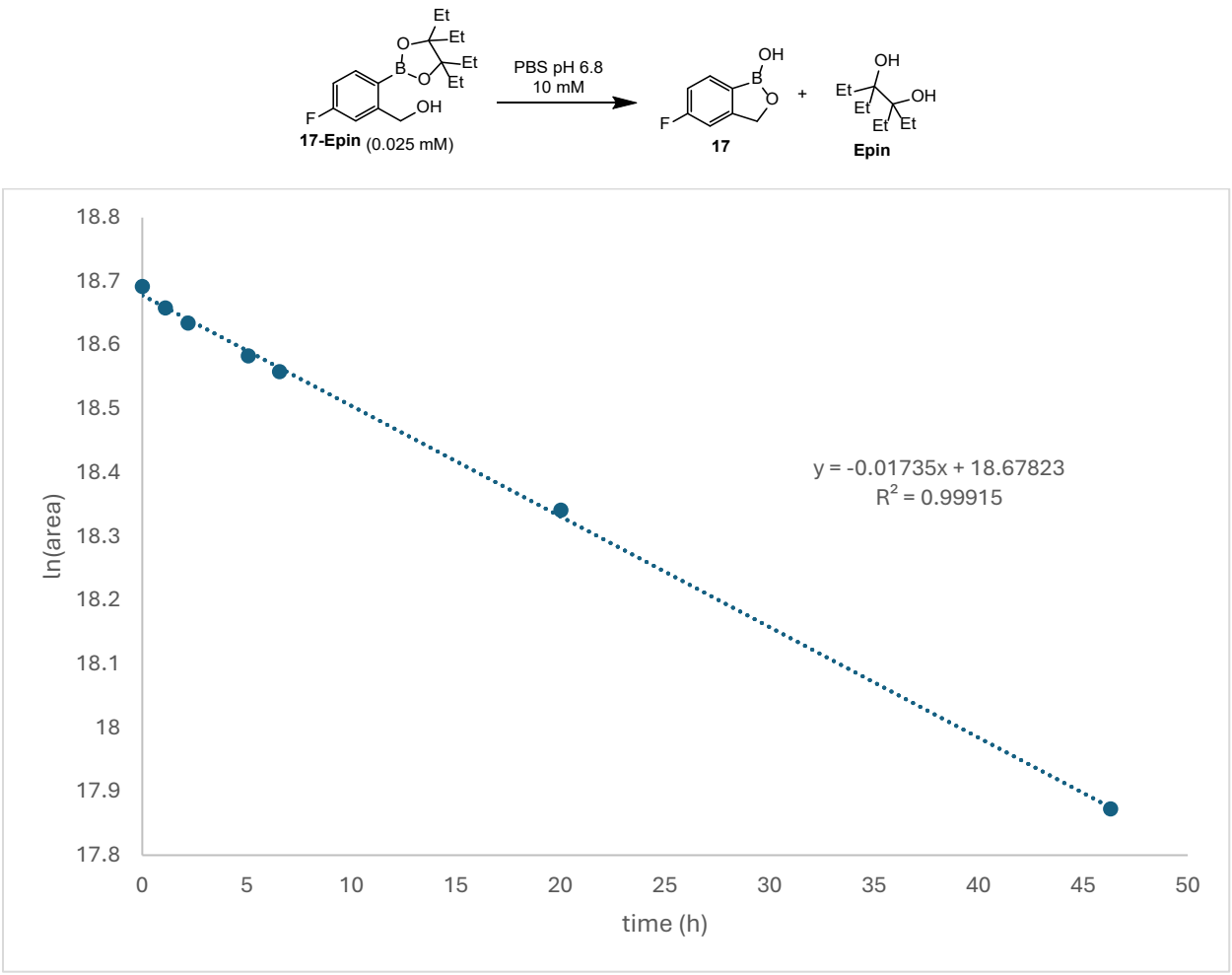

Figure S99. Plot of ln[boronic ester peak area] versus time at pH 6.8 for boronic ester **17-Epin**. Data were fitted to a first order decay model using linear regression. The slope of the best-fit line corresponds to the pseudo-first order rate constant (k), from which the hydrolysis half-life ($t_{1/2}$) of 40.0 h was calculated.

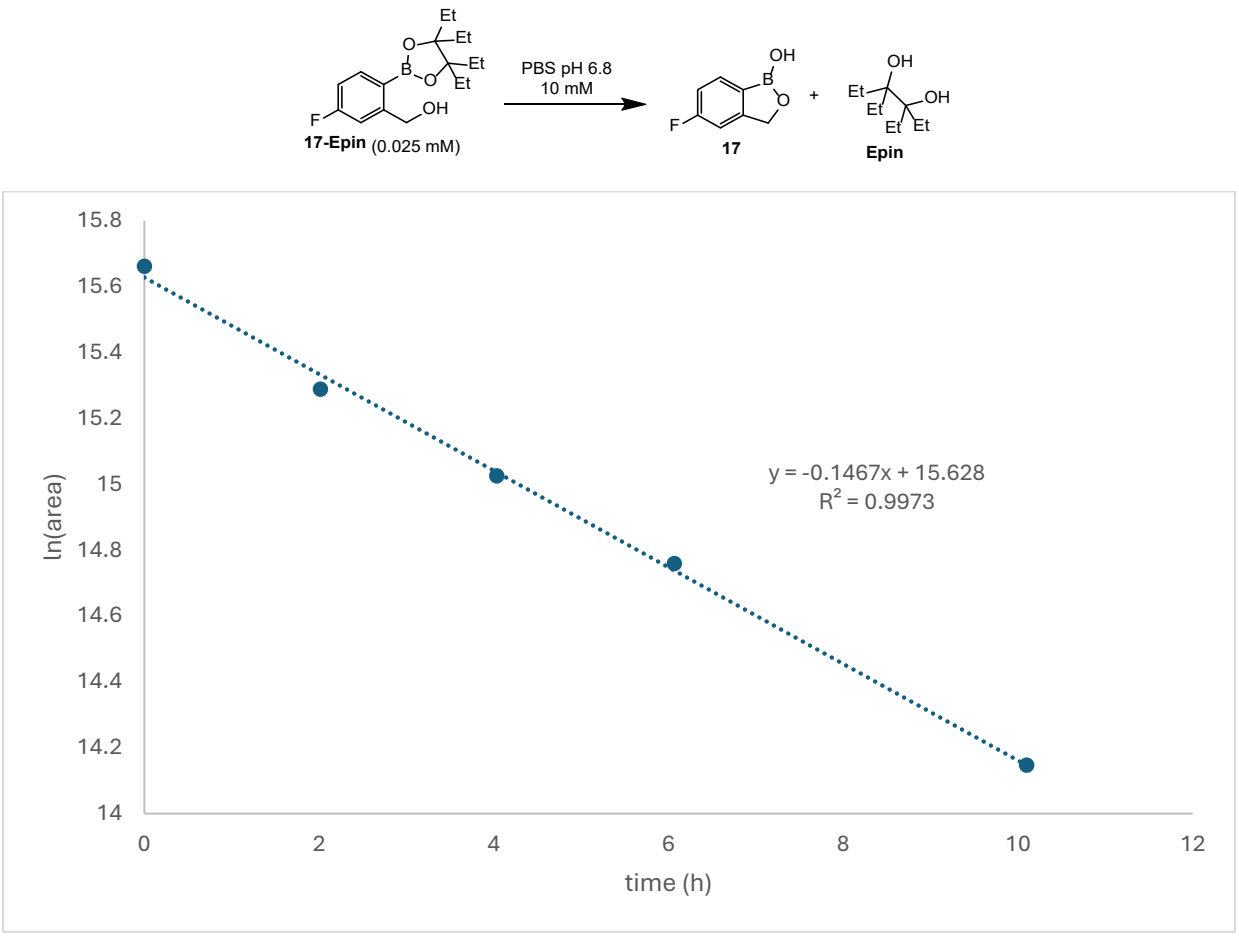

Figure S100. Plot of ln[boronic ester peak area] versus time at pH 8.0 for boronic ester **17-Epin**. Data were fitted to a first order decay model using linear regression. The slope of the best-fit line corresponds to the pseudo-first order rate constant (k), from which the hydrolysis half-life ($t_{1/2}$) of 4.7 h was calculated.

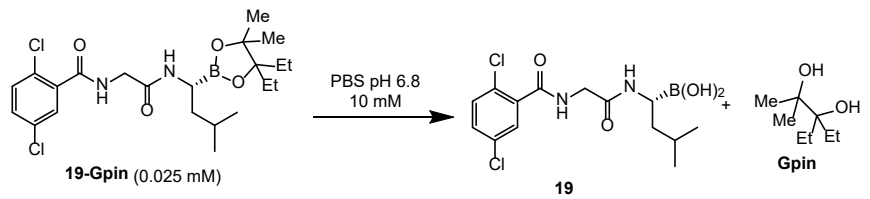

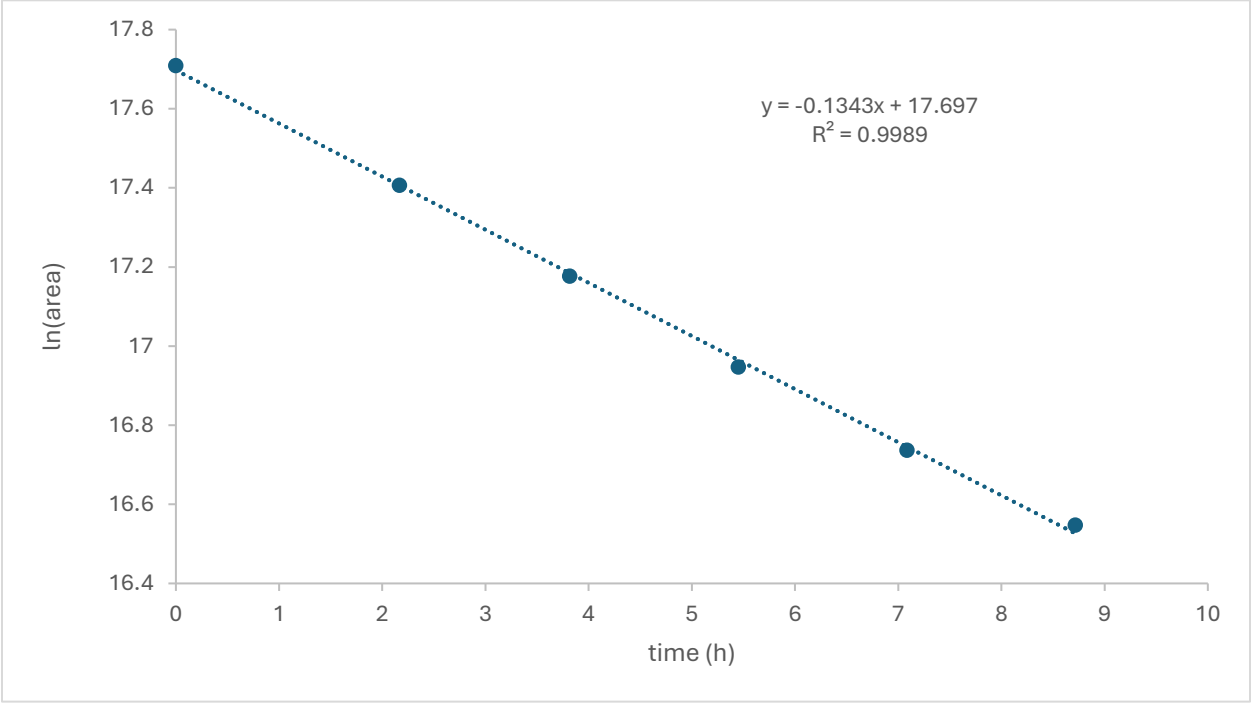

Figure S101. Plot of ln[boronic ester peak area] versus time at pH 6.8 for boronic ester **19-Gpin**. Data were fitted to a first order decay model using linear regression. The slope of the best-fit line corresponds to the pseudo-first order rate constant (k), from which the hydrolysis half-life ($t_{1/2}$) of 5.3 h was calculated.

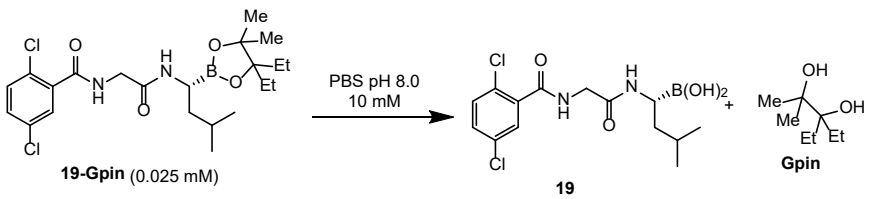

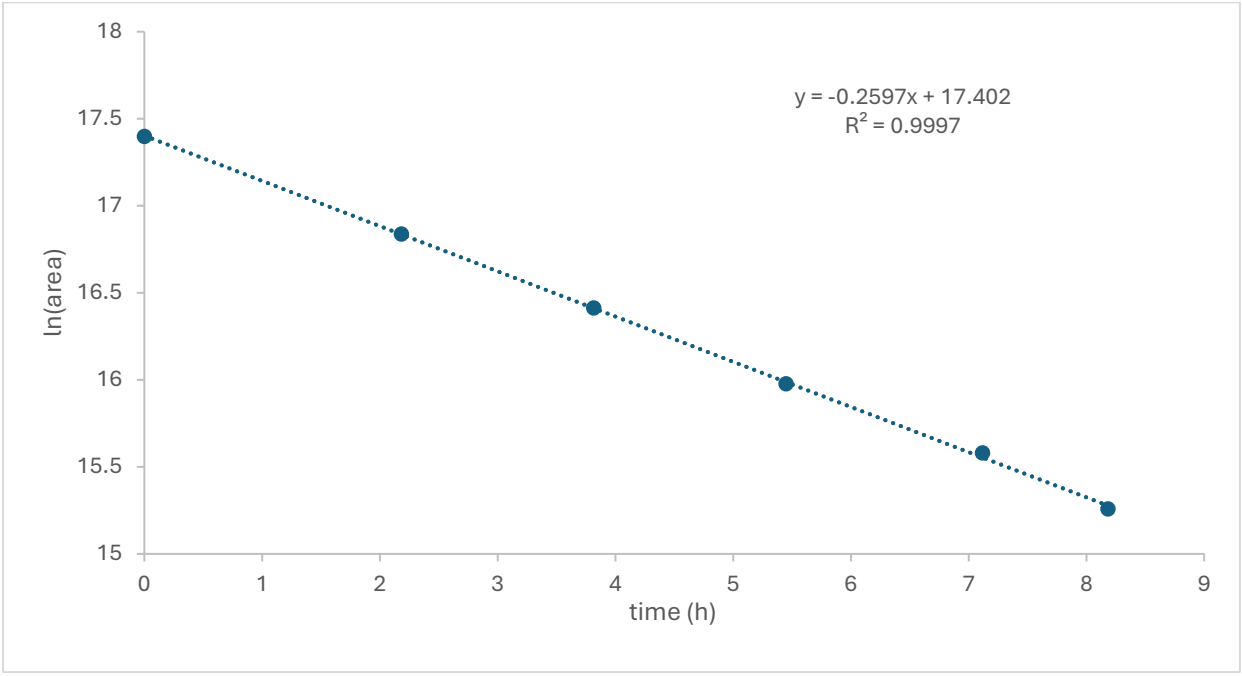

Figure S102. Plot of ln[boronic ester peak area] versus time at pH 8.0 for boronic ester **19-Gpin**. Data were fitted to a first order decay model using linear regression. The slope of the best-fit line corresponds to the pseudo-first order rate constant (k), from which the hydrolysis half-life ($t_{1/2}$) of 2.7 h was calculated.

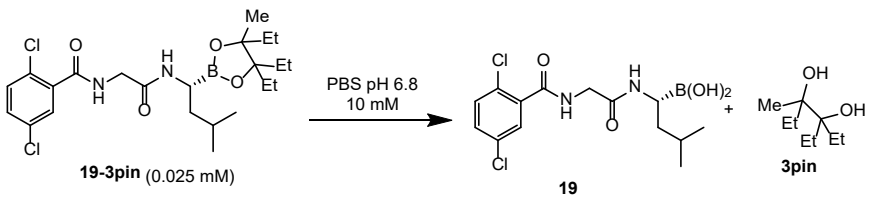

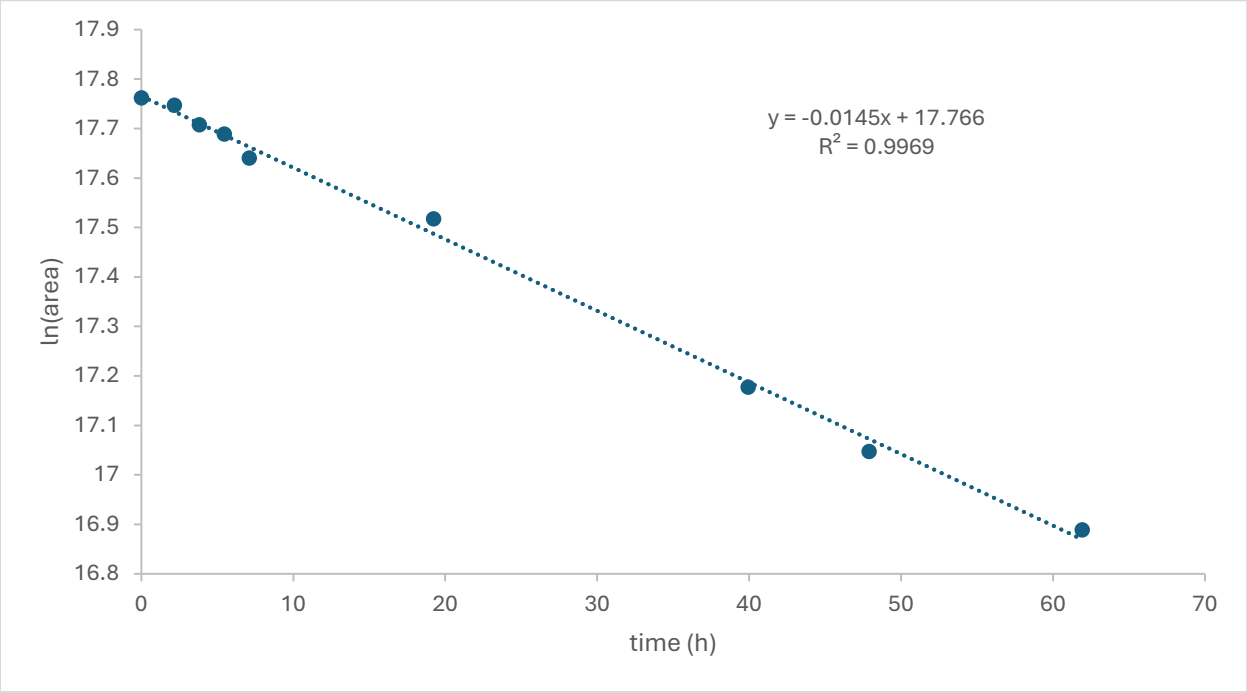

Figure S103. Plot of ln[boronic ester peak area] versus time at pH 8.0for boronic ester **19-3pin**. Data were fitted to a first order decay model using linear regression. The slope of the best-fit line corresponds to the pseudo-first order rate constant (k), from which the hydrolysis half-life ($t_{1/2}$) of 47.8 h was calculated.

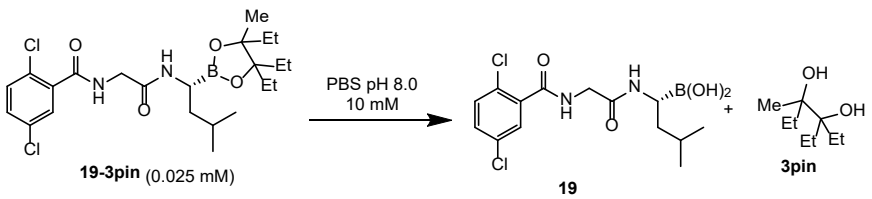

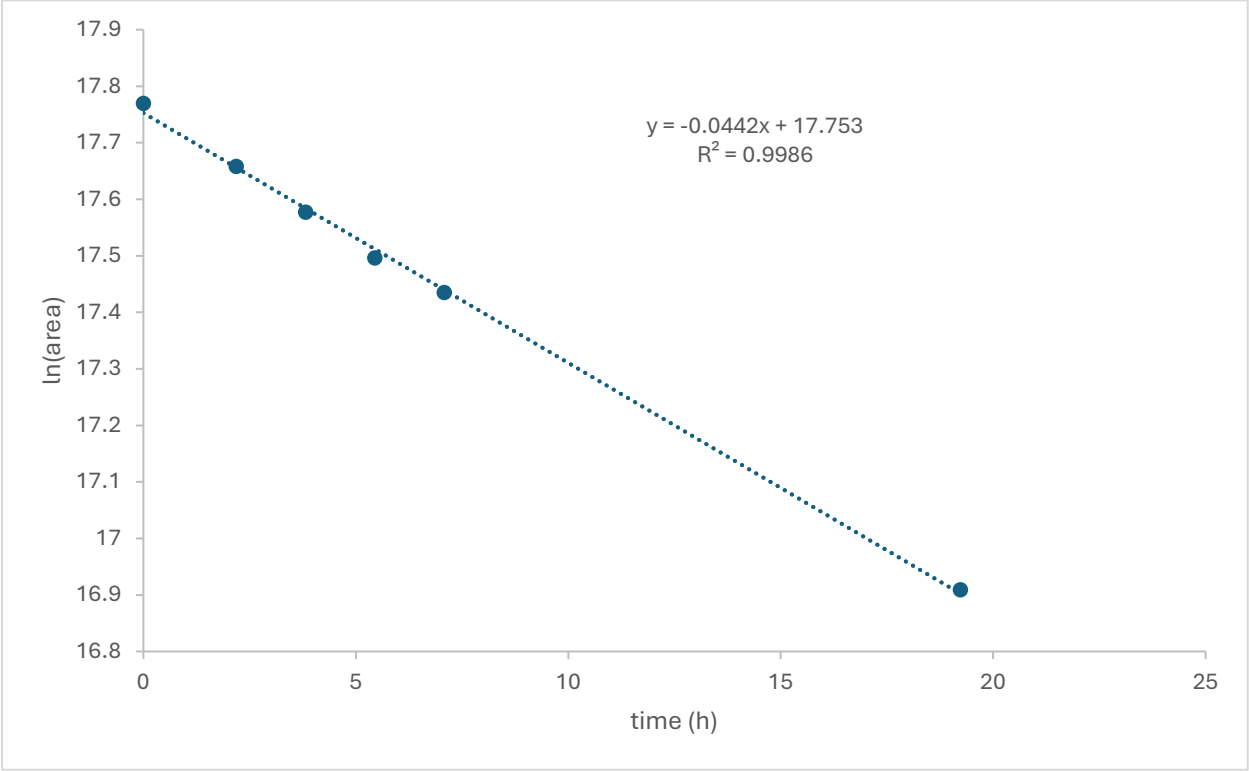

Figure S104. Plot of ln[boronic ester peak area] versus time at pH 8.0 for boronic ester **19-3pin**. Data were fitted to a first order decay model using linear regression. The slope of the best-fit line corresponds to the pseudo-first order rate constant (k), from which the hydrolysis half-life ($t_{1/2}$) of 15.7 h was calculated.

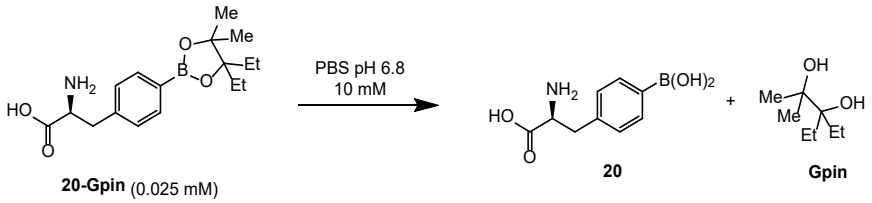

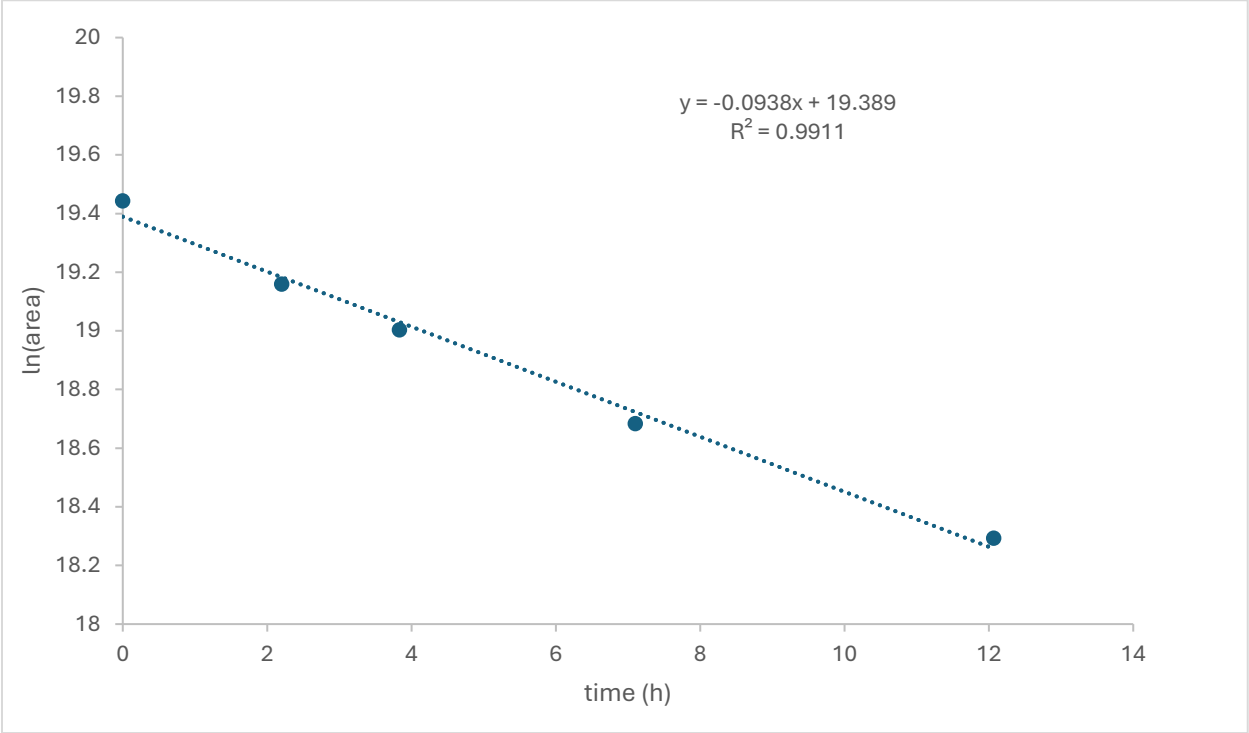

Figure S105. Plot of ln[boronic ester peak area] versus time at pH 6.8 for boronic ester **20-Gpin**. Data were fitted to a first order decay model using linear regression. The slope of the best-fit line corresponds to the pseudo-first order rate constant (k), from which the hydrolysis half-life ($t_{1/2}$) of 7.4 h was calculated.

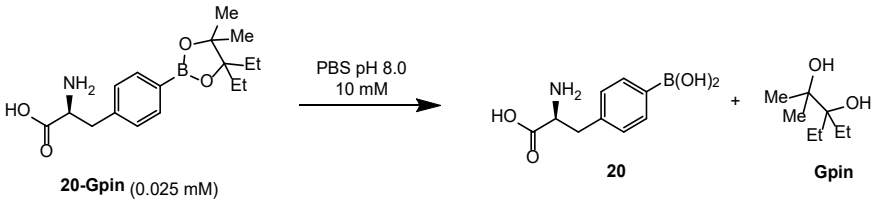

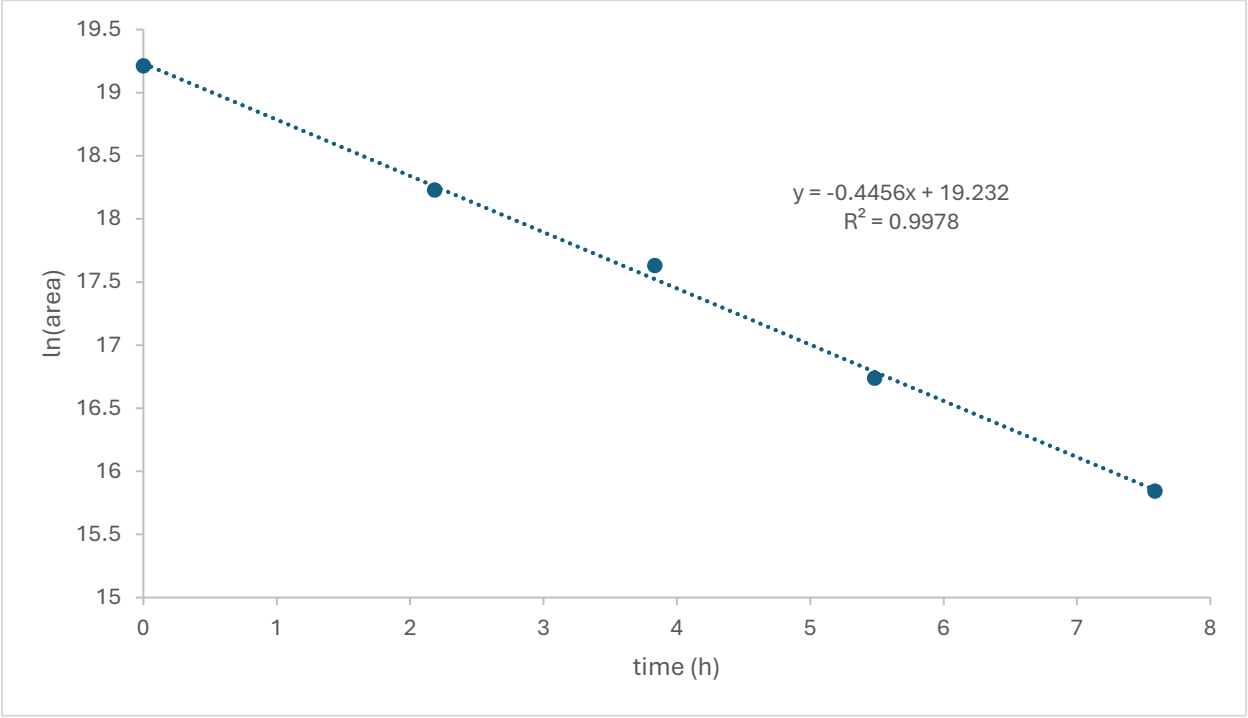

Figure S106. Plot of ln[boronic ester peak area] versus time at pH 8.0 for boronic ester **20-Gpin**. Data were fitted to a first order decay model using linear regression. The slope of the best-fit line corresponds to the pseudo-first order rate constant (k), from which the hydrolysis half-life ($t_{1/2}$) of 2.1 h was calculated.

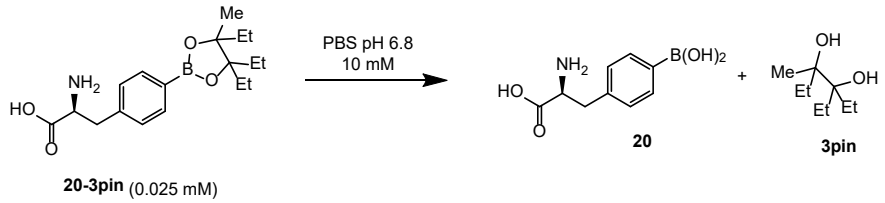

20-3pin (0.025 mM)

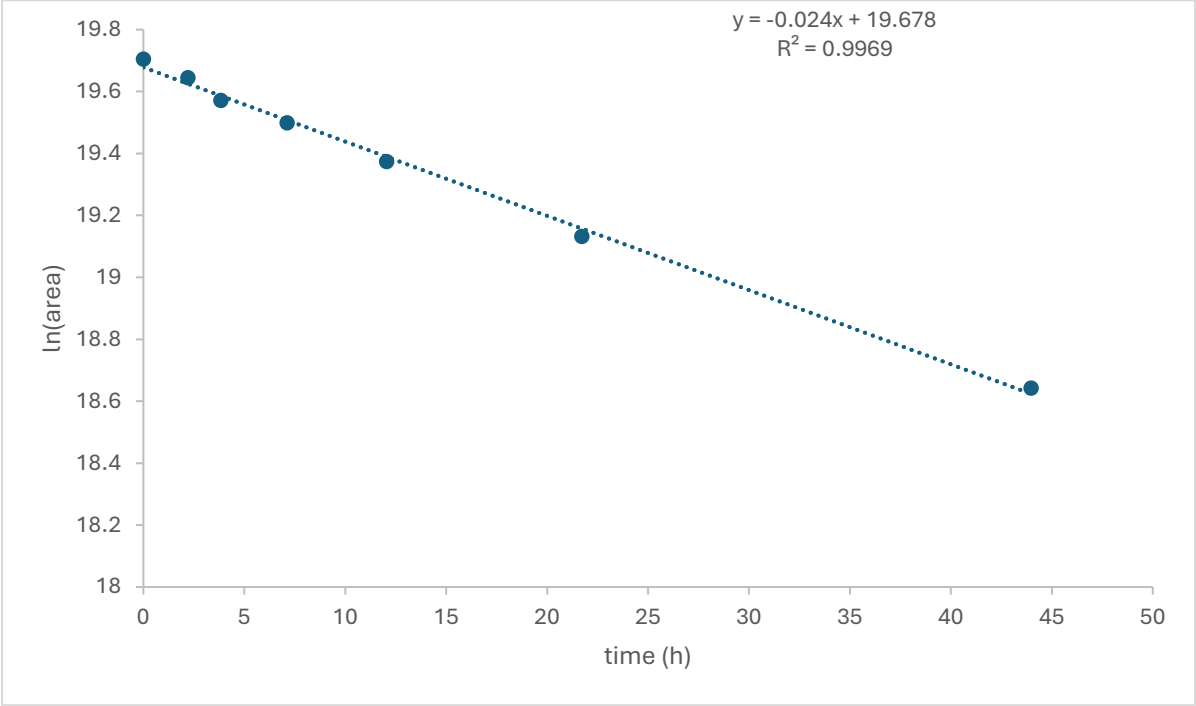

Figure S107. Plot of ln[boronic ester peak area] versus time at pH 8.0for boronic ester **20-3pin**. Data were fitted to a first order decay model using linear regression. The slope of the best-fit line corresponds to the pseudo-first order rate constant (k), from which the hydrolysis half-life ($t_{1/2}$) of 28.7 h was calculated.

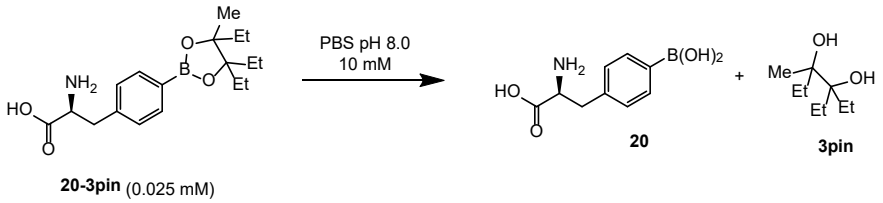

20-3pin (0.025 mM)

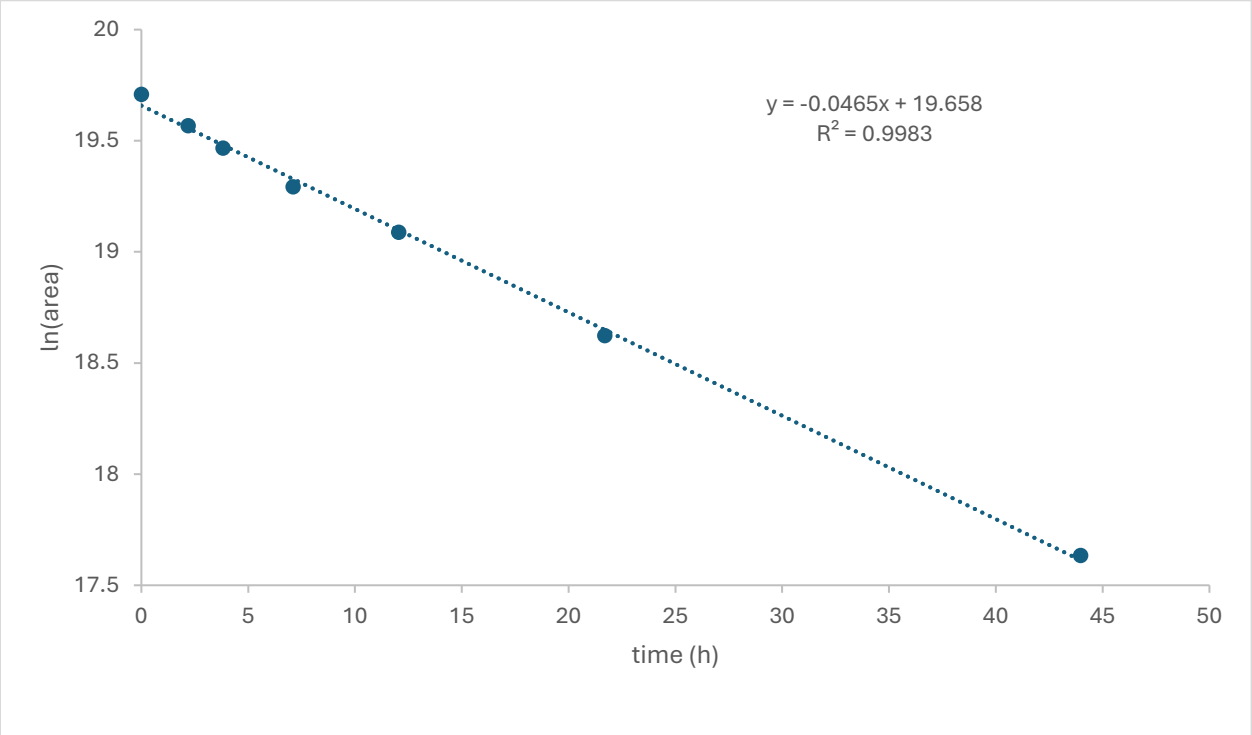

Figure S108. Plot of ln[boronic ester peak area] versus time at pH 8.0 for boronic ester **20-3pin**. Data were fitted to a first order decay model using linear regression. The slope of the best-fit line corresponds to the pseudo-first order rate constant (k), from which the hydrolysis half-life ($t_{1/2}$) of 14.9 h was calculated.

Characterization data

Small molecule boronic esters

Phenylboronic acid (**1**) esters characterization.

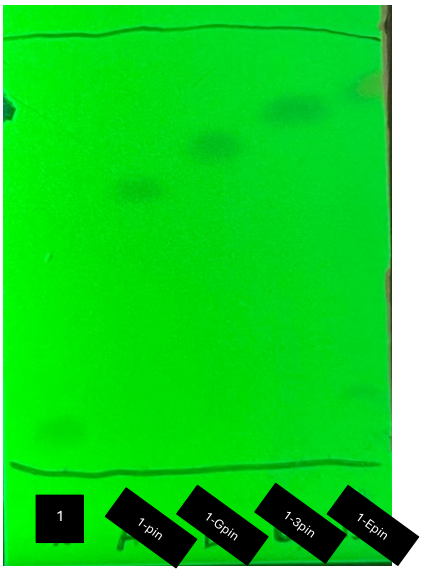

Figure S109. Boronic acid **1** and boronic esters TLC UV analysis using 20% ethyl acetate in hexanes as an eluent.

Formation and characterization of the Pinacol ester **1-pin**.

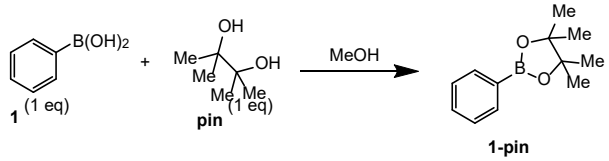

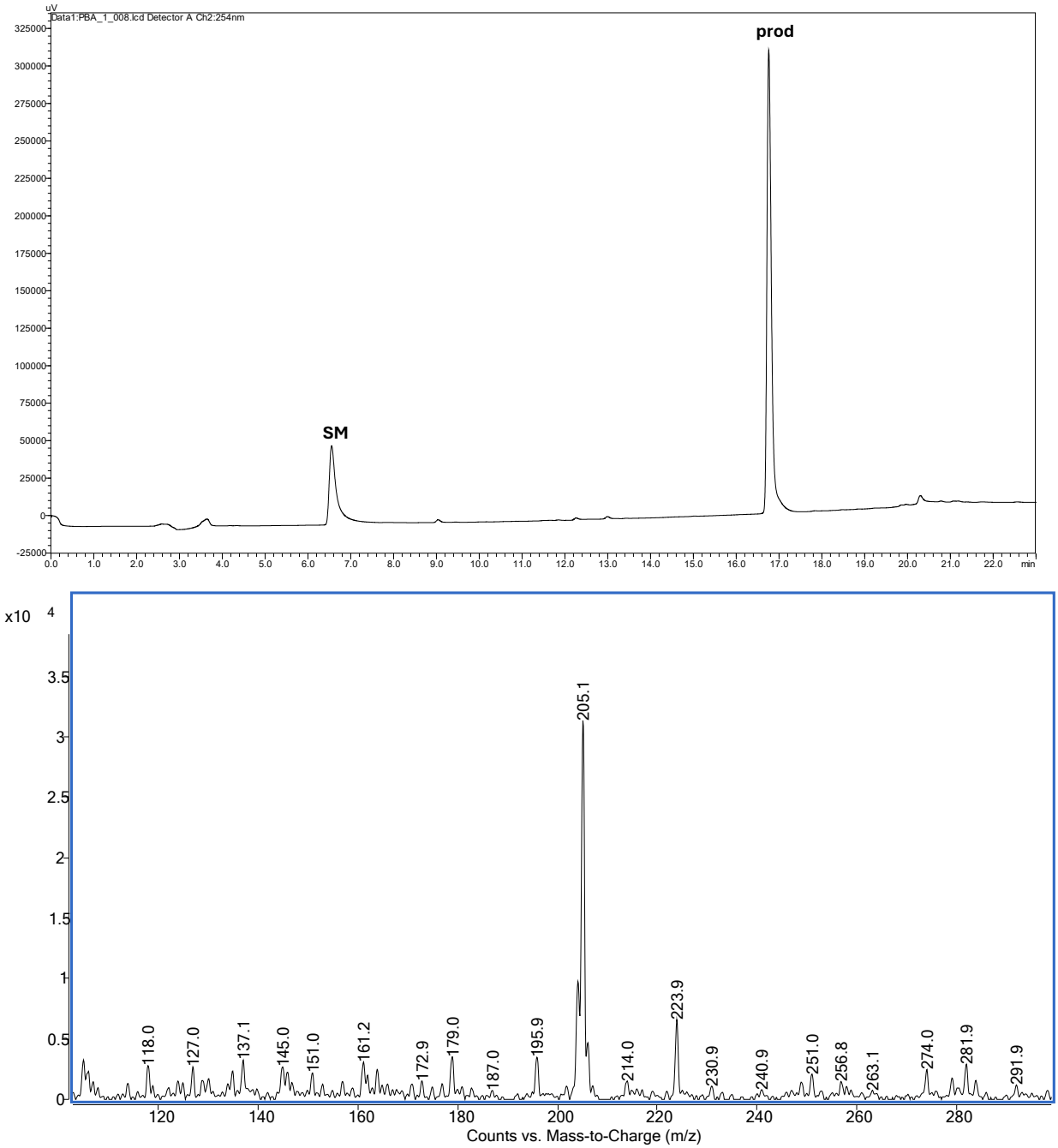

Figure S110. RP-HPLC trace at 254 nm (30-90% MeCN over 23 min) and ESI-MS spectrum of purified boronic ester **1-pin**. m/z 205.1 corresponds to $[M+H]^+$.

Formation and characterization of the Gpin ester **1-Gpin**.

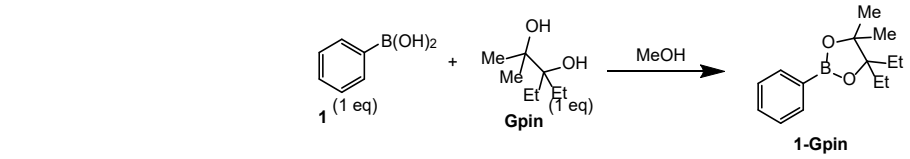

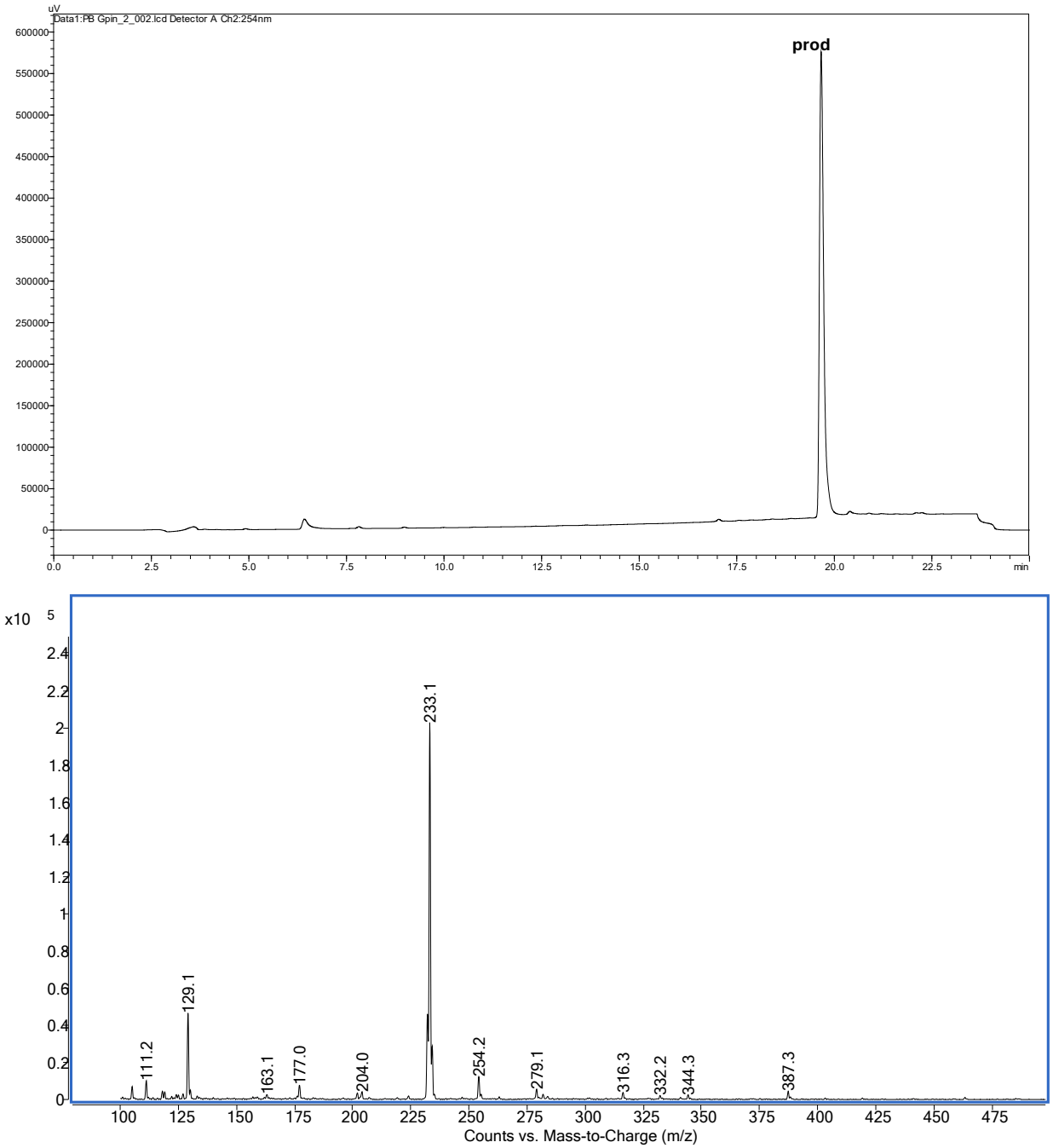

Figure S111. RP-HPLC trace at 254 nm (30-90% MeCN over 23 min) and ESI-MS spectrum of purified boronic ester **1-Gpin**. m/z 233.1 corresponds to $[M+H]^+$.

Formation and characterization of the 3pin ester **1-3pin**.

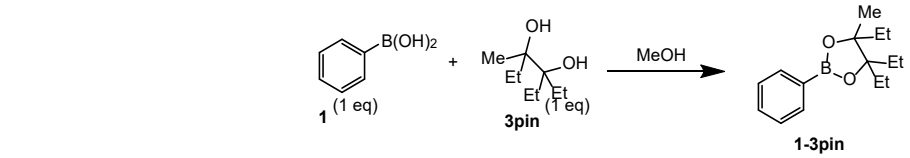

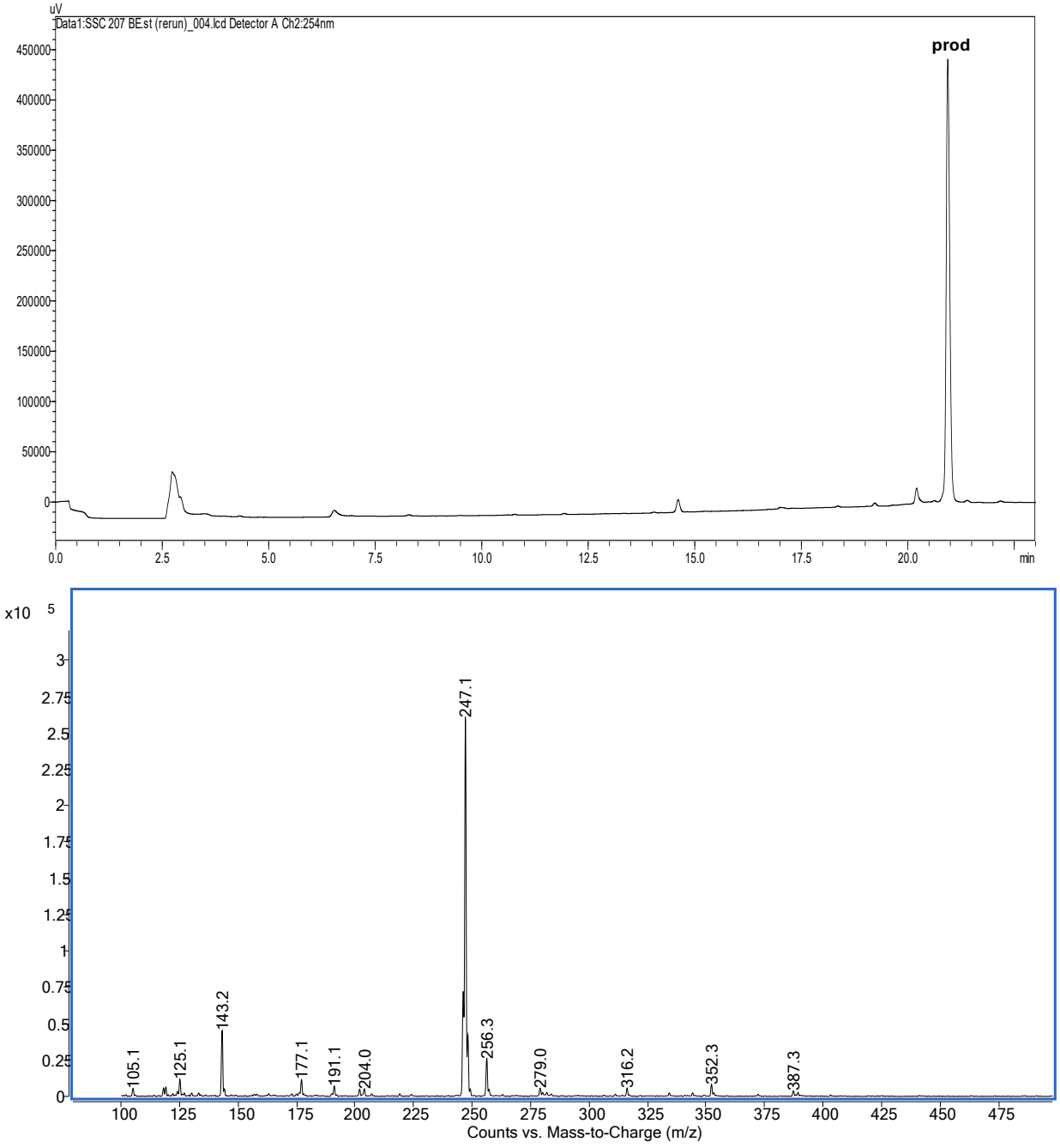

Figure S112. RP-HPLC trace at 254 nm (30-90% MeCN over 23 min) and ESI-MS spectrum of purified boronic ester **1-3pin**. m/z 247.1 corresponds to $[M+H]^+$.

Formation and characterization of the Epin ester **1-Epin**.

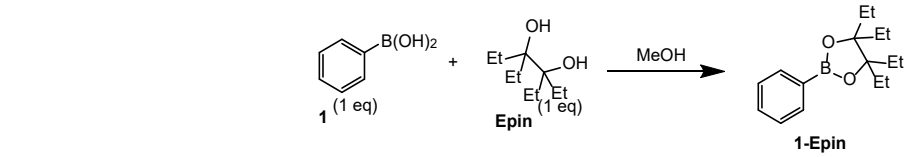

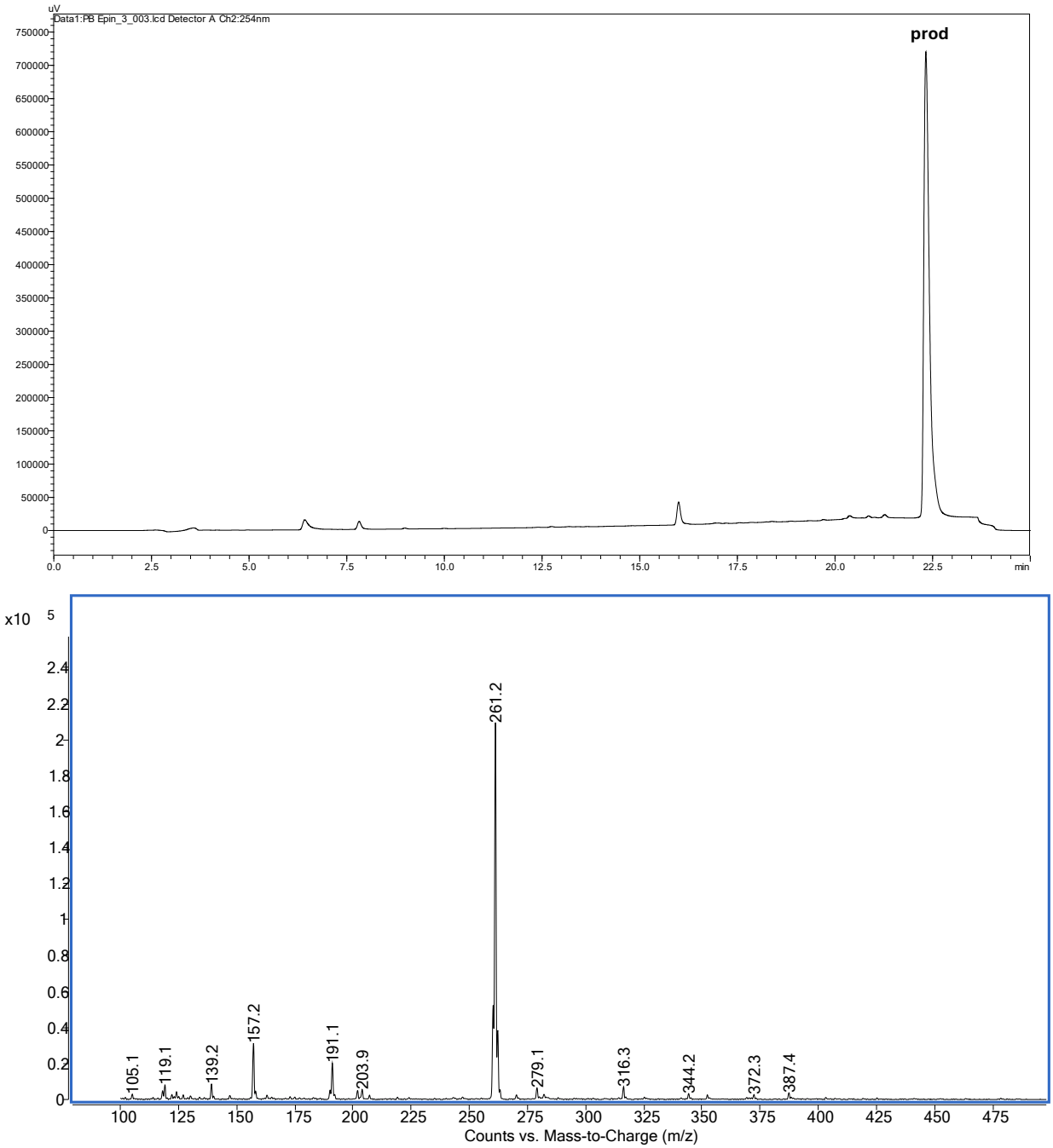

Figure S113. RP-HPLC trace at 254 nm (30-90% MeCN over 23 min) and ESI-MS spectrum of purified boronic ester **1-Epin**. m/z 261.2 corresponds to $[M+H]^+$.

Phenethylboronic acid (**2**) esters characterization.

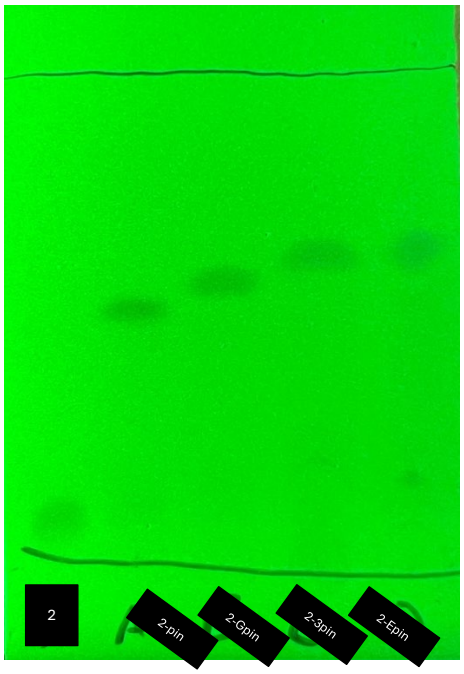

Figure S114. Boronic acid **2** and boronic esters TLC UV analysis using 10% ethyl acetate in hexanes as an eluent.

Formation and characterization of the Pinacol ester **2-pin**.

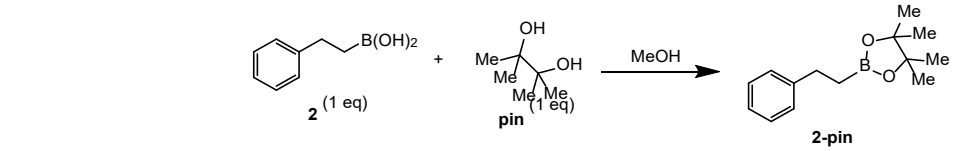

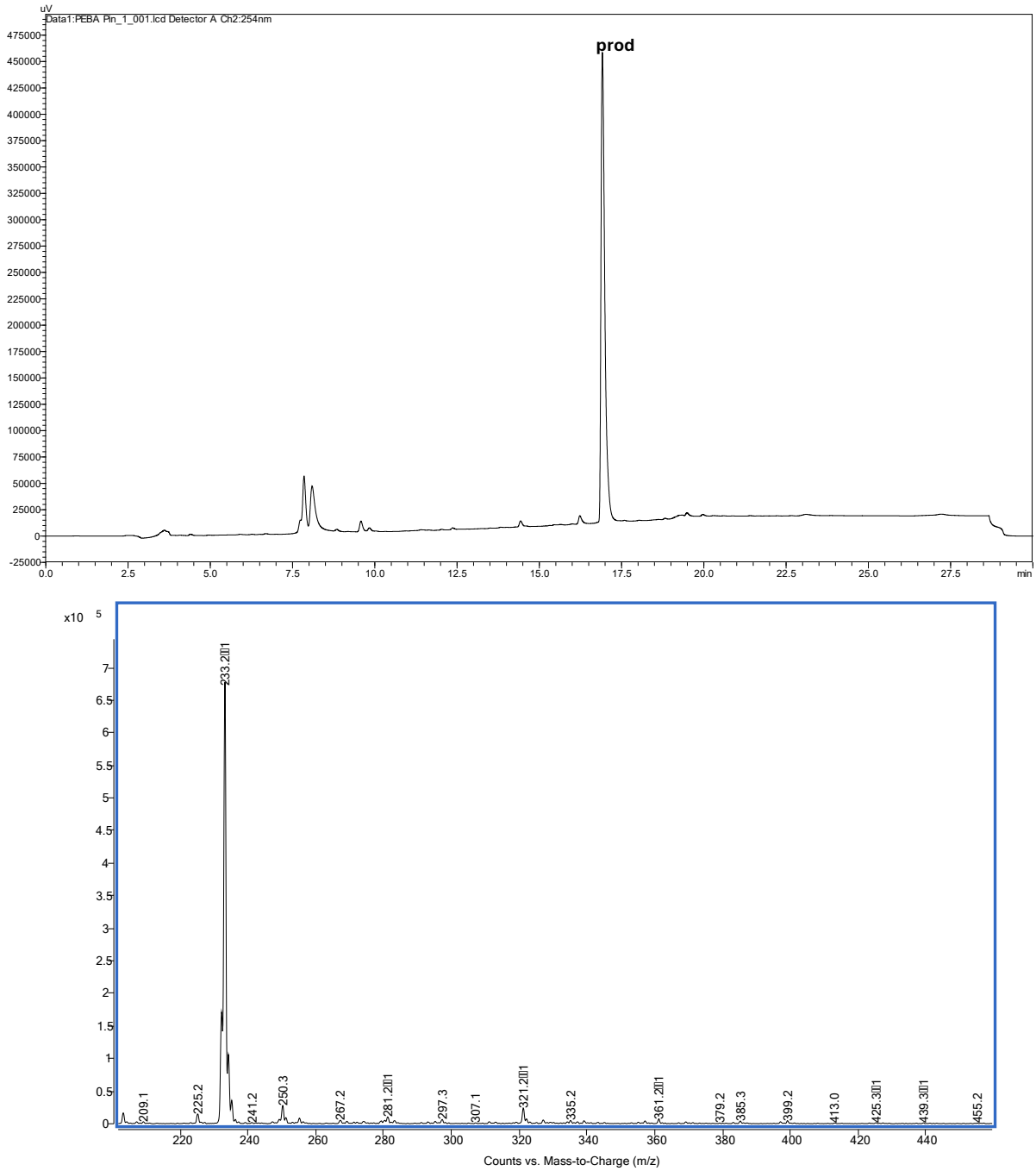

Figure S115. RP-HPLC trace at 254 nm (30-95% MeCN over 30 min) and ESI-MS spectrum of purified boronic ester **2-Pin**. m/z 233.2 corresponds to $[M+H]^+$.

Formation and characterization of the Gpin ester **2-Gpin**.

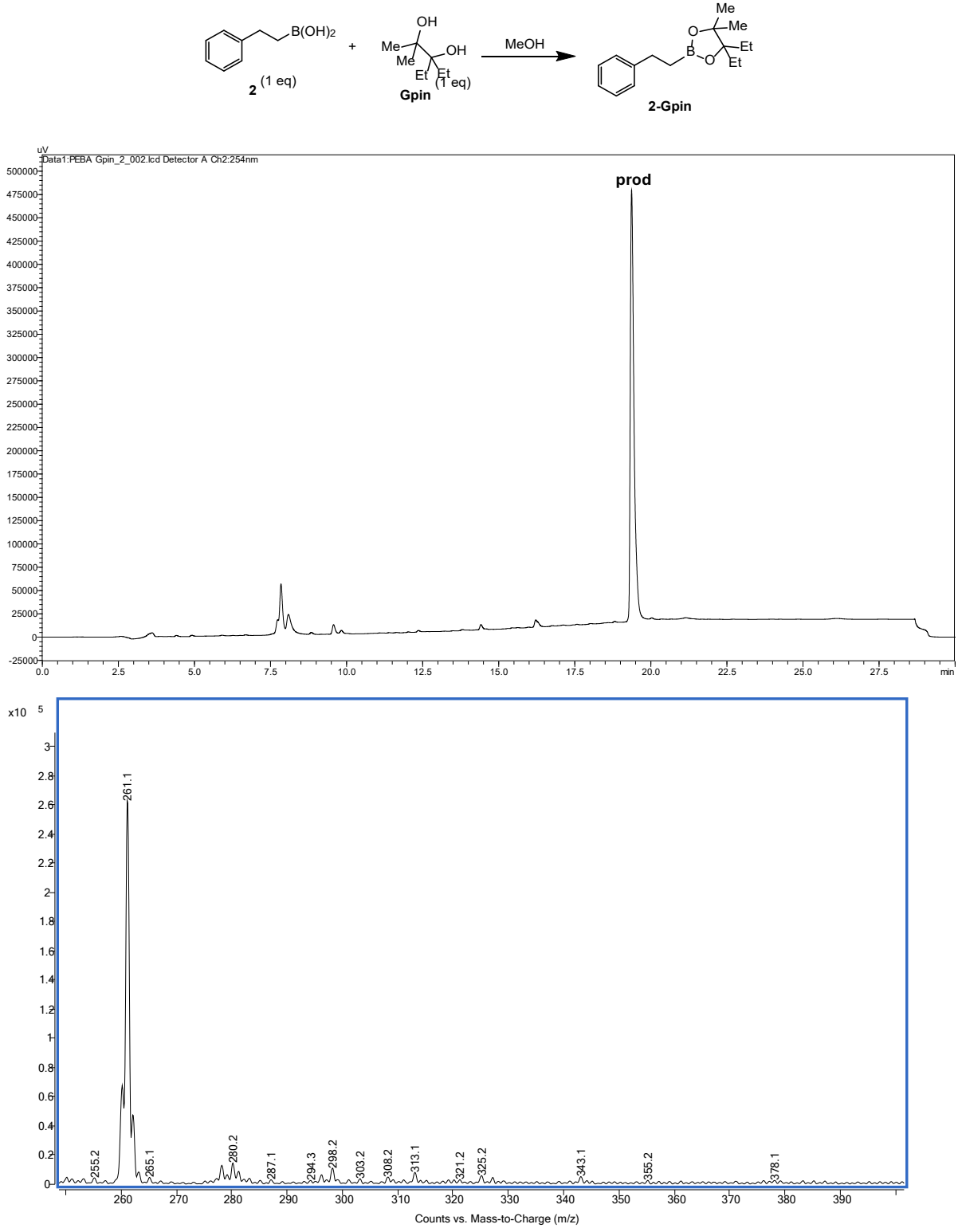

Figure S116. RP-HPLC trace at 254 nm (30-95% MeCN over 30 min) and ESI-MS spectrum of purified boronic ester **2-Gpin**. m/z 261.1 corresponds to $[M+H]^+$.

Formation and characterization of the 3pin ester **2-3pin**.

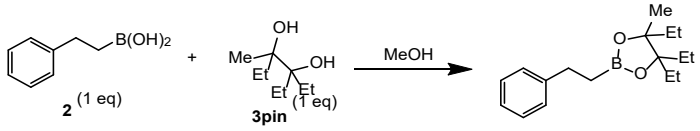

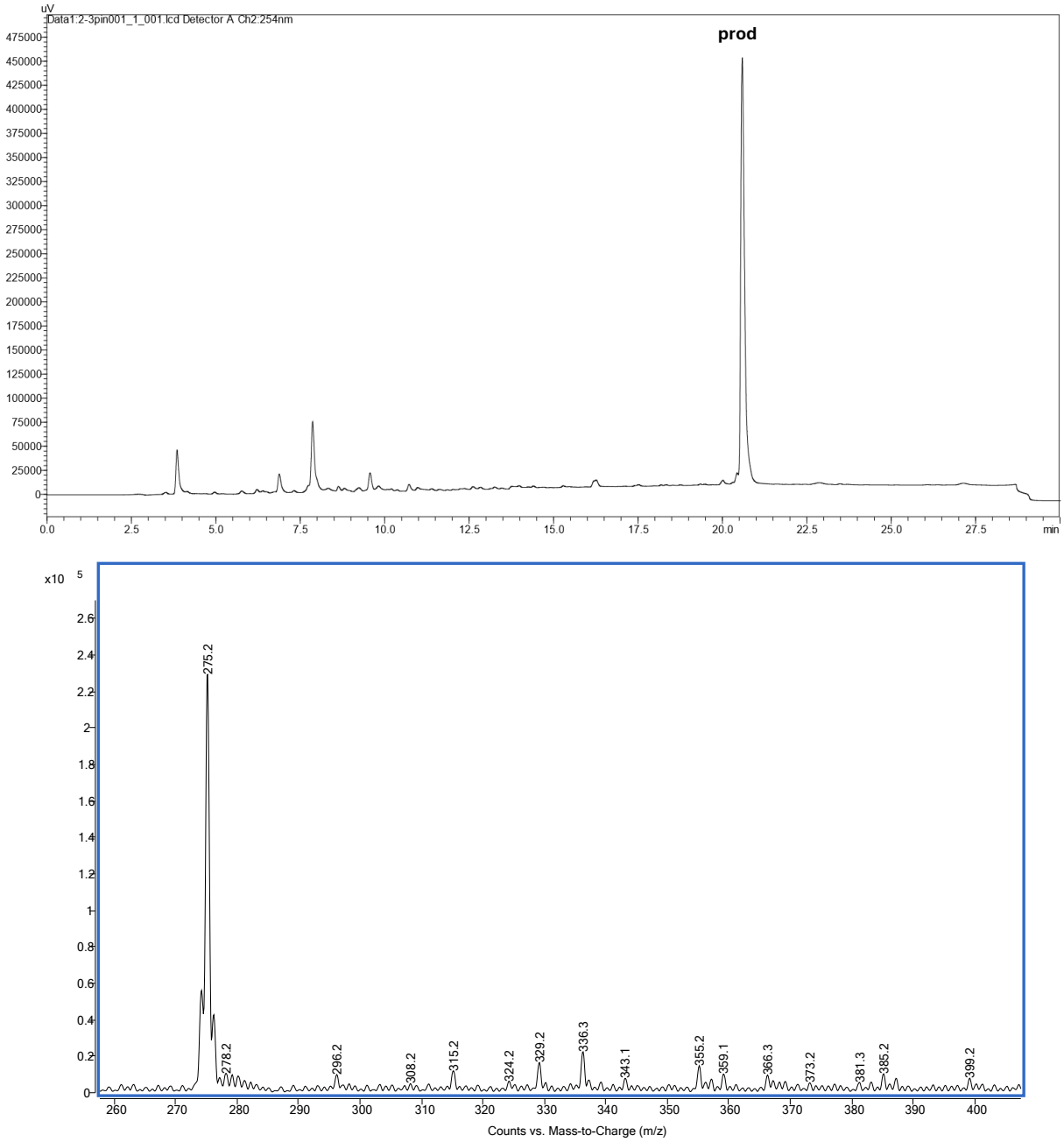

Figure S117. RP-HPLC trace at 254 nm (30-95% MeCN over 30 min) and ESI-MS spectrum of purified boronic ester **2-3pin**. m/z 275.2 corresponds to $[M+H]^+$.

Formation and characterization of the Epin ester **2-Epin**.

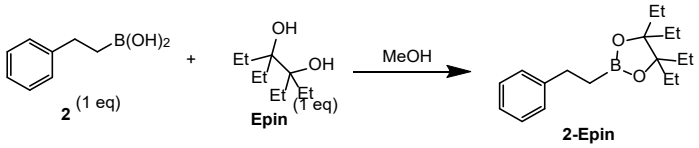

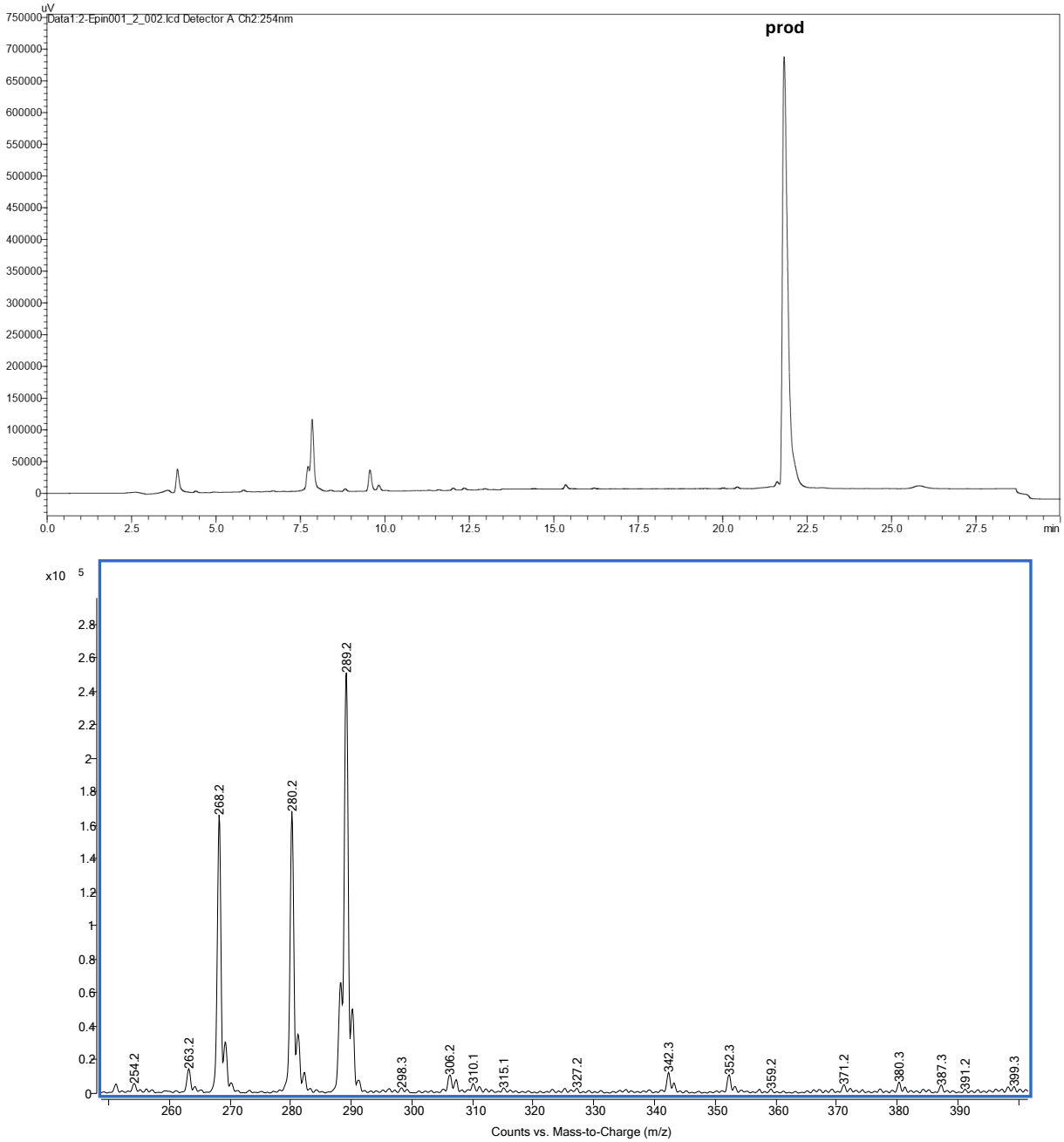

Figure S118. RP-HPLC trace at 254 nm (30-95% MeCN over 30 min) and ESI-MS spectrum of purified boronic ester **2-Epin**. m/z 289.2 corresponds to $[M+H]^+$.

(E)-styrylboronic acid (**3**) esters characterization.

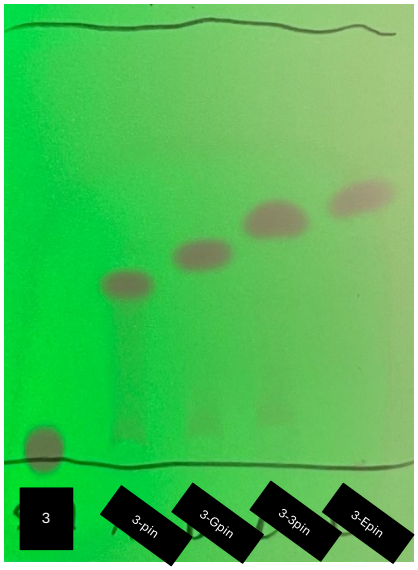

Figure S119. Boronic acid **3** and boronic esters TLC UV analysis using 10% ethyl acetate in hexanes as an eluent.

Formation and characterization of the Pinacol ester **3-pin**.

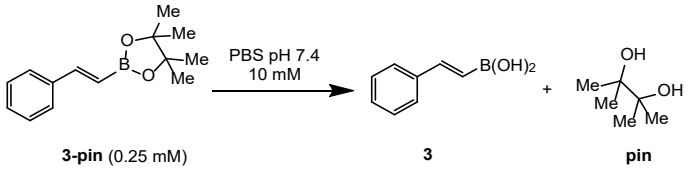

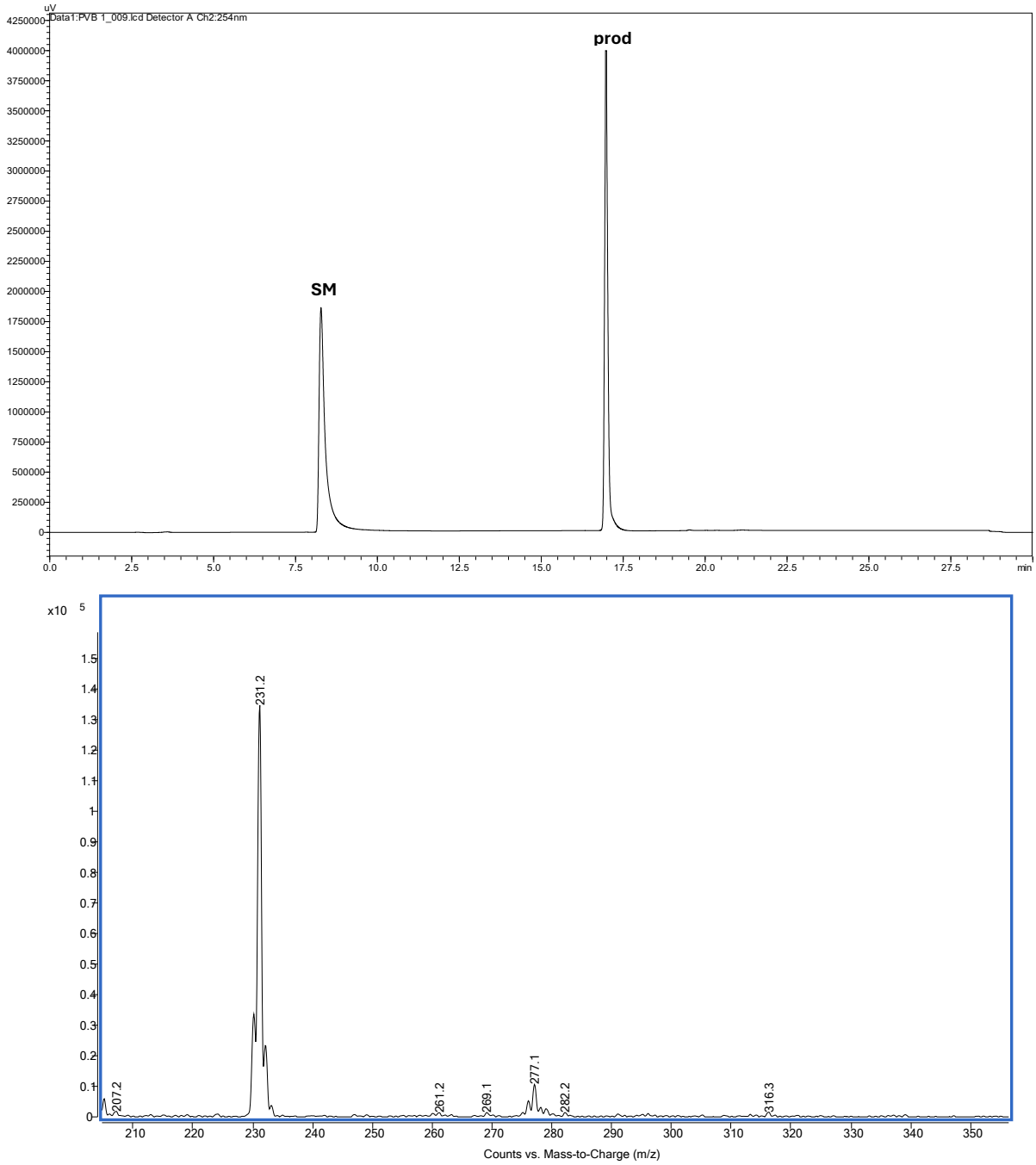

Figure S120. RP-HPLC trace at 254 nm (30-95% MeCN over 30 min) and ESI-MS spectrum of purified boronic ester **3-Pin**. m/z 231.2 corresponds to $[M+H]^+$.

Formation and characterization of the Gpin ester **3-Gpin**.

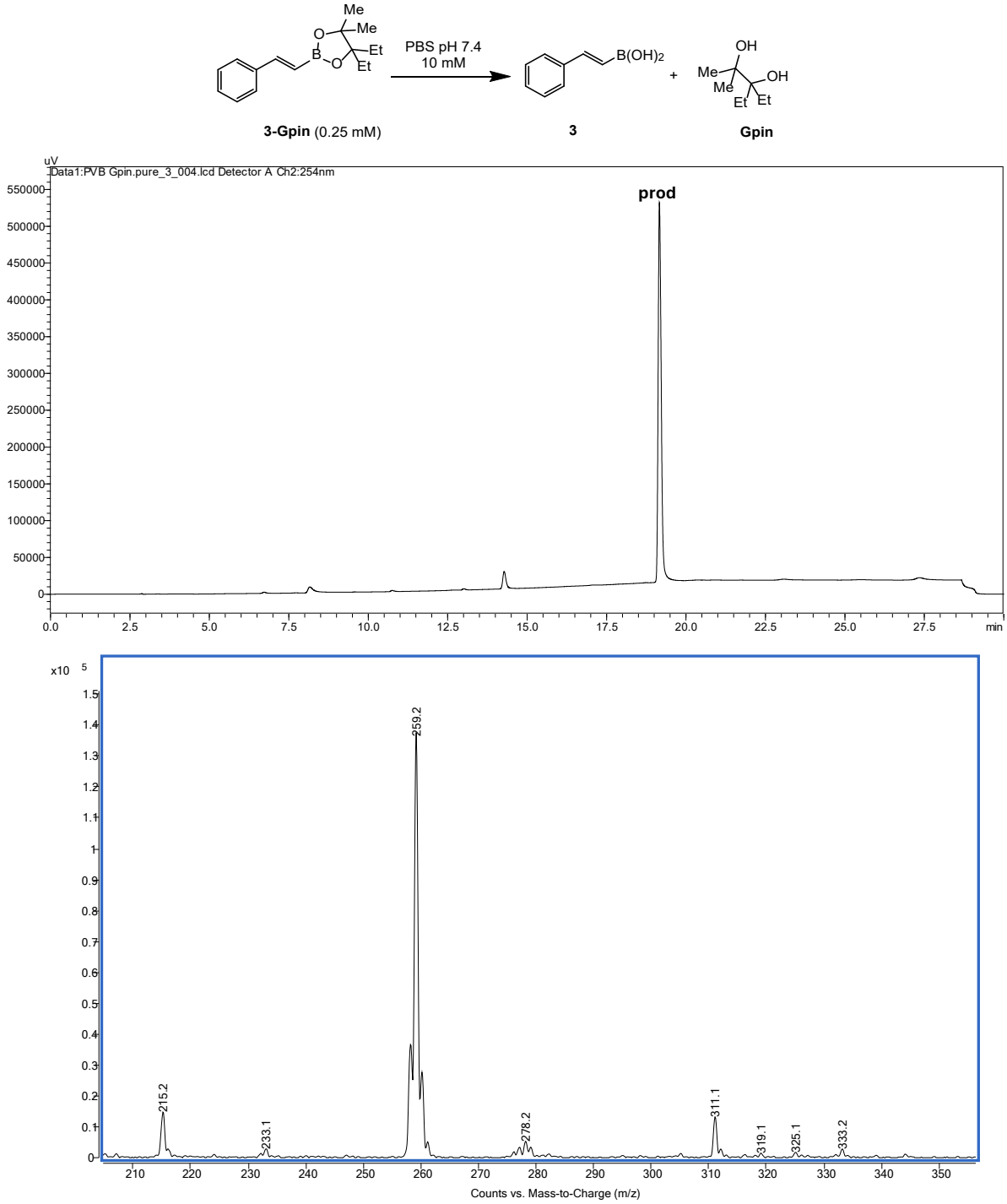

Figure S121. RP-HPLC trace at 254 nm (30-95% MeCN over 30 min) and ESI-MS spectrum of purified boronic ester **3-Gpin**. m/z 259.2 corresponds to $[M+H]^+$.

Formation and characterization of the 3pin ester **3-3pin**.

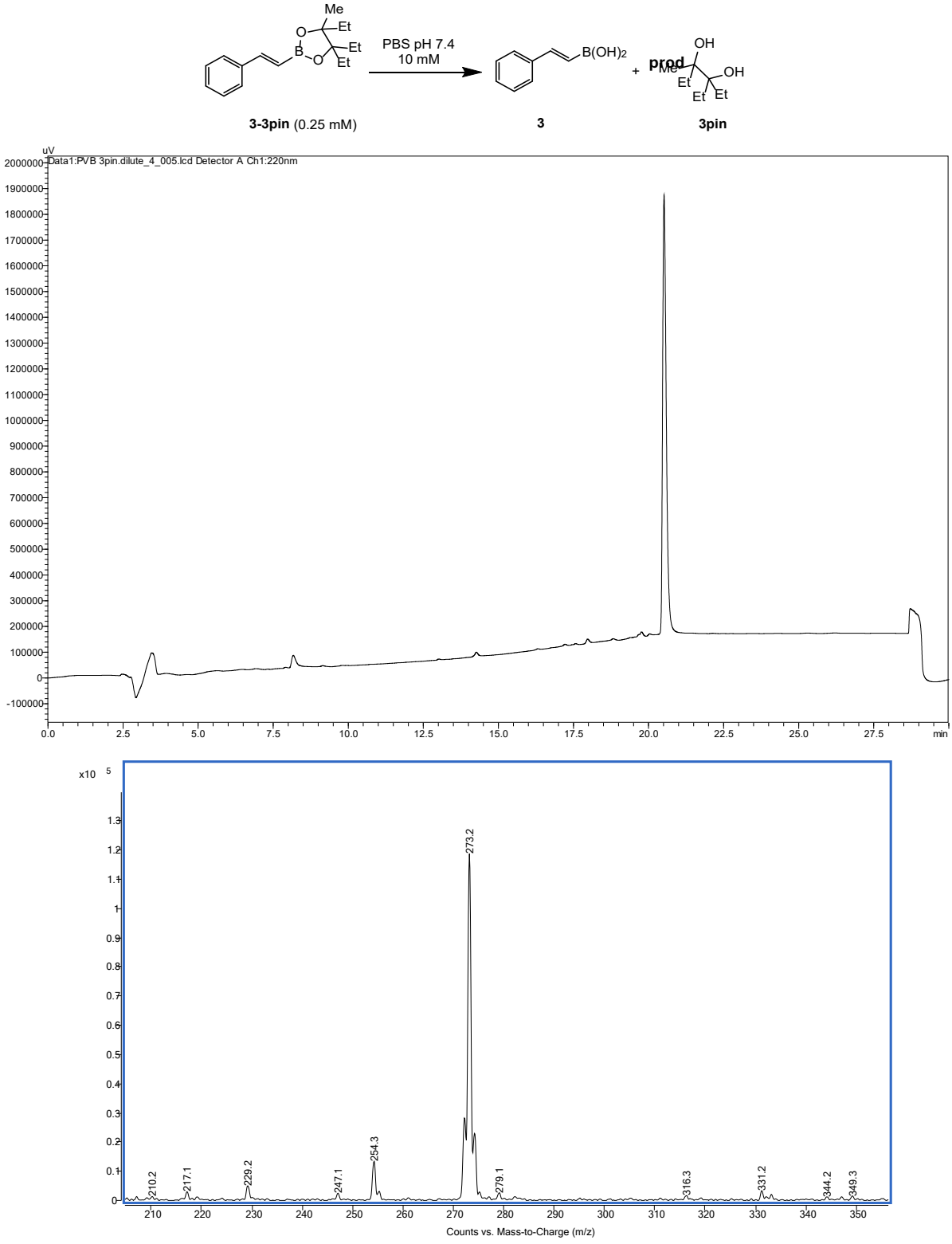

Figure S122. RP-HPLC trace at 254 nm (30-95% MeCN over 30 min) and ESI-MS spectrum of purified boronic ester **3-3pin**. m/z 273.2 corresponds to $[M+H]^+$.

Formation and characterization of the Epin ester **3-Epin**.

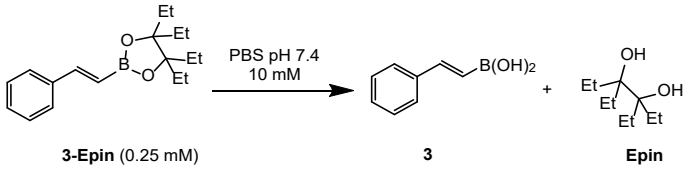

3-Epin (0.25 mM) **3** **Epin**

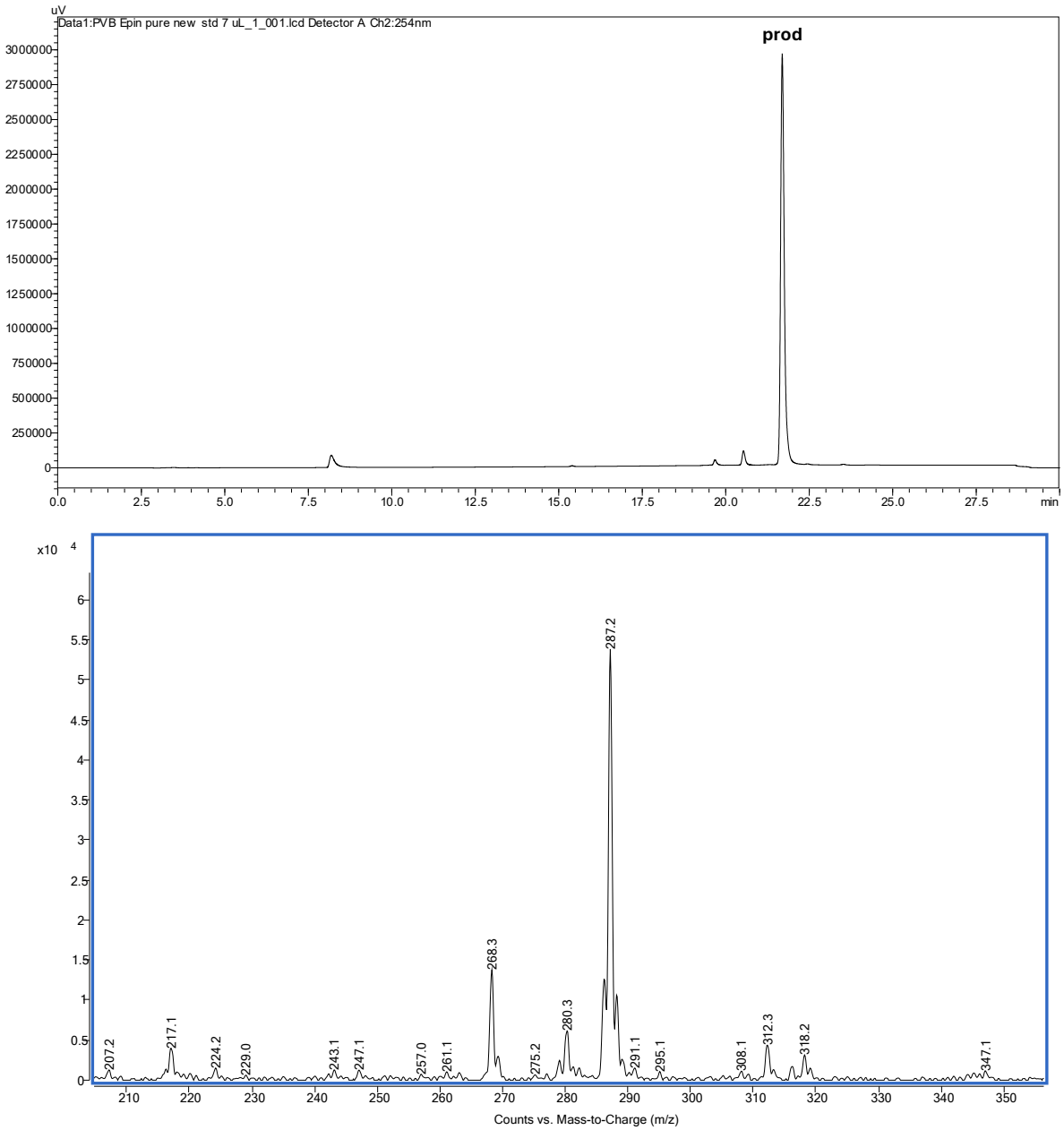

Figure S123. RP-HPLC trace at 254 nm (30-95% MeCN over 30 min) and ESI-MS spectrum of purified boronic ester **3-Epin**. m/z 287.2 corresponds to $[M+H]^+$.

(4-hydroxyphenyl)boronic acid (**4**) esters characterization.

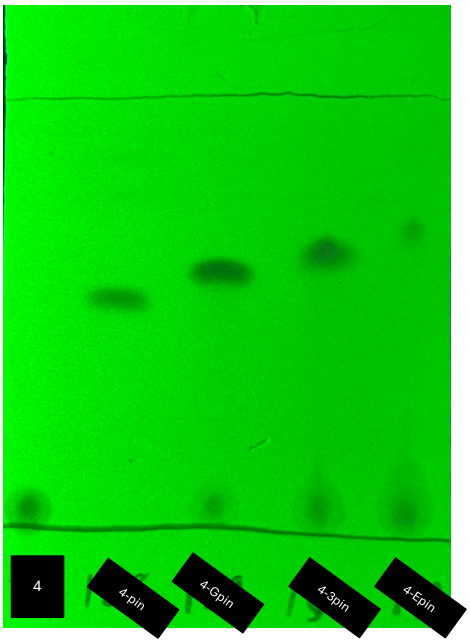

Figure S124. Boronic acid **4** and boronic esters TLC UV analysis using 15% ethyl acetate in hexanes as an eluent

Formation and characterization of the pinacol ester **4-pin**.

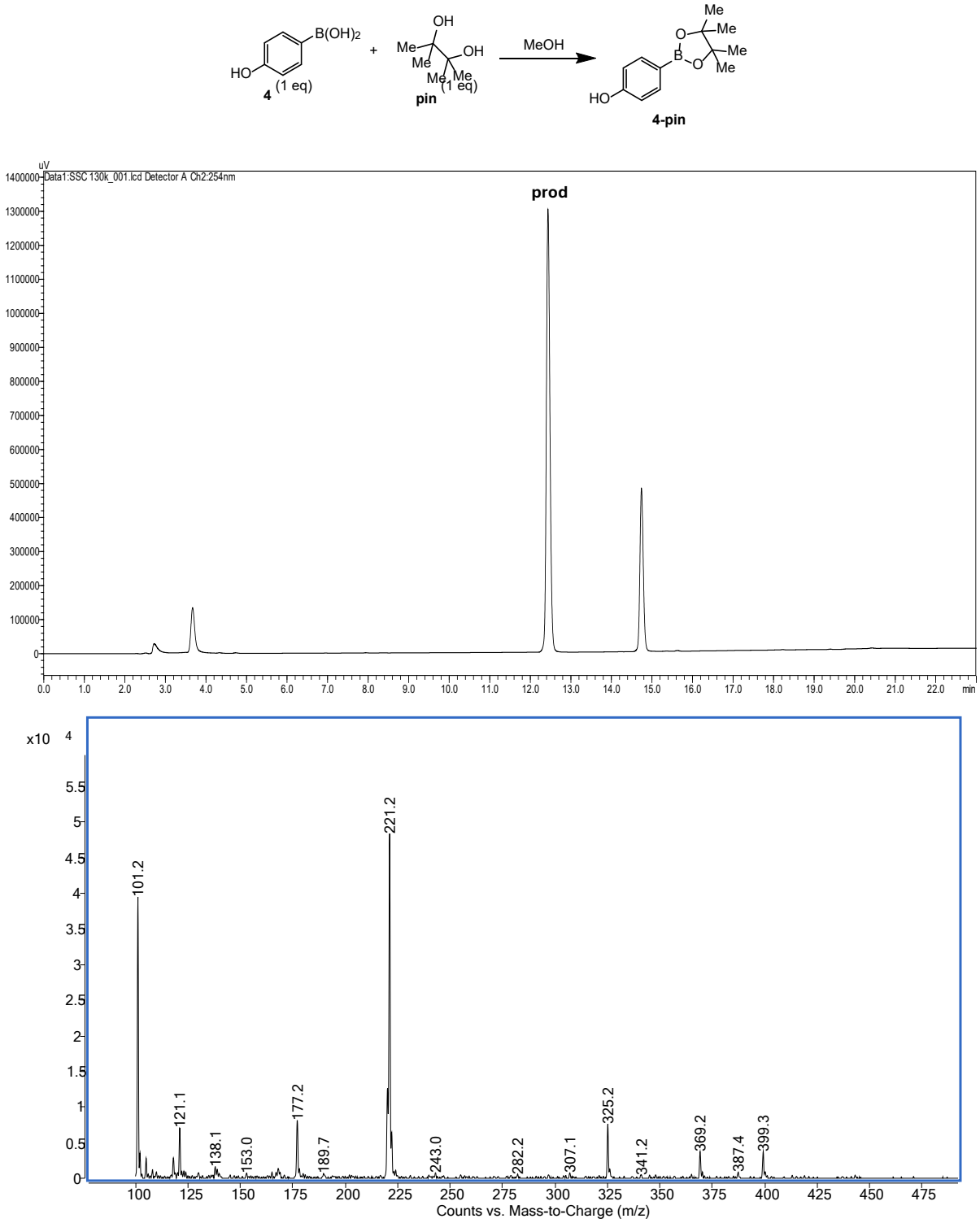

Figure S125. RP-HPLC trace at 254 nm (30-95% MeCN over 30 min) and ESI-MS spectrum of purified boronic ester **4-pin**. m/z 221.2 corresponds to $[M+H]^+$.

Formation and characterization of the Gpinacol ester **4-Gpin**.

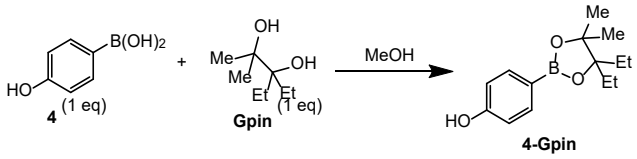

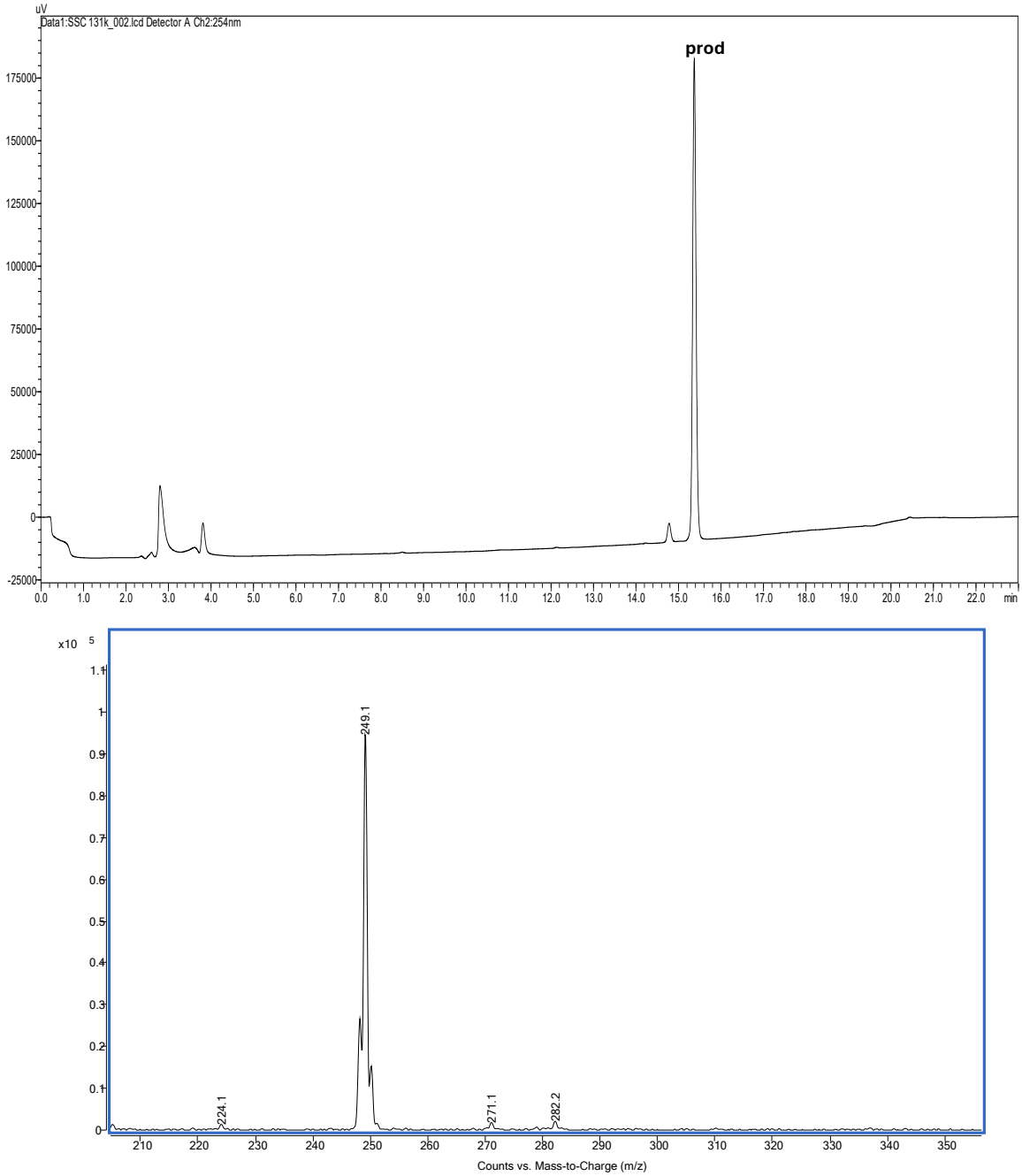

Figure S126. RP-HPLC trace at 254 nm (30-95% MeCN over 30 min) and ESI-MS spectrum of purified boronic ester **4-Gpin**. m/z 249.1 corresponds to $[M+H]^+$.

Formation and characterization of the 3-Ethyl Pinacol ester **4-3pin**

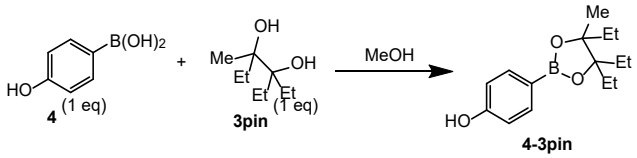

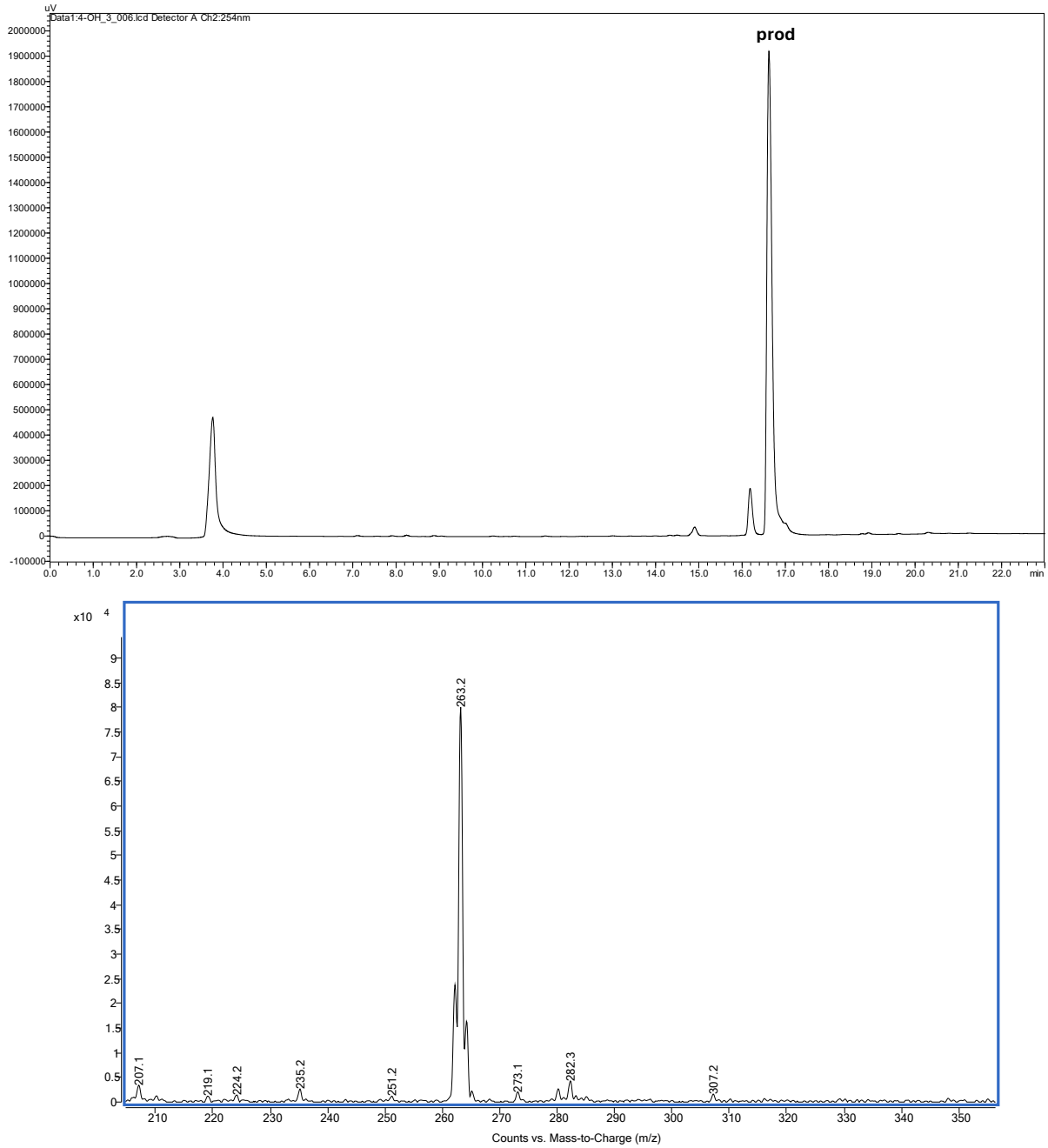

Figure S127. RP-HPLC trace at 254 nm (30-95% MeCN over 30 min) and ESI-MS spectrum of purified boronic ester **4-3pin**. m/z 263.2 corresponds to $[M+H]^+$.

Formation and characterization of Epin **4-Epin**.

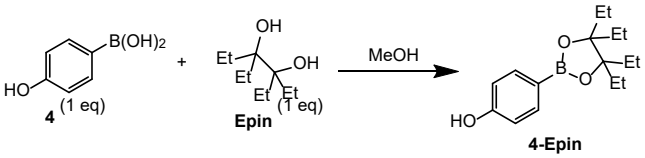

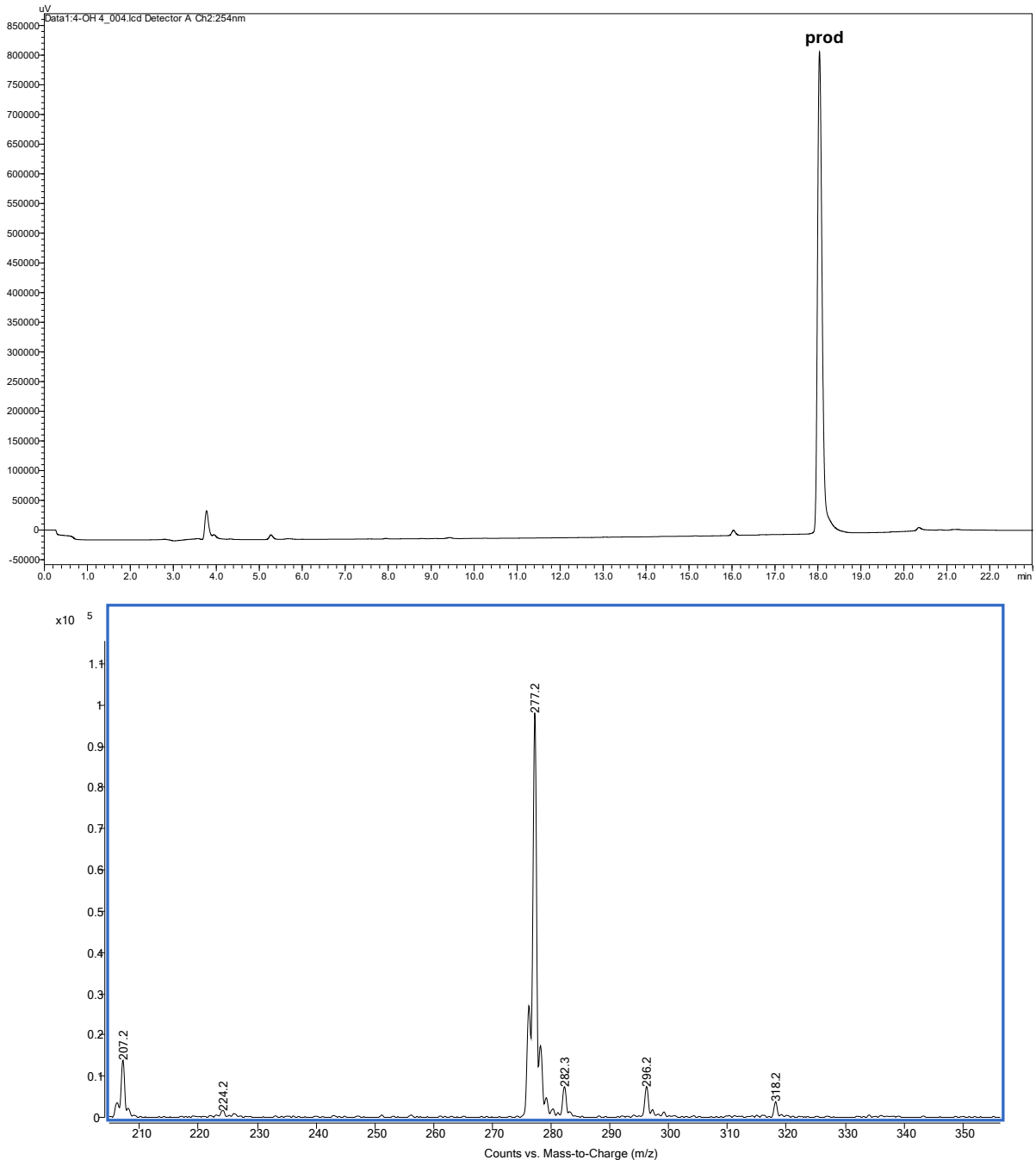

Figure S128. RP-HPLC trace at 254 nm (30-95% MeCN over 30 min) and ESI-MS spectrum of purified boronic ester **4-Epin**. m/z 277.2 corresponds to $[M+H]^+$.

(4-methoxyphenyl)boronic acid (**5**) esters characterization.

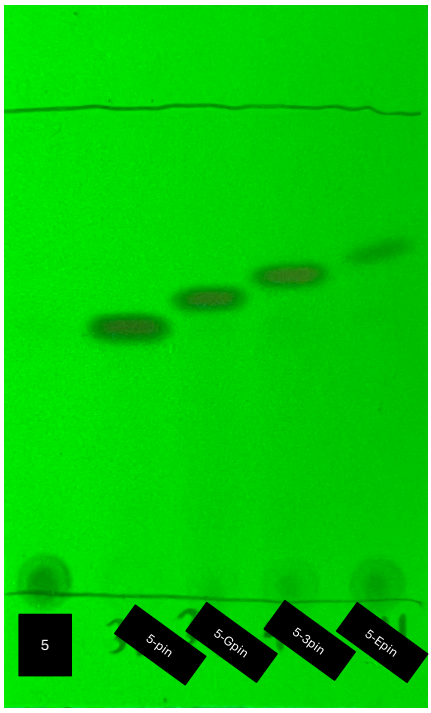

Figure S129. Boronic acid **5** and boronic esters TLC UV analysis using 15% ethyl acetate in hexanes as an eluent.

Formation and characterization of the Pinacol ester **5-pin**.

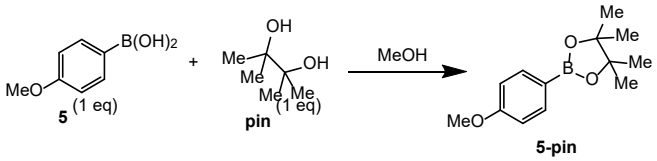

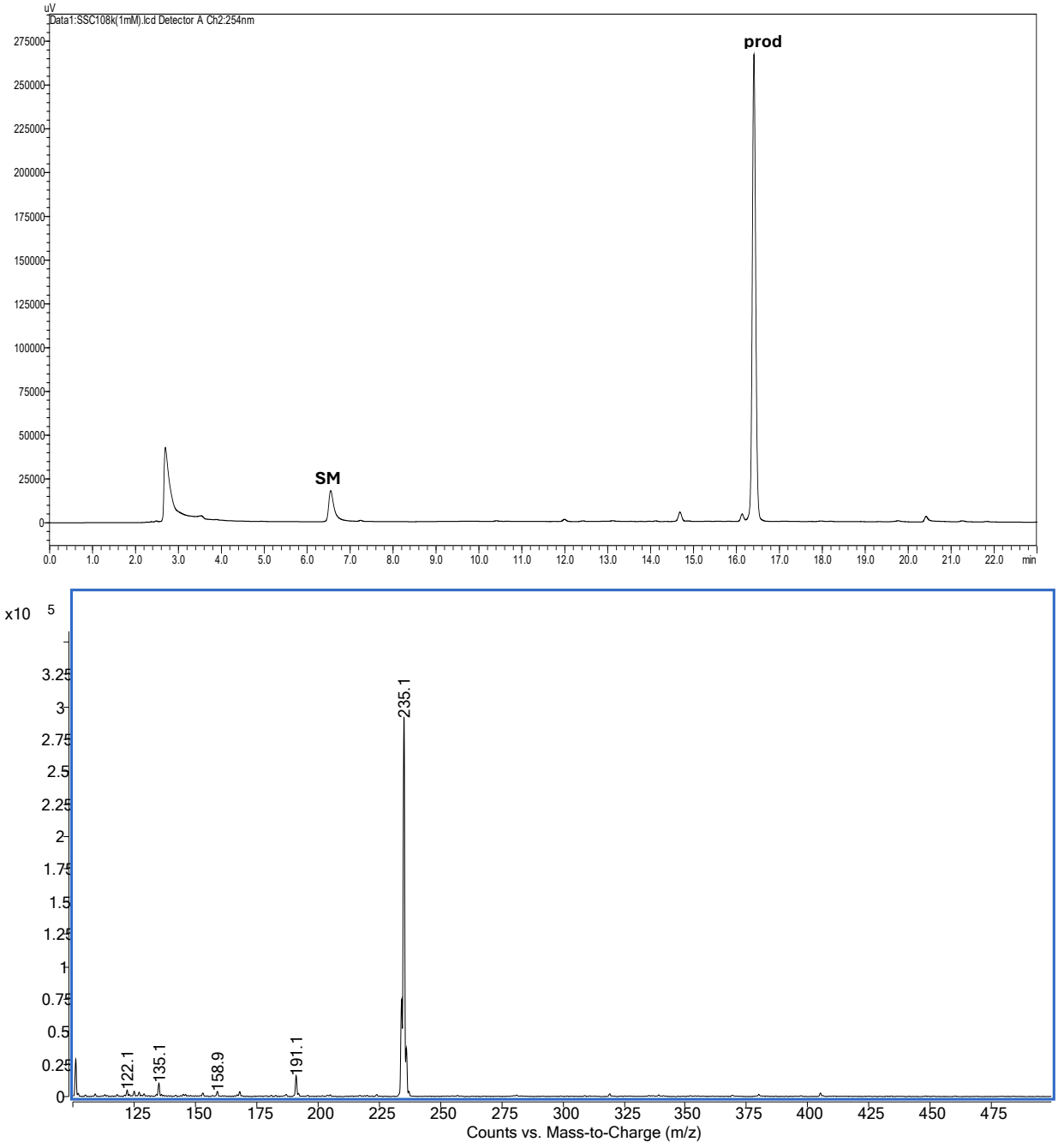

Figure S130. RP-HPLC trace at 254 nm (30-95% MeCN over 30 min) and ESI-MS spectrum of purified boronic ester **5-pin**. m/z 235.1 correspond to $[M+H]^+$.

Formation and characterization of Gpin ester **5-Gpin**.

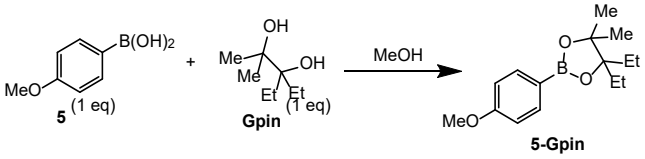

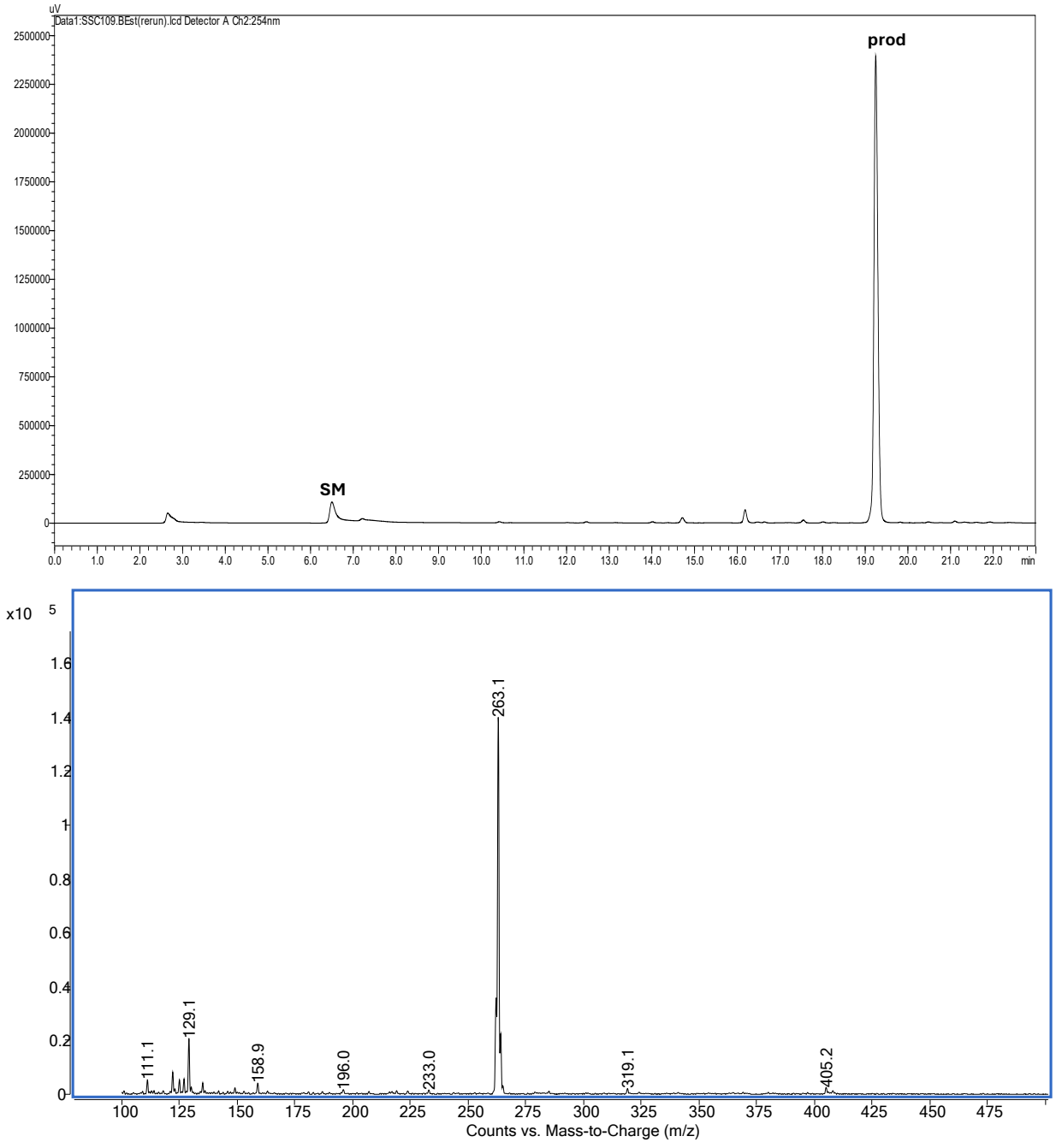

Figure S131. RP-HPLC trace at 254 nm (30-95% MeCN over 30 min) and ESI-MS spectrum of purified boronic ester **5-Gpin**. m/z 263.1 corresponds to $[M+H]^+$.

Formation and characterization of 3pin ester **5-3pin**.

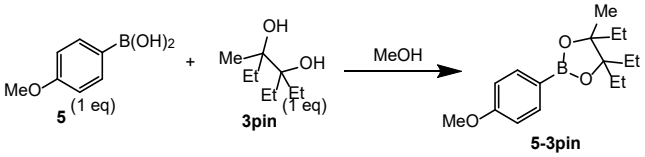

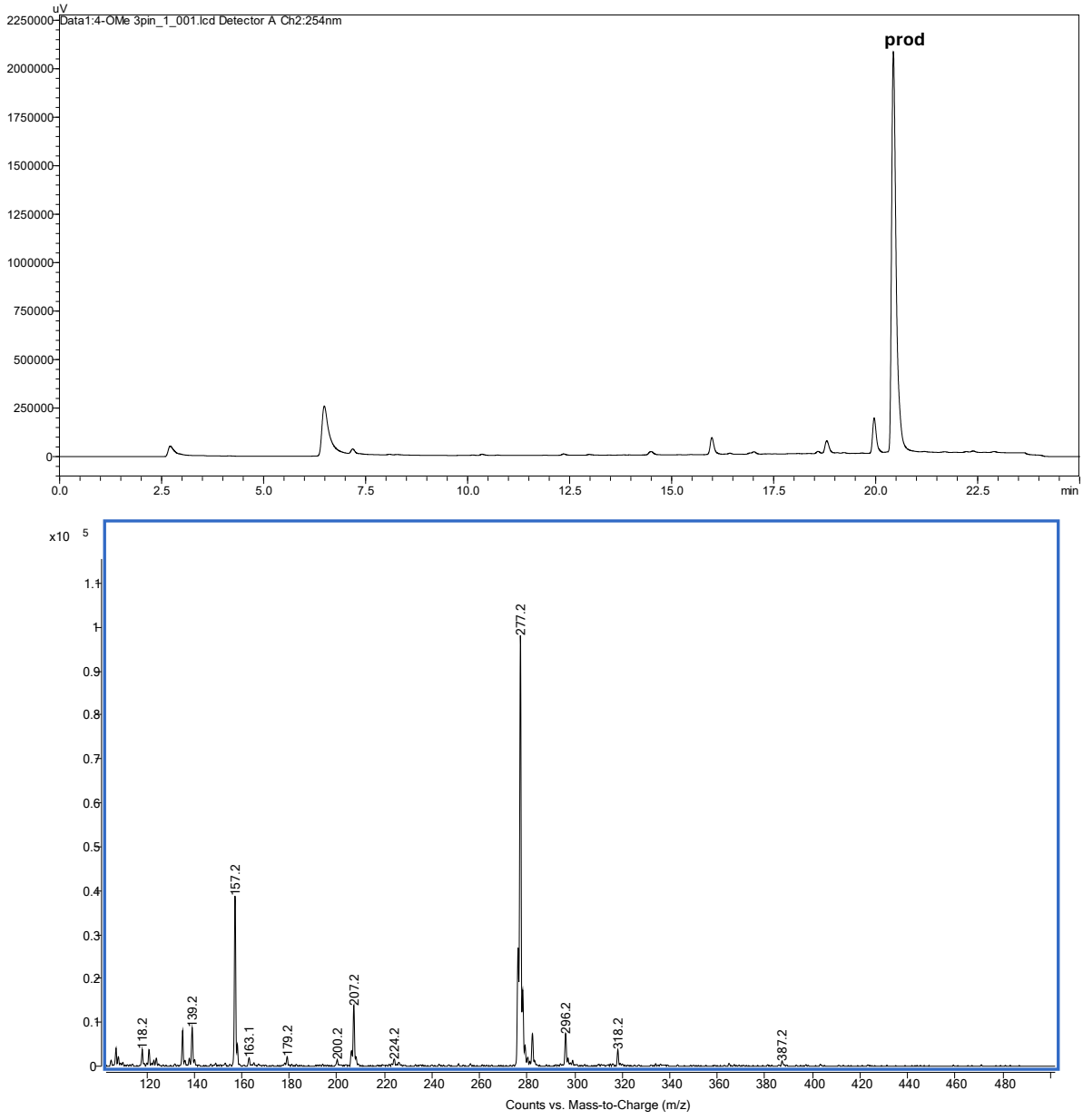

Figure S132. RP-HPLC trace at 254 nm (30-95% MeCN over 30 min) and ESI-MS spectrum of purified boronic ester **5-3pin**. m/z 277.2 $[M+H]^+$.

Formation and characterization of Epin ester **5-Epin**.

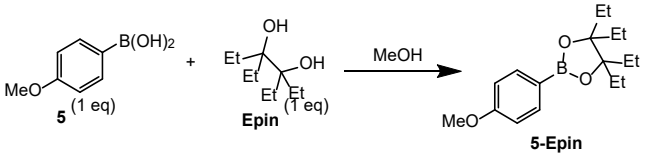

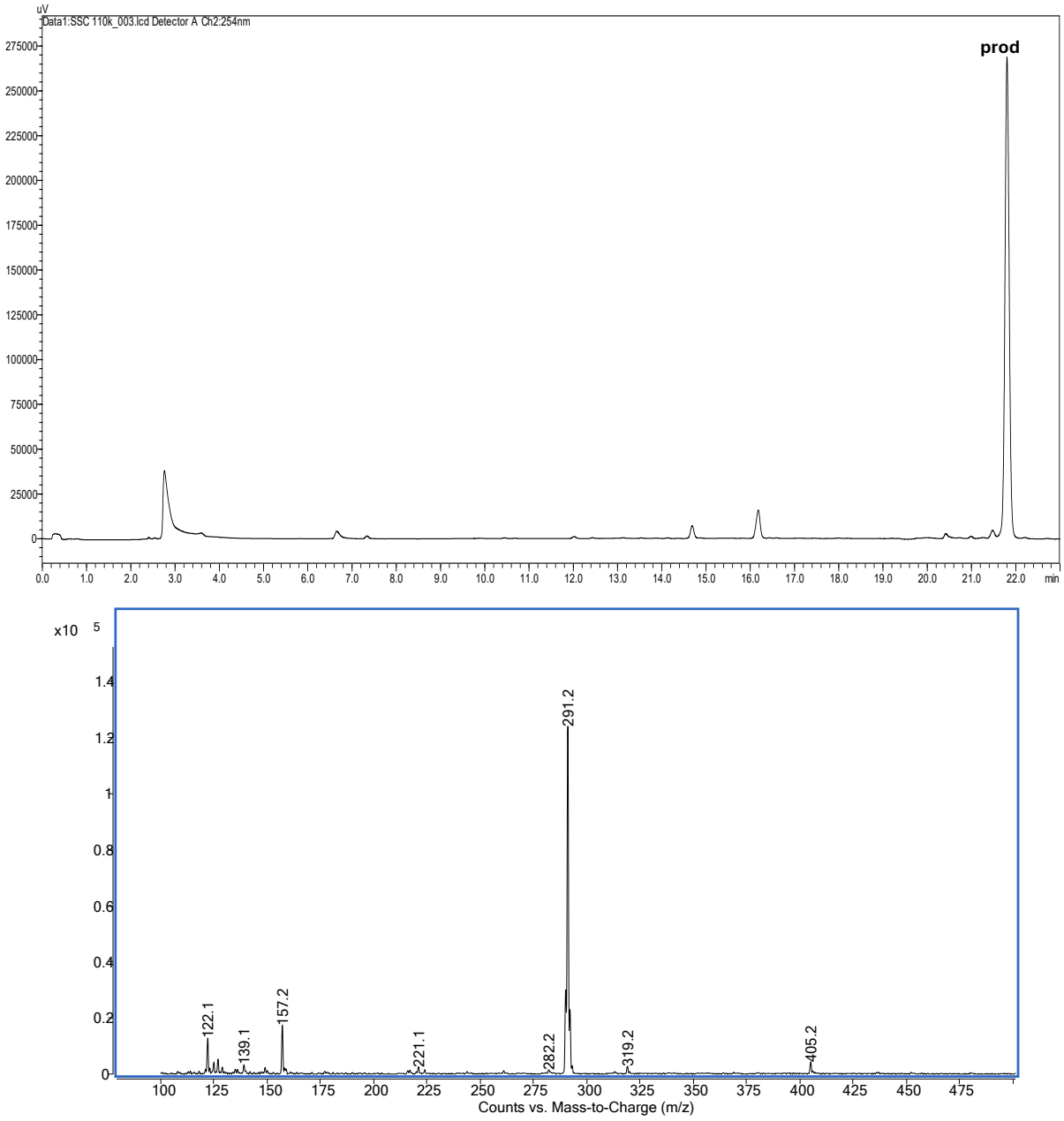

Figure S133. RP-HPLC trace at 254 nm (30-95% MeCN over 30 min) and ESI-MS spectrum of purified boronic ester **5-Epin**. m/z 291.2 corresponds to $[M+H]^+$.

(2-methoxyphenyl)boronic acid (**6**) esters characterization.

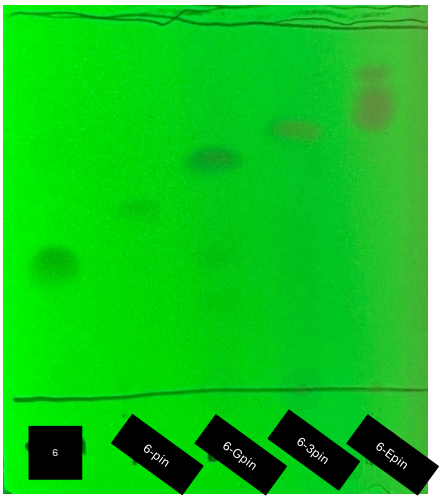

Figure S134. Boronic acid **6** and boronic esters TLC UV analysis using 15% ethyl acetate in hexanes as an eluent.

Formation and characterization of Pinacol ester **6-pin**.

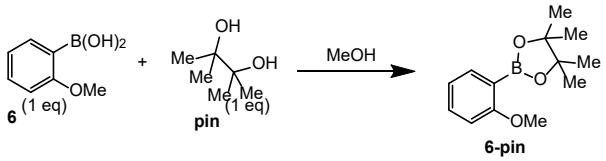

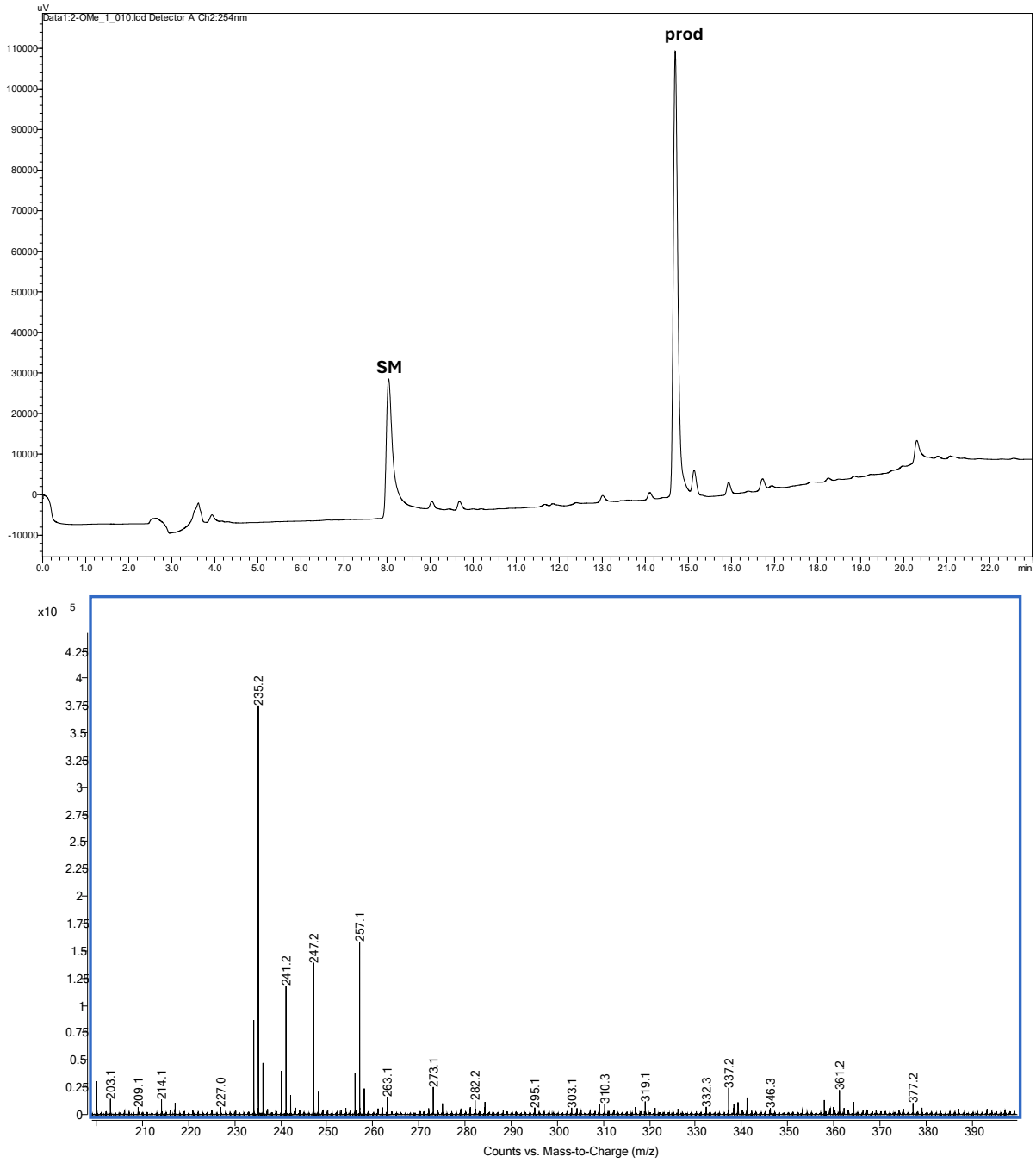

Figure S135. RP-HPLC trace at 254 nm (30-95% MeCN over 30 min) and ESI-MS spectrum of purified boronic ester **6-pin**. m/z 235.2 corresponds to $[M+H]^+$.

Formation and characterization of Gpin ester **6-Gpin**.

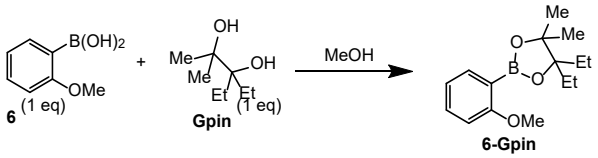

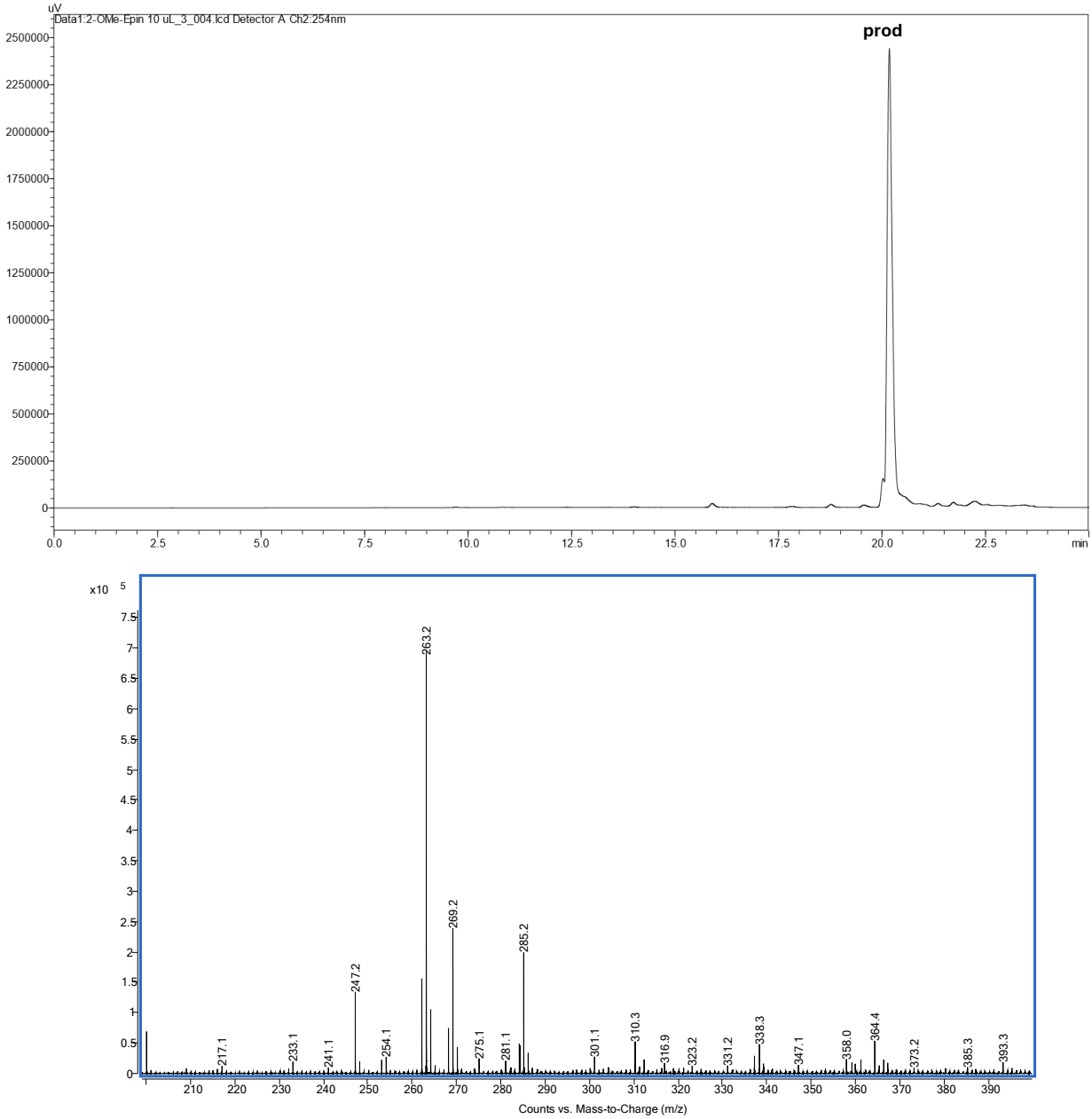

Figure S136. RP-HPLC trace at 220 nm (30-95% MeCN over 30 min) and ESI-MS spectrum of purified boronic ester **6-Gpin**. m/z 263.2 $[M+H]^+$.

Formation and characterization of 3pin ester **6-3pin**.

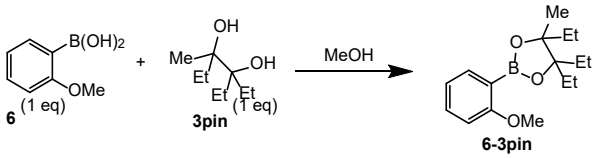

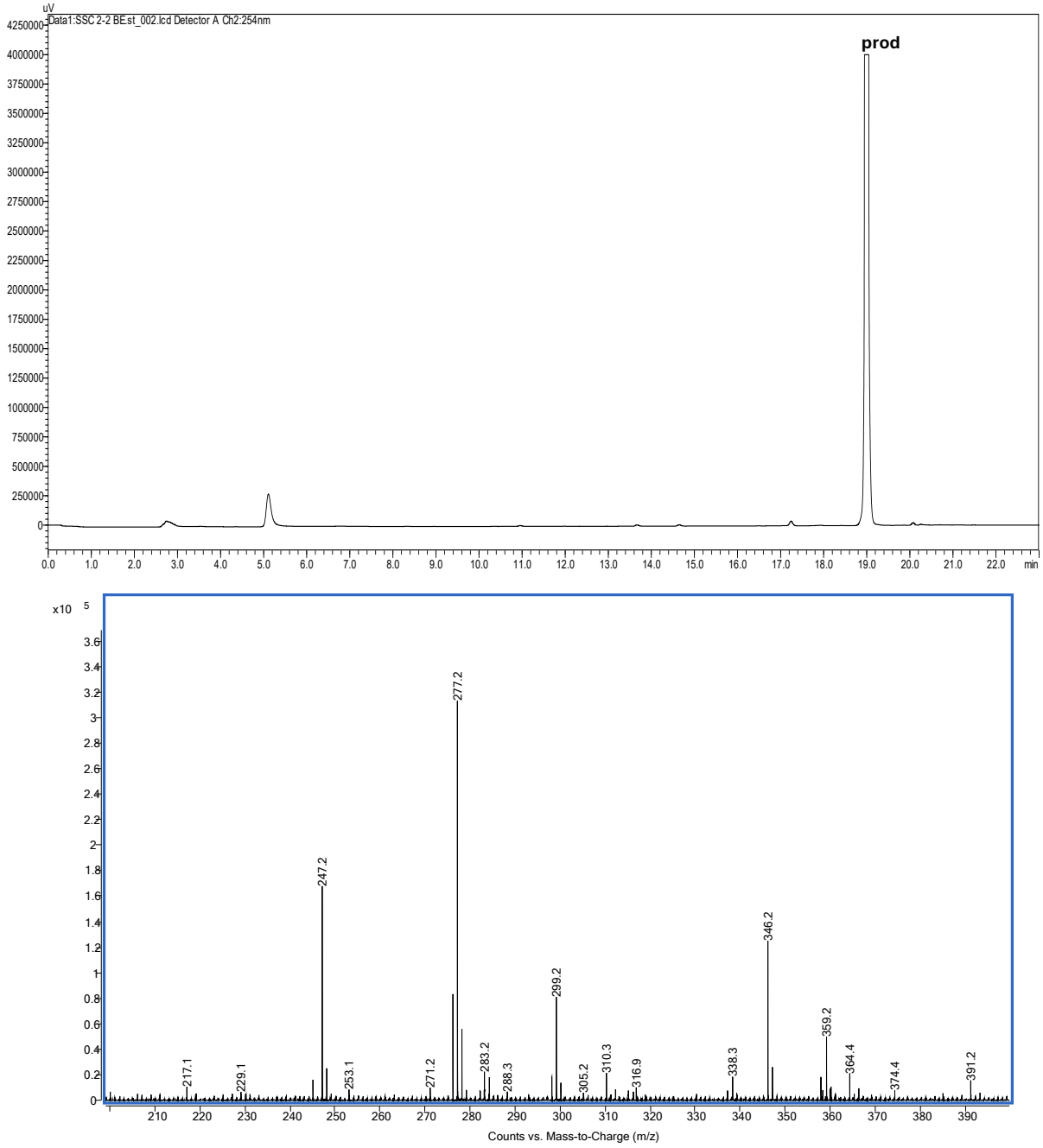

Figure S137. RP-HPLC trace at 254 nm (30-95% MeCN over 30 min) and ESI-MS spectrum of purified boronic ester **6-3pin**. m/z 277.2 $[M+H]^+$.

Formation and characterization of Epin ester **6-Epin**.

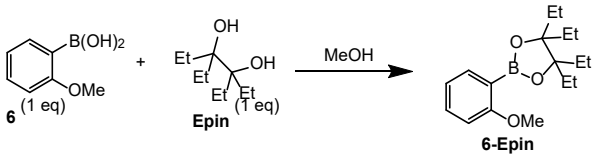

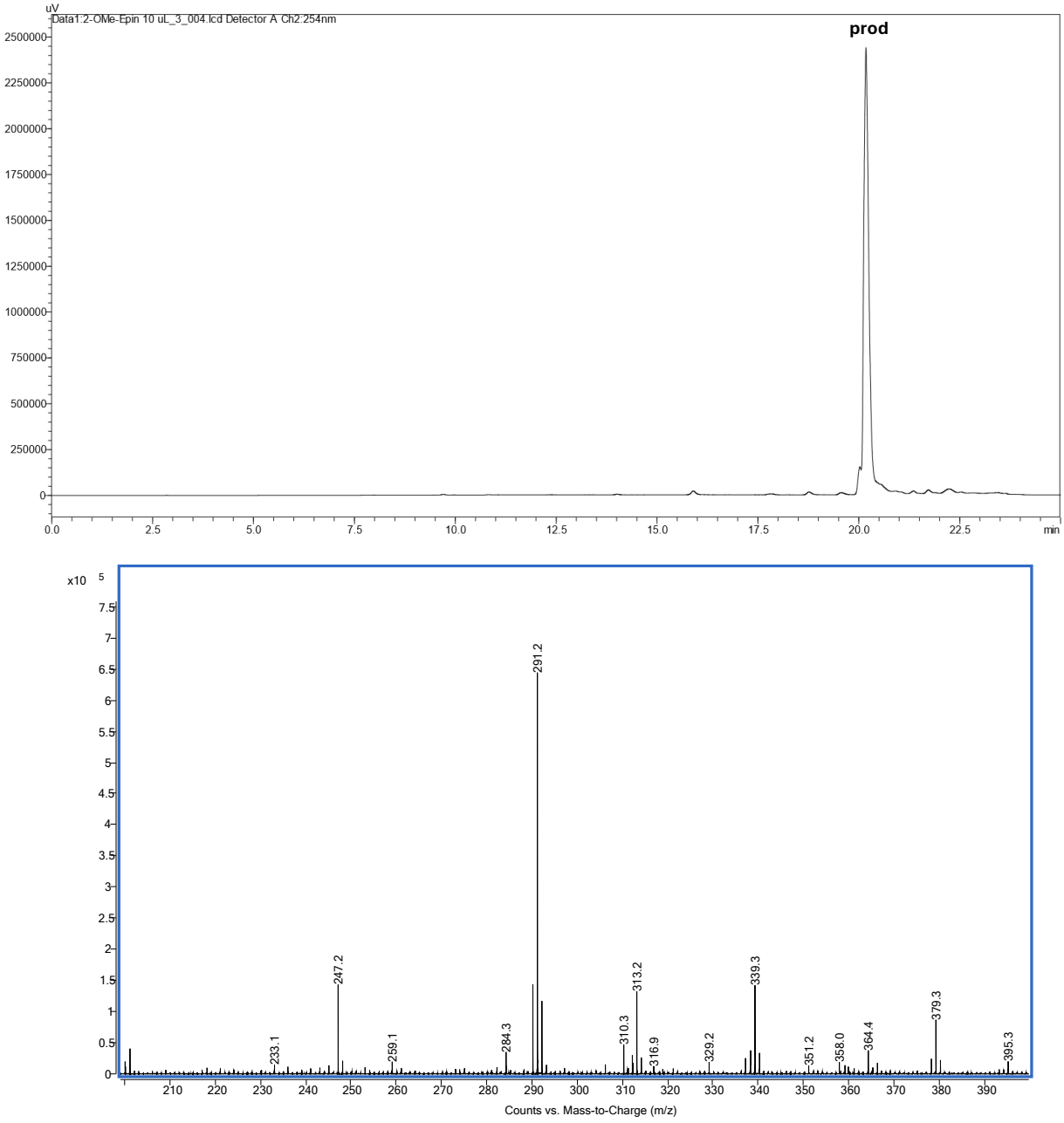

Figure S138. RP-HPLC trace at 254 nm (30-95% MeCN over 30 min) and ESI-MS spectrum of purified boronic ester **6-Epin**. m/z 291.2 $[M+H]^+$.

(4-nitrophenyl)boronic acid (**7**) esters characterization.

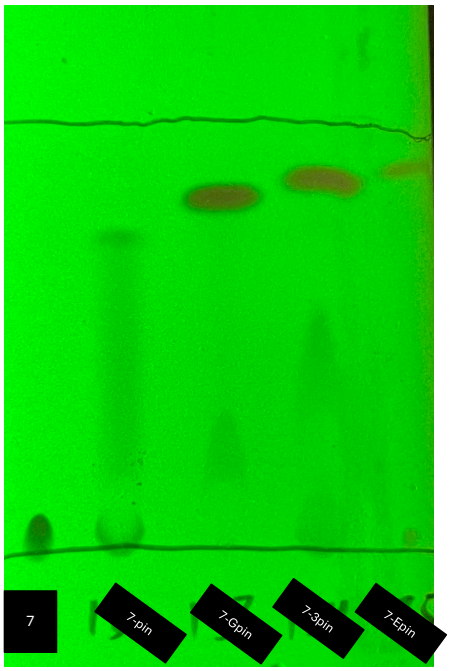

Figure S139. Boronic acid **7** and boronic esters TLC UV analysis using 15% ethyl acetate in hexanes as an eluent.

Formation and characterization of Gpin ester **7-Gpin**.

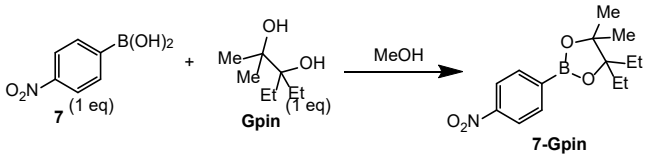

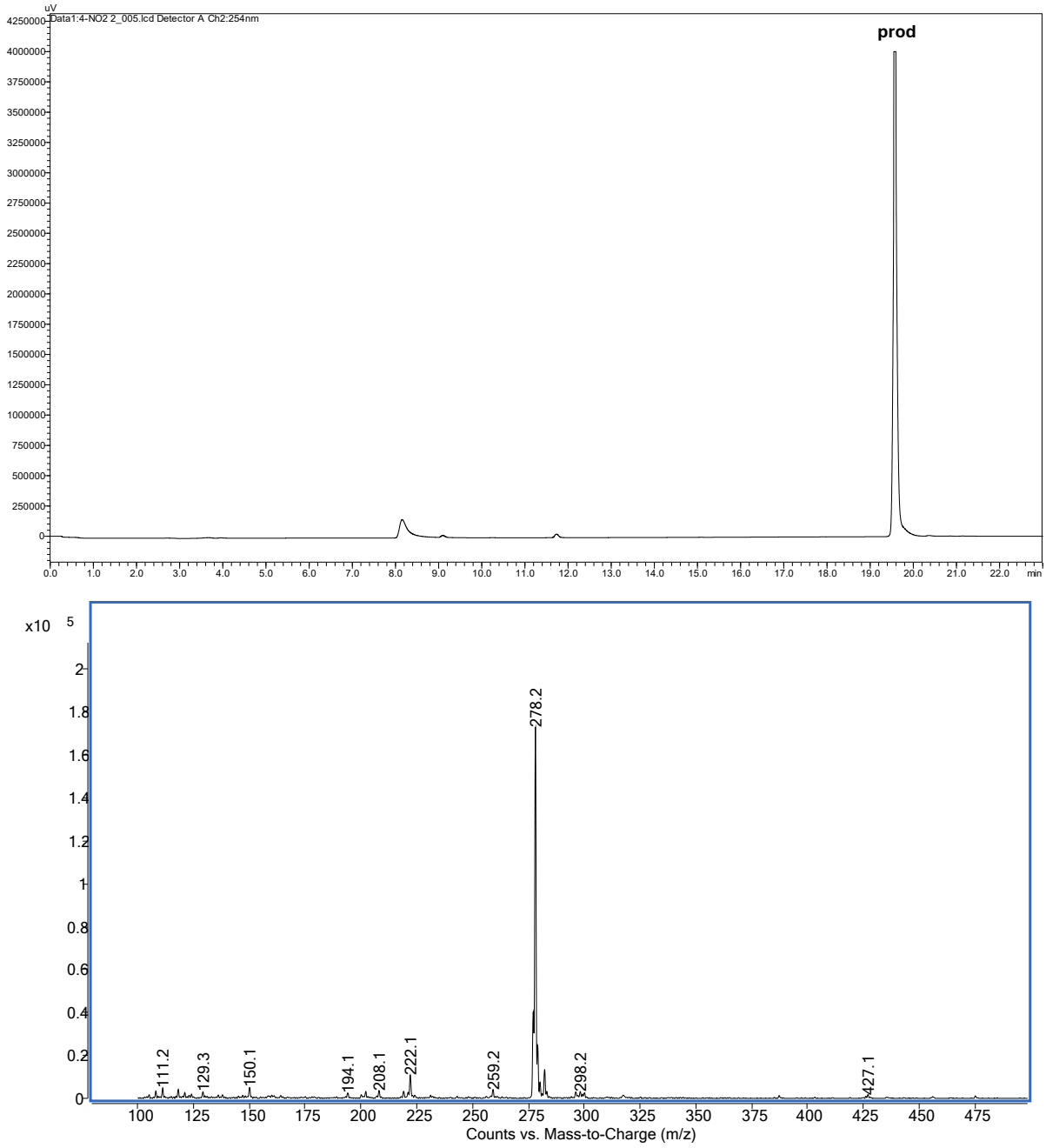

Figure S140. RP-HPLC trace at 254 nm (30-95% MeCN over 30 min) and ESI-MS spectrum of purified boronic ester **7-Gpin**. m/z 278.2 corresponds to $[M+H]^+$.

Formation and characterization of 3pin ester **7-3pin**.

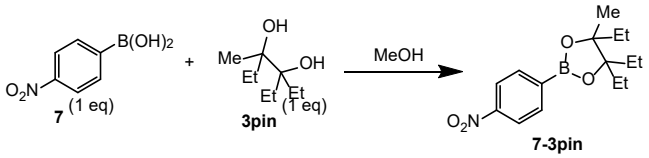

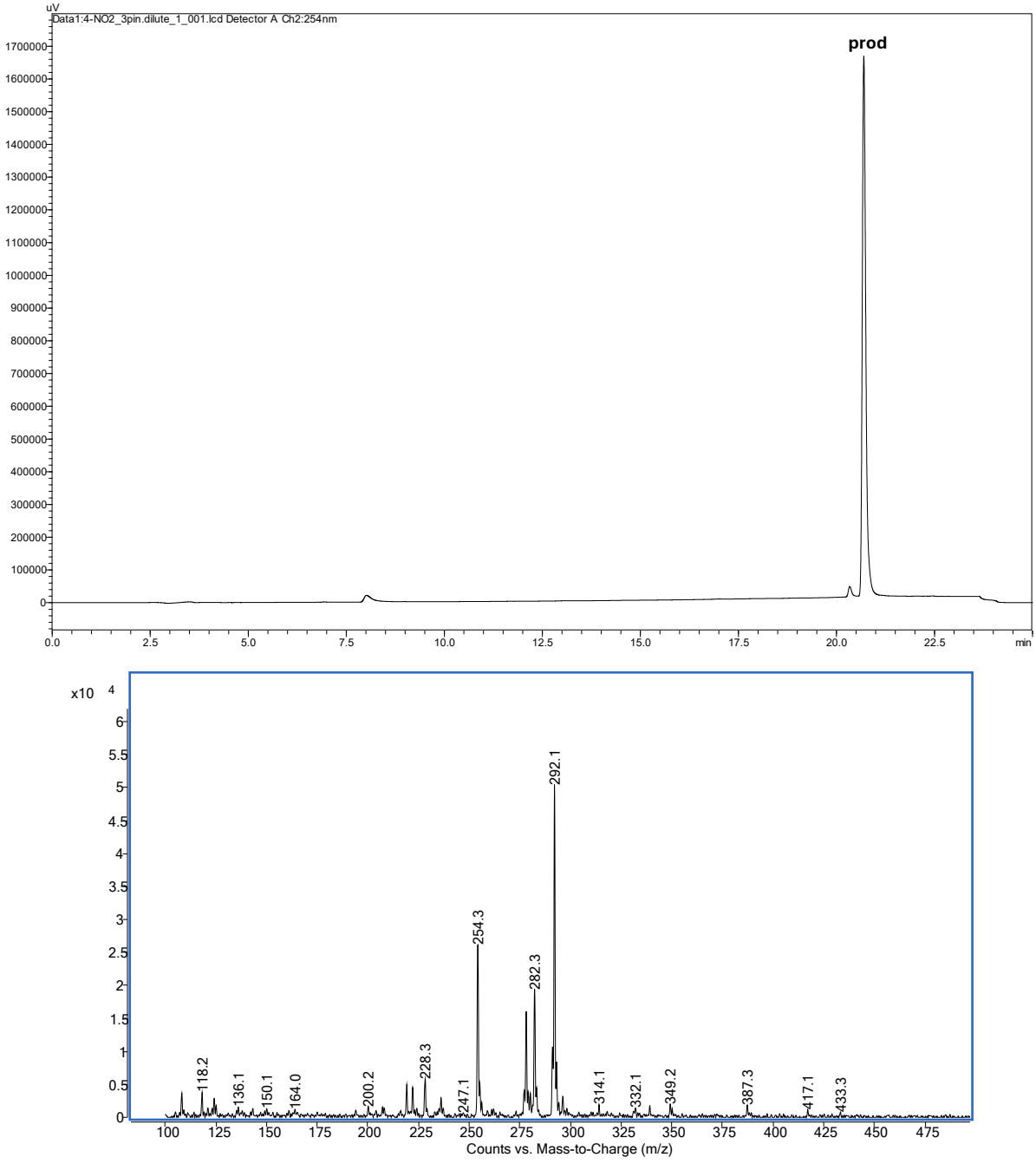

Figure S141. RP-HPLC trace at 254 nm (30-95% MeCN over 30 min) and ESI-MS spectrum of purified boronic ester **7-3pin**. m/z 292.1 corresponds to $[M+H]^+$.

Formation and characterization of Epin ester **7-Epin**.

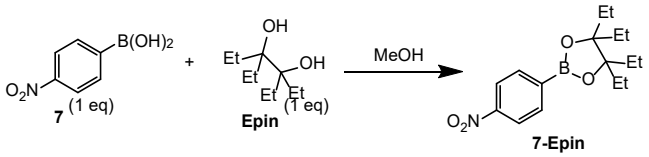

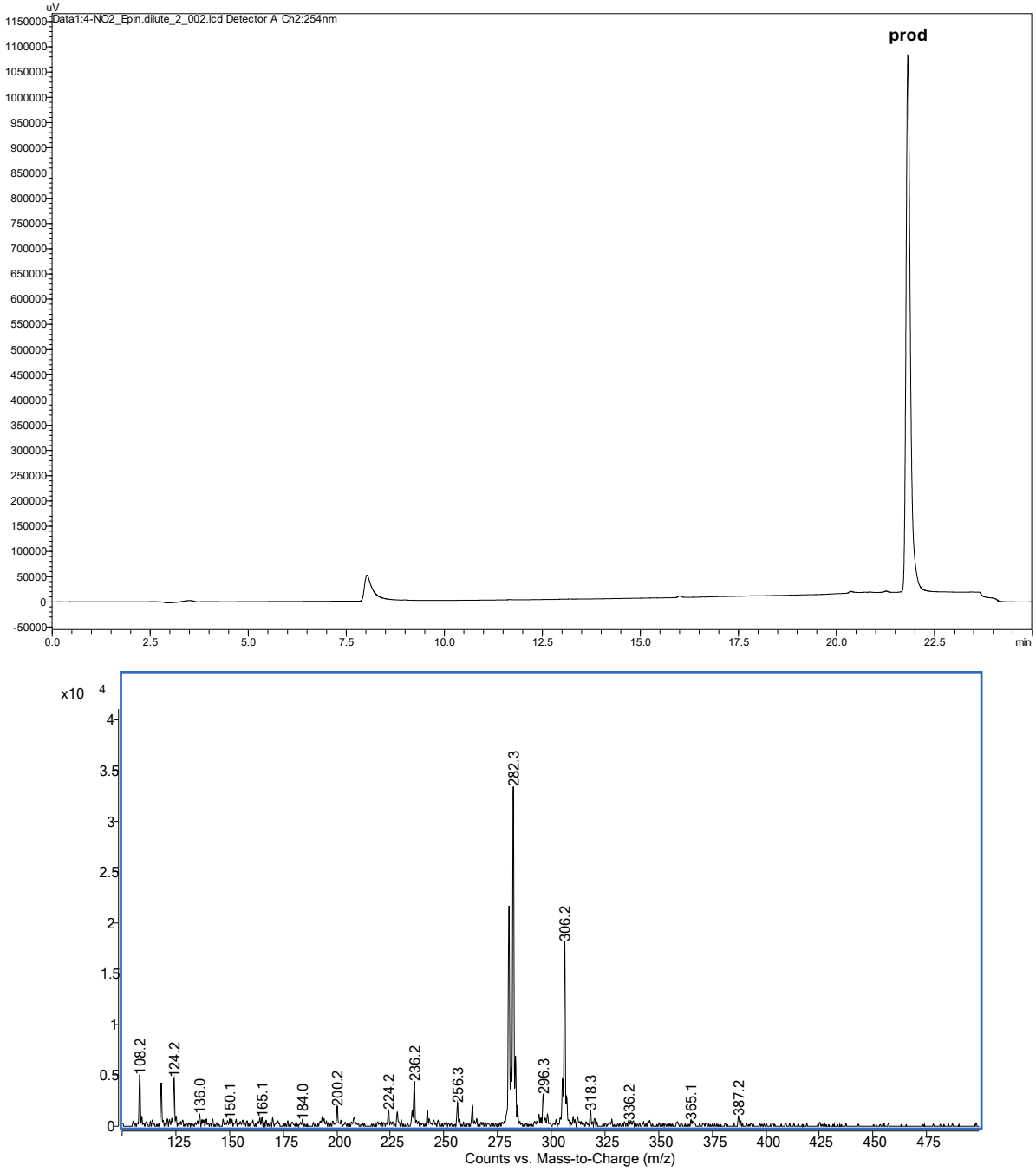

Figure S142. RP-HPLC trace at 254 nm (30-95% MeCN over 30 min) and ESI-MS spectrum of purified boronic ester **7-Epin**. m/z 306.2 corresponds to $[M+H]^+$.

(3-nitrophenyl)boronic acid (**8**) esters characterization.

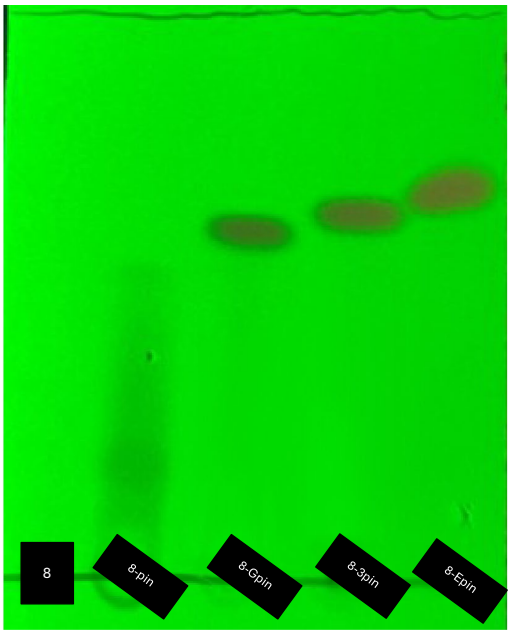

Figure S143. Boronic acid **8** and boronic esters TLC UV analysis using 20% ethyl acetate in hexanes as an eluent.

Standard of free boronic acid **8.**

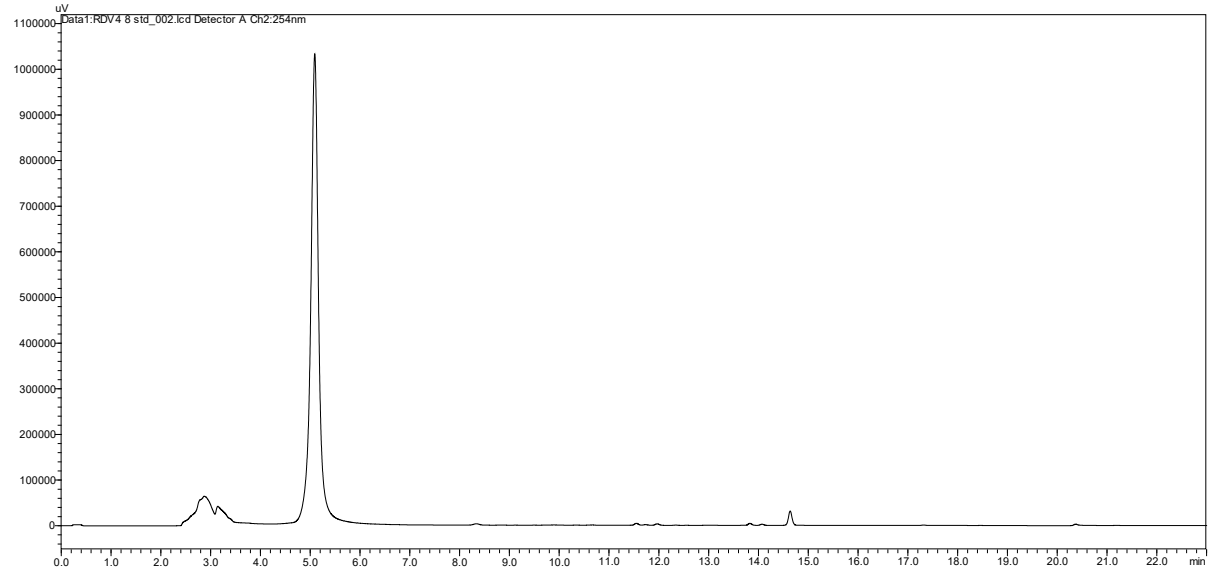

Figure S144. RP-HPLC trace at 254 nm (30-95% MeCN over 23 min) of free boronic acid 8**.**

Formation and characterization of pinacol ester **8-pin**.

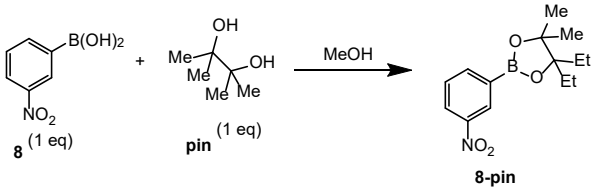

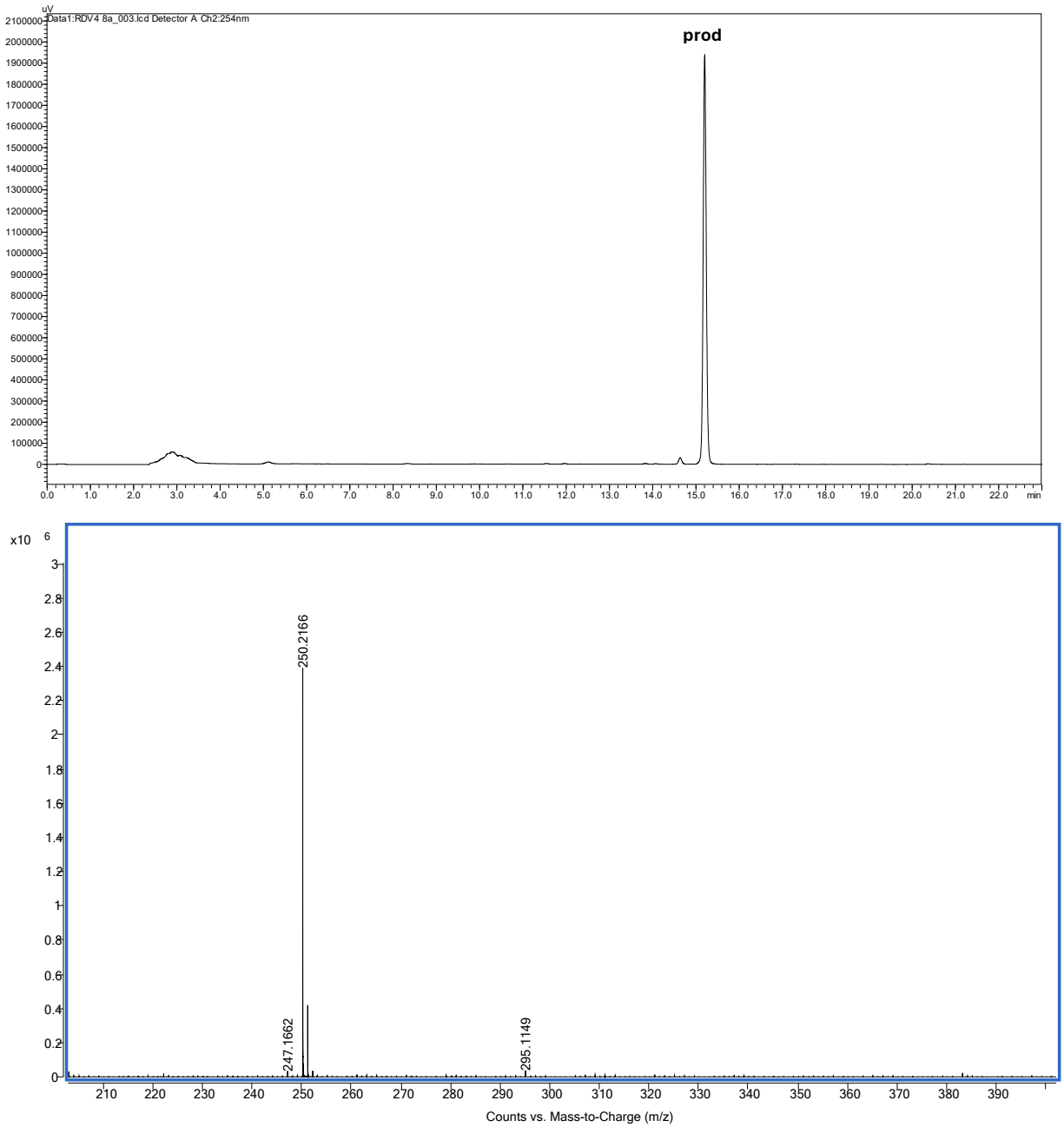

Figure S145. RP-HPLC trace at 254 nm (30-95% MeCN over 30 min) and ESI-MS spectrum of purified boronic ester **8-pin**. m/z 250.2166 corresponds to $[M+H]^+$.

Formation and characterization of **Gpin** ester **8-Gpin**.

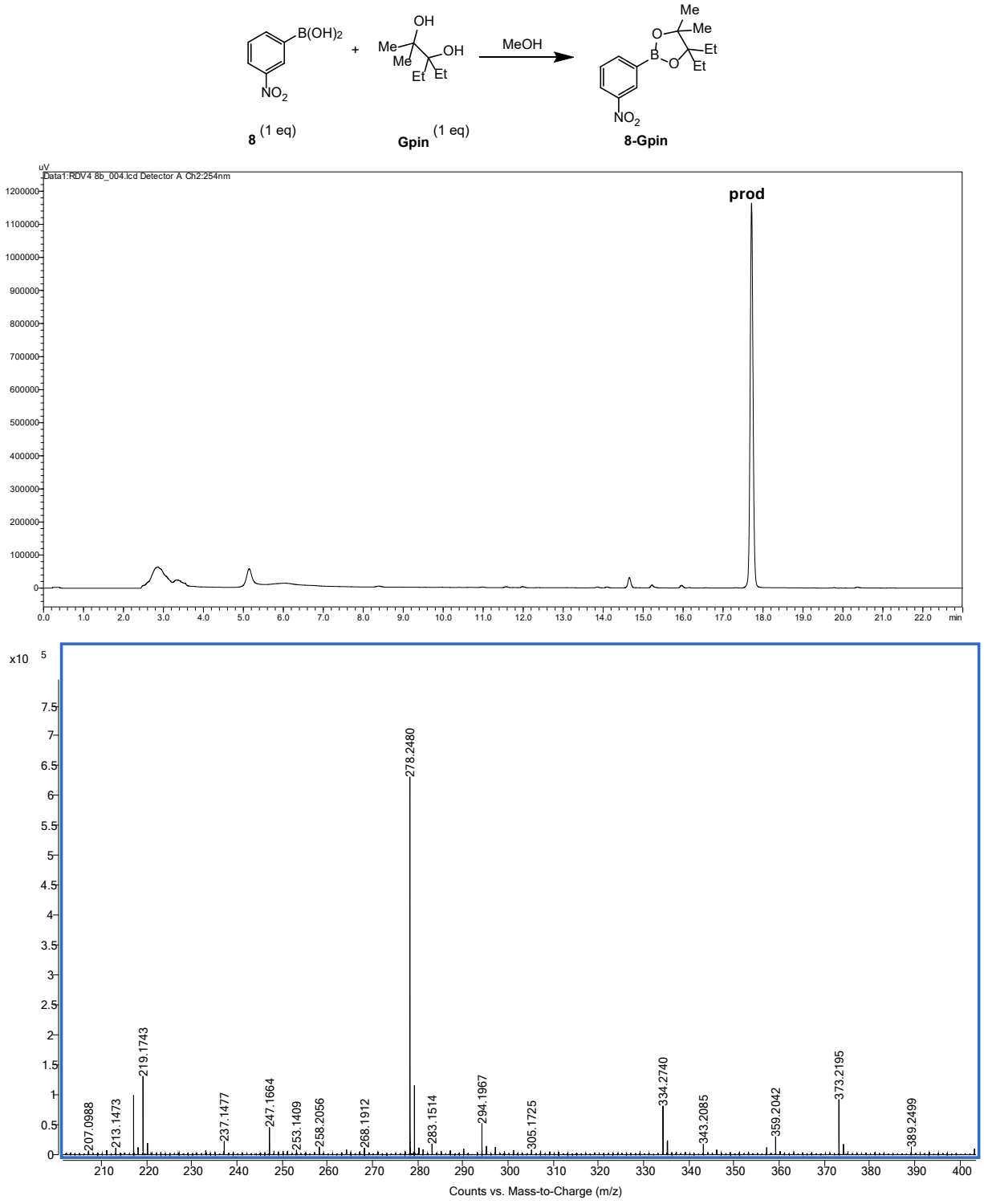

Figure S146. RP-HPLC trace at 254 nm (30-95% MeCN over 30 min) and ESI-MS spectrum of purified boronic ester **8-Gpin**. m/z 278.2480 corresponds to $[M+H]^+$.

Formation and characterization of 3-Ethyl Pinacol ester **8-3pin**.

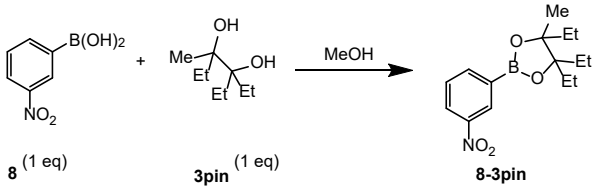

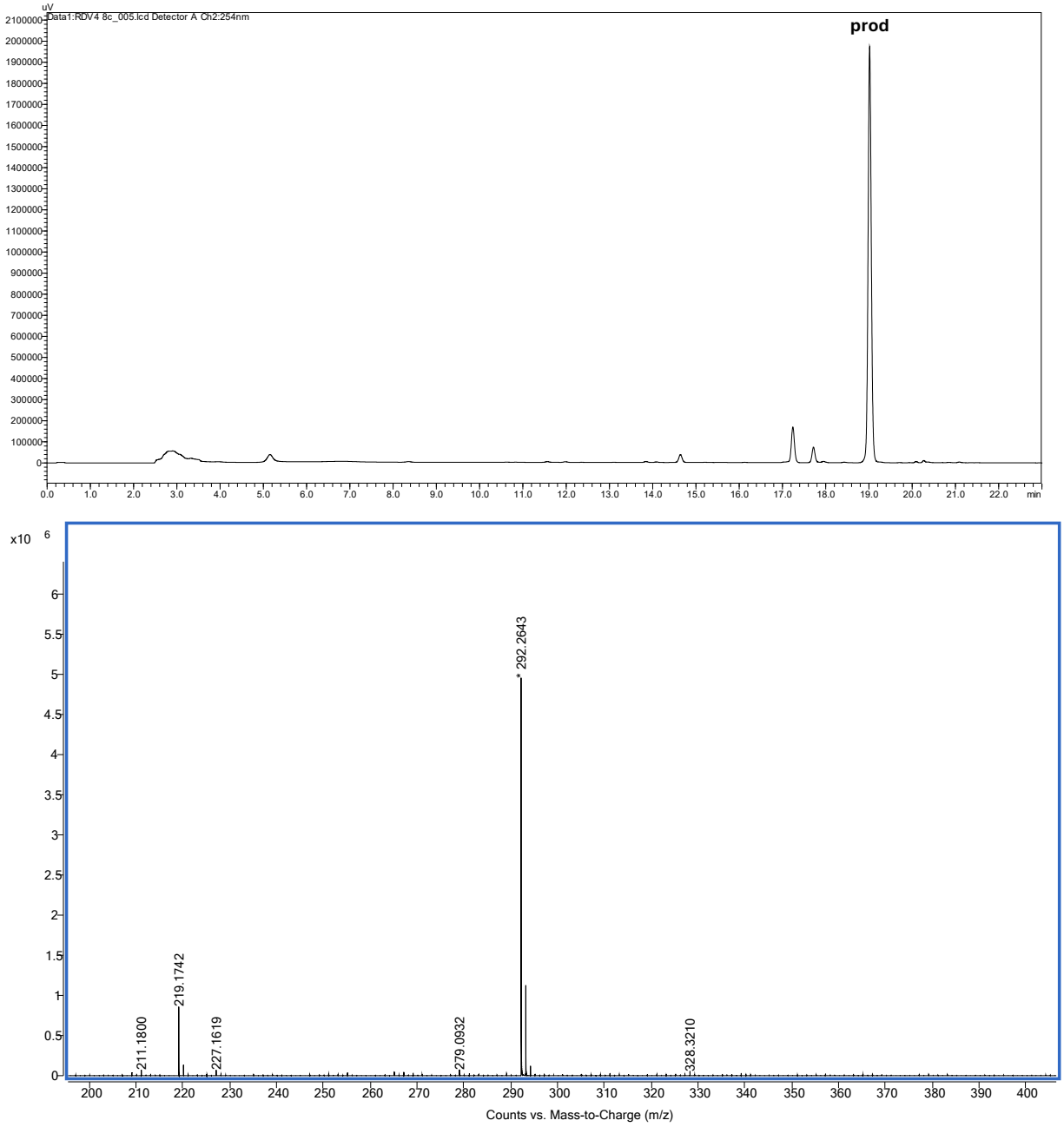

Figure S147. RP-HPLC trace at 254 nm (30-95% MeCN over 30 min) and ESI-MS spectrum of purified boronic ester **8-3pin**. m/z 292.2643 corresponds to $[M+H]^+$.

Formation and characterization of Epin ester **8-Epin**.

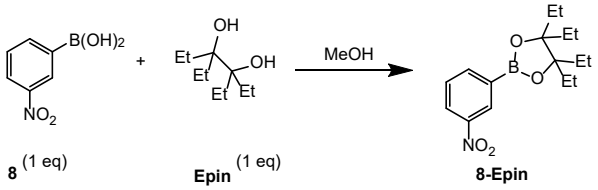

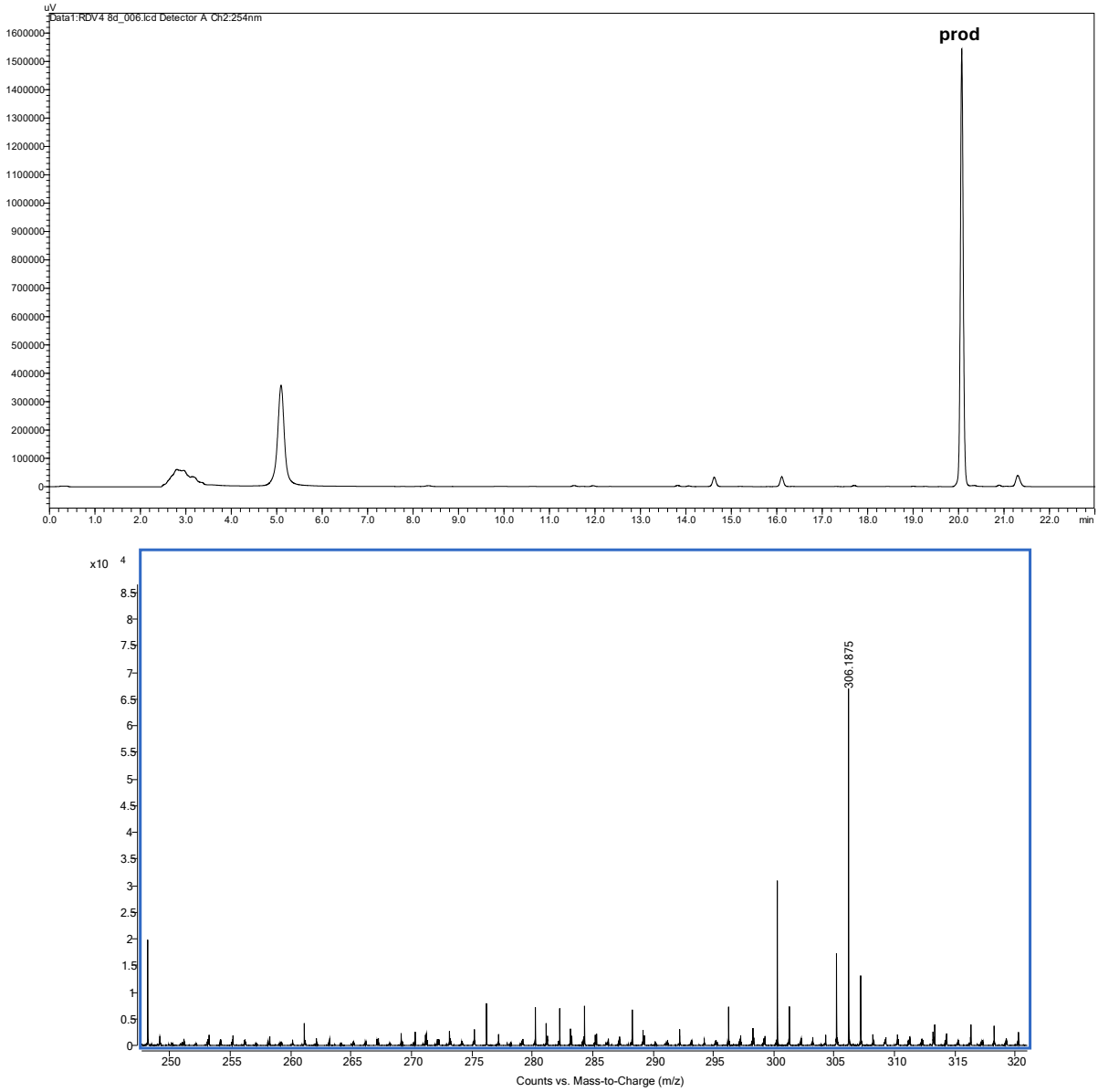

Figure S148. RP-HPLC trace at 254 nm (30-95% MeCN over 30 min) and ESI-MS spectrum of purified boronic ester **8-Epin**. m/z 306.1875 corresponds to $[M+H]^+$.

(2-nitrophenyl)boronic acid (**9**) esters characterization.

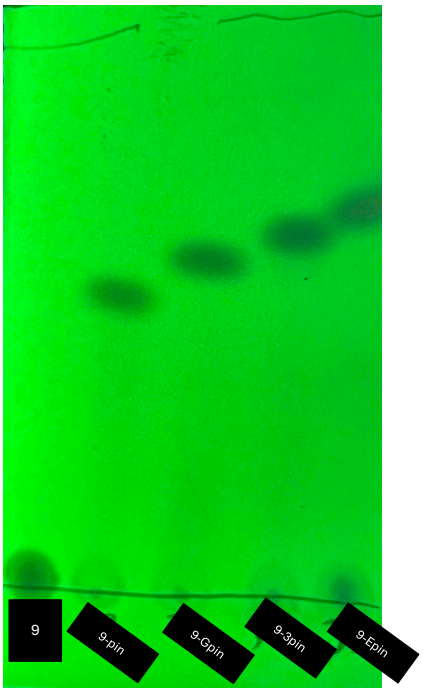

Figure S149. Boronic acid **9** and boronic esters TLC UV analysis using 20% ethyl acetate in hexanes as an eluent

Formation and characterization of Pinacol ester **9-pin**.

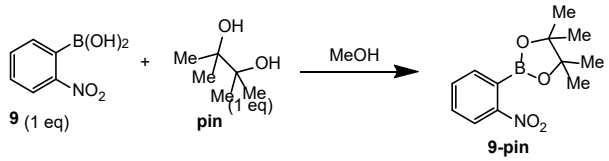

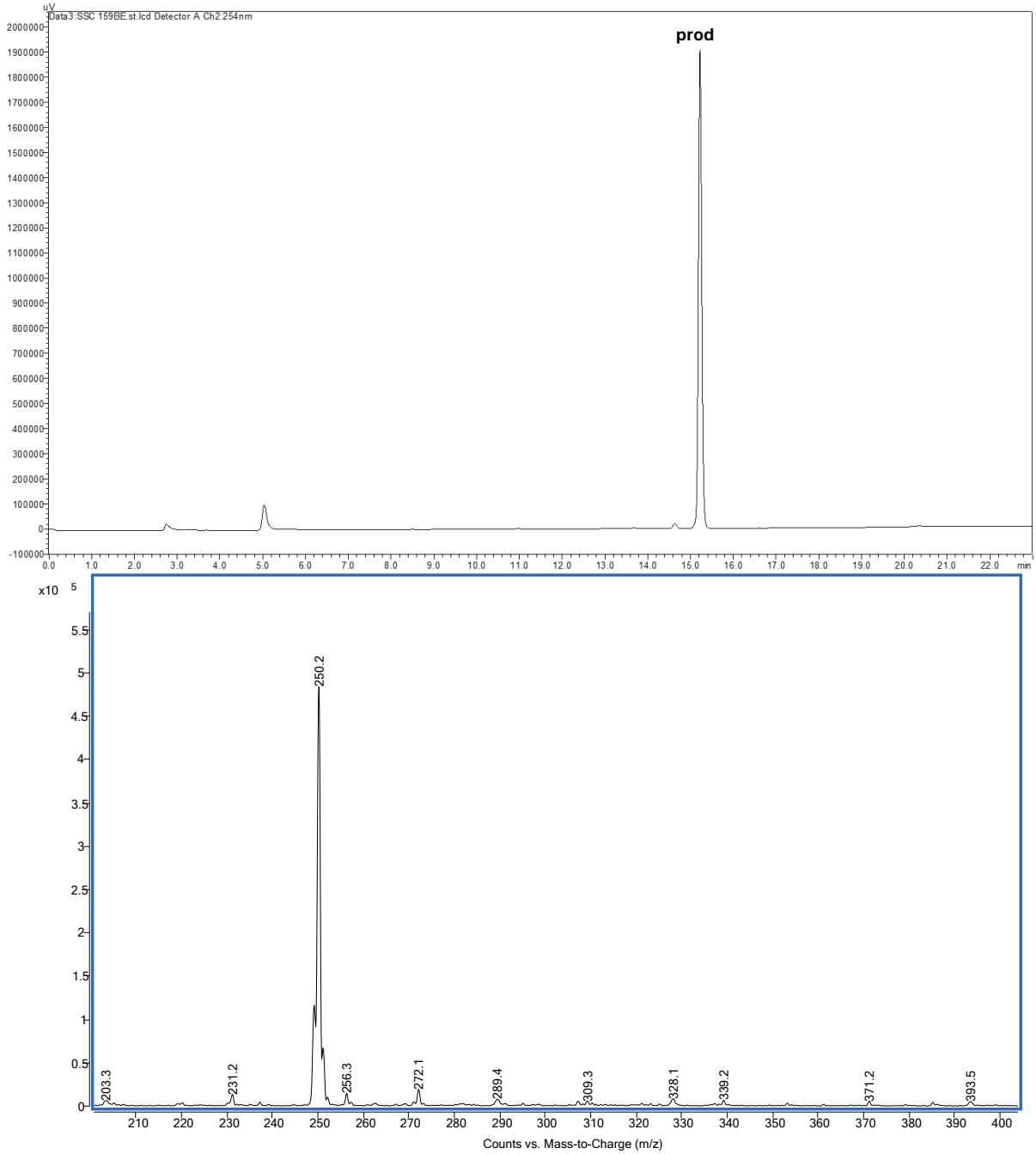

Figure S150. RP-HPLC trace at 254 nm (30-95% MeCN over 30 min) and ESI-MS spectrum of purified boronic ester **9-pin**. m/z 250.2 corresponds to $[M+H]^+$.

Formation and characterization of Gpin ester **9-Gpin**.

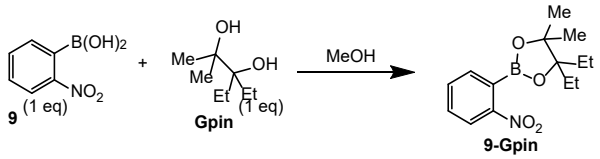

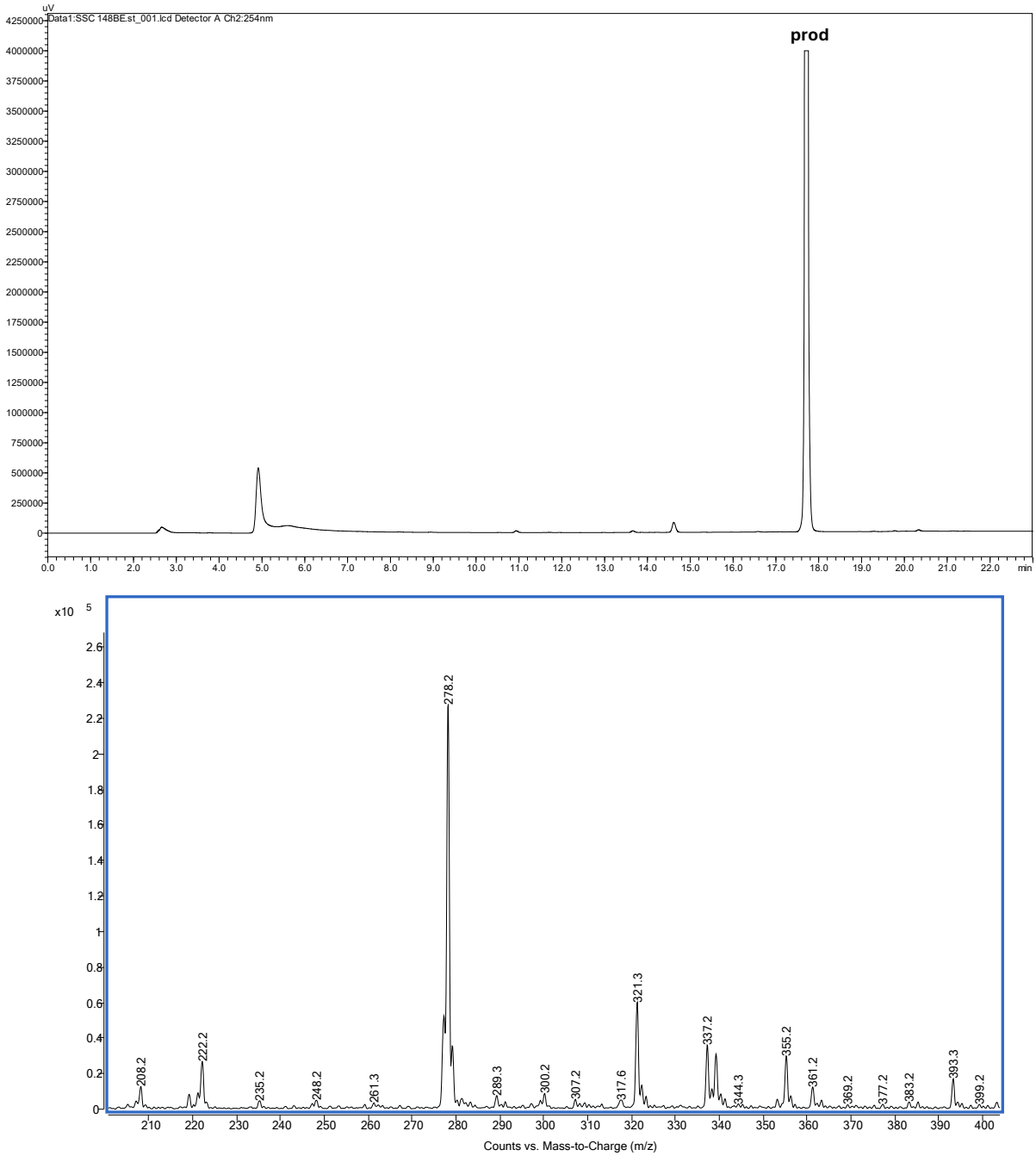

Figure S151. RP-HPLC trace at 254 nm (30-95% MeCN over 30 min) and ESI-MS spectrum of purified boronic ester **9-Gpin**. m/z 278.2 corresponds to $[M+H]^+$.

Formation and characterization of 3pin ester **9-3pin**.

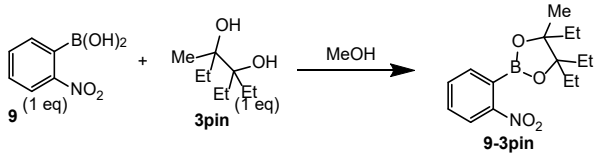

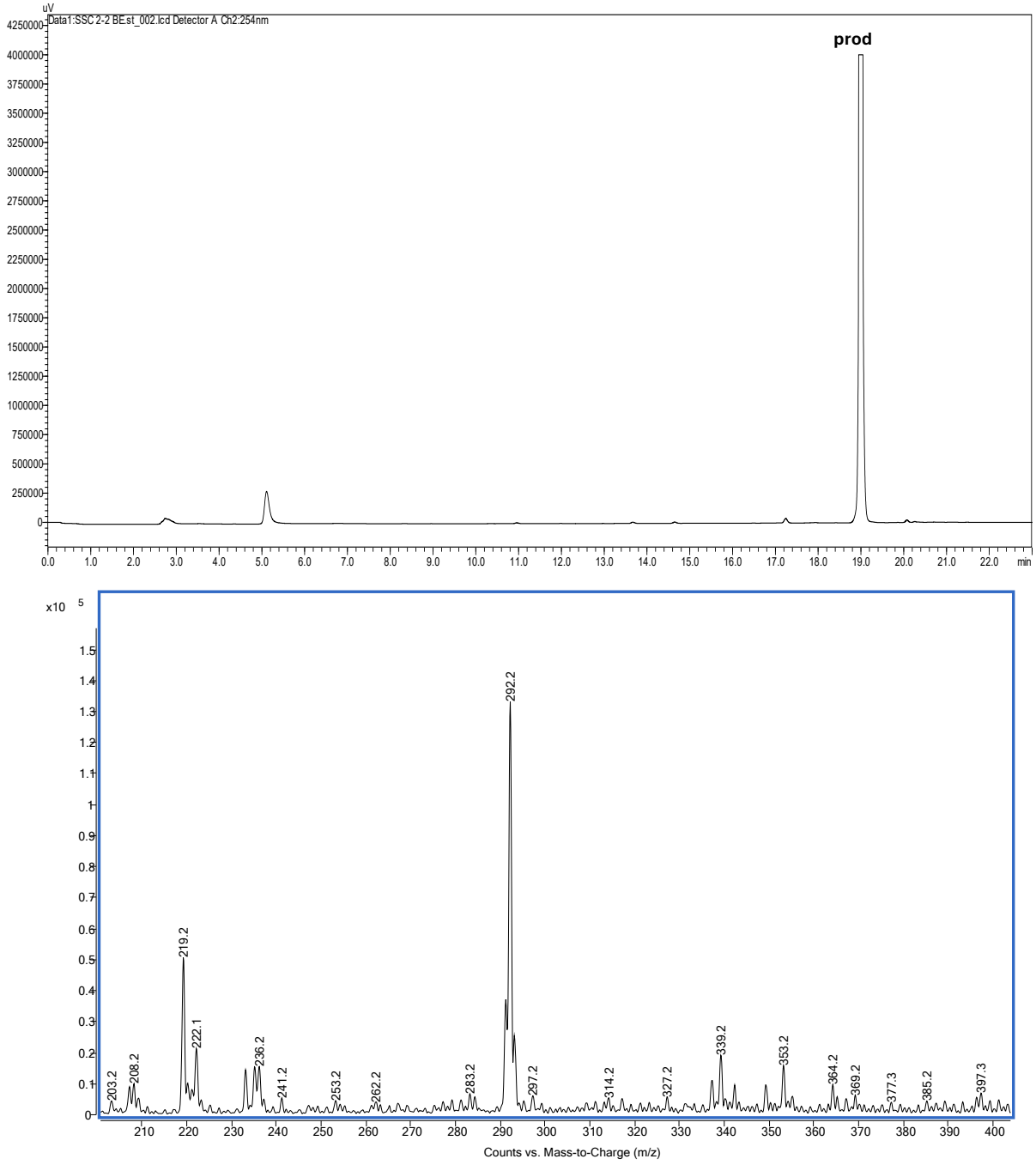

Figure S152. RP-HPLC trace at 254 nm (30-95% MeCN over 30 min) and ESI-MS spectrum of purified boronic ester **9-3pin**. m/z 292.2 corresponds to $[M+H]^+$.

Formation and characterization of Epin ester **9-Epin**.

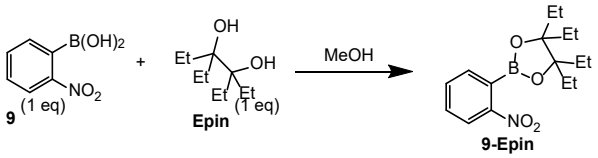

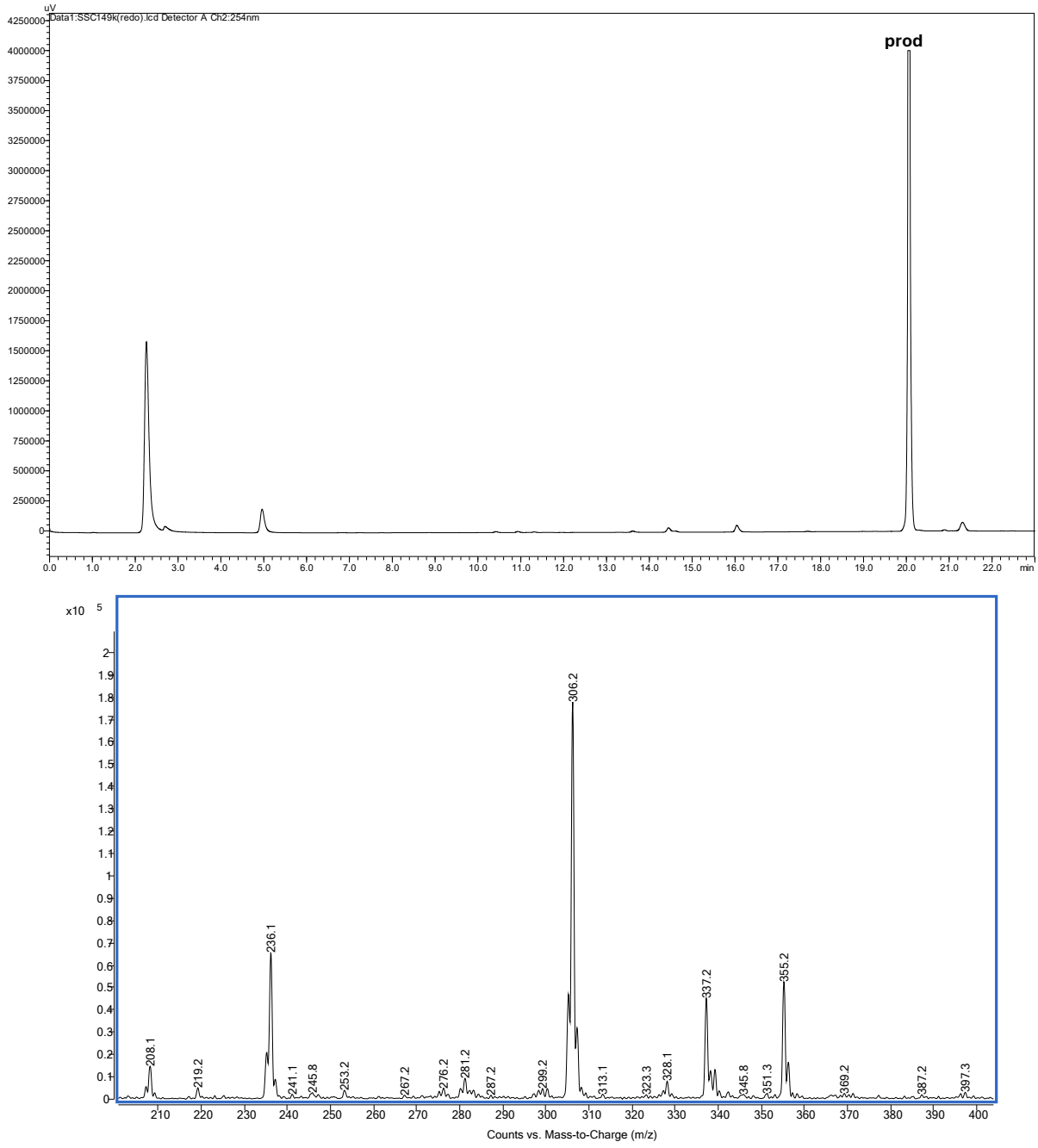

Figure S153. RP-HPLC trace at 254 nm (30-95% MeCN over 30 min) and ESI-MS spectrum of purified boronic ester **9-Epin**. m/z 306.2 corresponds to $[M+H]^+$.

4-borono-3-fluorobenzoic acid (**10**) esters characterization.

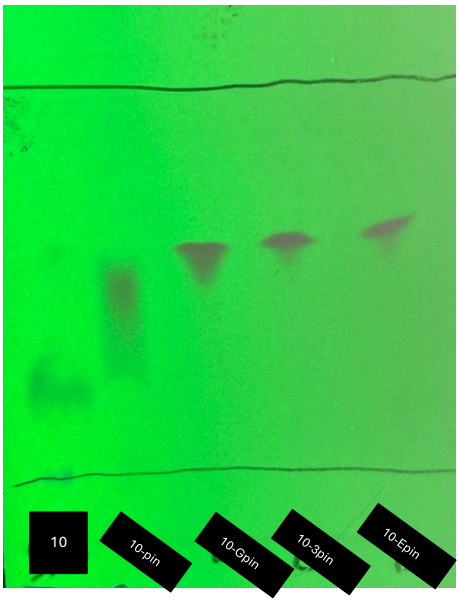

Figure S154. Boronic acid **10** and boronic esters TLC analysis using 0.1% acetic acid and 20% ethyl acetate in hexanes as an eluent.

Formation and characterization of Gpin ester **10-Gpin**.

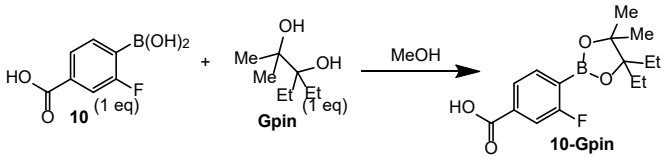

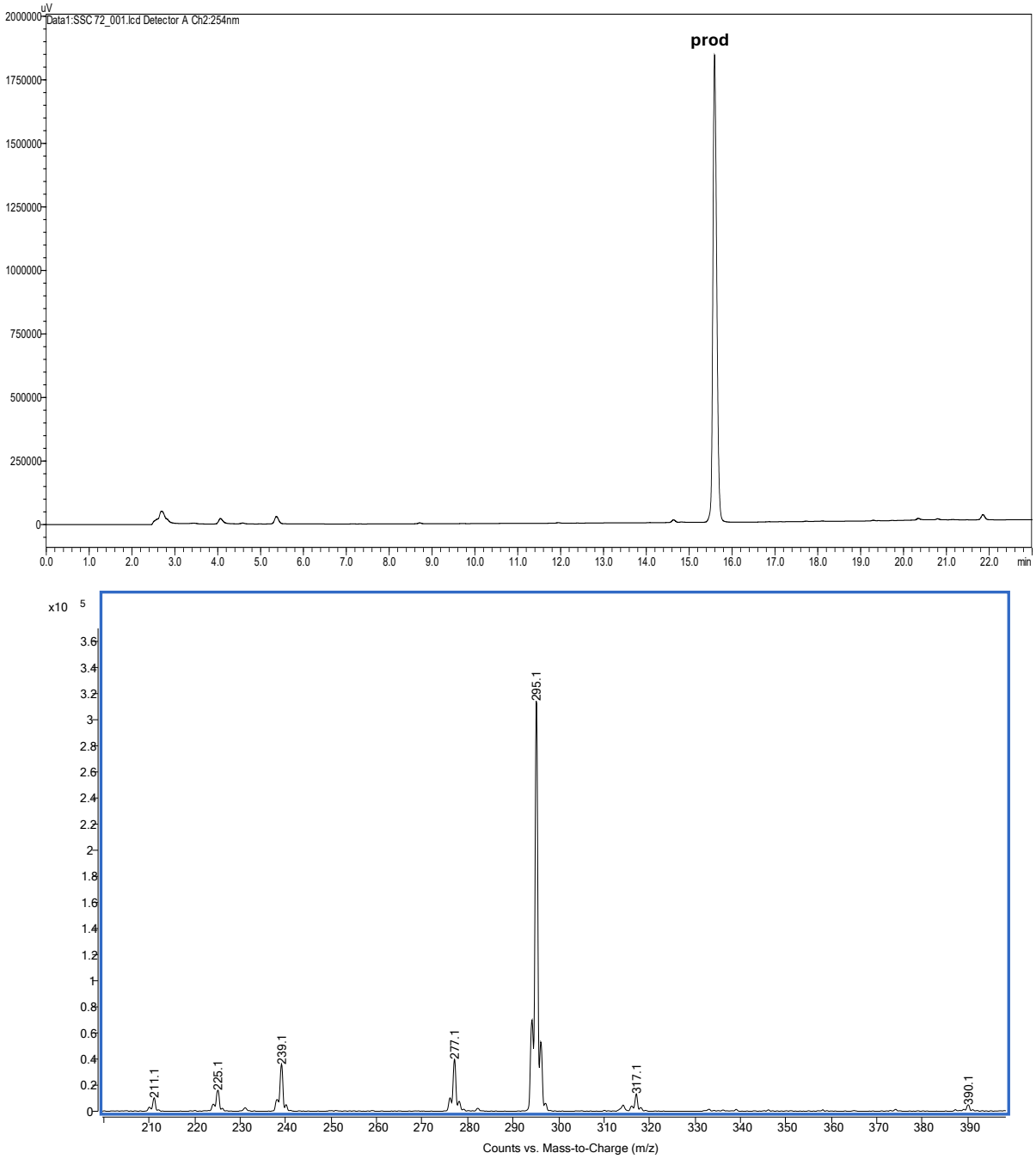

Figure S155. RP-HPLC trace at 254 nm (30-95% MeCN over 30 min) and ESI-MS spectrum of purified boronic ester **10-Gpin**. m/z 295.1 corresponds to $[M+H]^+$.

Formation and characterization of 3pin ester **10-3pin**.

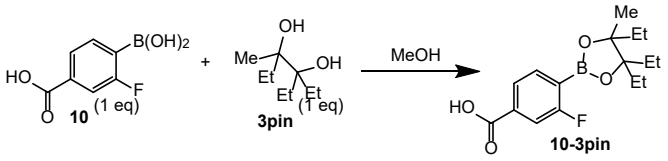

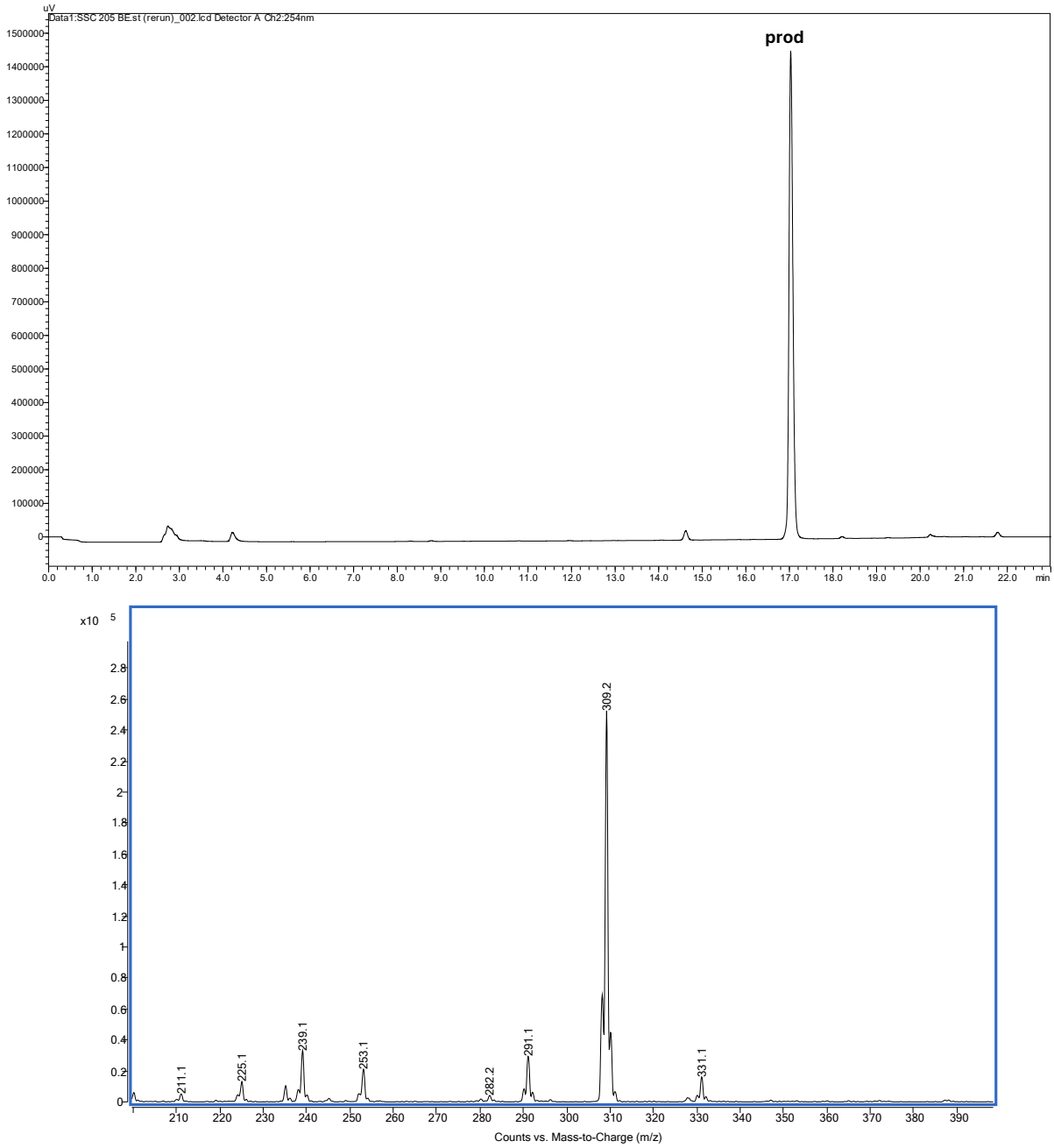

Figure S156. RP-HPLC trace at 254 nm (30-95% MeCN over 30 min) and ESI-MS spectrum of purified boronic ester **10-3pin**. m/z 309.2 $[M+H]^+$.

Formation and characterization of Epin ester **10-Epin**.

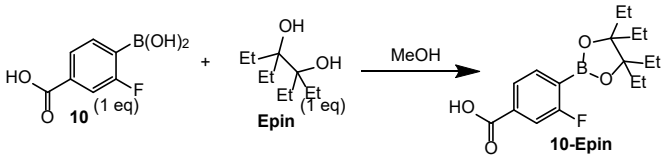

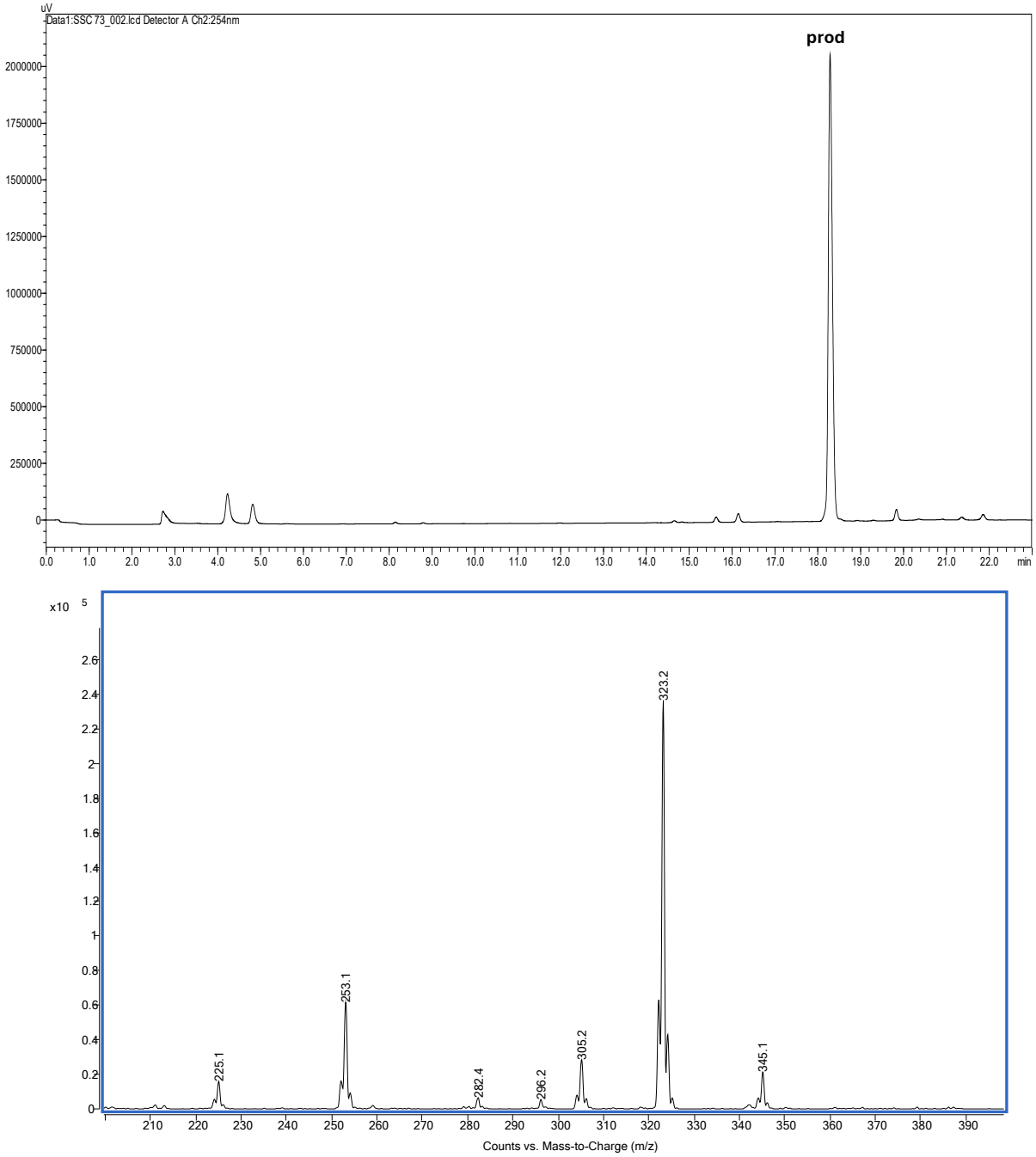

Figure S157. RP-HPLC trace at 254 nm (30-95% MeCN over 30 min) and ESI-MS spectrum of purified boronic ester **10-Epin**. m/z 323.2 corresponds to $[M+H]^+$.

(2-fluoro-4-methoxyphenyl)boronic acid (**11**) esters characterization.

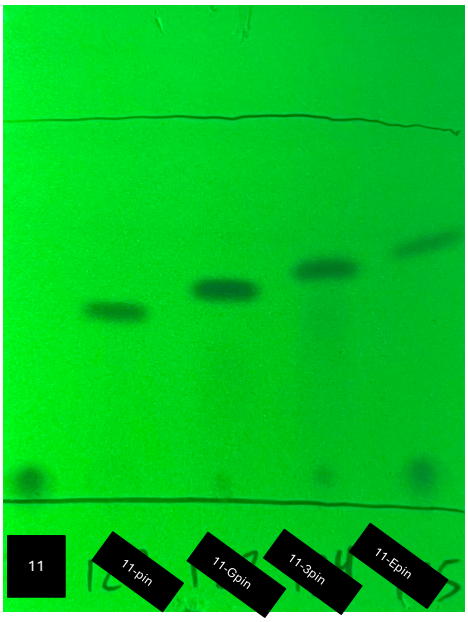

Figure S158. Boronic acid **11** and boronic esters TLC UV analysis using 20% ethyl acetate in hexanes as an eluent.

Formation and characterization of Pinacol ester **11-pin**.

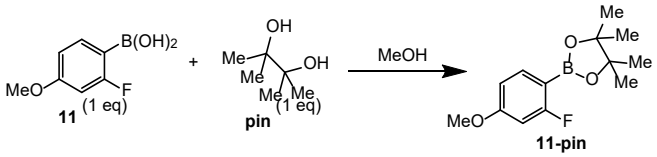

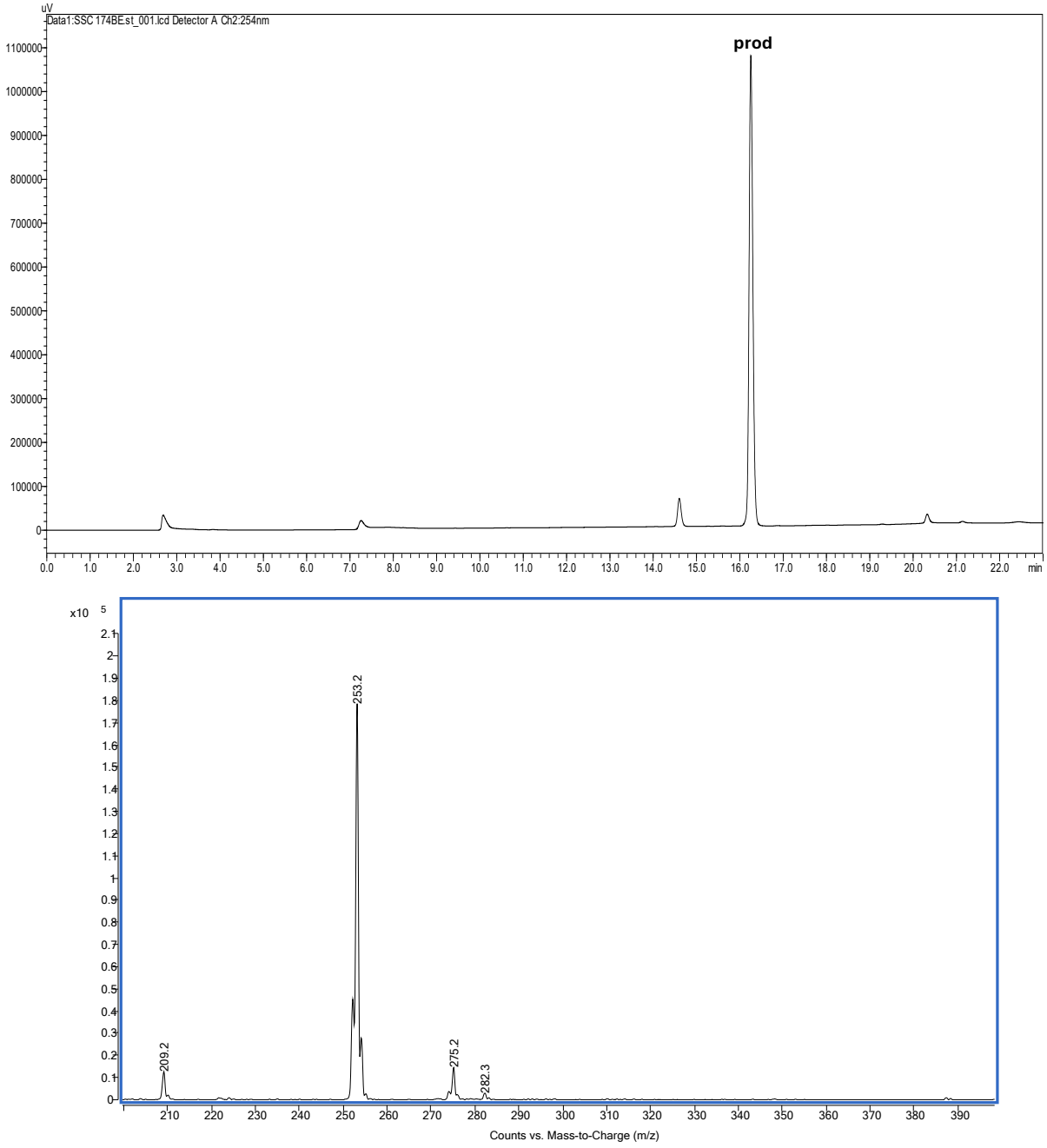

Figure S159. RP-HPLC trace at 254 nm (30-95% MeCN over 30 min) and ESI-MS spectrum of purified boronic ester **11-pin**. m/z 253.2 corresponds to $[M+H]^+$.

Formation and characterization of Gpin ester **11-Gpin**.

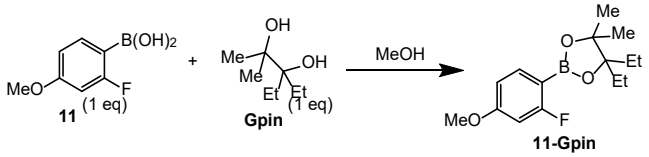

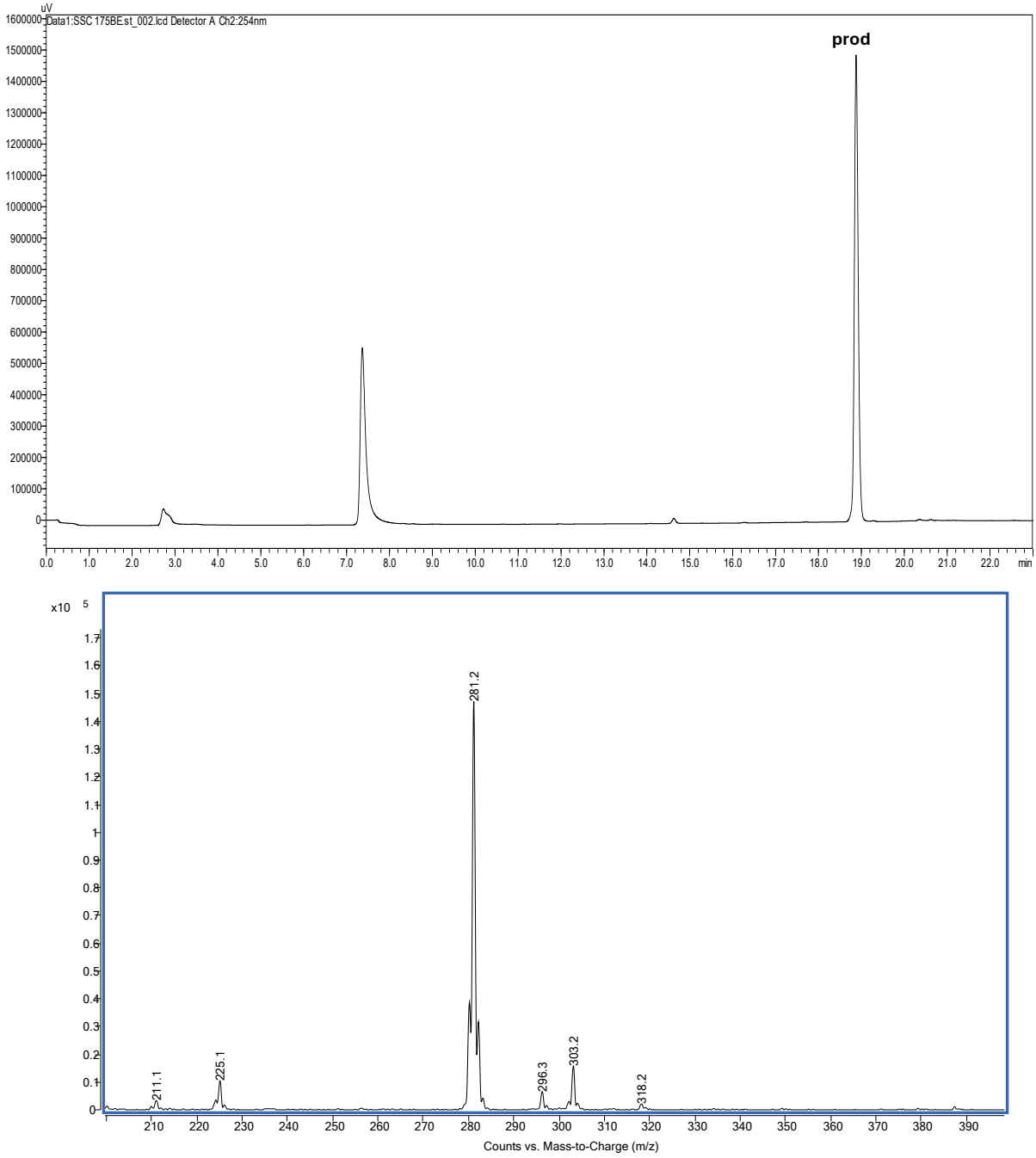

Figure S160. RP-HPLC trace at 254 nm (30-95% MeCN over 30 min) and ESI-MS spectrum of purified boronic ester **11-Gpin**. m/z 281.2 corresponds to $[M+H]^+$.

Formation and characterization of 3pin ester **11-3pin**.

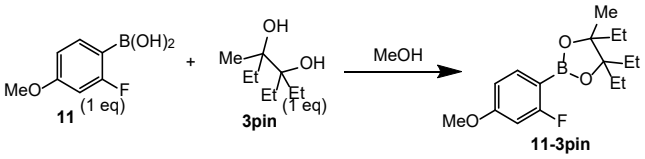

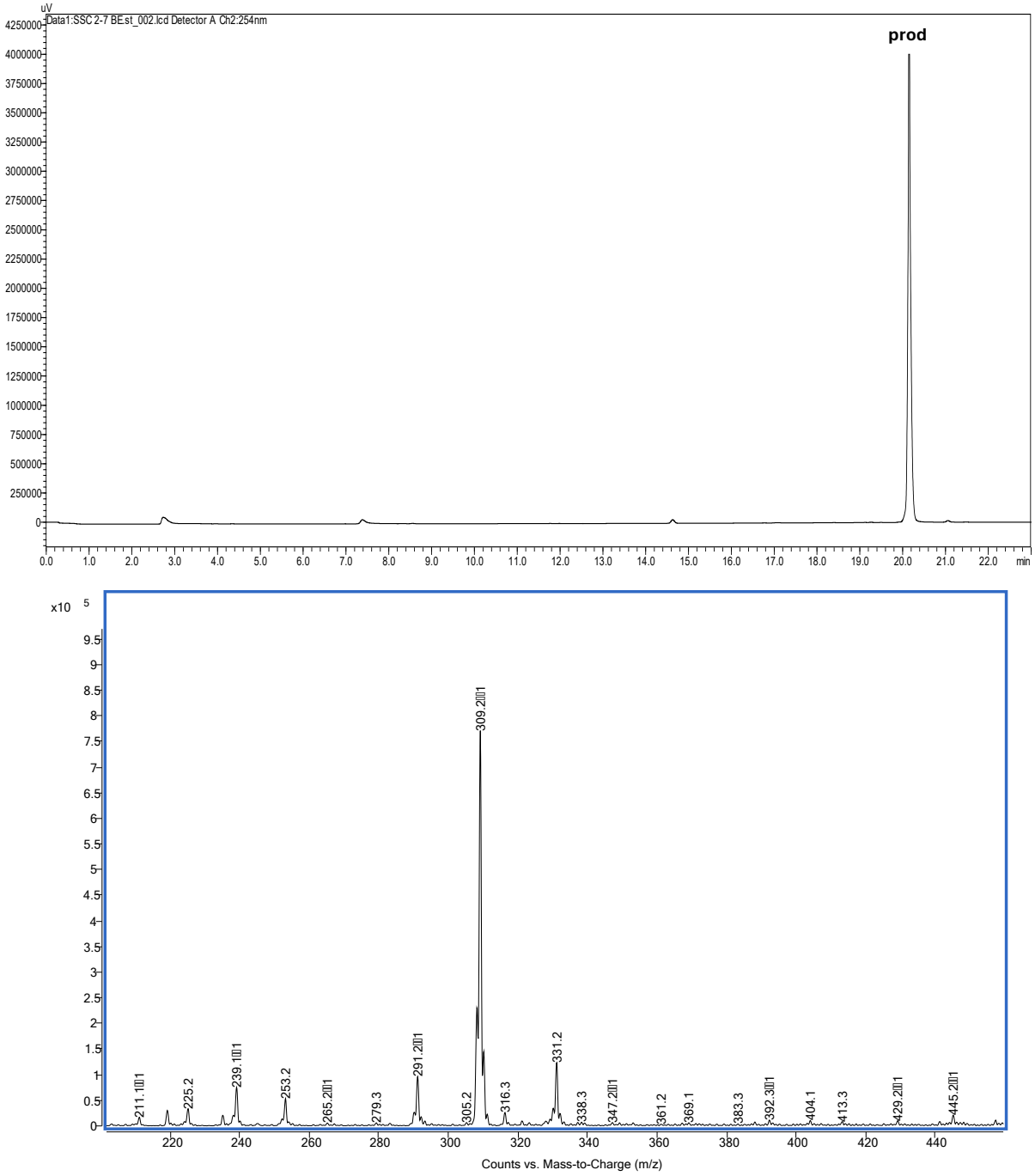

Figure S161. RP-HPLC trace at 254 nm (30-95% MeCN over 30 min) and ESI-MS spectrum of purified boronic ester **11-3pin**. m/z 295.2 corresponds to $[M+H]^+$.

Formation and characterization of Epin ester **11-Epin**.

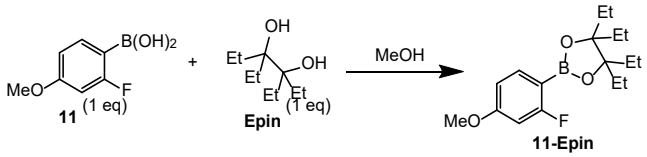

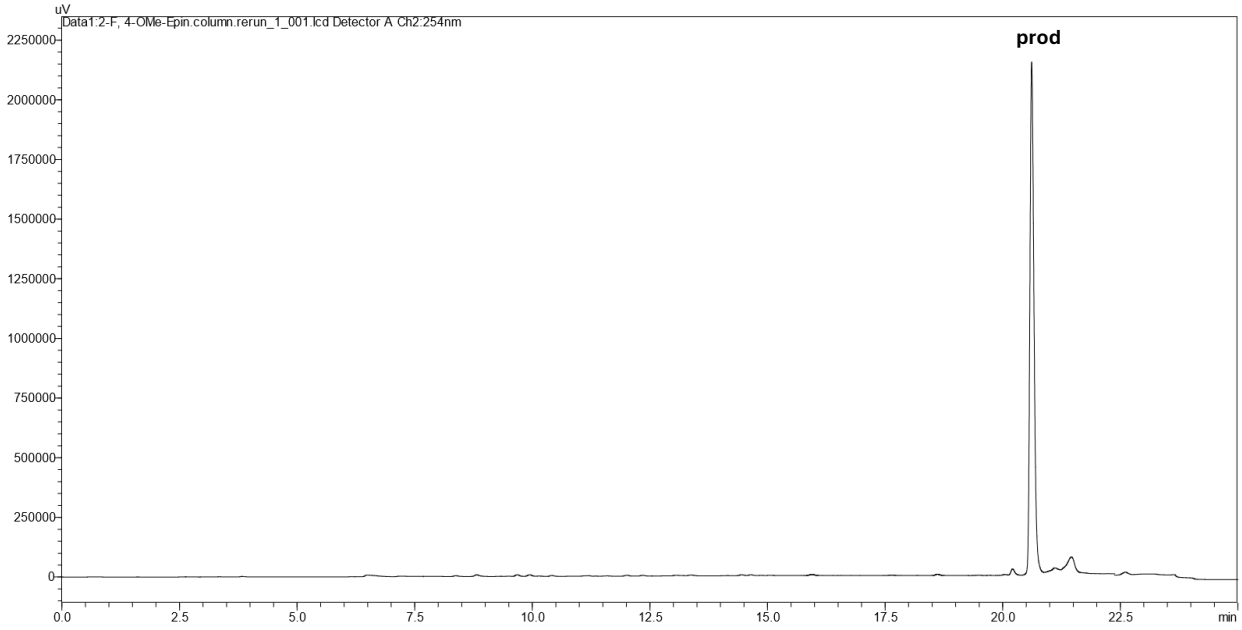

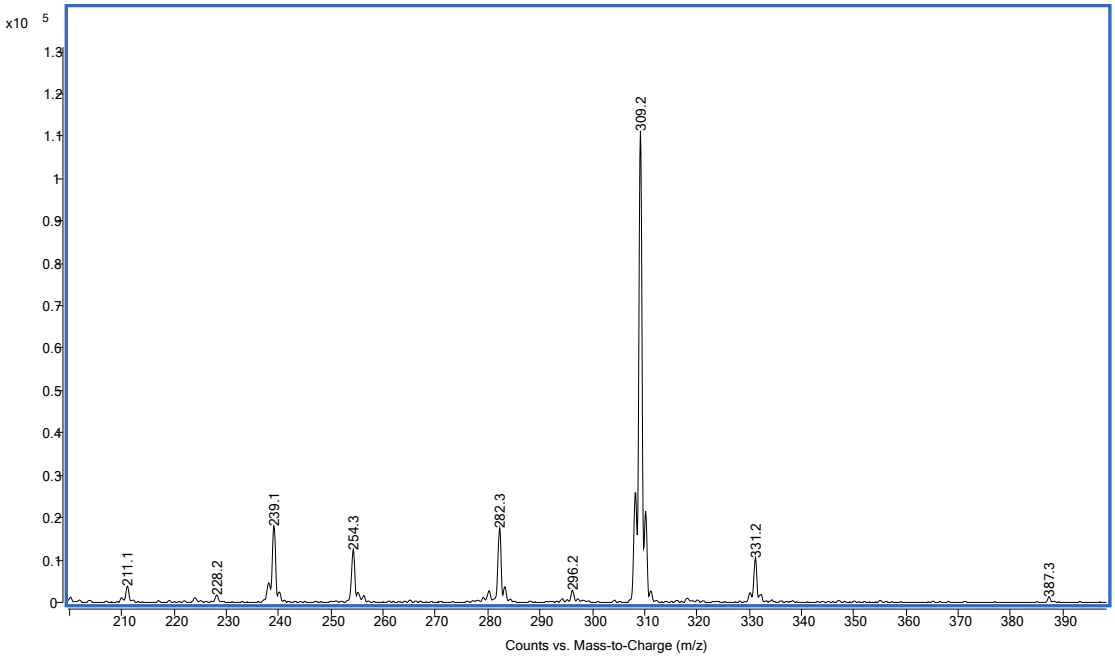

Figure S162. RP-HPLC trace at 254 nm (30-95% MeCN over 30 min) and ESI-MS spectrum of purified boronic ester **11-Epin**. m/z 309.2 $[M+H]^+$.

2-(*N,N*-dimethylaminomethyl)phenylboronic acid (**13**) esters characterization.

Formation and characterization of Gpin ester **13-Gpin**.

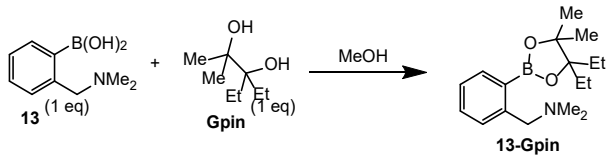

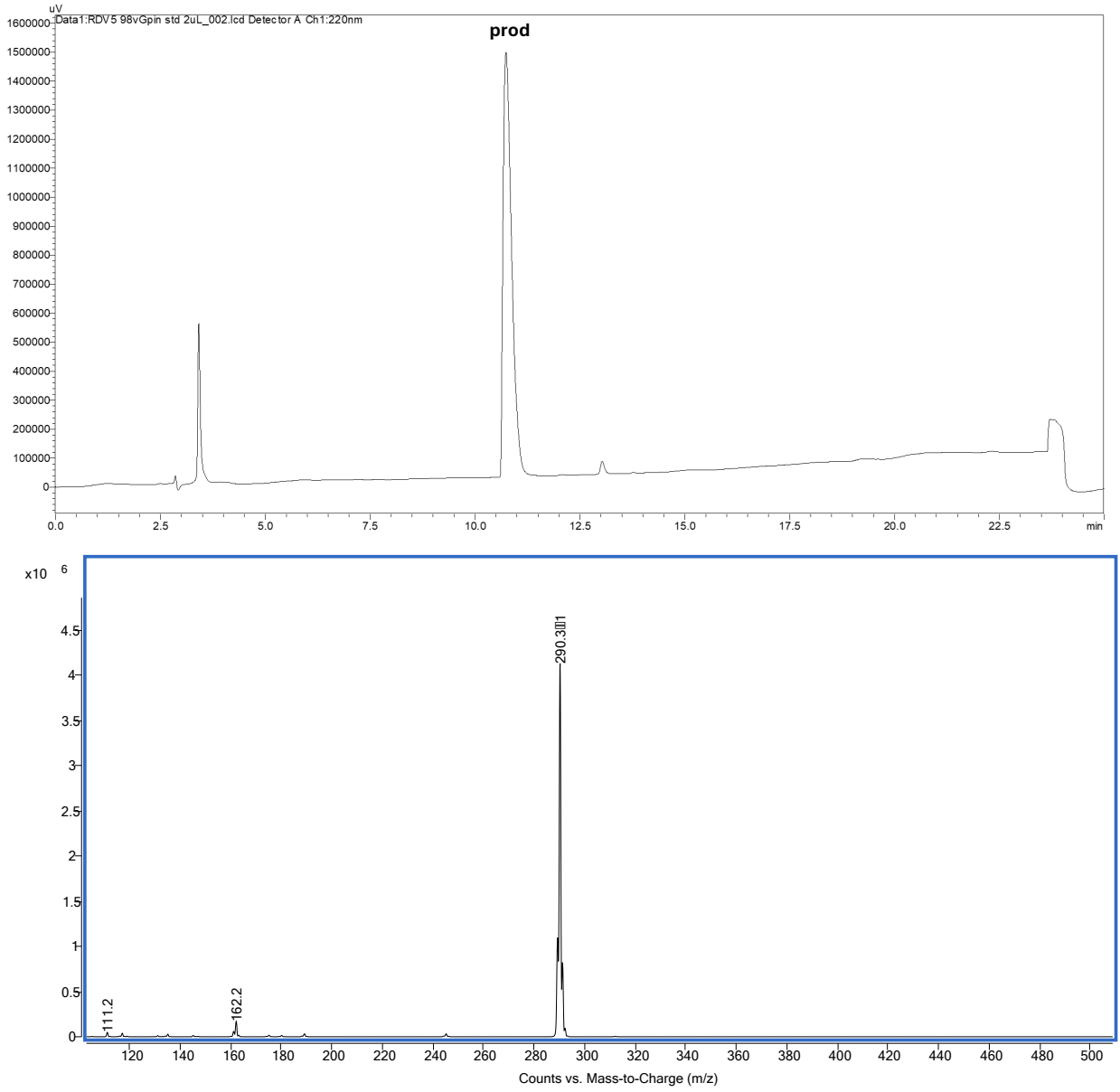

Figure S163. RP-HPLC trace at 254 nm (30-95% MeCN over 30 min) and ESI-MS spectrum of purified boronic ester **13-Gpin**. m/z 290.3 corresponds to $[M+H]^+$.

Formation and characterization of 3pin ester **13-3pin**.

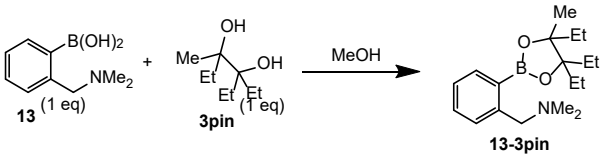

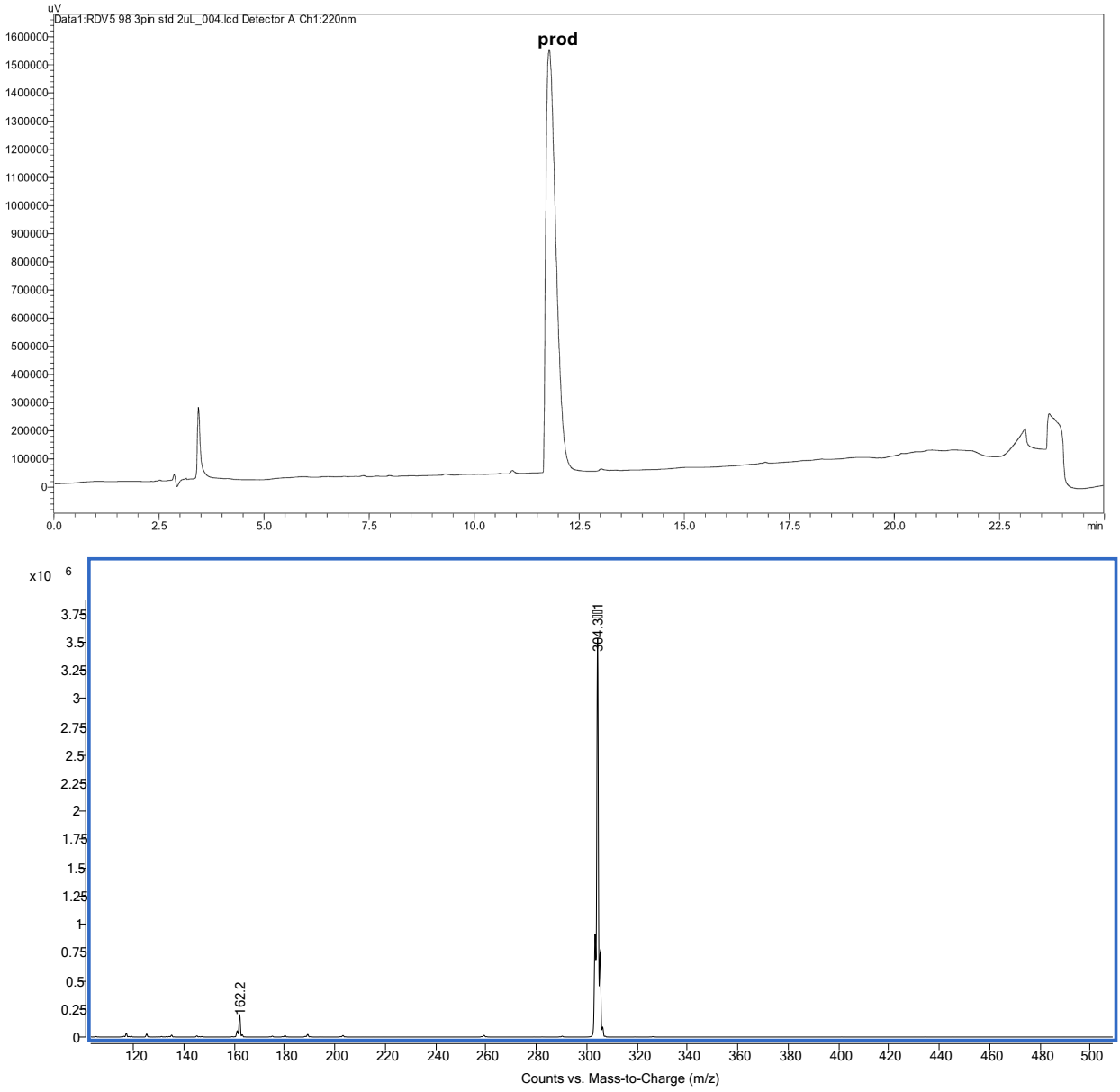

Figure S164. RP-HPLC trace at 254 nm (30-95% MeCN over 30 min) and ESI-MS spectrum of purified boronic ester **13-3pin**. m/z 304.3 corresponds to $[M+H]^+$.

Formation and characterization of Epin ester **13-Epin**.

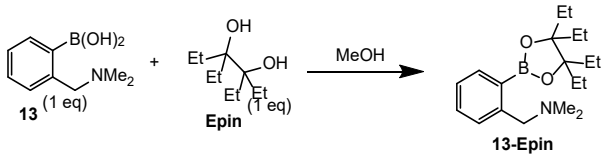

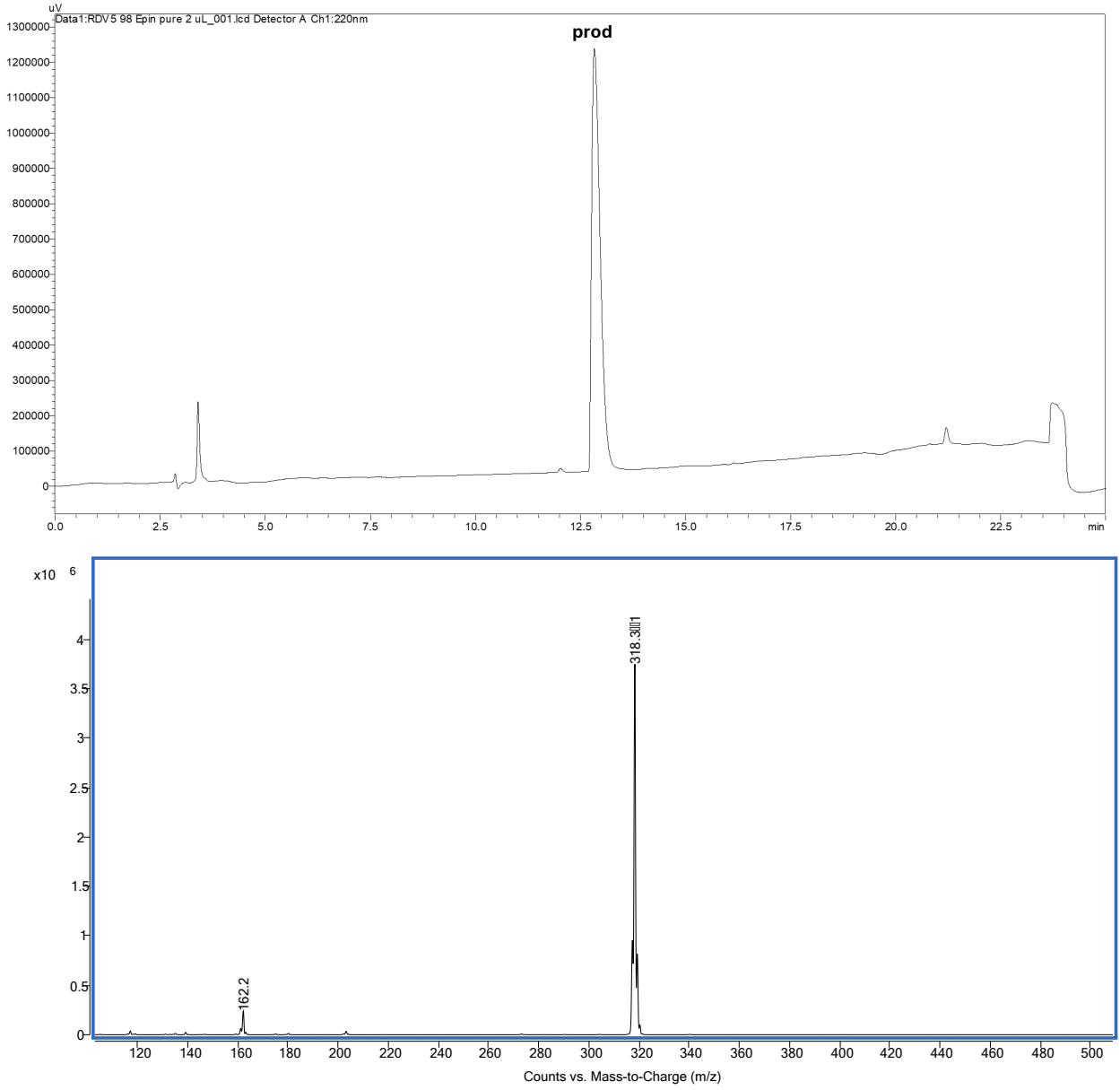

Figure S165. RP-HPLC trace at 254 nm (30-95% MeCN over 30 min) and ESI-MS spectrum of purified boronic ester **13-Epin**. m/z 318.3 $[M+H]^+$.

2-thienylboronic acid (**14**) esters characterization.

Formation and characterization of Gpin ester **14-Gpin**.

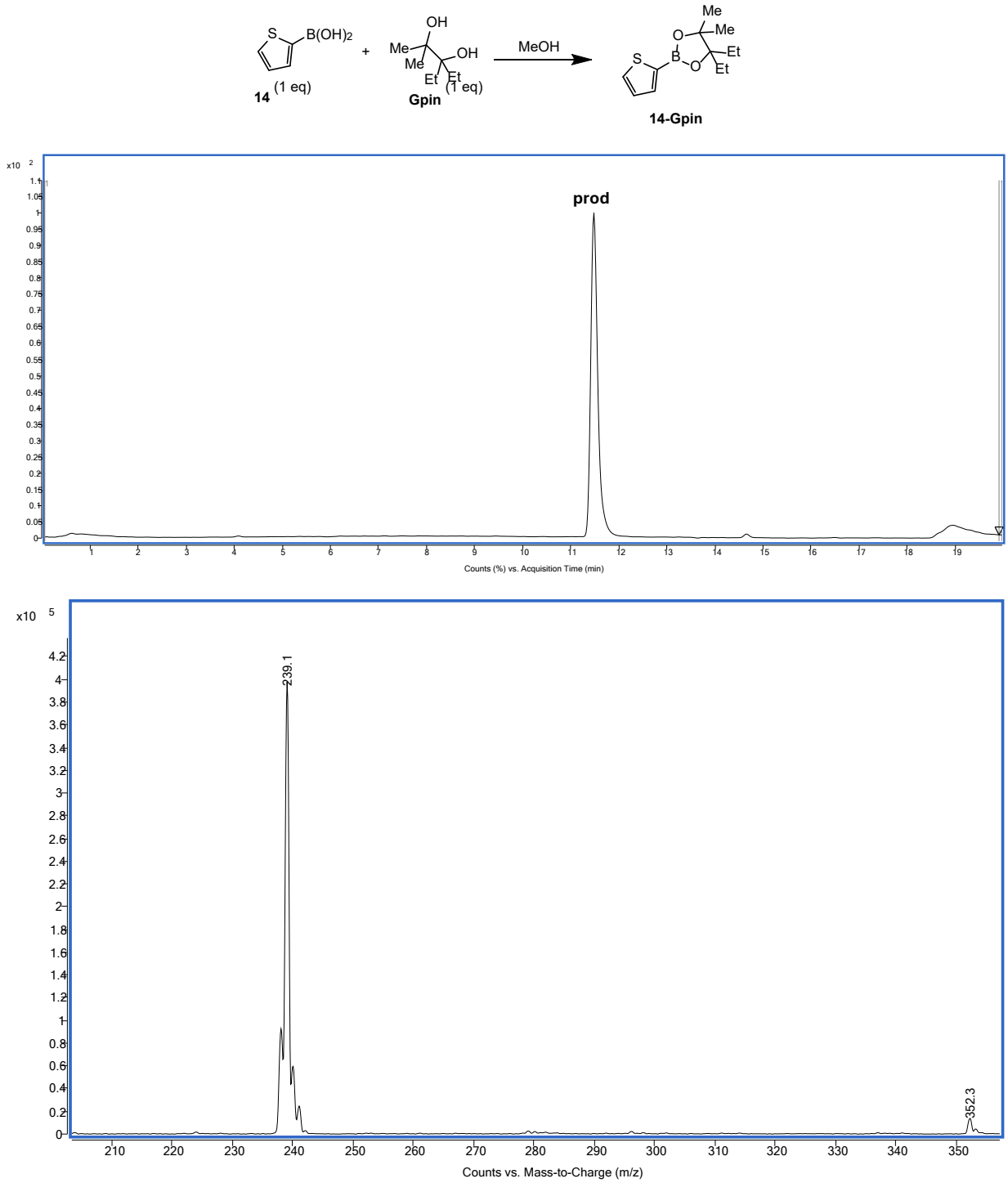

Figure S166. RP-LCMS trace at 254 nm (30-90% MeCN over 30 min) and ESI-MS spectrum of purified boronic ester **14-Gpin**. m/z 239.1 corresponds to $[M+H]^+$.

Formation and characterization of 3pin ester **14-3pin**.

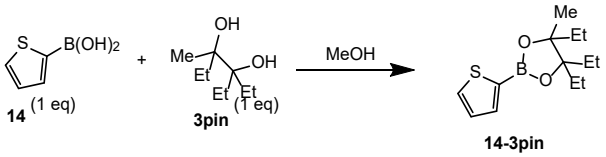

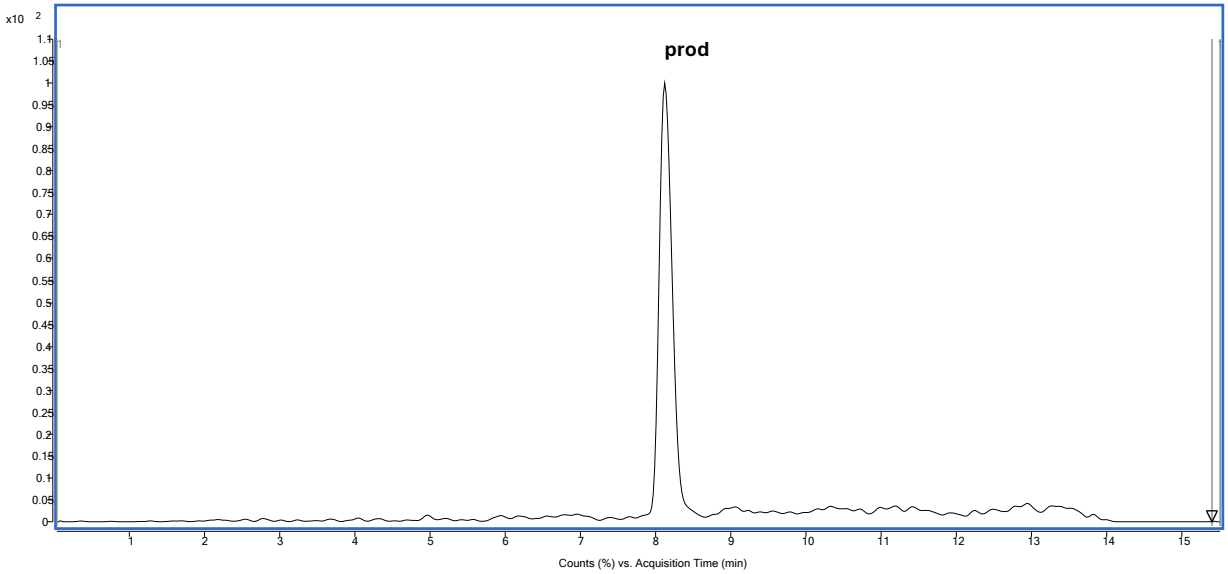

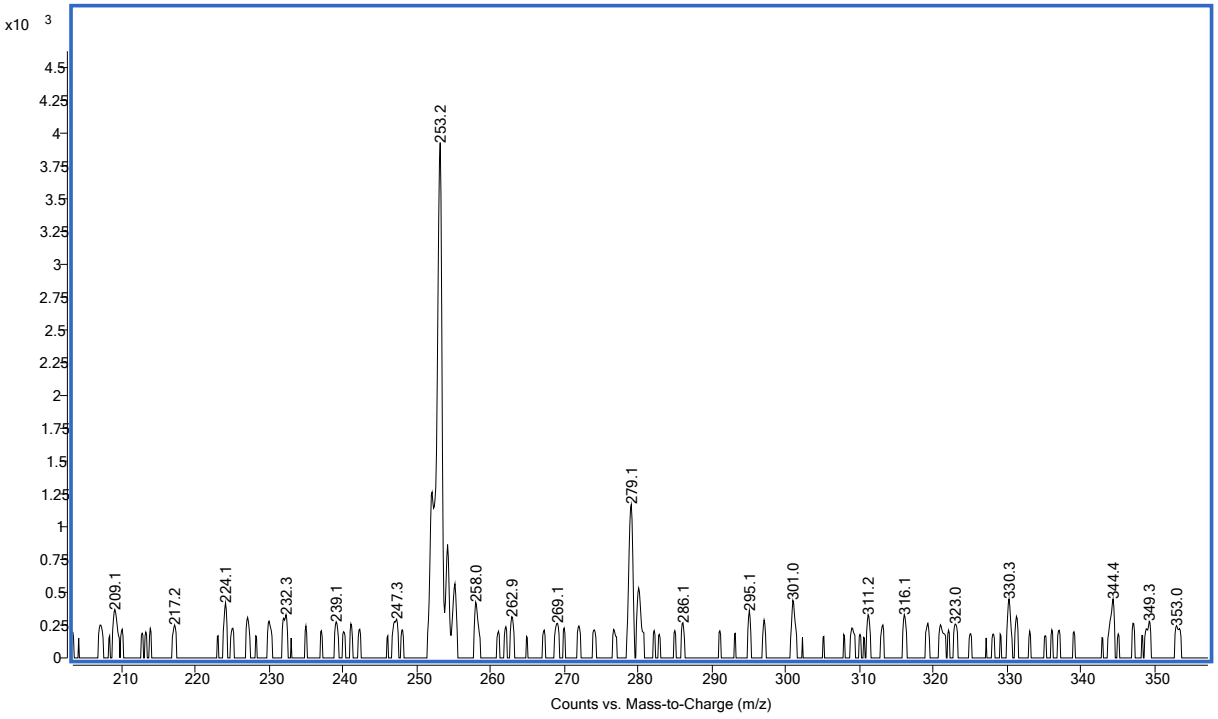

Figure S167. RP-LCMS trace at 254 nm (30-90% MeCN over 30 min) and ESI-MS spectrum of purified boronic ester **14-3pin**. m/z 253.22 corresponds to $[M+H]^+$.

2-furylboronic acid (**15**) esters characterization.

Formation and characterization of Gpin ester **15-Gpin**.

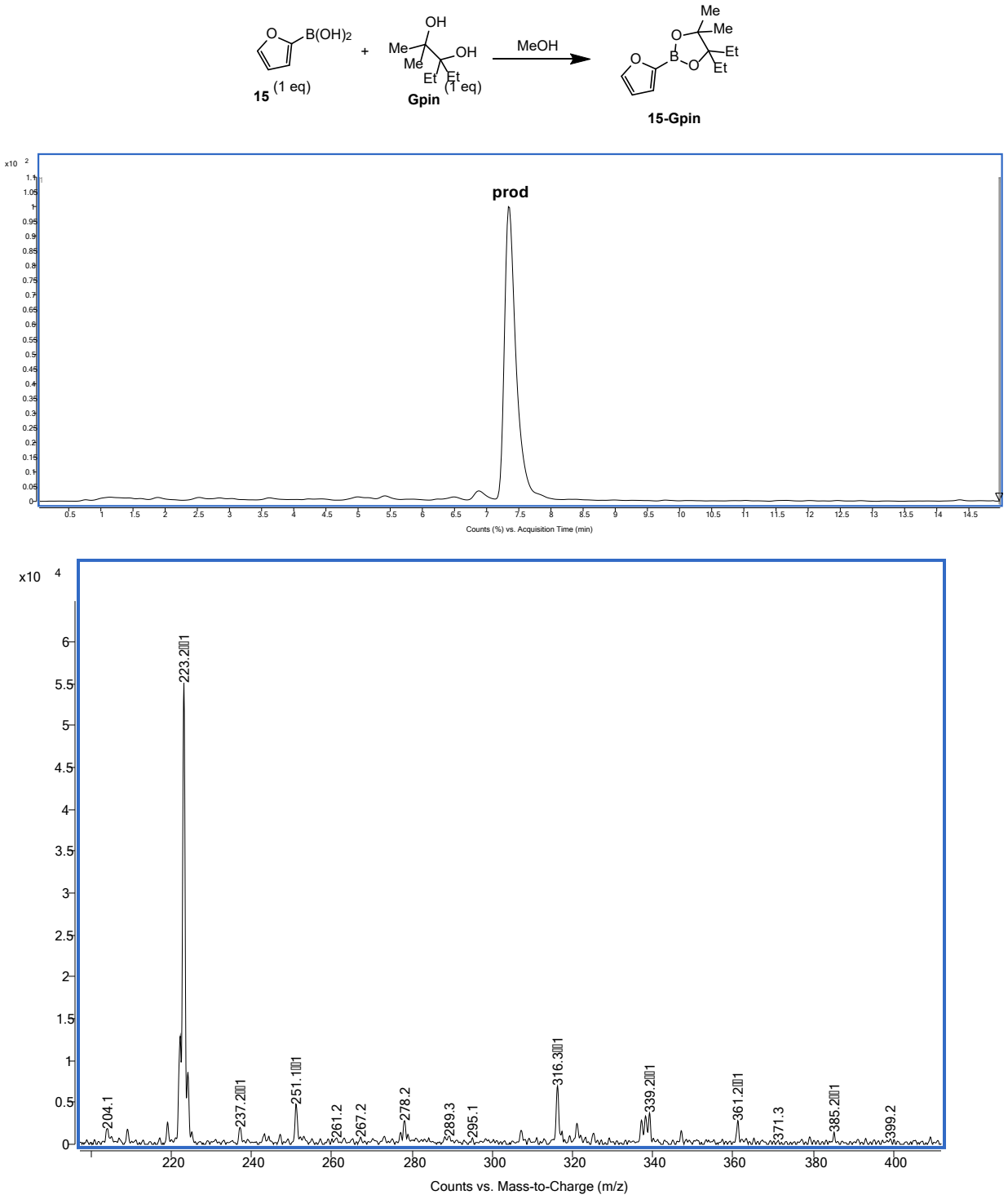

Figure S168. RP-LCMS trace at 254 nm (30-90% MeCN over 15 min) and ESI-MS spectrum of purified boronic ester **15-Gpin**. m/z 223.2 corresponds to $[M+H]^+$.

Formation and characterization of 3pin ester **15-3pin**.

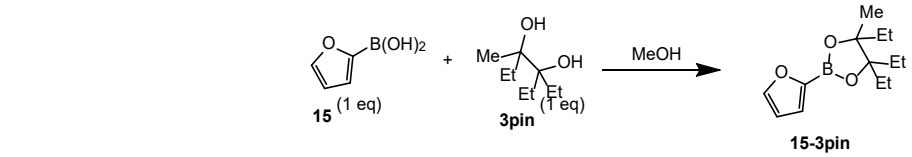

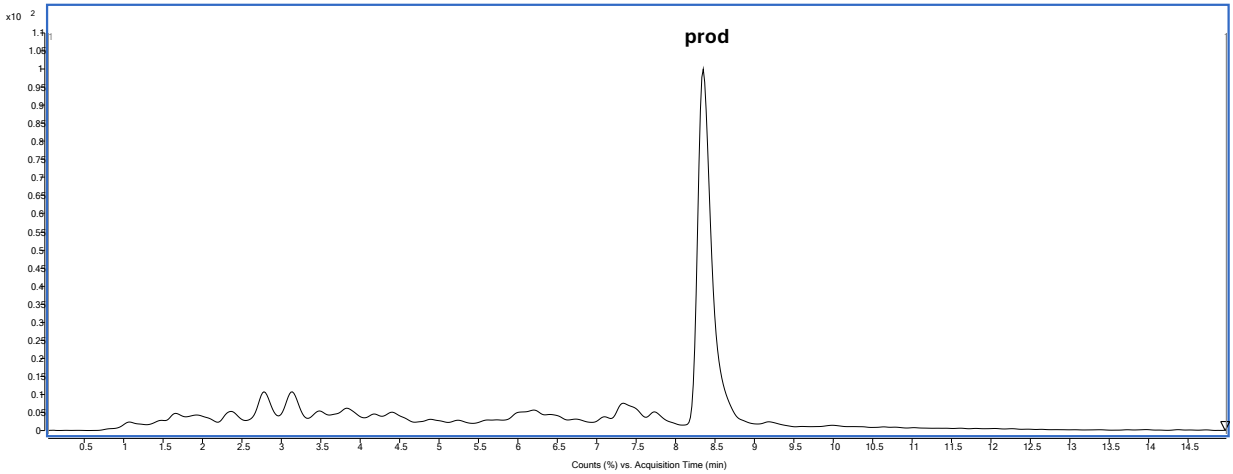

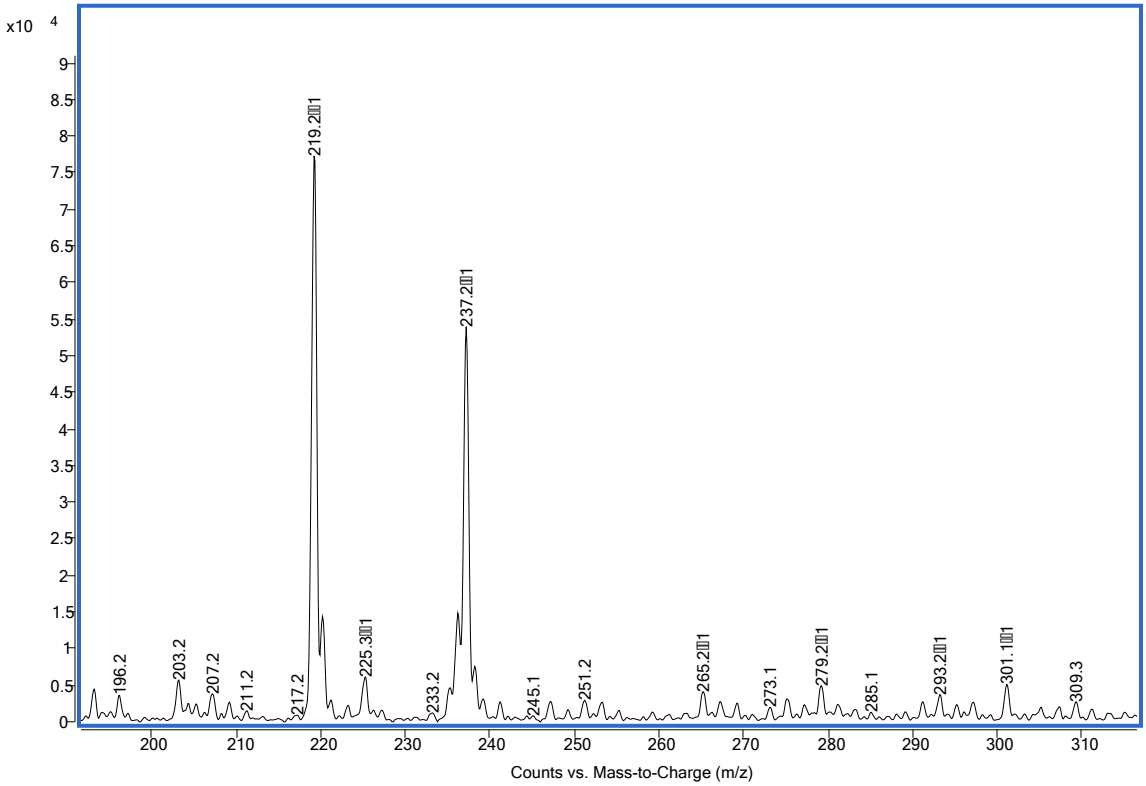

Figure S169. RP-LCMS trace at 254 nm (30-90% MeCN over 15 min) and ESI-MS spectrum of purified boronic ester **15-3pin**. m/z 237.2 corresponds to $[M+H]^+$.

Formation and characterization of 3pin ester **15-Epin**.

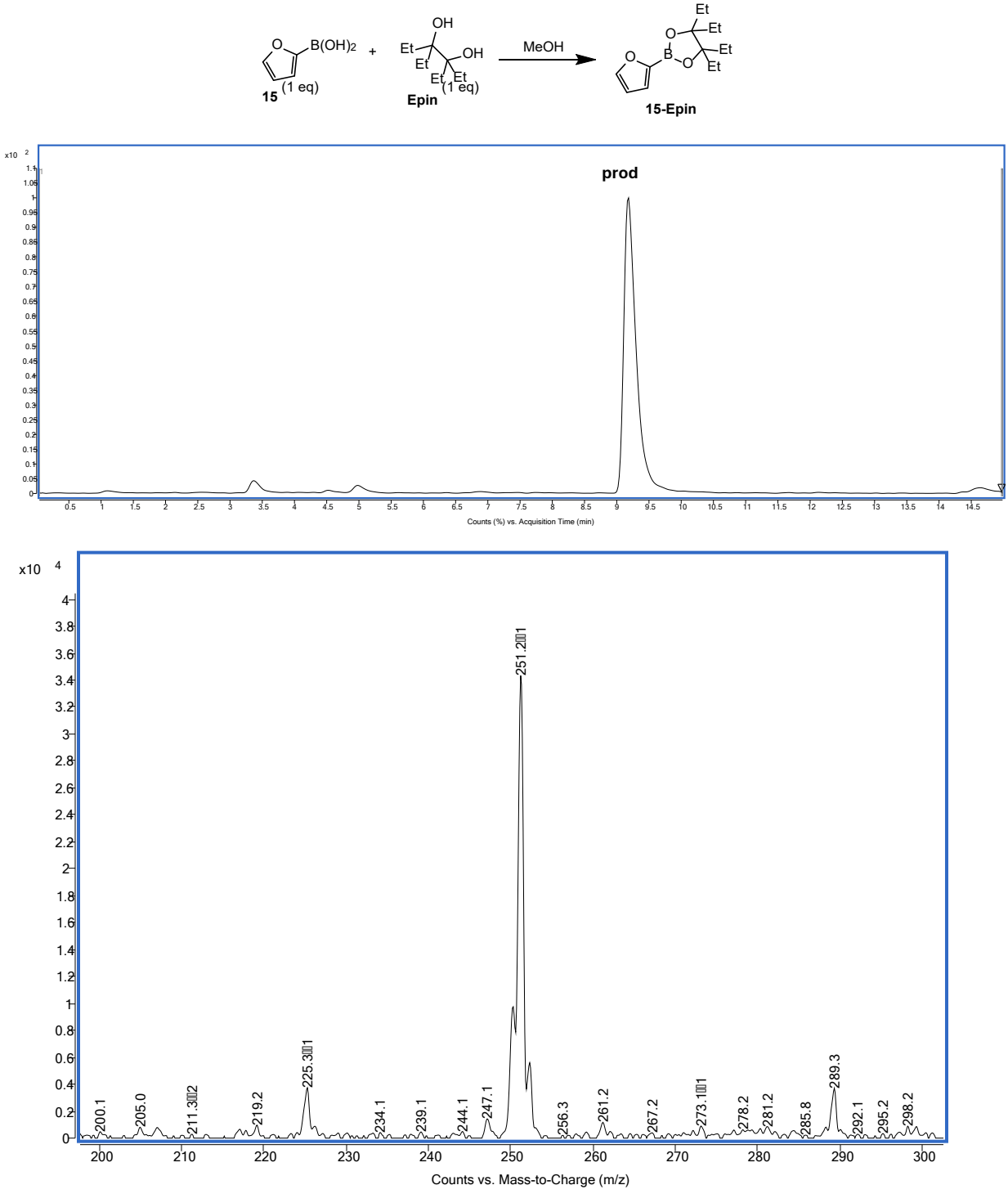

Figure S170. RP-LCMS trace at 254 nm (30-90% MeCN over 30 min) and ESI-MS spectrum of purified boronic ester **15-Epin.** m/z 251.2 corresponds to $[M+H]^+$.

2-pyridylboronic acid (**16**) esters characterization.

Formation and characterization of Gpin ester **16-Gpin**.

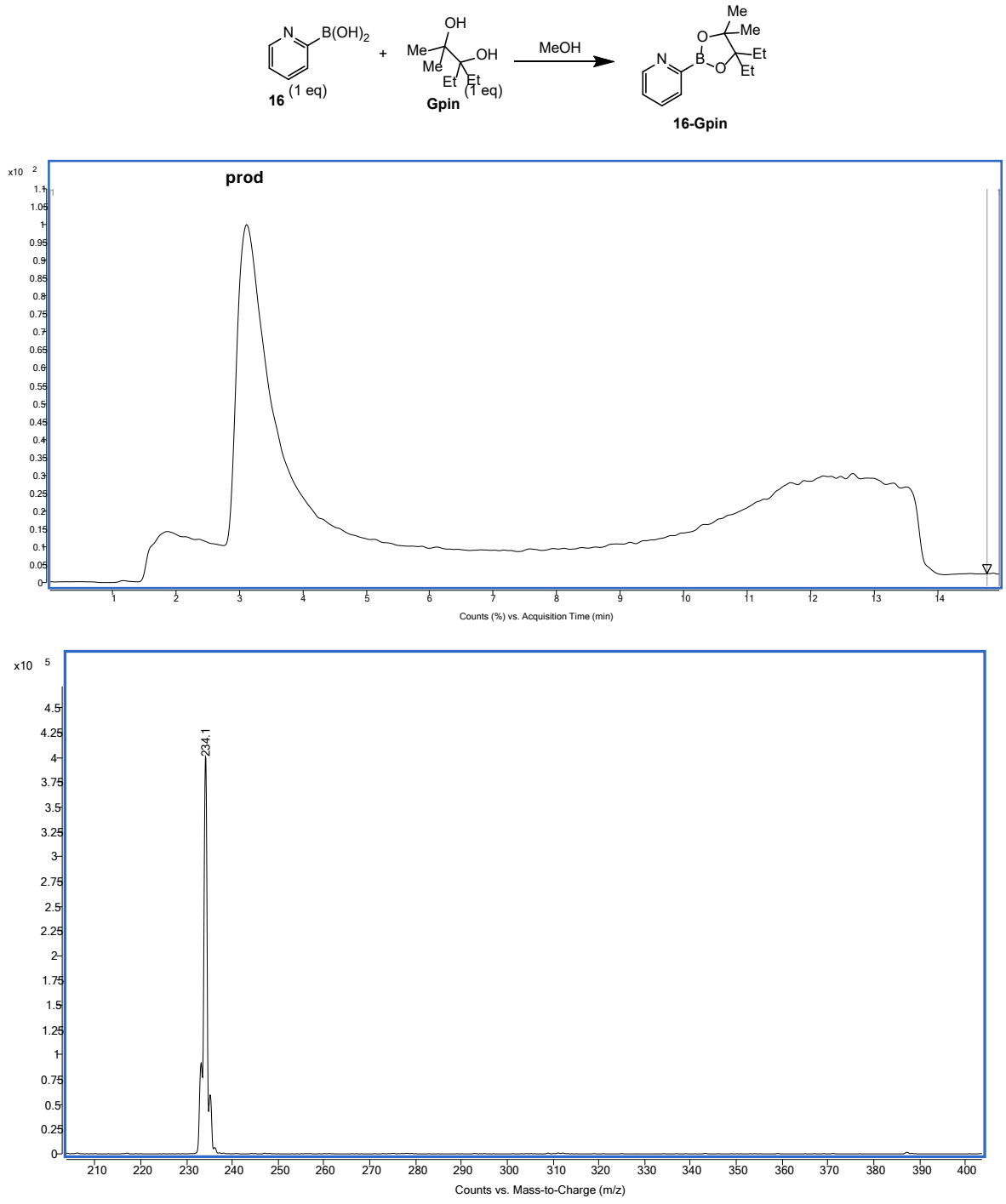

Figure S171. RP-LCMS trace at 254 nm (30-90% MeCN over 15 min) and ESI-MS spectrum of purified boronic ester **16-Gpin**. m/z 234.1 corresponds to $[M+H]^+$.

Formation and characterization of 3pin ester **16-3pin**.

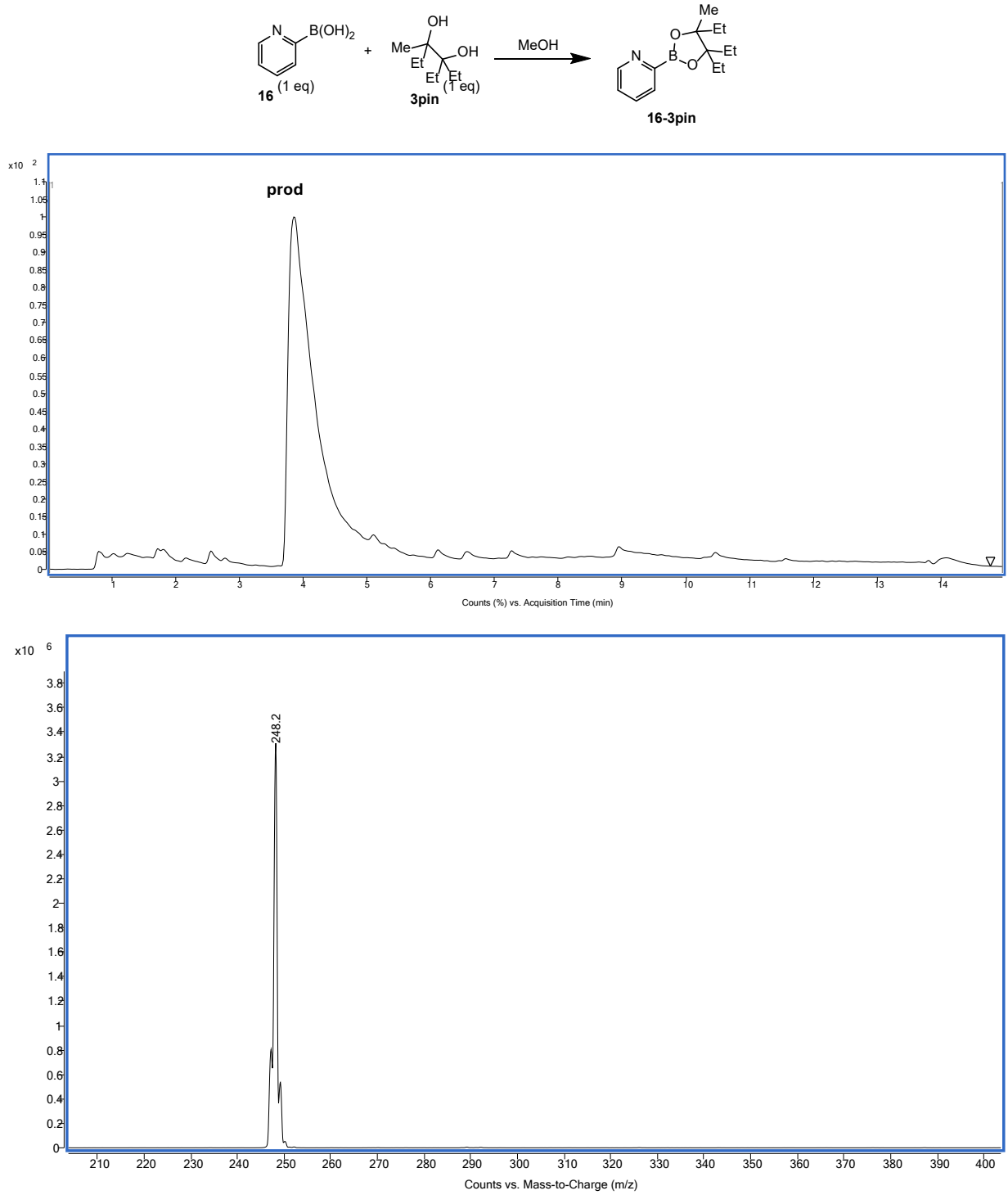

Figure S172. RP-LCMS trace at 254 nm (30-90% MeCN over 15 min) and ESI-MS spectrum of purified boronic ester **16-3pin**. m/z 248.2 corresponds to $[M+H]^+$.

Formation and characterization of 3pin ester **16-Epin**.

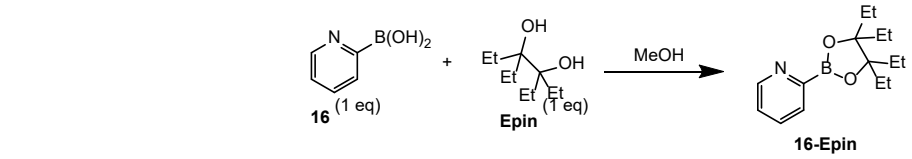

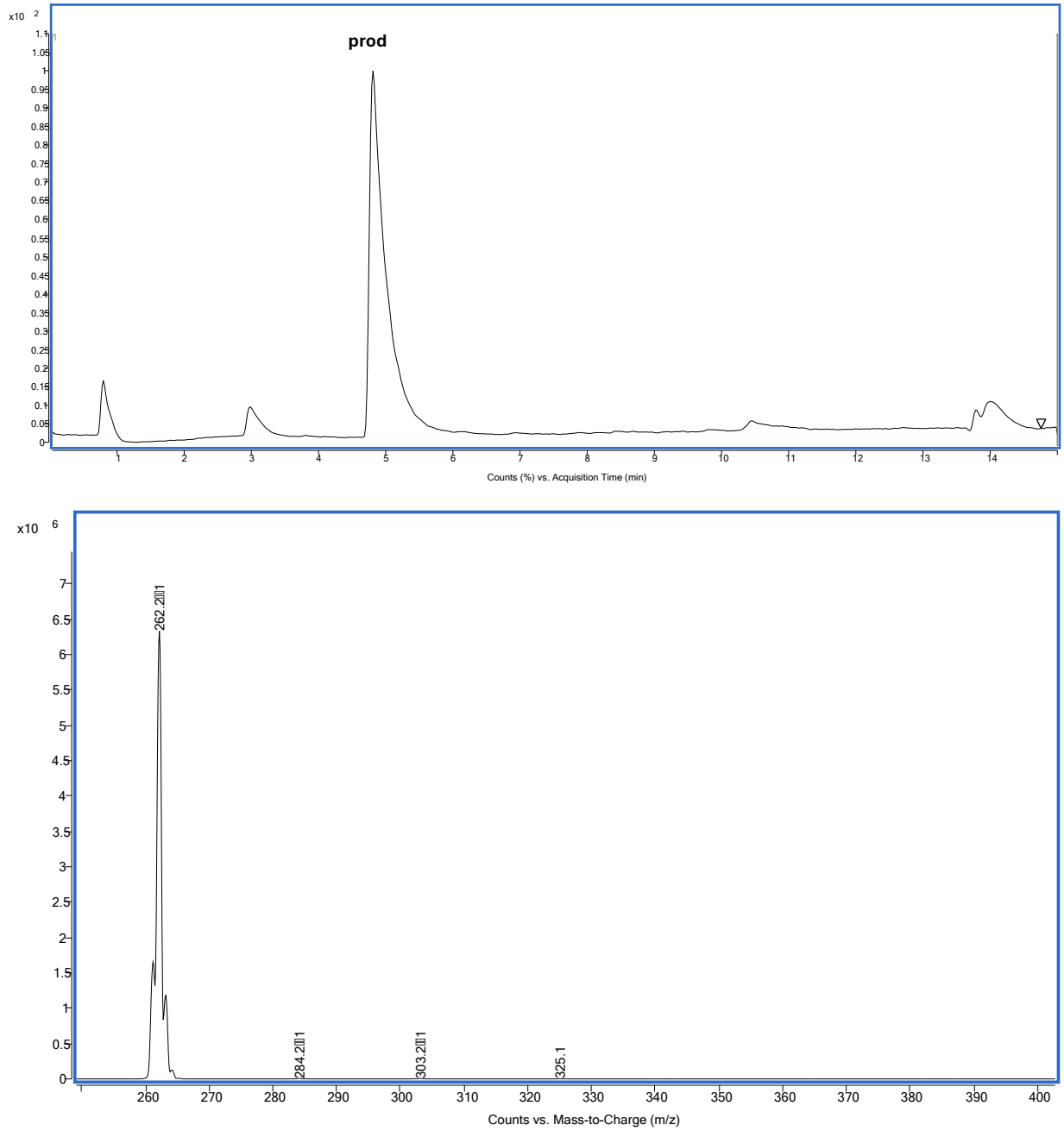

Figure S173. RP-LCMS trace at 254 nm (30-90% MeCN over 15 min) and ESI-MS spectrum of purified boronic ester **16-Epin**. m/z 262.2 corresponds to $[M+H]^+$.

Tavaborole (**17**) esters characterization.

Formation and characterization of Gpin ester **17-Gpin**.

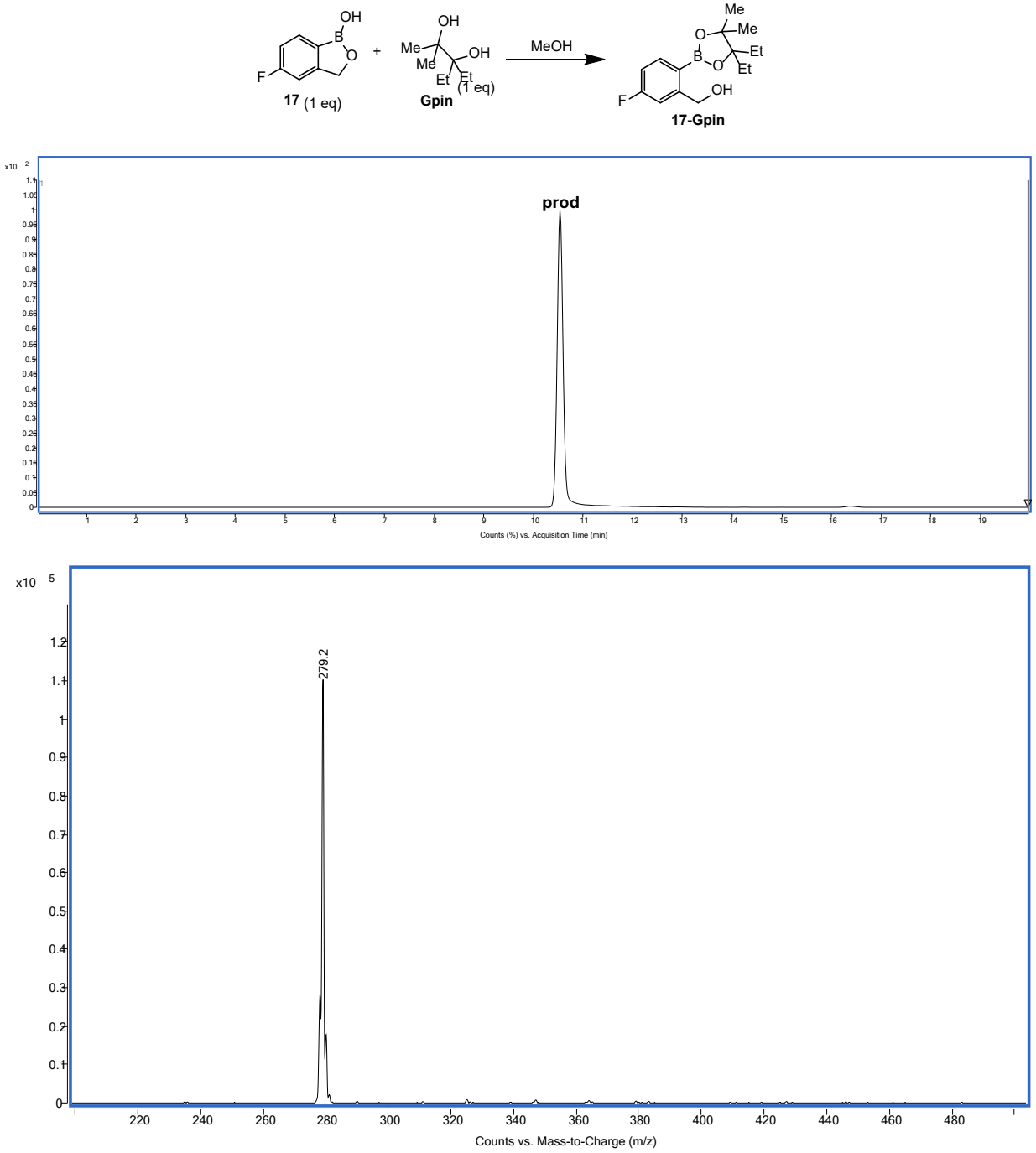

Figure S174. RP-LCMS trace at 254 nm (5-50% MeCN over 20 min) and ESI-MS spectrum of purified boronic ester **17-Gpin**. m/z 279.2 corresponds to $[M-H]^-$.

Formation and characterization of 3pin ester **17-3pin**.

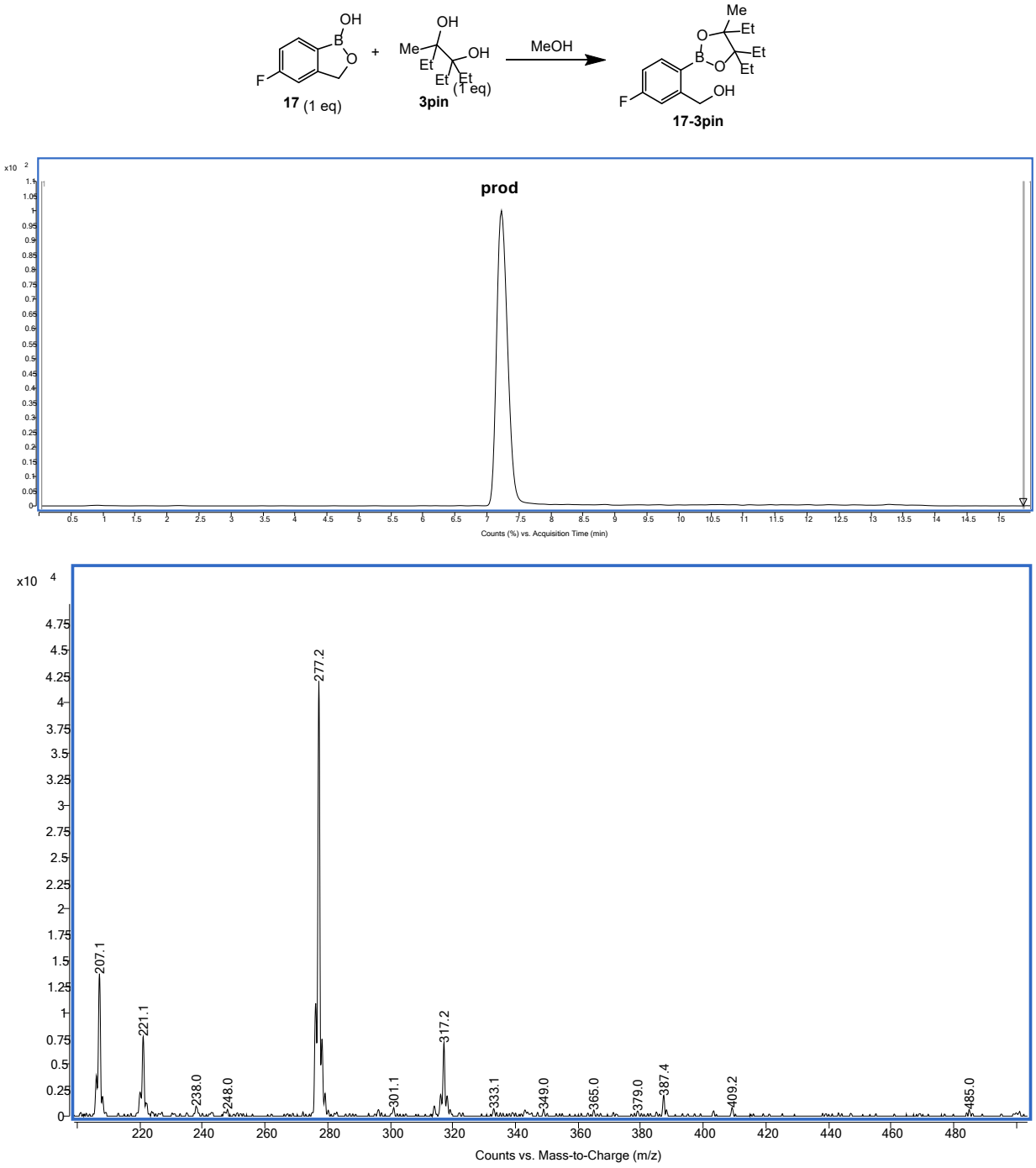

Figure S175. RP-LCMS trace at 254 nm (30-90% MeCN over 15 min) and ESI-MS spectrum of purified boronic ester **17-3pin**. m/z 295.2 corresponds to $[M\text{-}OH]^+$.

Formation and characterization of Epin ester **17-Epin**.

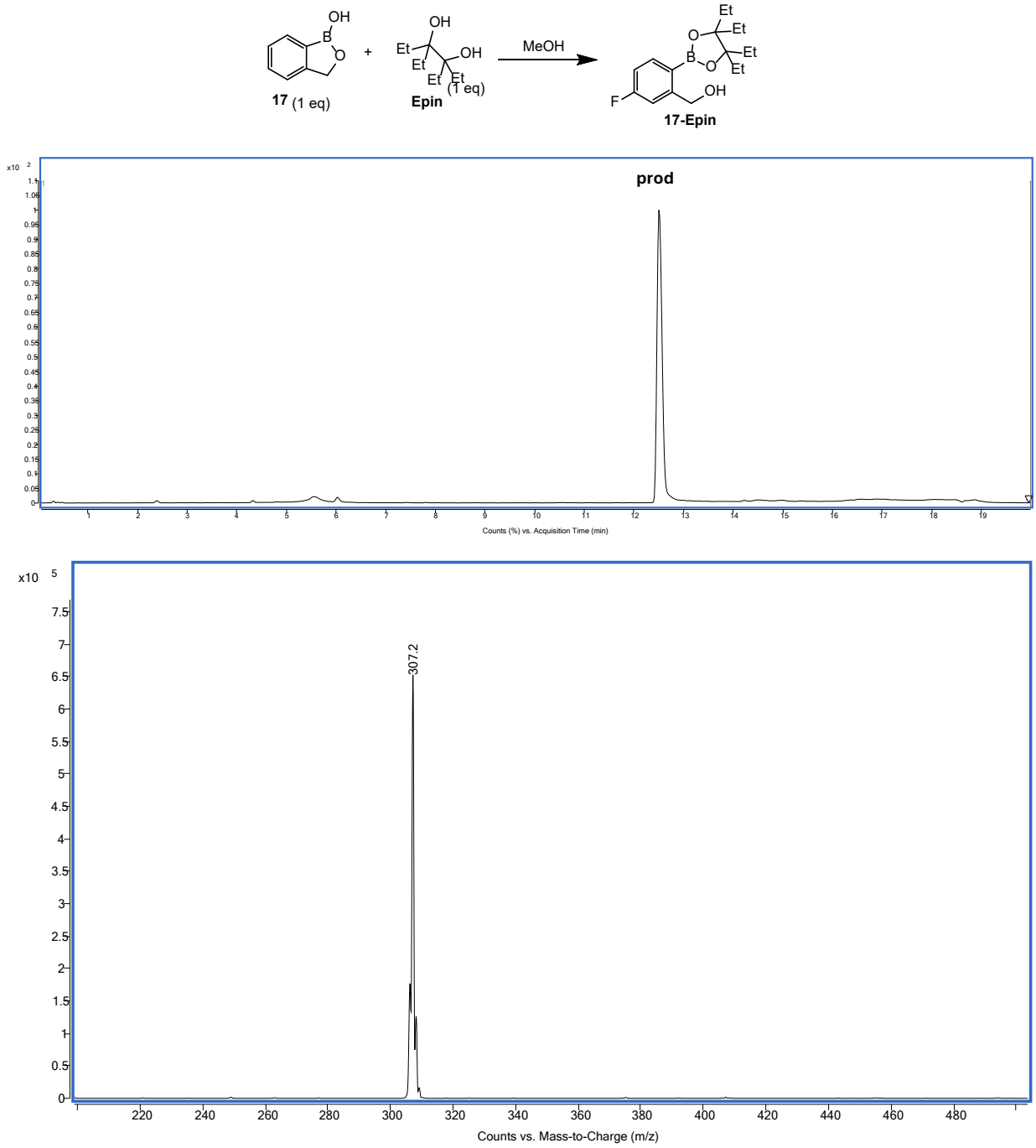

Figure S176. RP-LCMS trace at 254 nm (5-50% MeCN over 20 min) and ESI-MS spectrum of purified boronic ester **17-Epin**. m/z 307.2 corresponds to $[M-H]^-$.

Crisaborole (**18**) esters characterization.

Formation and characterization of Gpin ester **18-Gpin**.

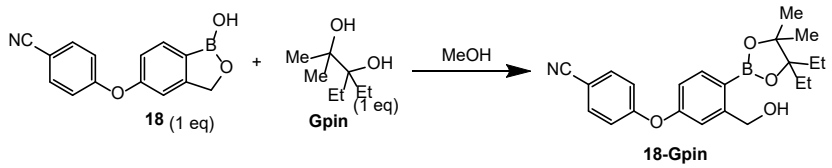

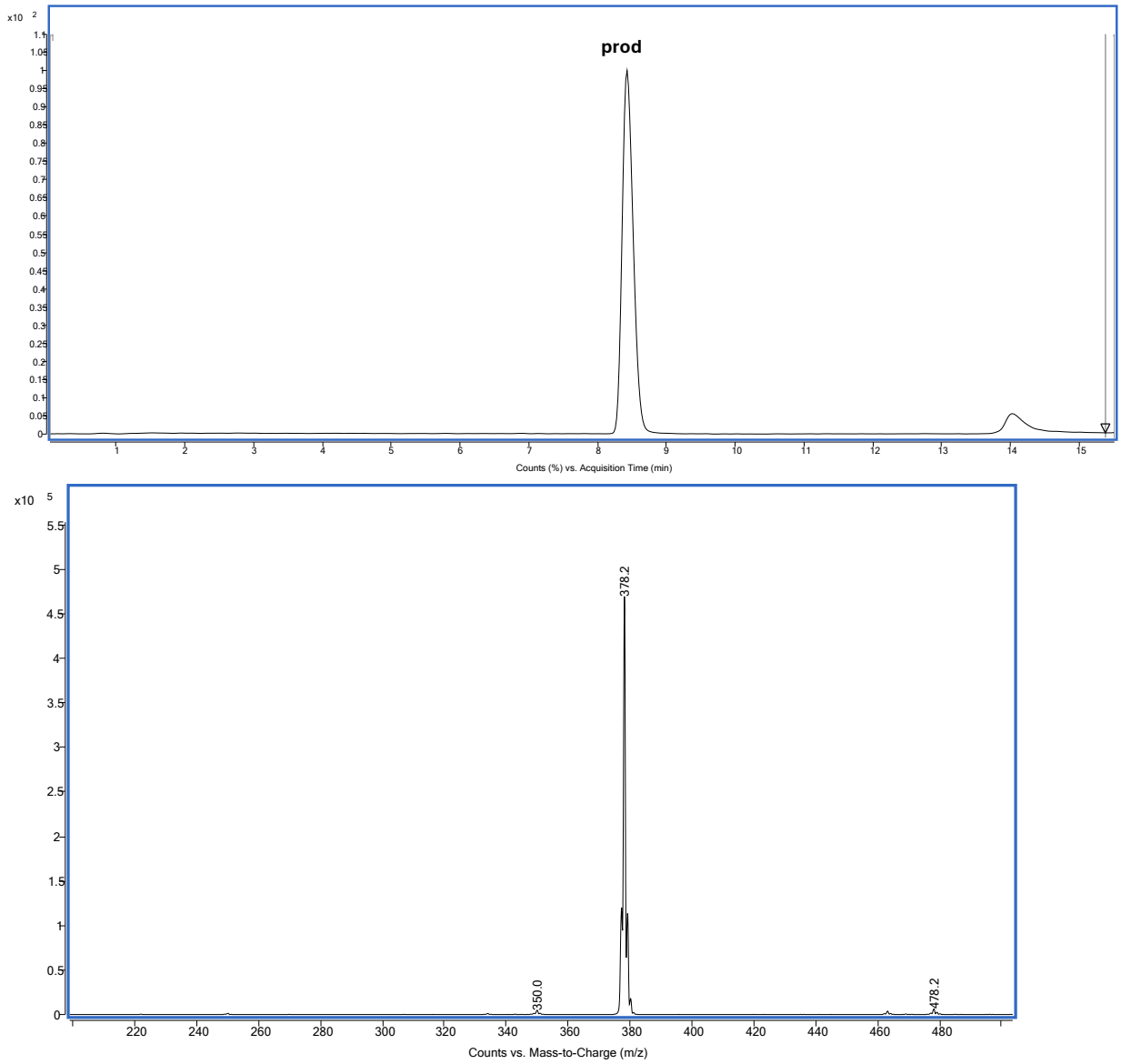

Figure S177. RP-LCMS trace at 254 nm (30-90% MeCN over 15 min) and ESI-MS spectrum of purified boronic ester **18-Gpin**. m/z 378.2 corresponds to $[M-H]^-$.

Formation and characterization of 3pin ester **18-3pin**.

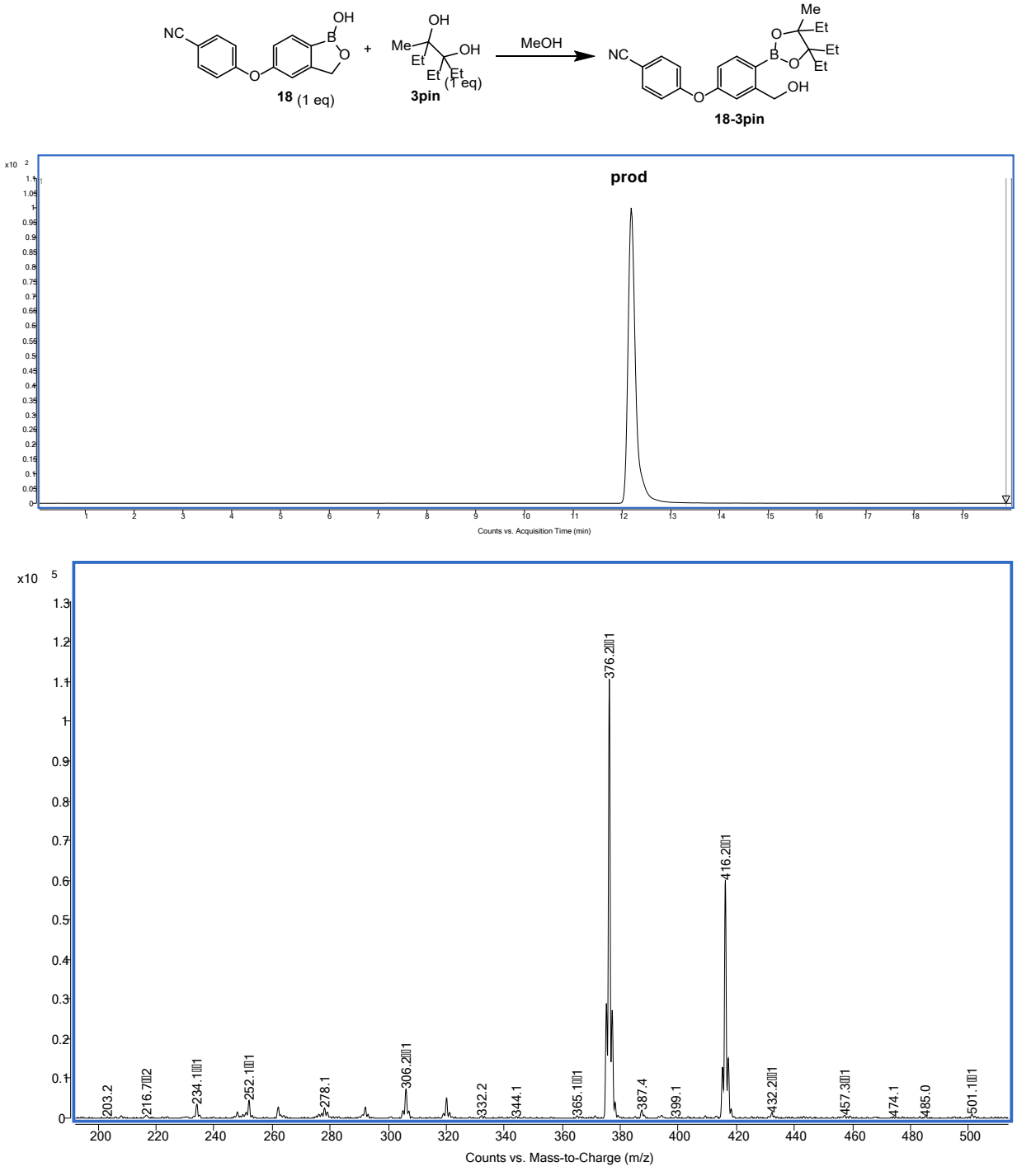

Figure S178. RP-LCMS trace at 254 nm (30-90% MeCN over 20 min) and ESI-MS spectrum of purified boronic ester **18-3pin**. m/z 376.2 and 416.2 corresponds to $[M\text{-}OH]^+$ and $[M+H]^+$ respectively.

Ixazomib (**19**) esters characterization.

Formation and characterization of Gpin ester **19-Gpin**.

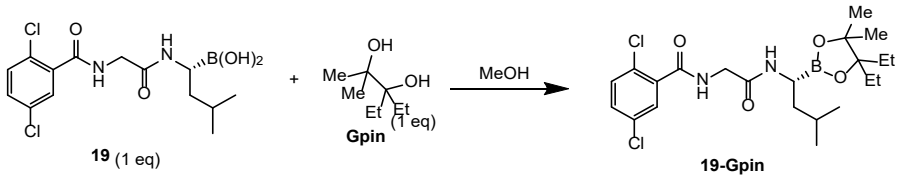

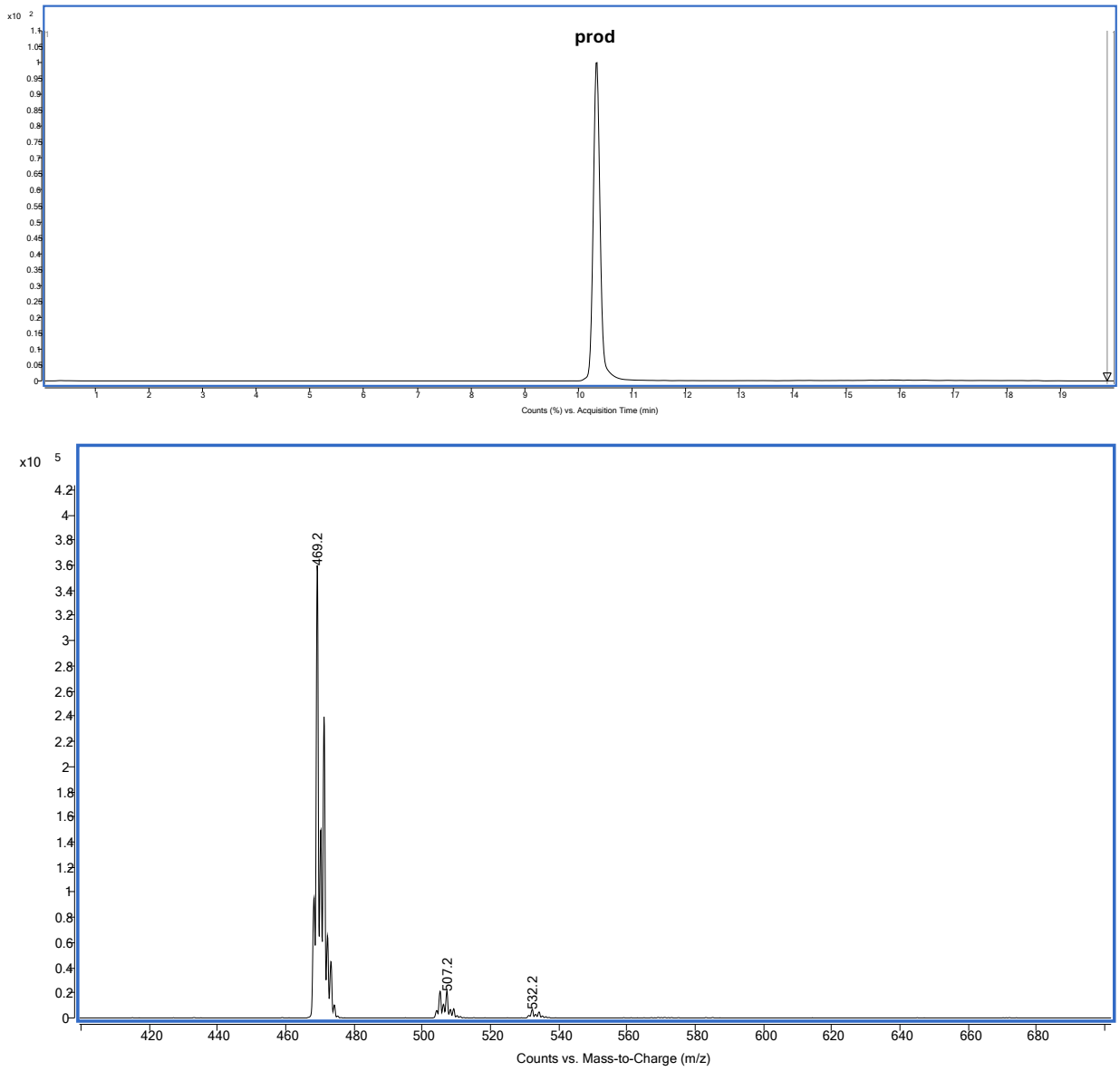

Figure S179. RP-LCMS trace at 254 nm (5-50% MeCN over 20 min) and ESI-MS spectrum of purified boronic ester **19-Gpin**. m/z 469.2 corresponds to $[M-H]^-$.

Formation and characterization of 3pin ester **19-3pin**.

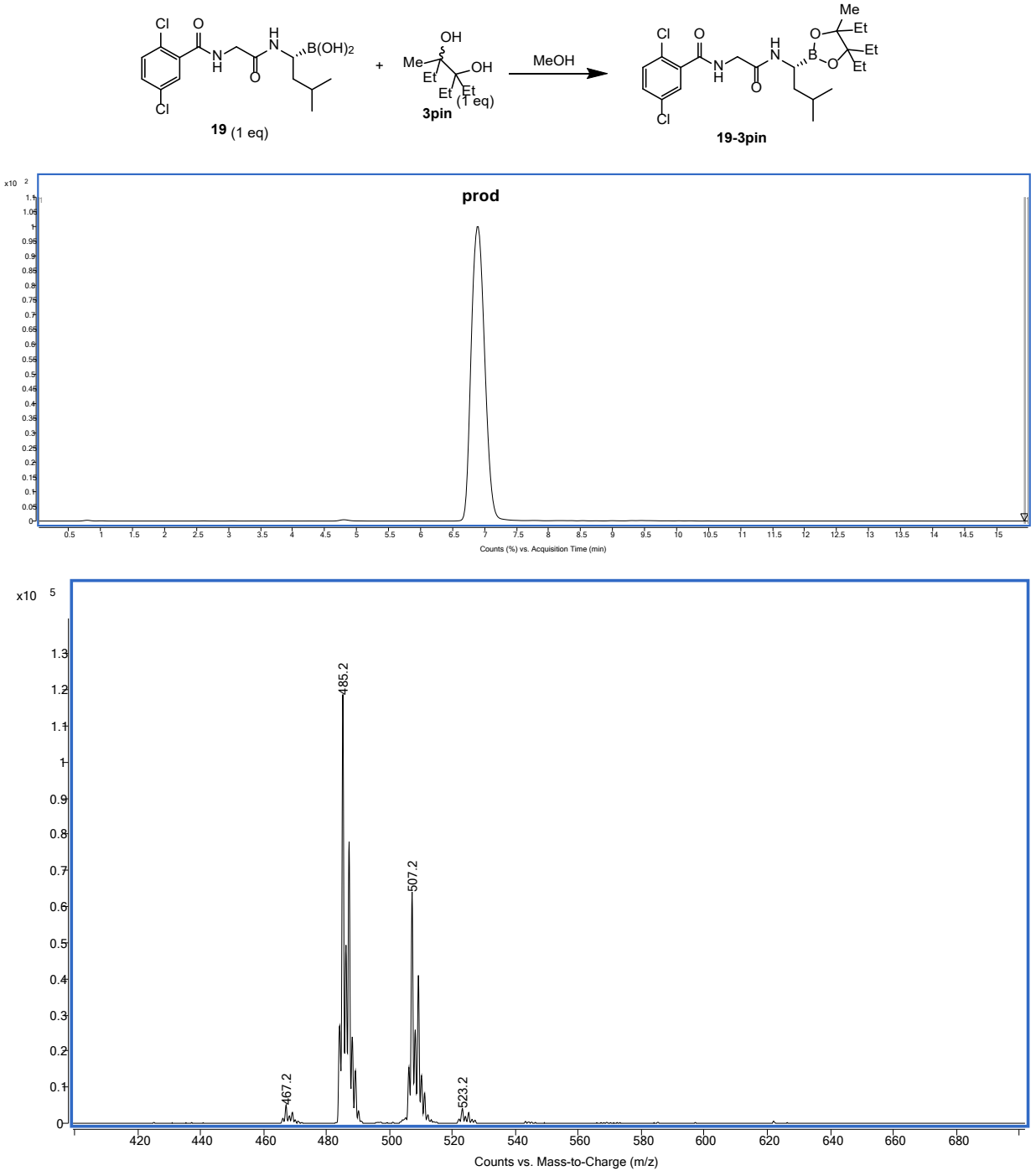

Figure S180. RP-LCMS trace at 254 nm (30-90% MeCN over 30 min) and ESI-MS spectrum of purified boronic ester **19-3pin**. m/z 485.2 corresponds to $[M+H]^+$.

Phenylalanine boronic acid (**20**) esters characterization.

Formation and characterization of Gpin ester **20-Gpin**.

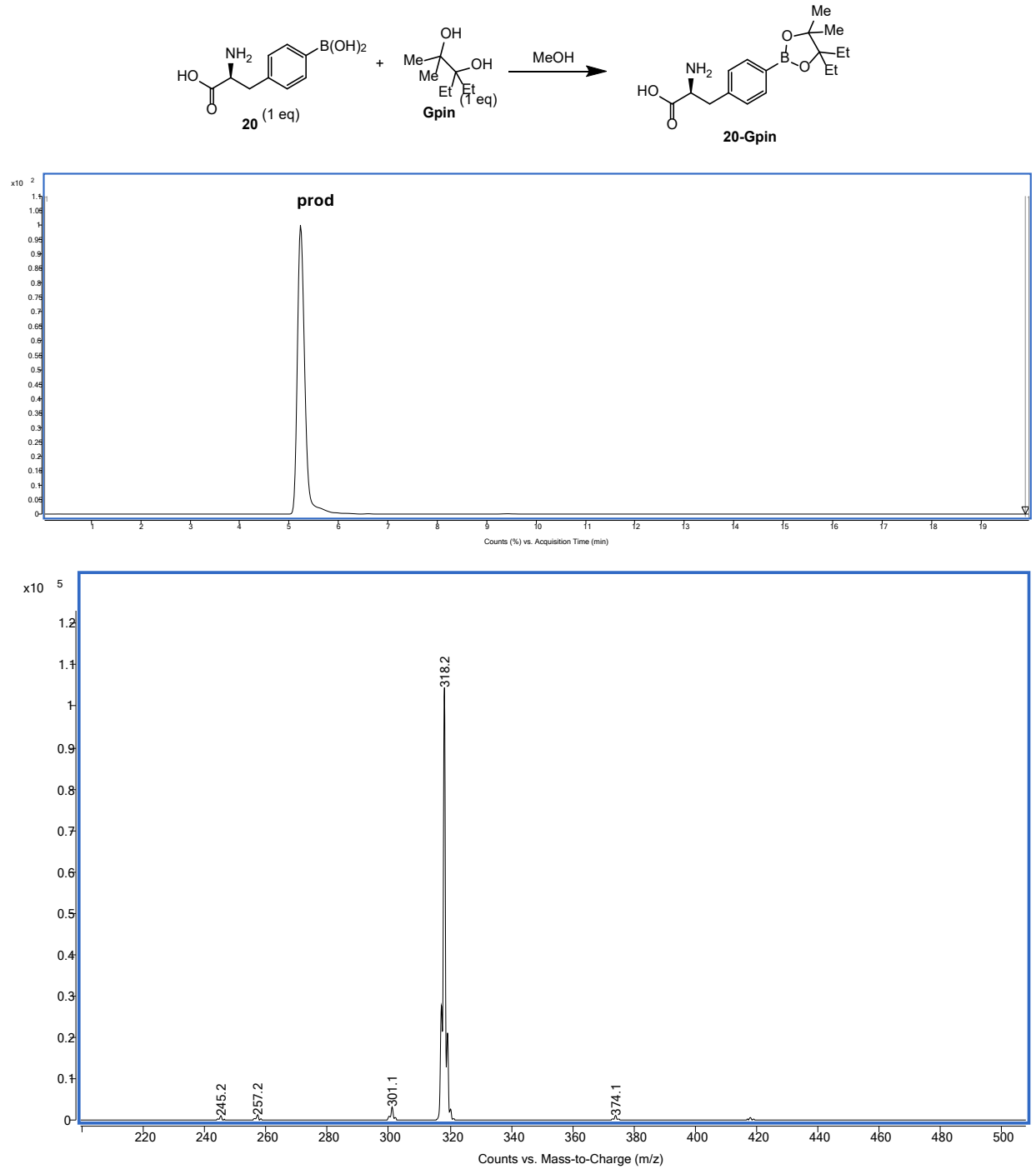

Figure S181. RP-LCMS trace at 254 nm (5-50% MeCN over 20 min) and ESI-MS spectrum of purified boronic ester **20-Gpin**. m/z 318.2 corresponds to $[M-H]^-$.

Formation and characterization of 3pin ester **20-3pin.**

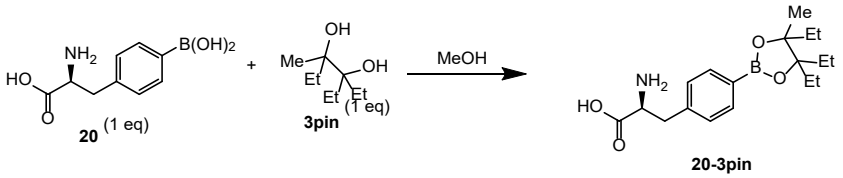

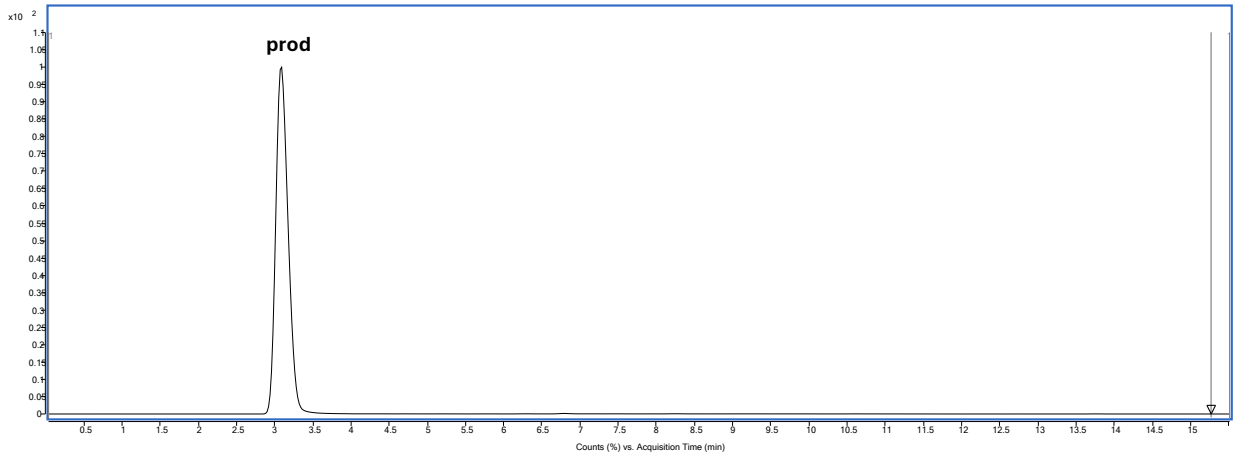

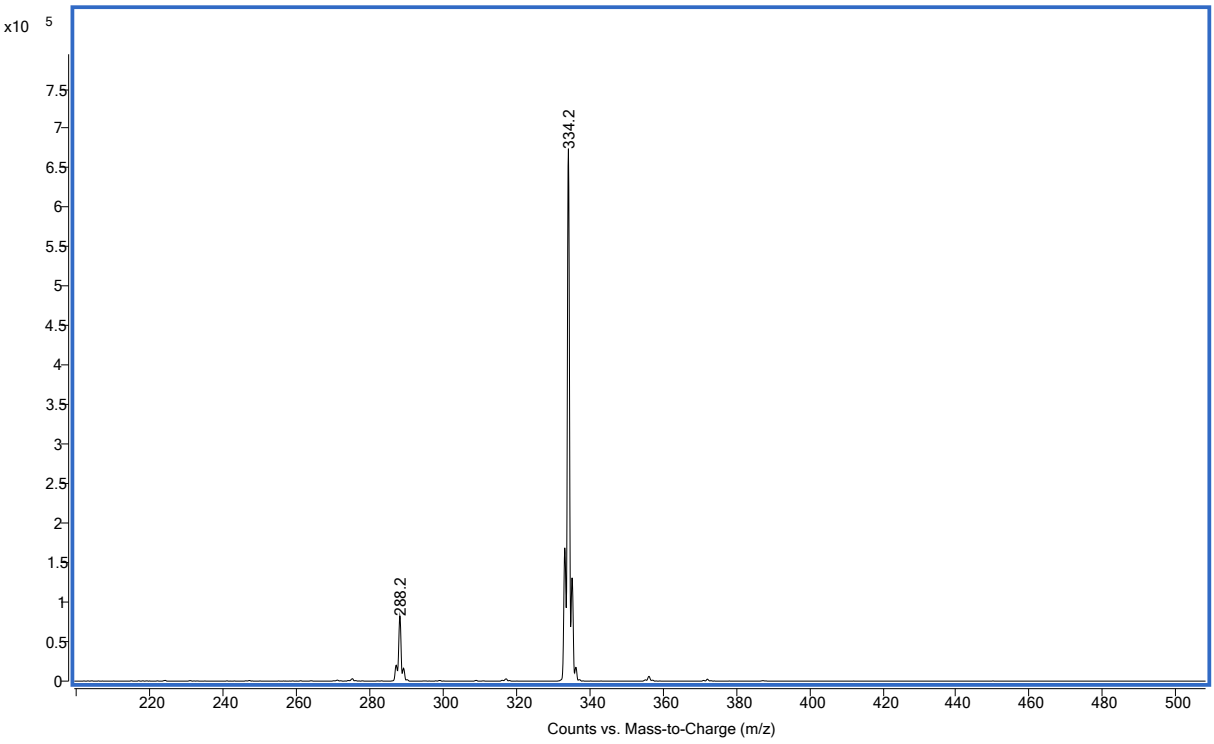

Figure S182. RP-LCMS trace at 254 nm (30-90% MeCN over 15 min) and ESI-MS spectrum of purified boronic ester **20-3pin**. m/z 334.2 corresponds to $[M-H]^-$.

4-carboxyphenylboronic acid (**S6**) ester characterization.

Formation and characterization of Gpin ester **S6-Gpin**.

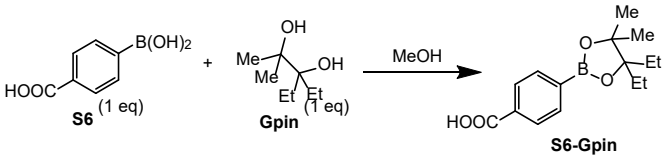

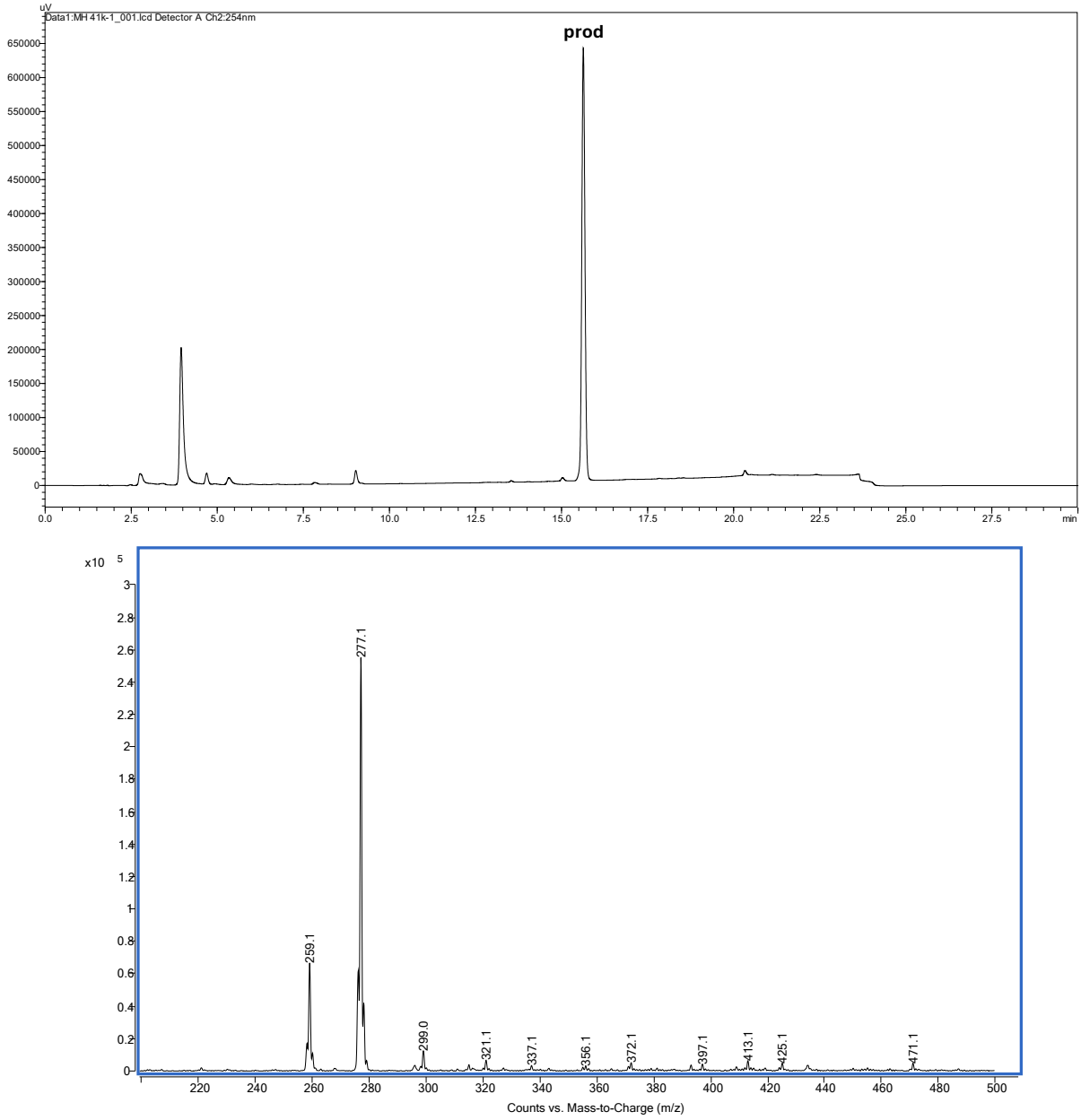

Figure S183. RP-HPLC trace at 254 nm (30-95% MeCN over 30 min) and ESI-MS spectrum of purified boronic ester **S6-Gpin**. m/z 277.1 corresponds to $[M+H]^+$.

4-(2-carboxyethyl)benzeneboronic acid (**S7**) ester characterization.

Formation and characterization of Ethyl Pinacol ester **S7-Gpin**.

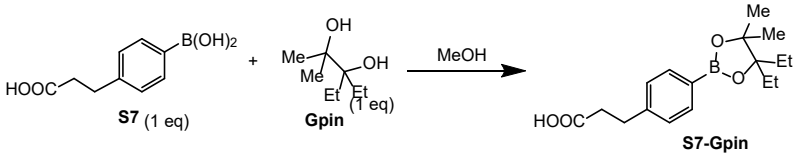

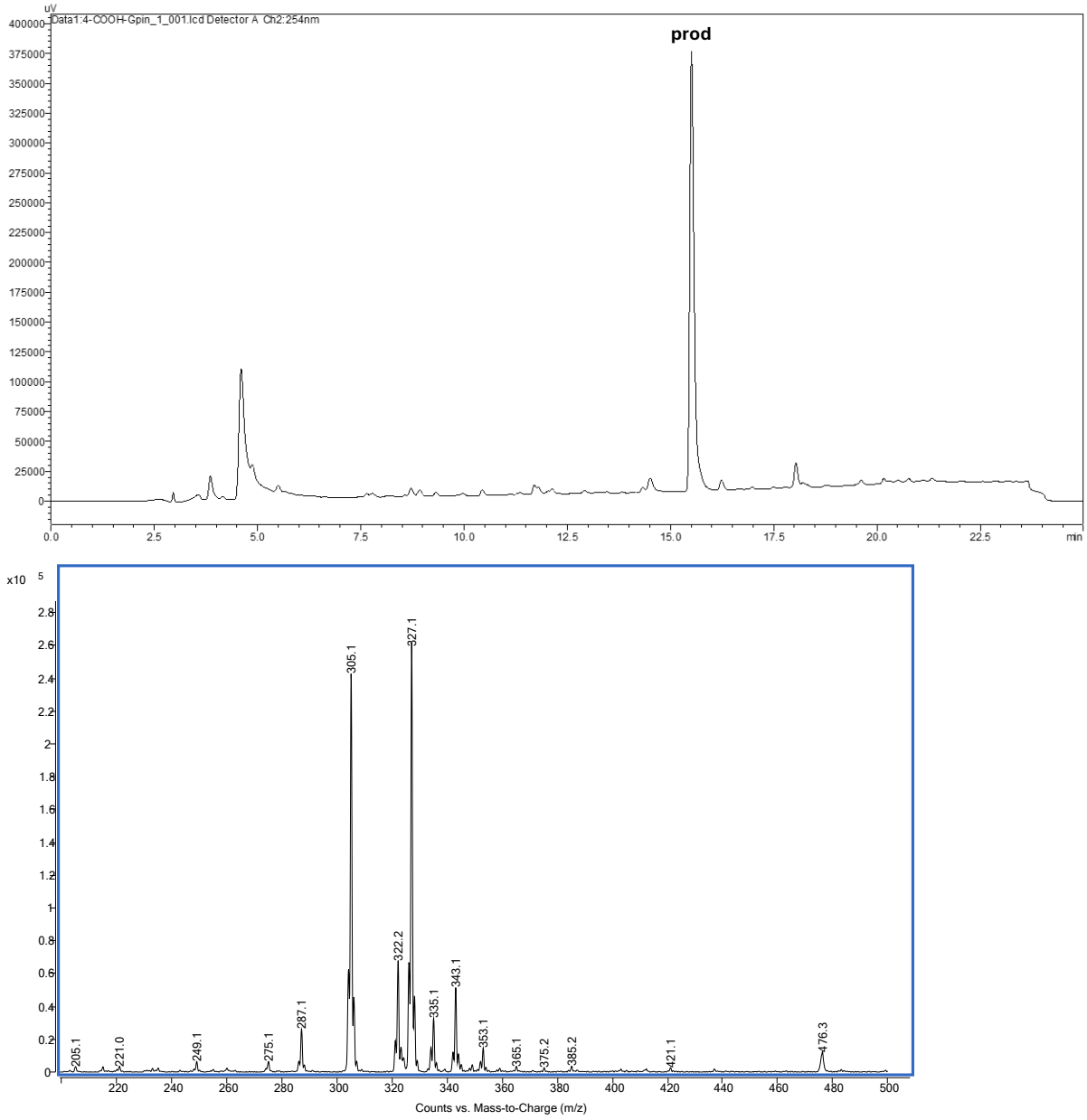

Figure S184. RP-HPLC trace at 254 nm (30-95% MeCN over 30 min) and ESI-MS spectrum of purified boronic ester **S7-Gpin**. m/z 305.1 and 327.1 corresponds to $[M+H]^+$ and $[M+Na]^+$ respectively.

Synthesized peptides characterization data

Peptide 21

Precursor **(**Ac-PF(4-I)RRYI-NH_2**)**

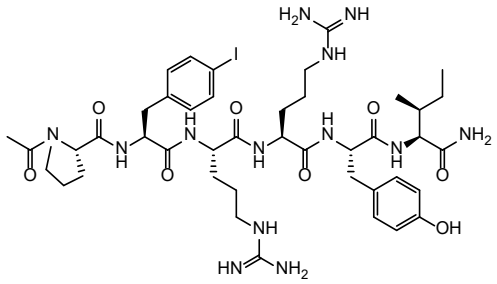

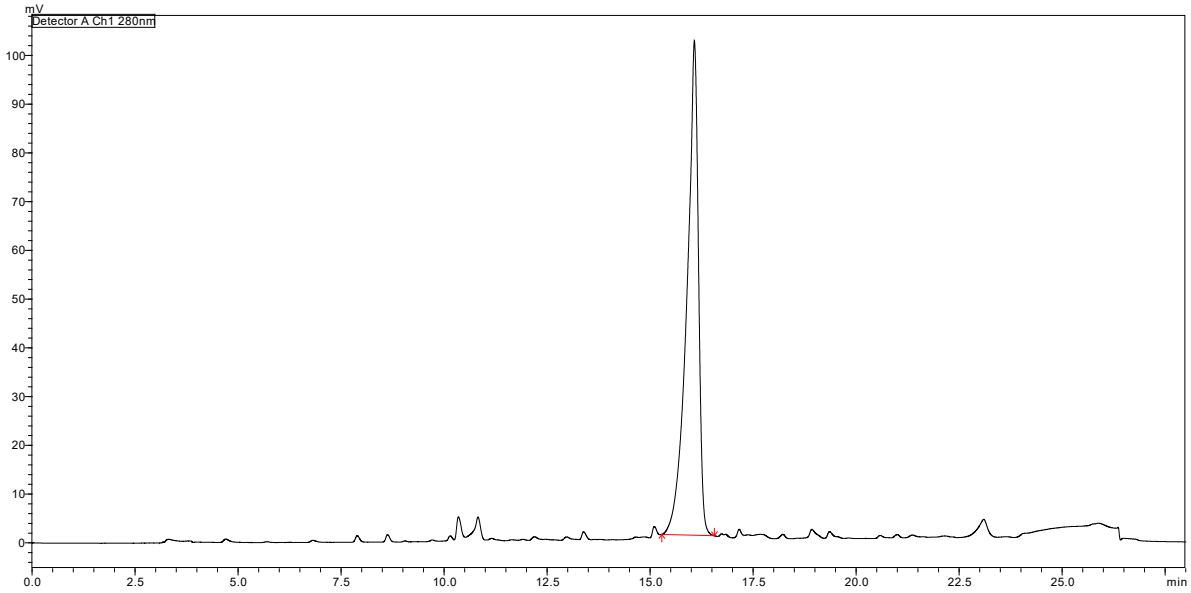

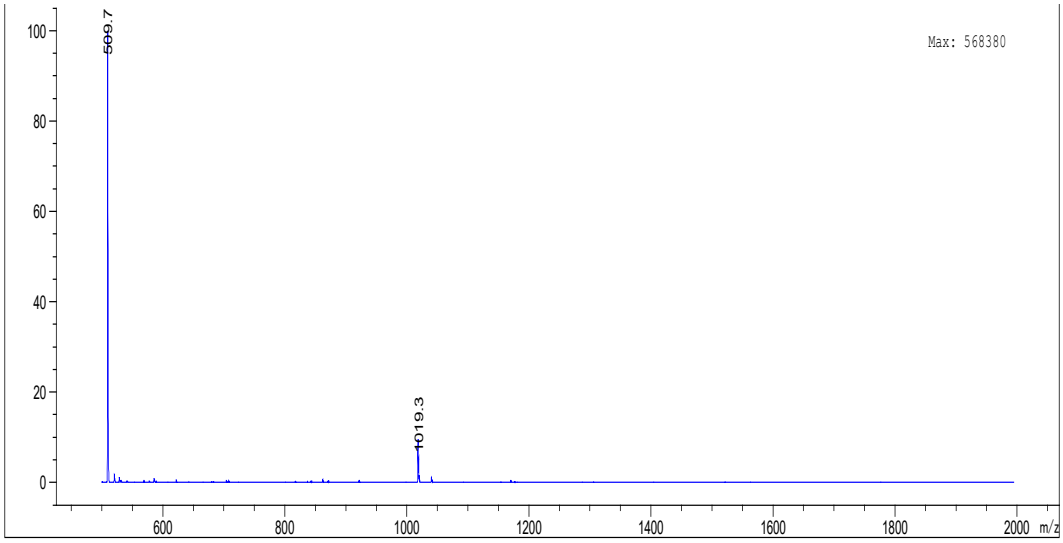

Figure S185. RP-HPLC trace at 280 nm (20-80% MeCN over 20 min) and ESI-MS spectrum of purified peptide **21** precursor. m/z 509.7 and 1019.3 correspond to $[M+2H]^{2+}$ and $[M+H]^{+}$ respectively.

Peptide 21 (Ac-PF(4-B(OH)$_2$)RRYI-NH$_2$)

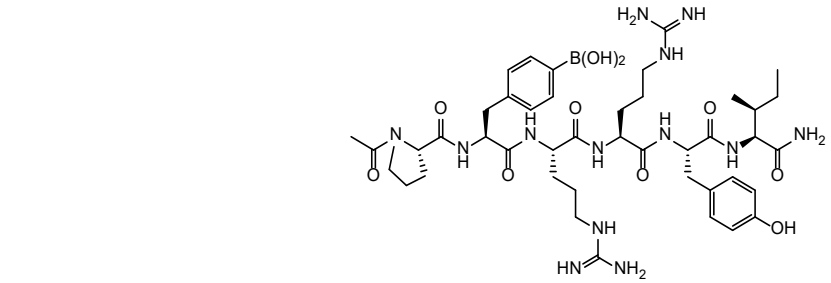

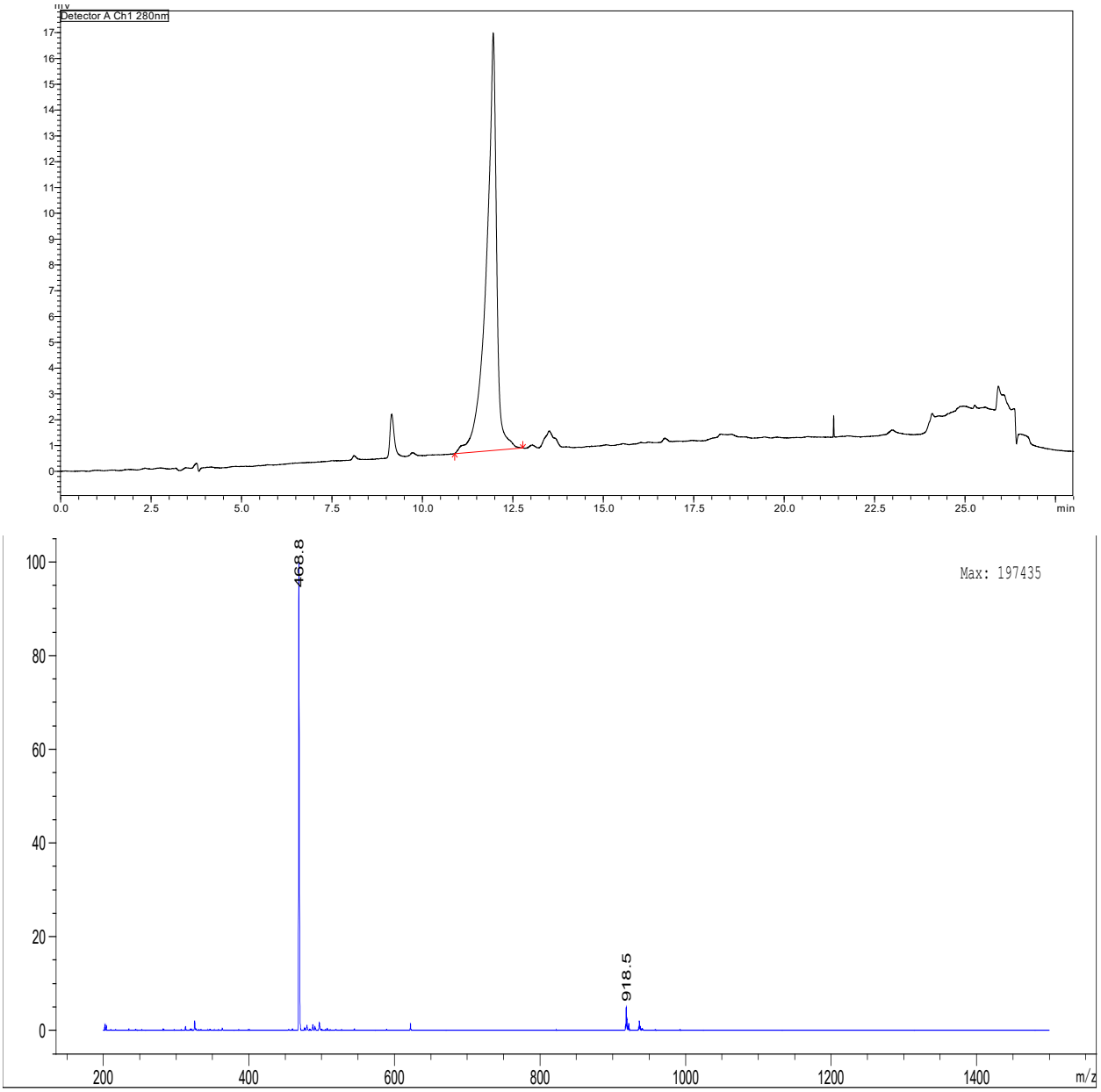

Figure S186. RP-HPLC trace at 280 nm (20-80% MeCN over 20 min) and ESI-MS spectrum of purified peptide **21**. m/z 468.8 and 918.5 correspond to $[M+2H]^{2+}$ and $[M-OH]^{+}$ respectively.

Peptide 22

Precursor **(**Ac-PF(2-I)RRYI-NH_2**)**

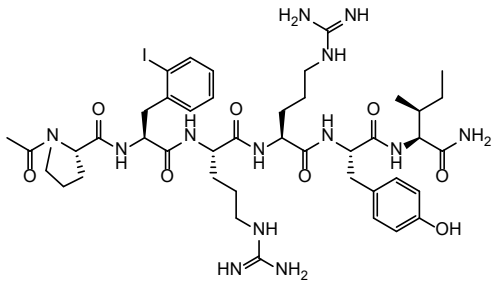

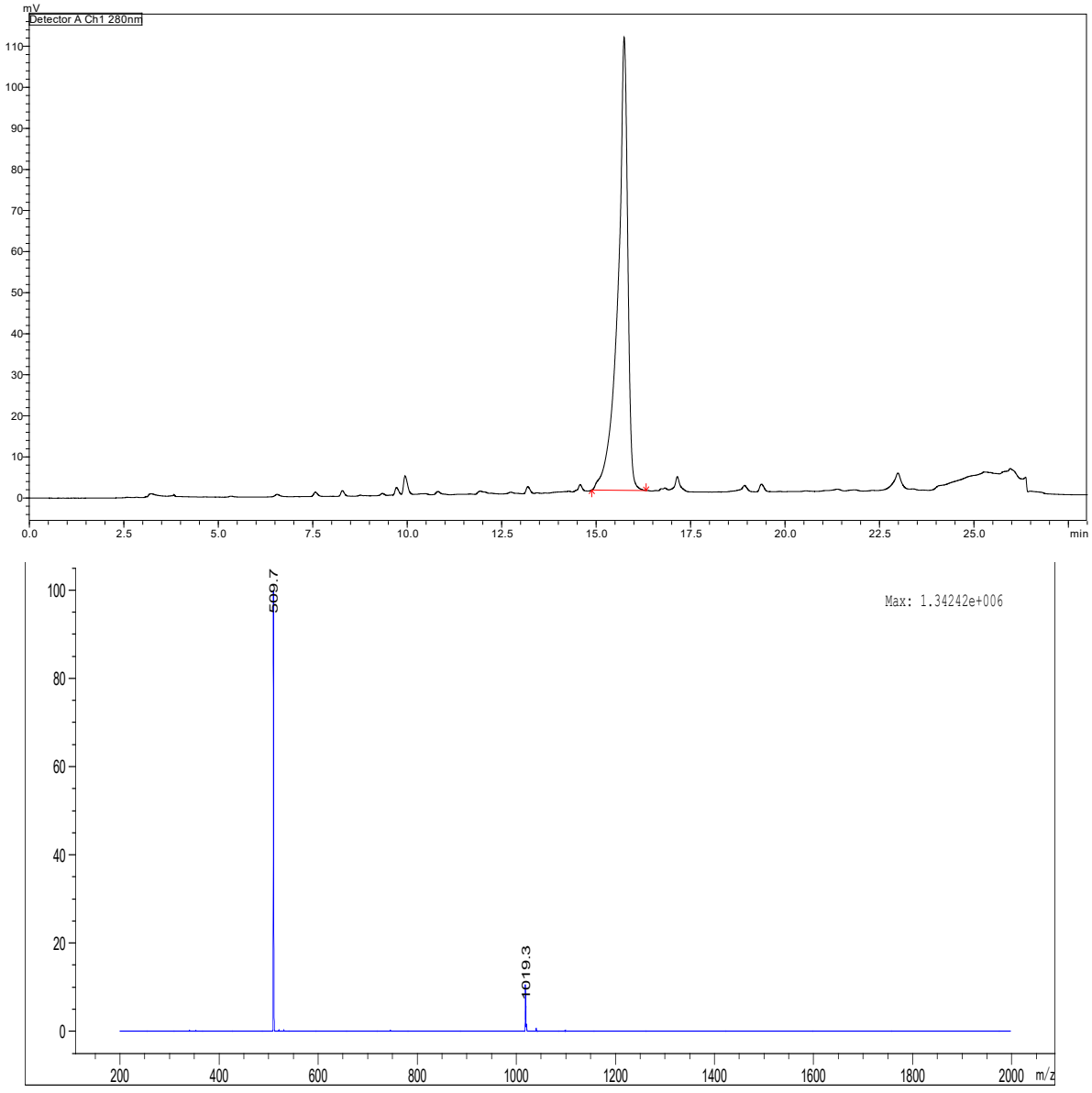

Figure S187. RP-HPLC trace at 280 nm (20-80% MeCN over 20 min) and ESI-MS spectrum of purified peptide **22** precursor. m/z 509.7 and 1019.3 correspond to $[M+2H]^{2+}$ and $[M+H]^{+}$ respectively.

Peptide 22 (Ac-PF(2-B(OH)$_2$)RRYI-NH$_2$)

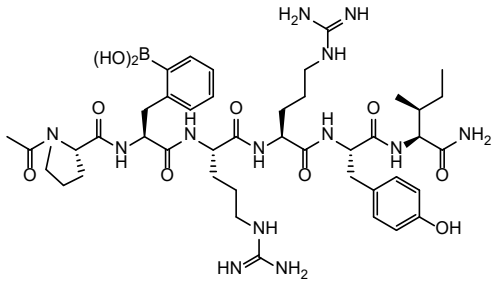

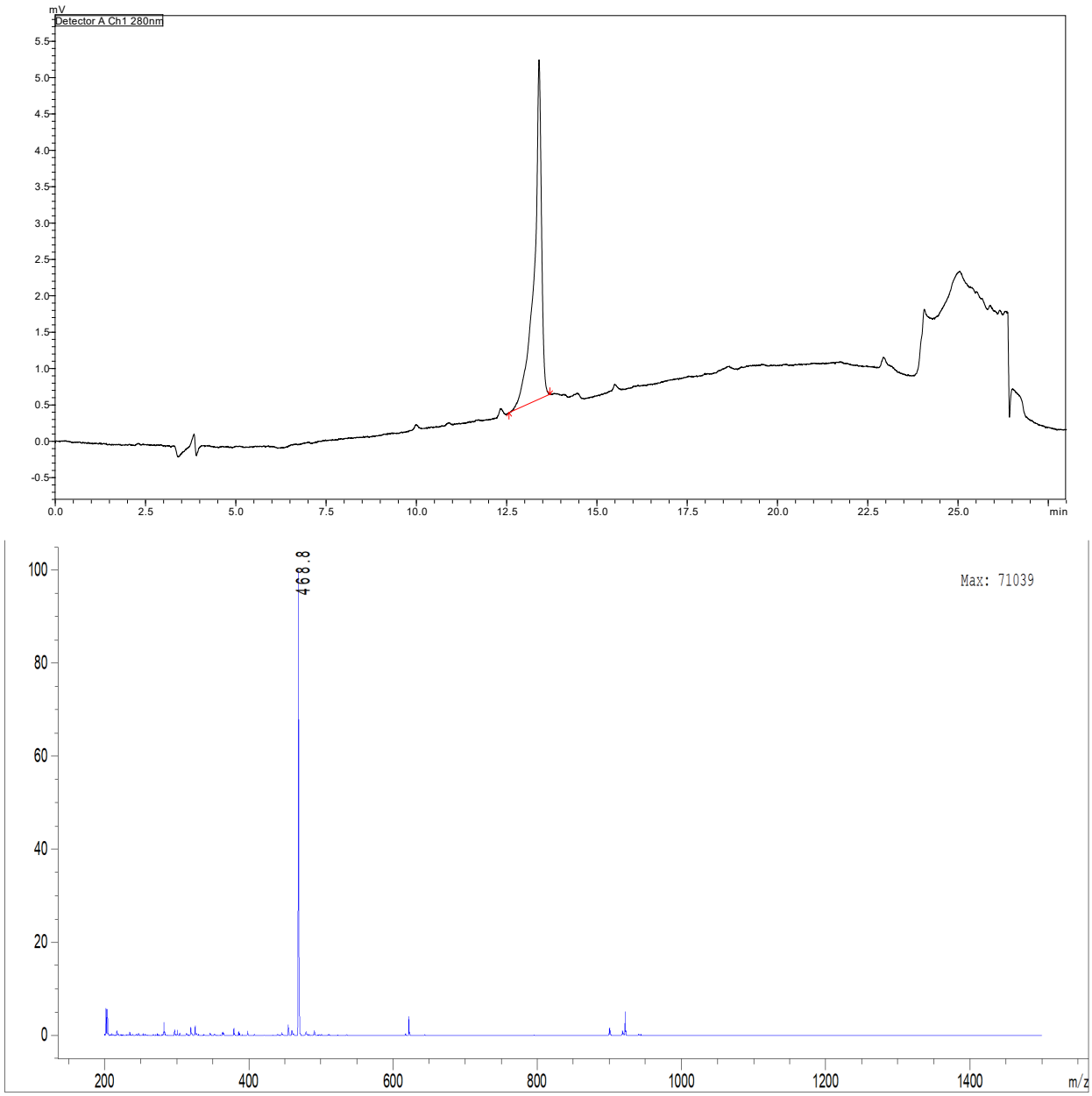

Figure S188. RP-HPLC trace at 280 nm (20-80% MeCN over 20 min) and ESI-MS spectrum of purified peptide **22**. m/z 468.8 correspond to $[M+2H]^{2+}$.

NMR spectra

^{1}H and ^{13}CNMR spectra of Gpin

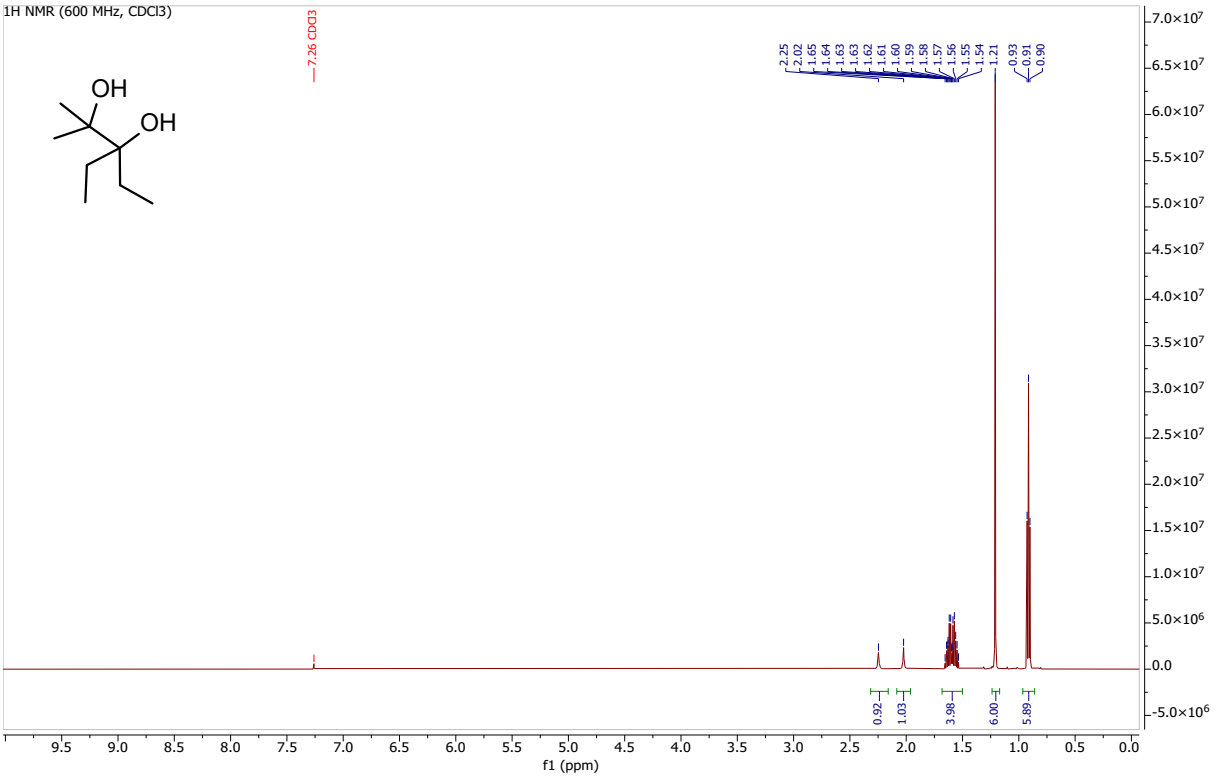

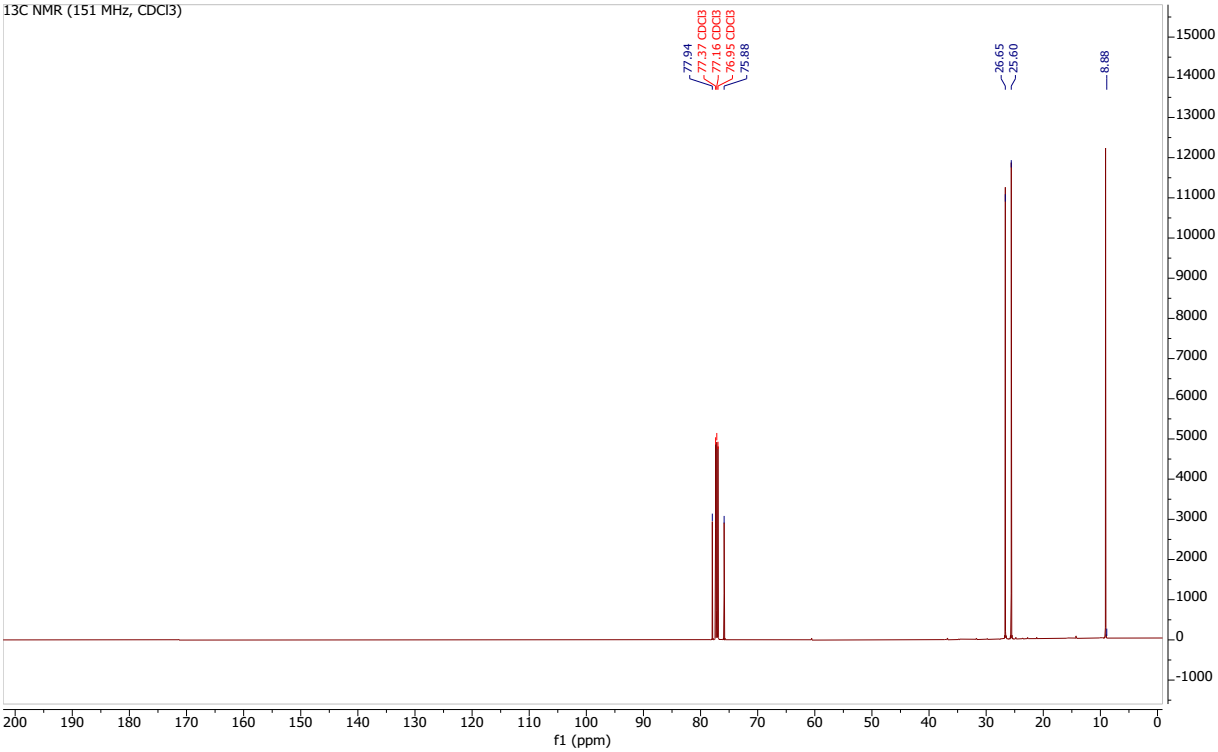

^{1}H and ^{13}CNMR spectra of ester S1

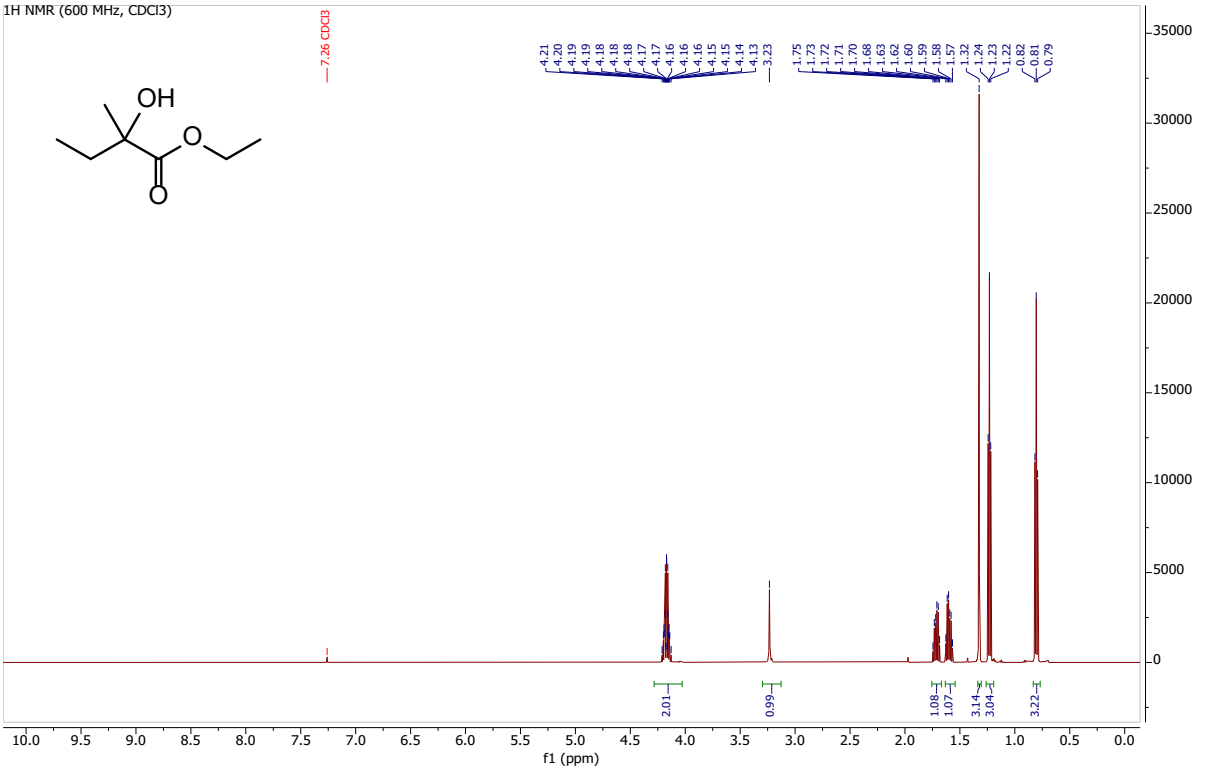

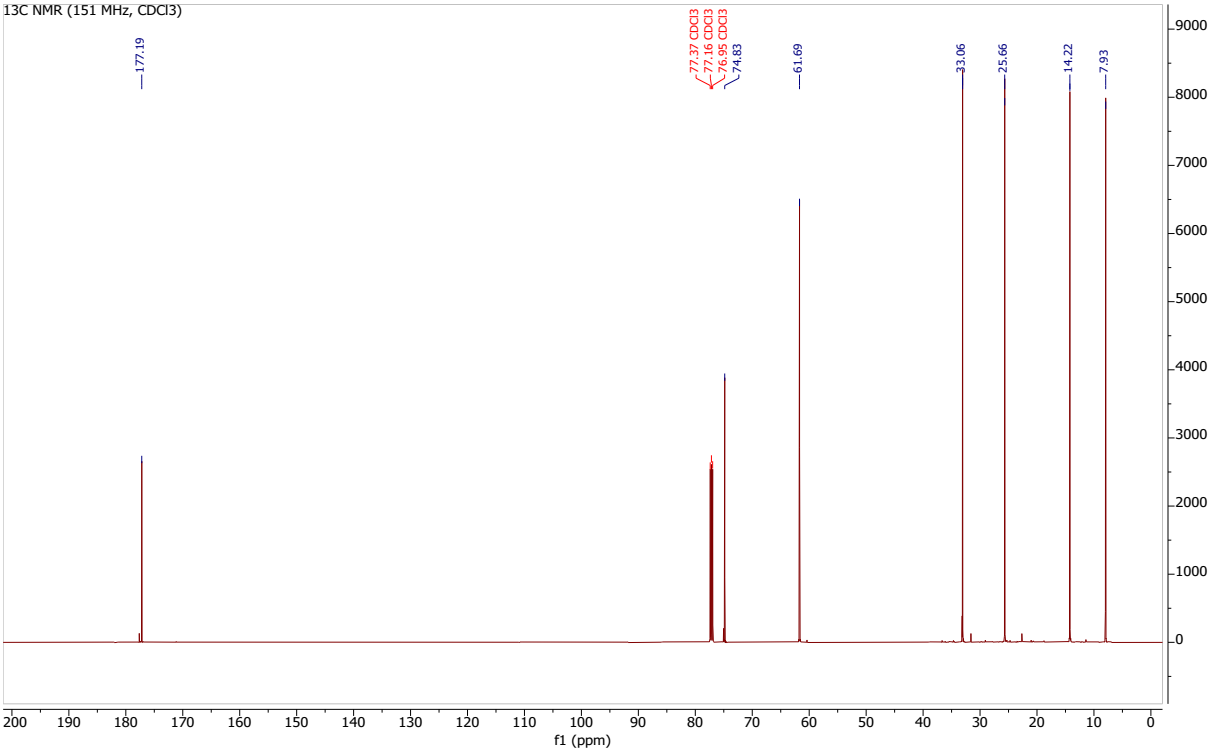

^{1}H and ^{13}CNMR spectra of 3pin

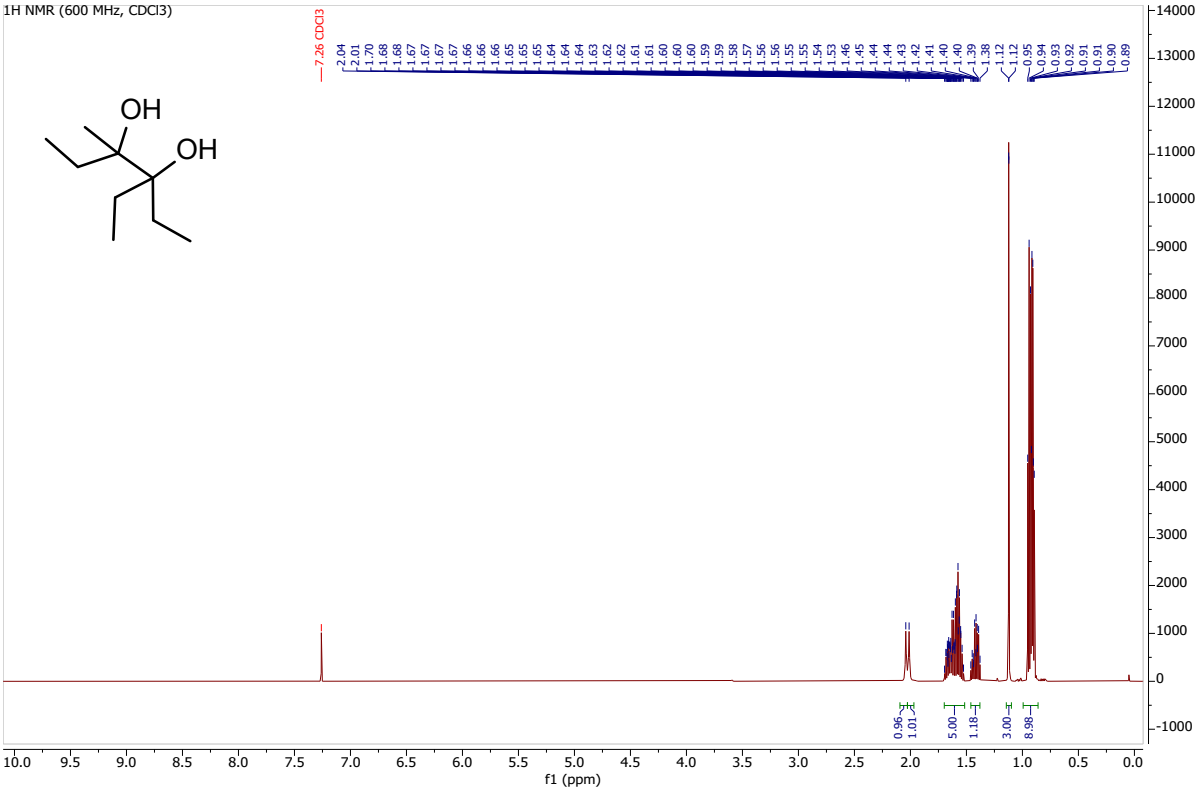

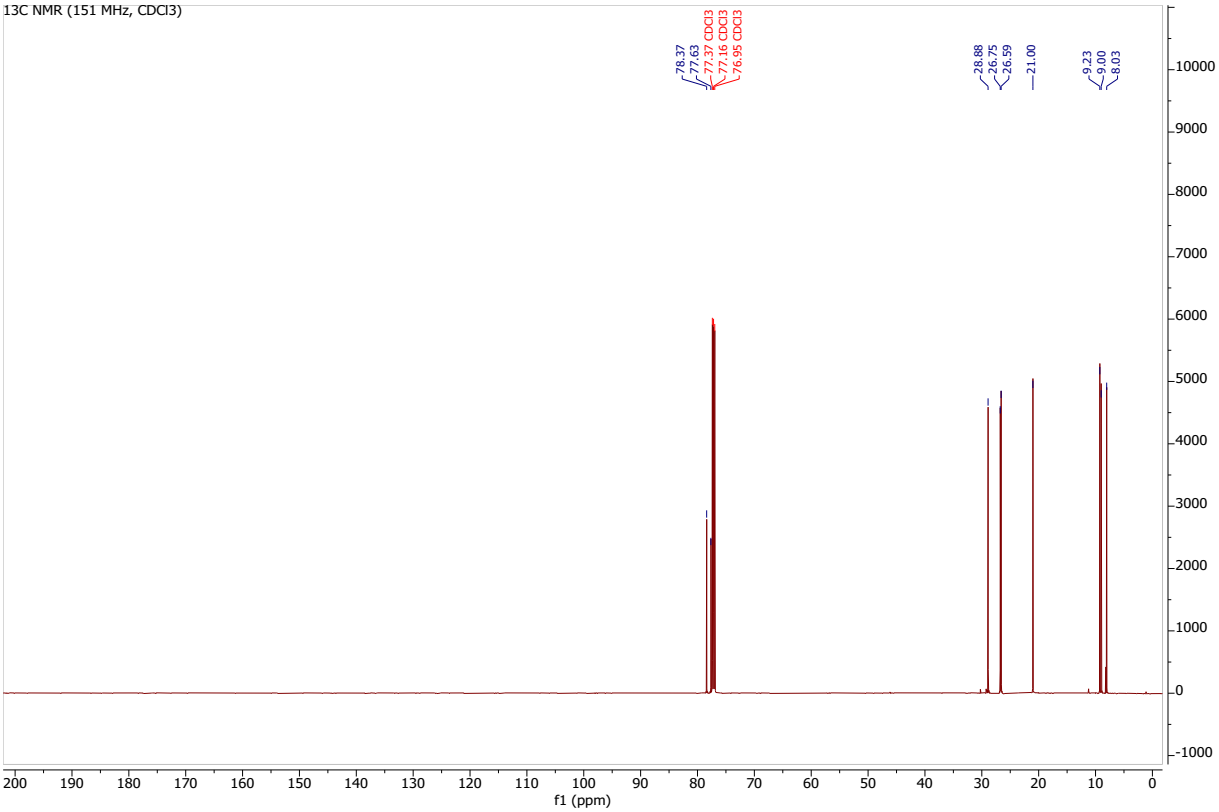

^{1}H, ^{13}C and ^{11}B NMR spectra of B_2Gpin_2

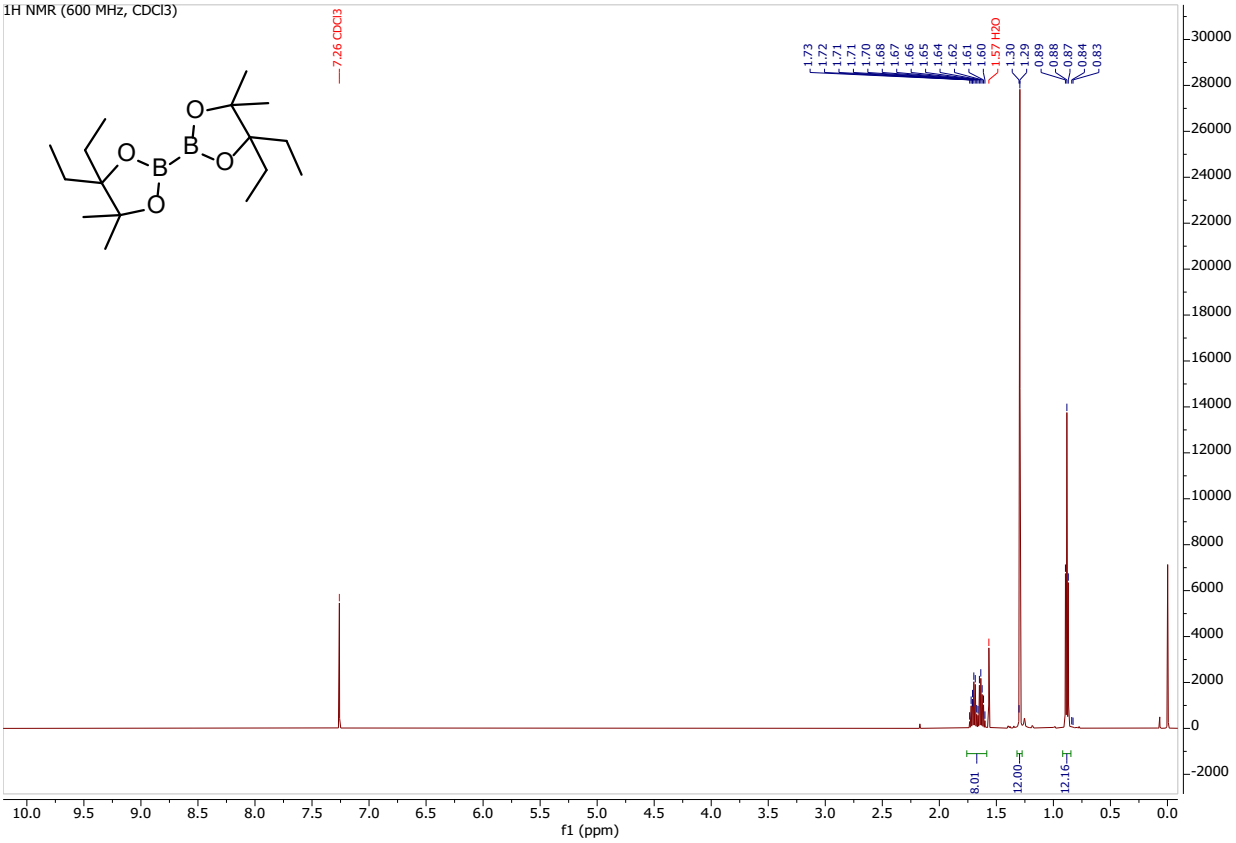

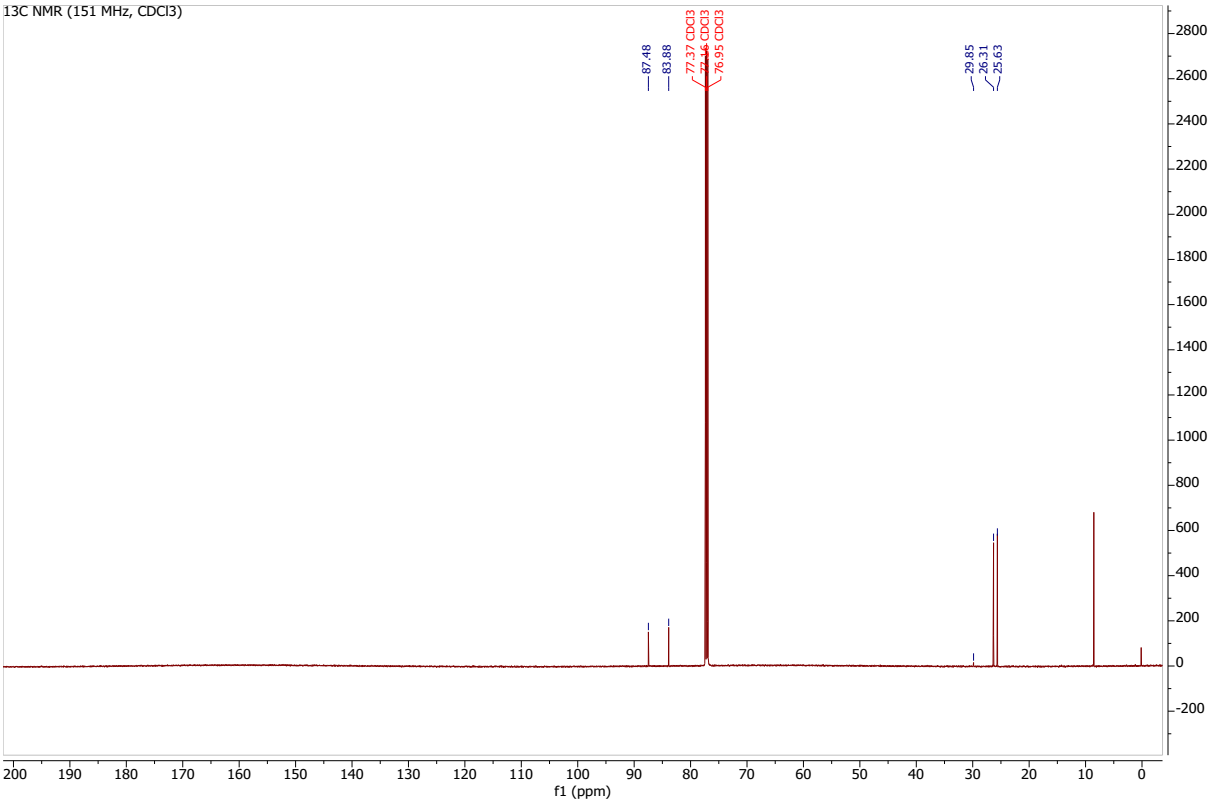

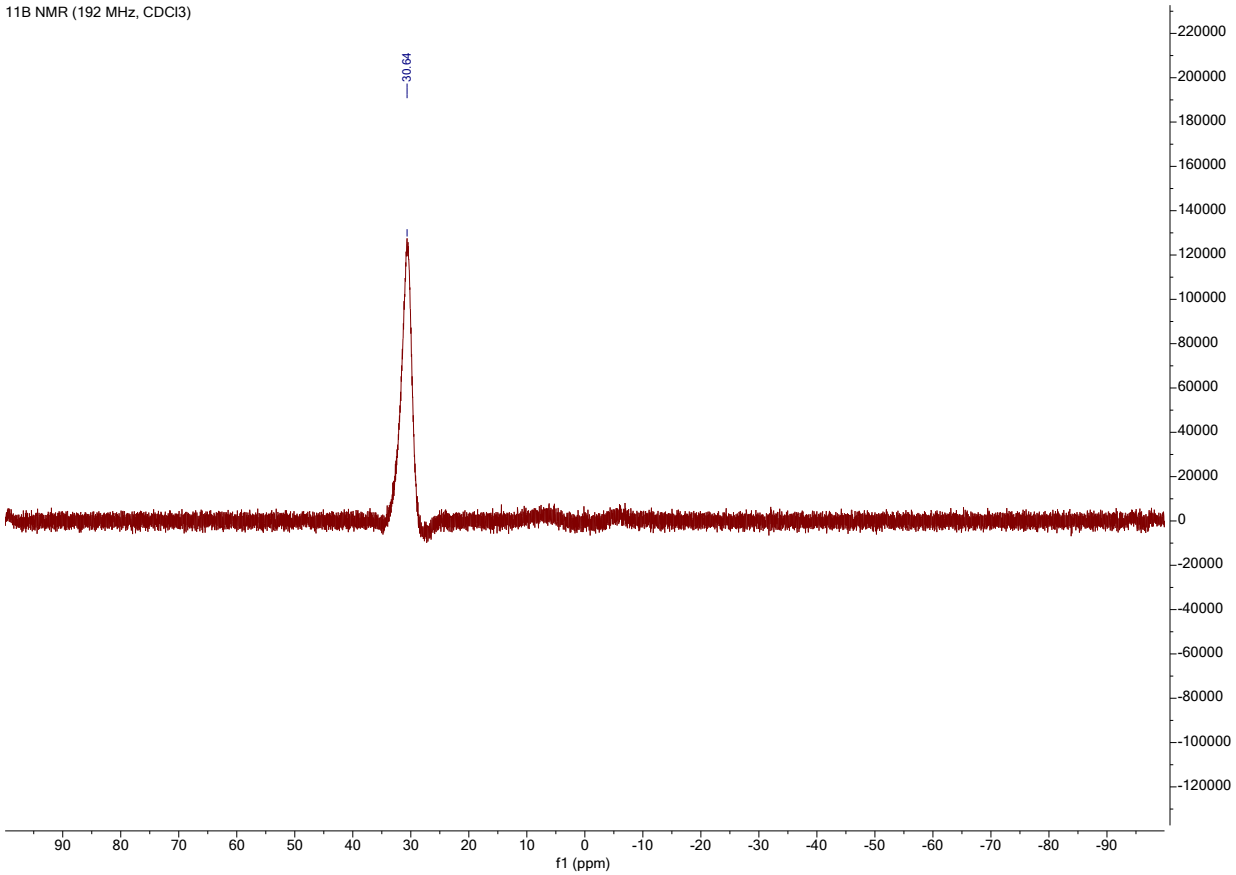
11B NMR (192 MHz, CDCl3)
30.64
220000
200000
180000
160000
140000
120000
100000
80000
60000
40000
20000
0
-20000
-40000
-60000
-80000
-100000
-120000
90
80
70
60
50
40
30
20
10
0
-10
-20
-30
-40
-50
-60
-70
-80
-90
f1 (ppm)

^{1}H and ^{13}CNMR spectra of S4

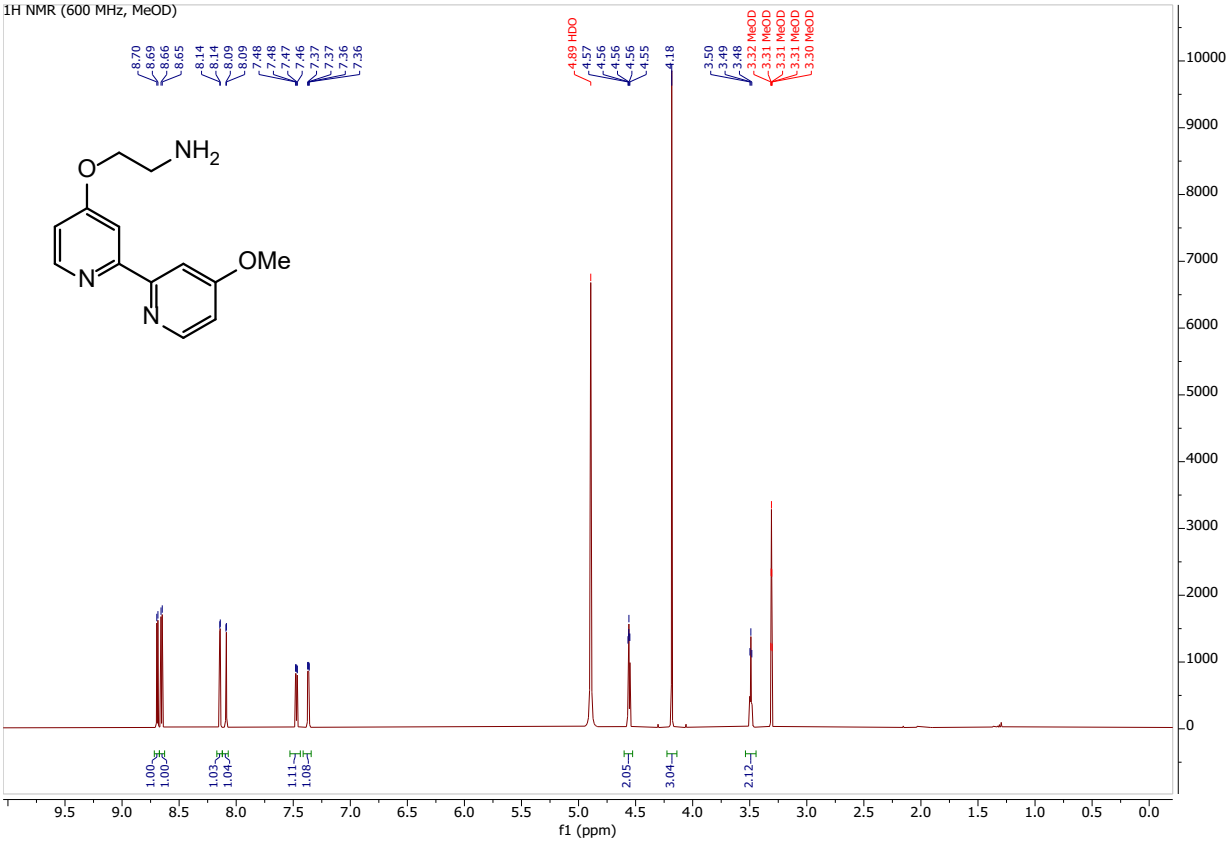

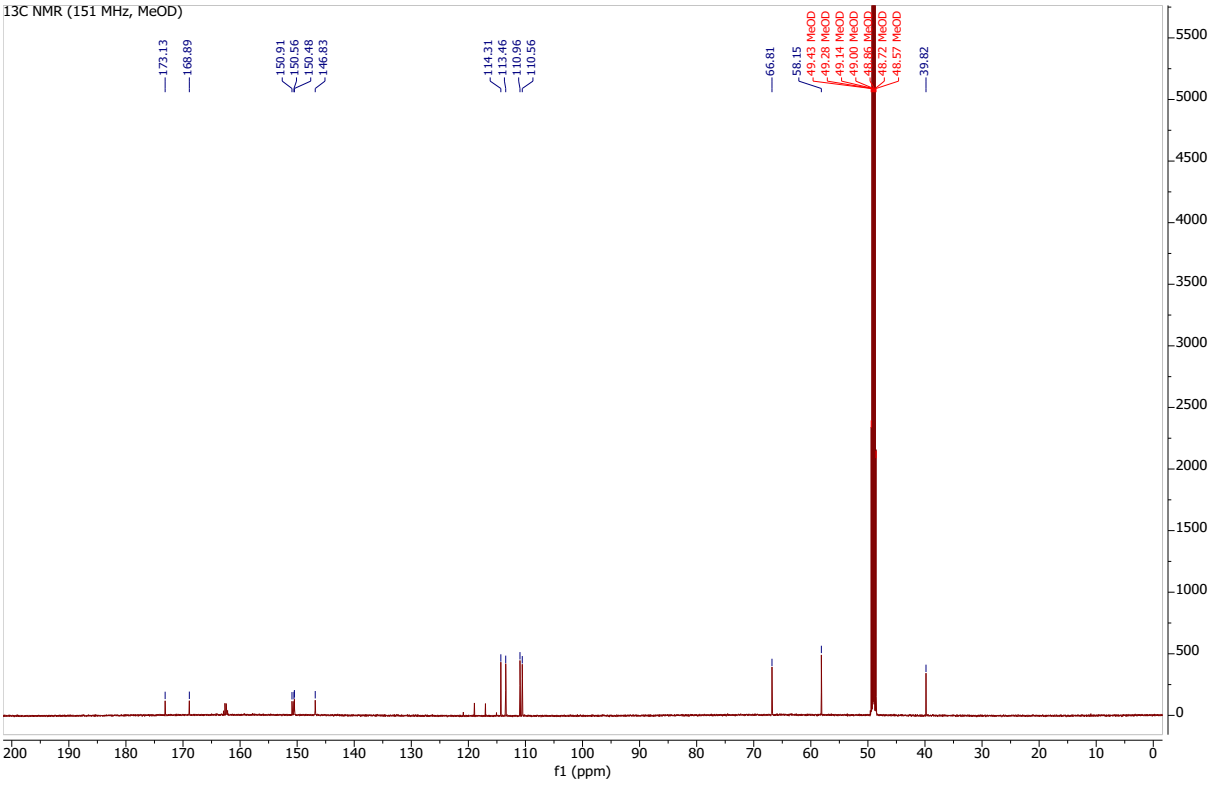

^{1}H and ^{13}CNMR spectra of 12-Gpin

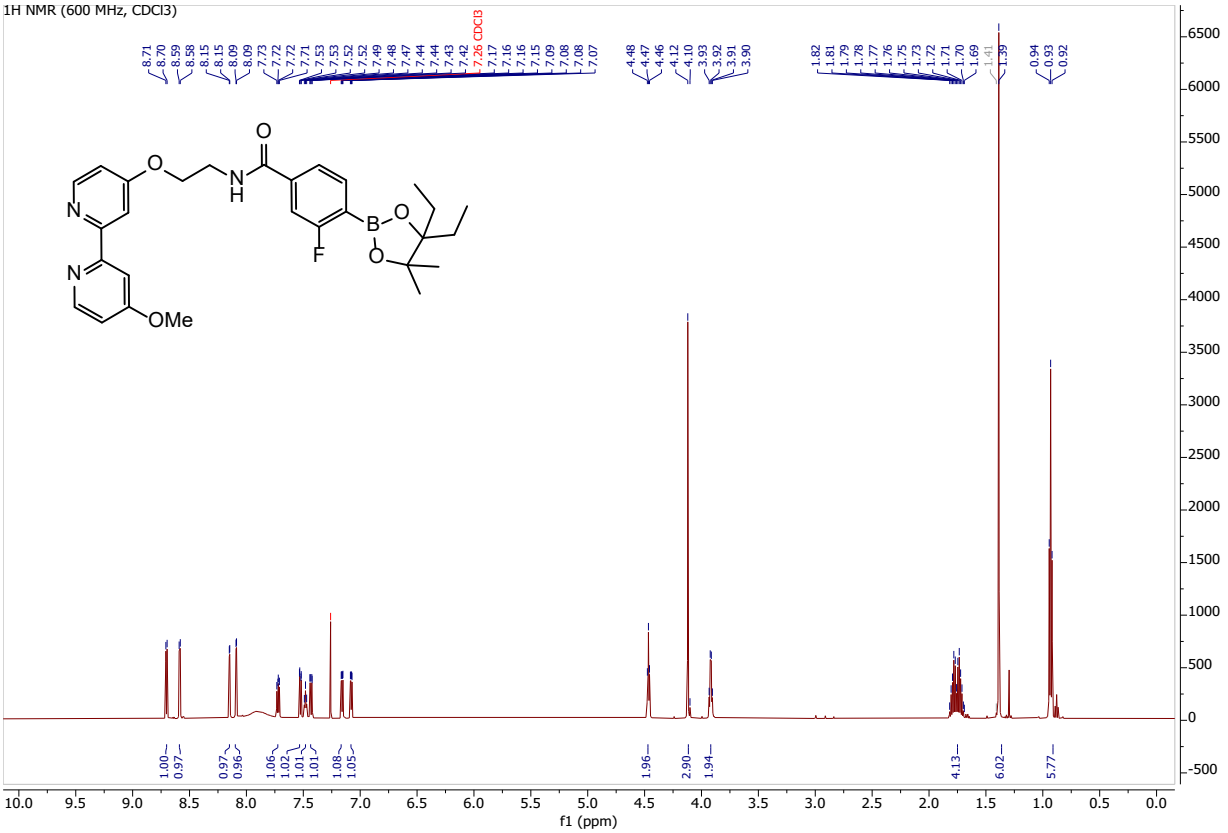

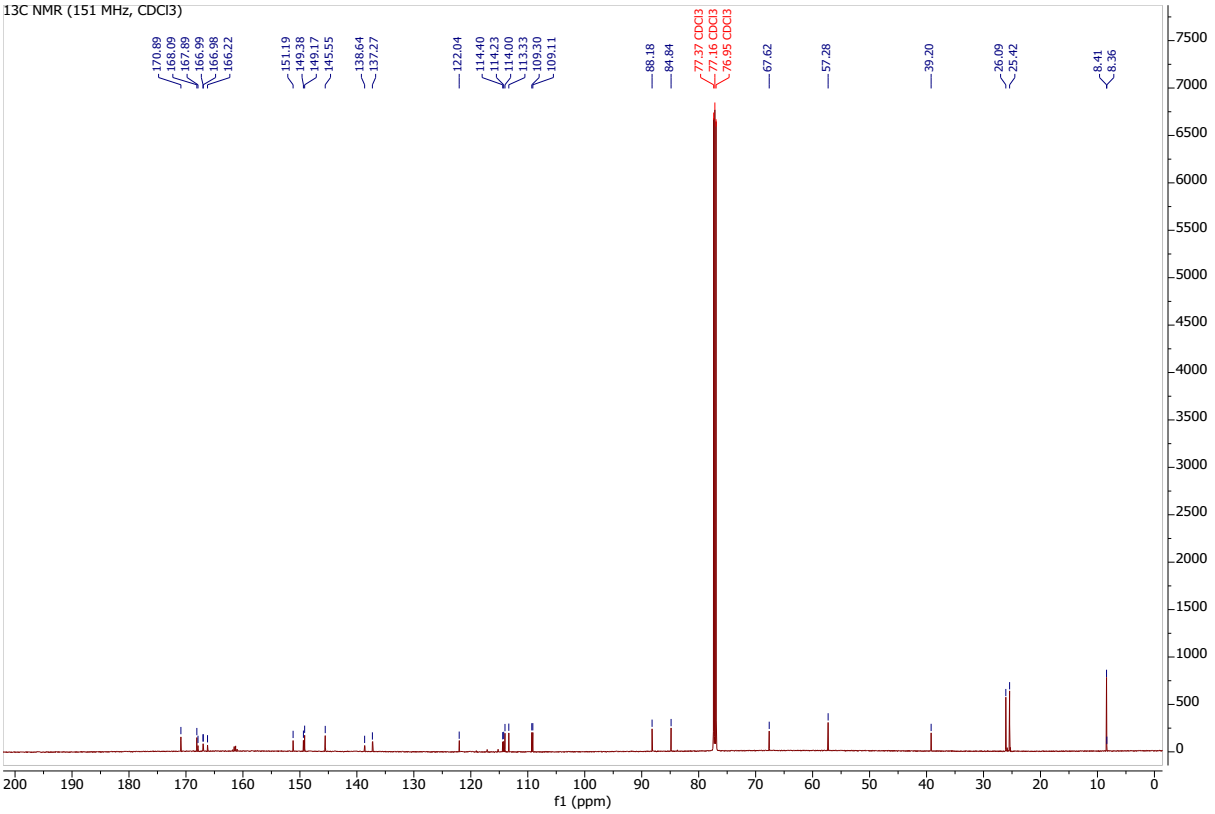

^{1}H and ^{13}CNMR spectra of 12-3pin

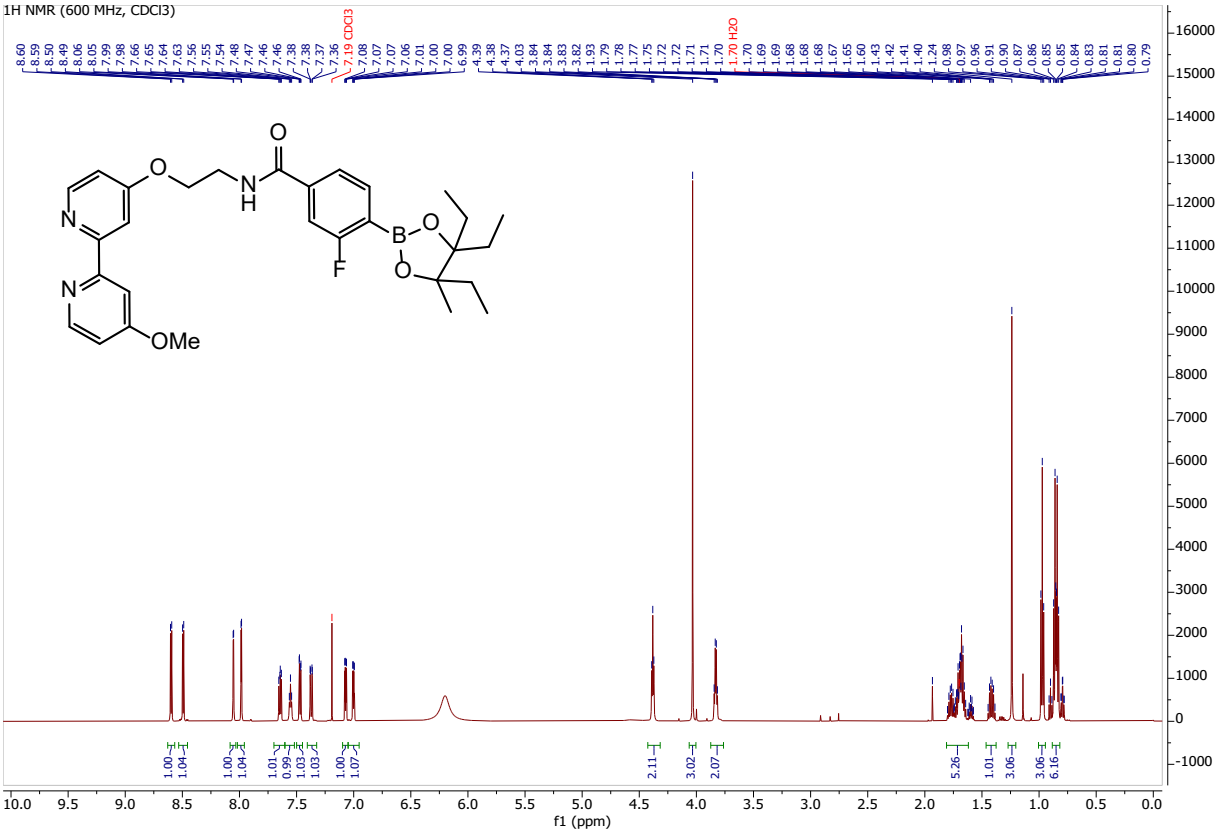

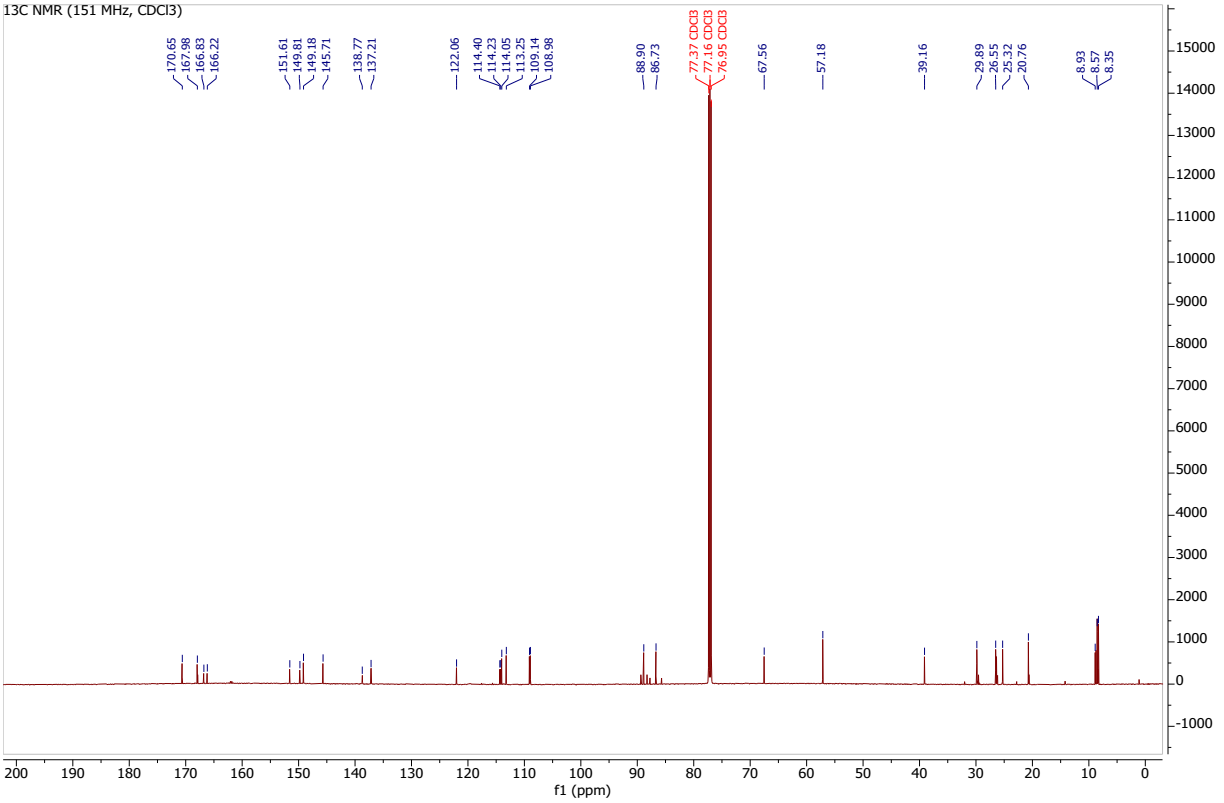

^{1}H and ^{13}CNMR spectra of 12-Epin

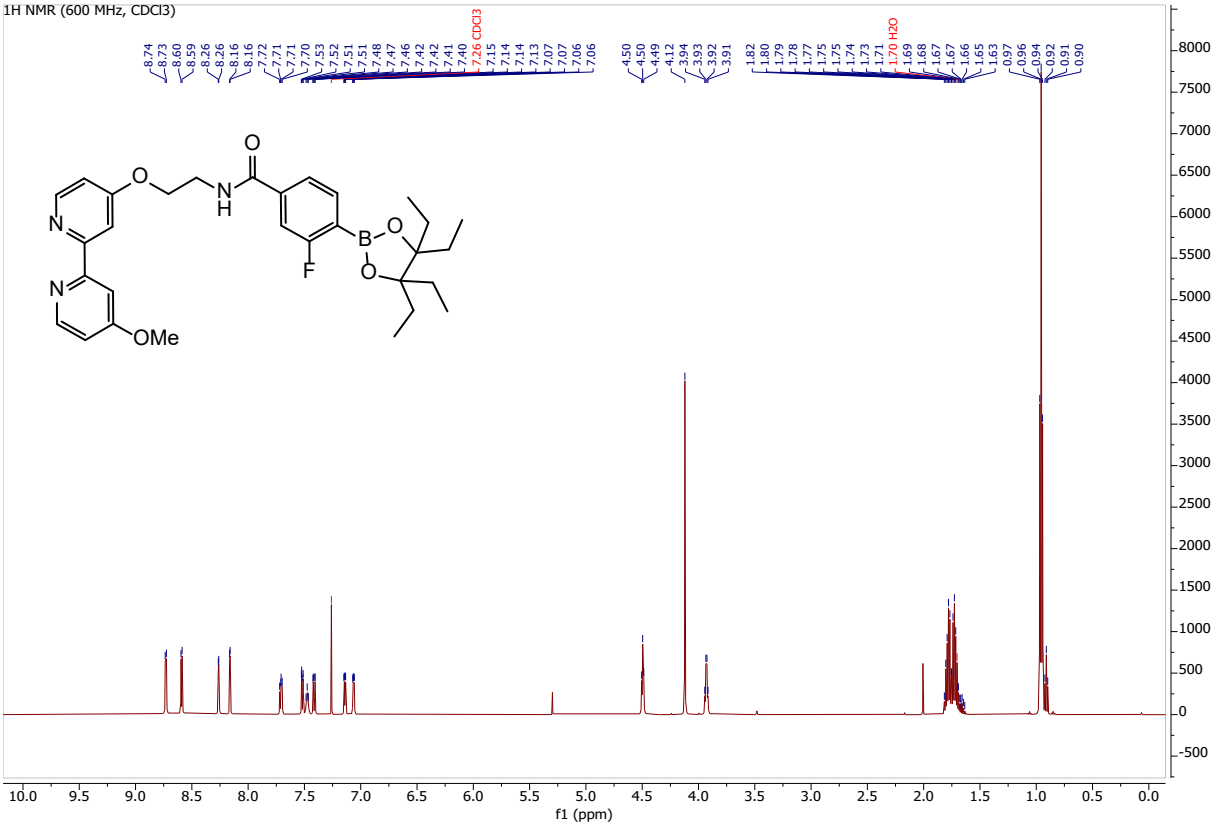

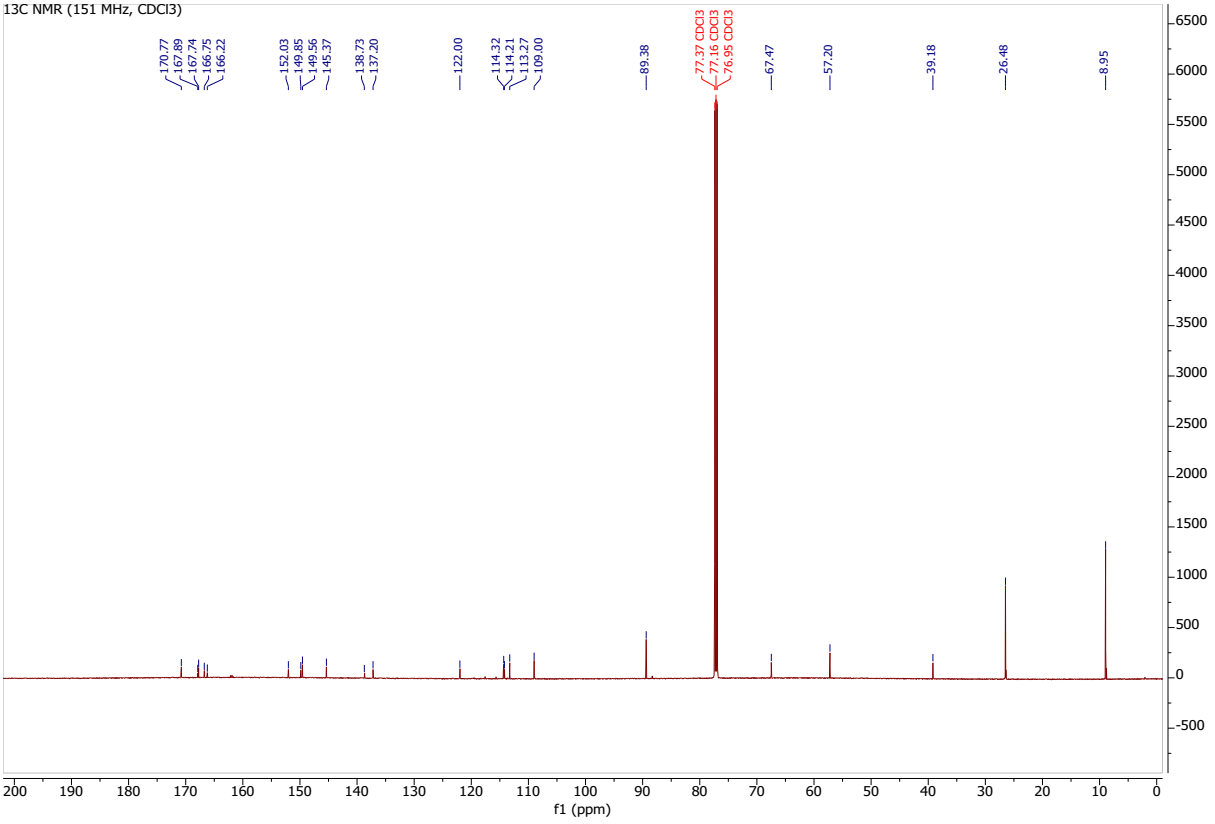

^{1}H and ^{13}CNMR spectra of 5-Pin

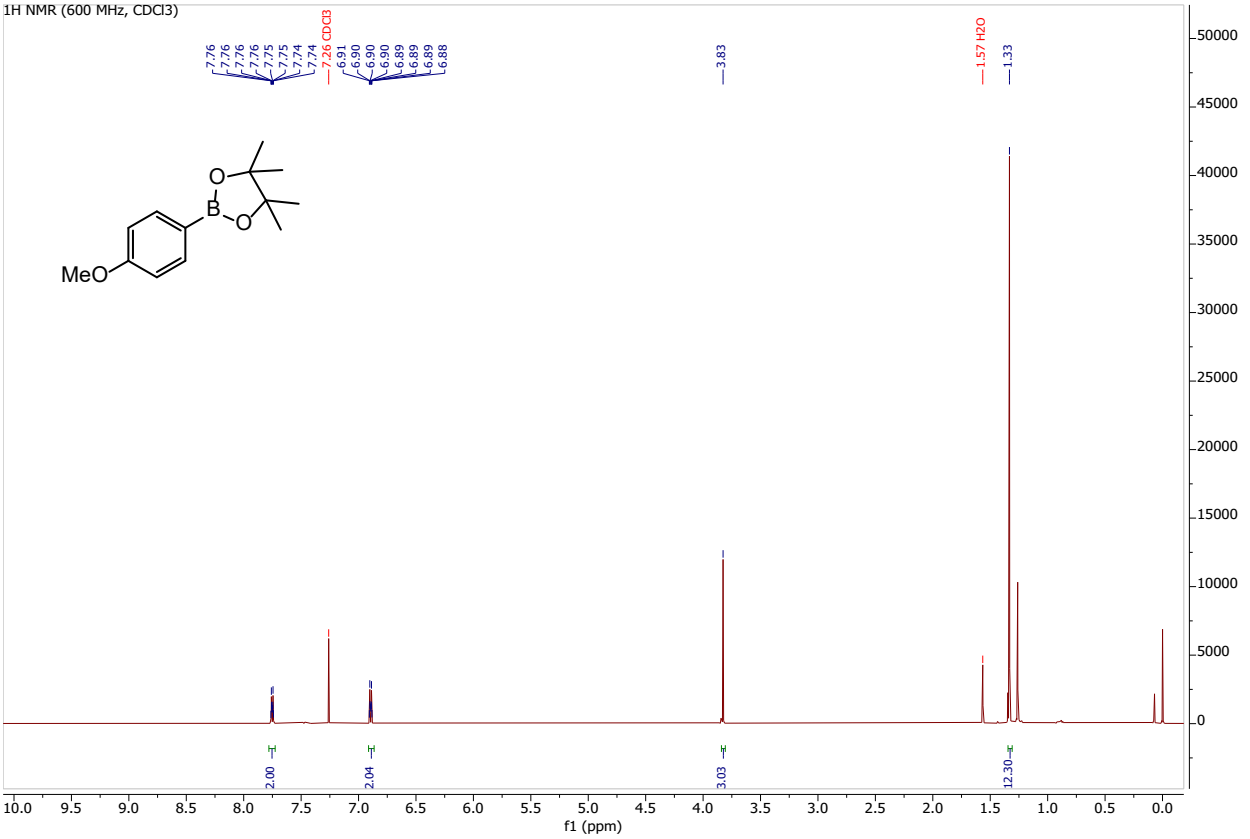

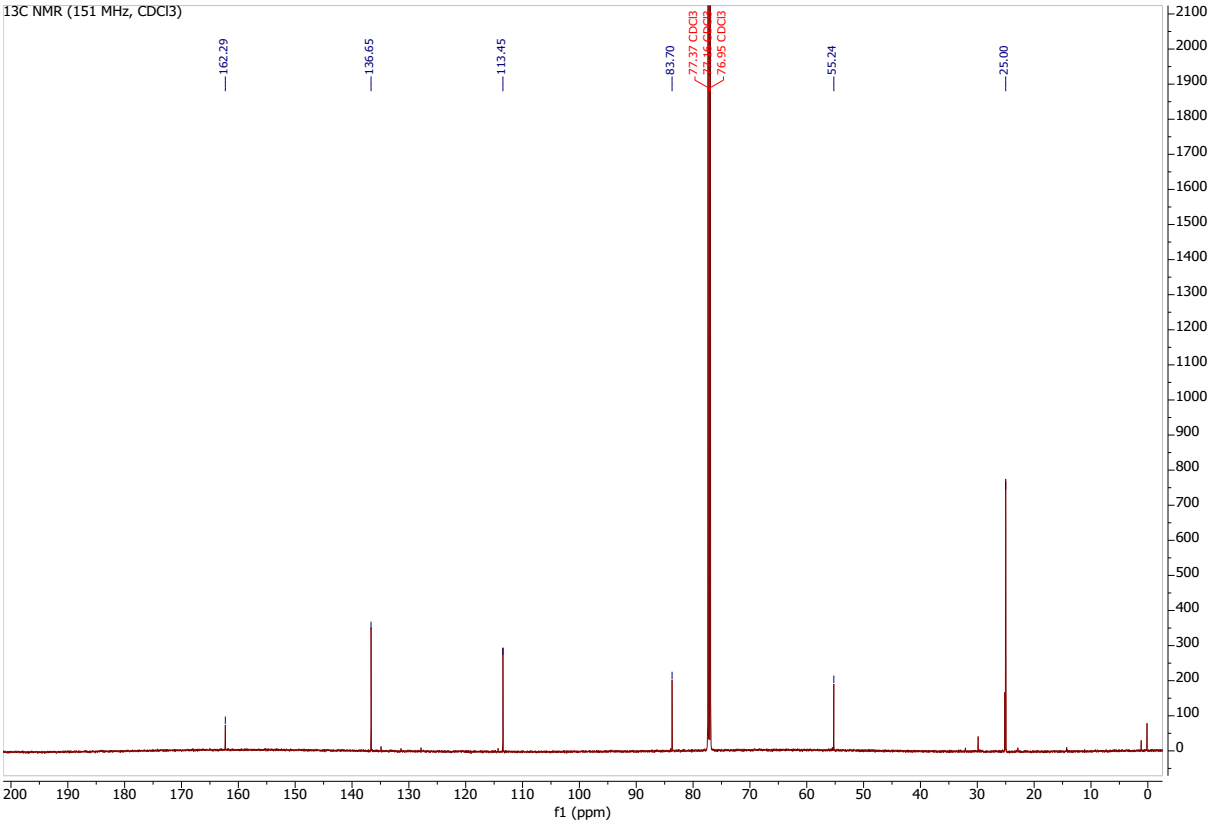

^{1}H and ^{13}CNMR spectra of 5-Gpin

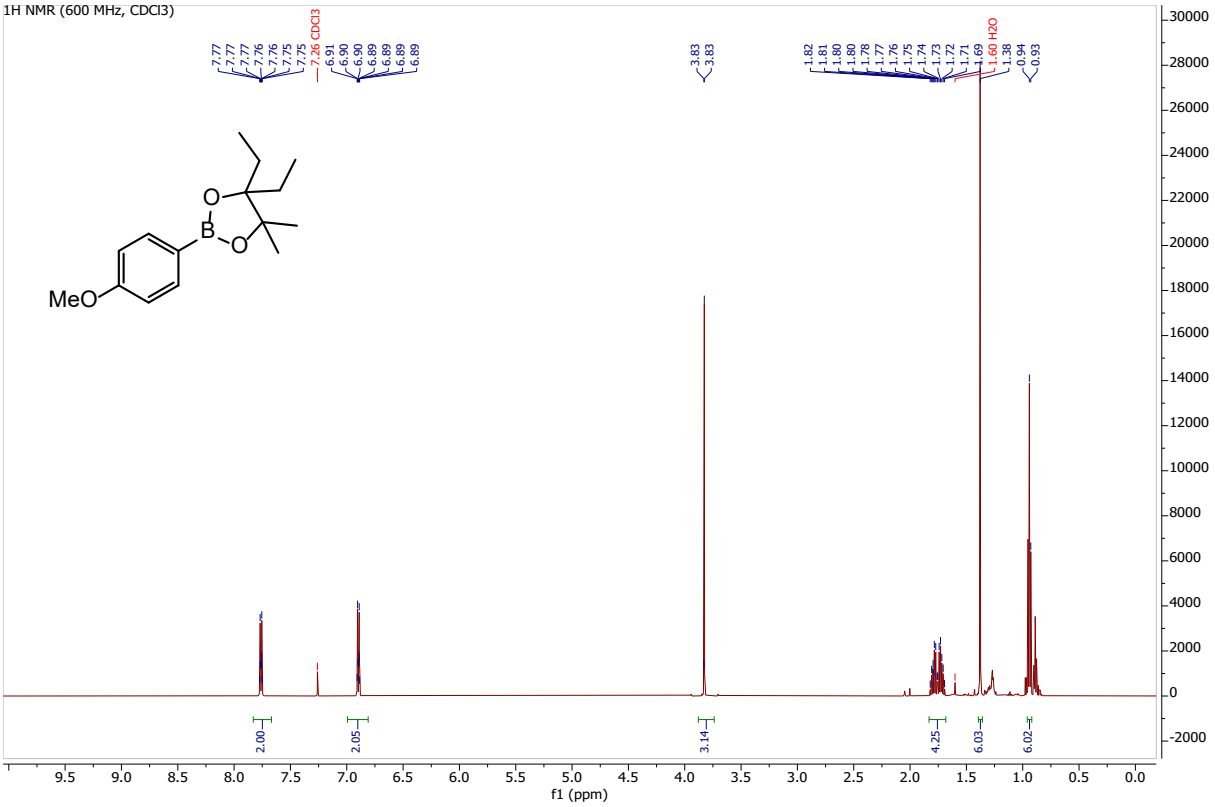

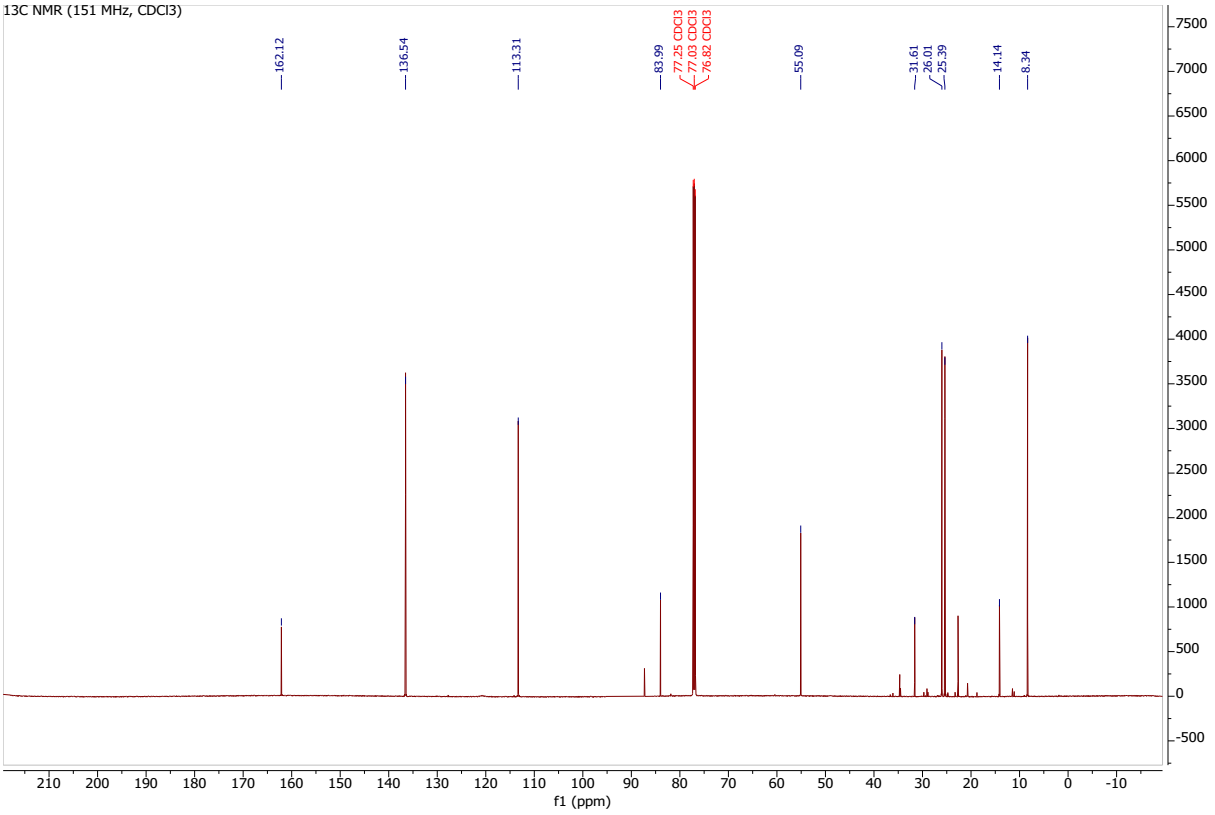

^{1}H and ^{13}CNMR spectra of 24-3pin

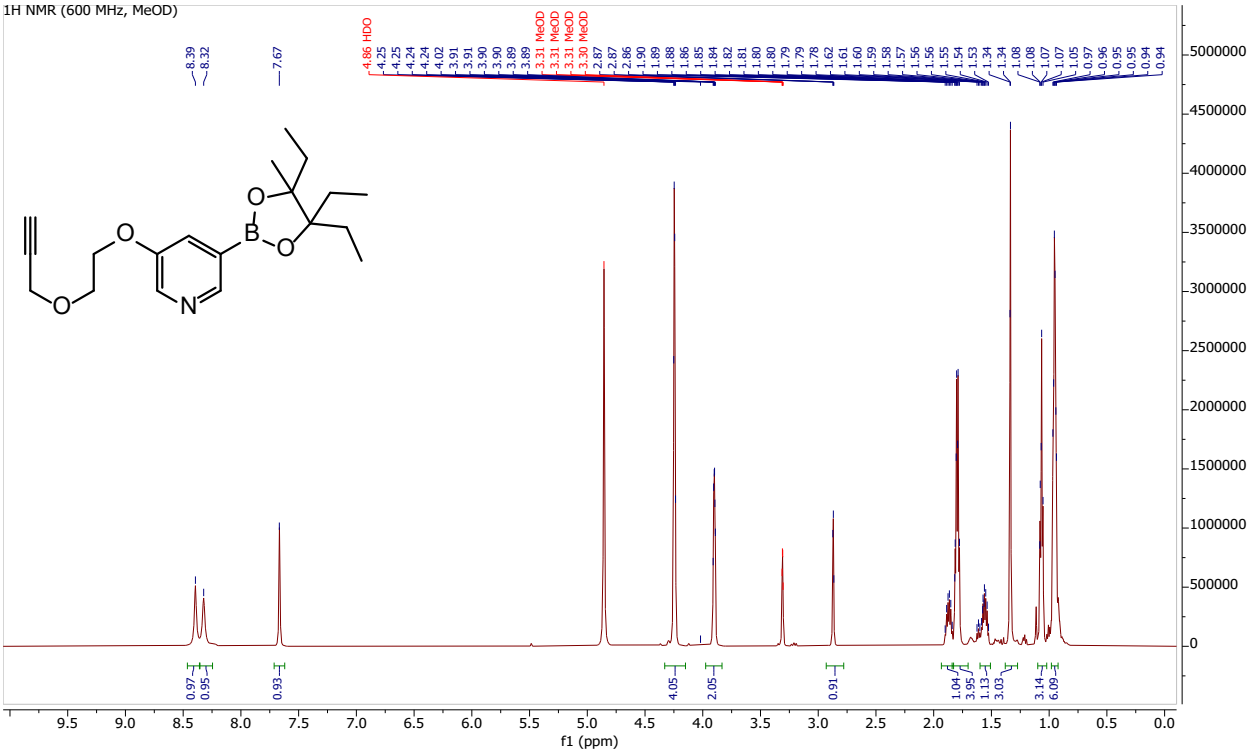

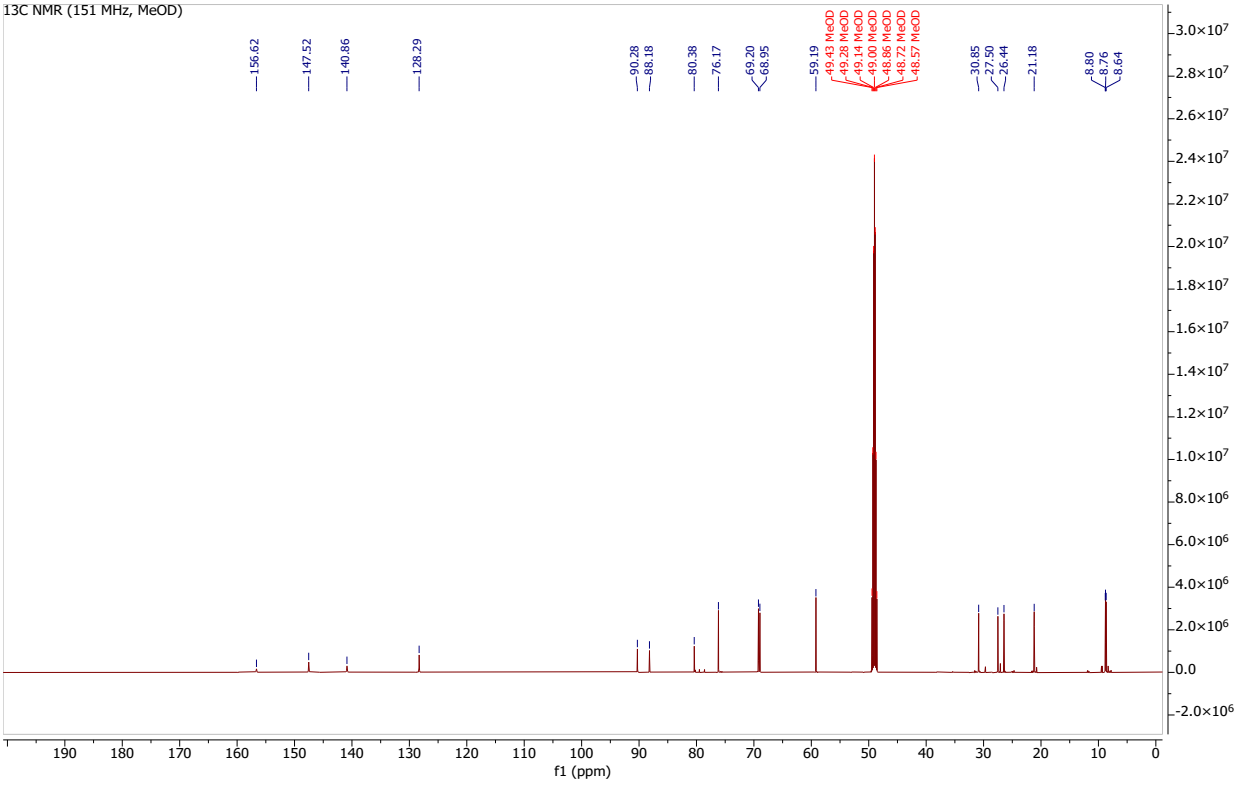

^{1}H and ^{13}CNMR spectra of 24-Epin

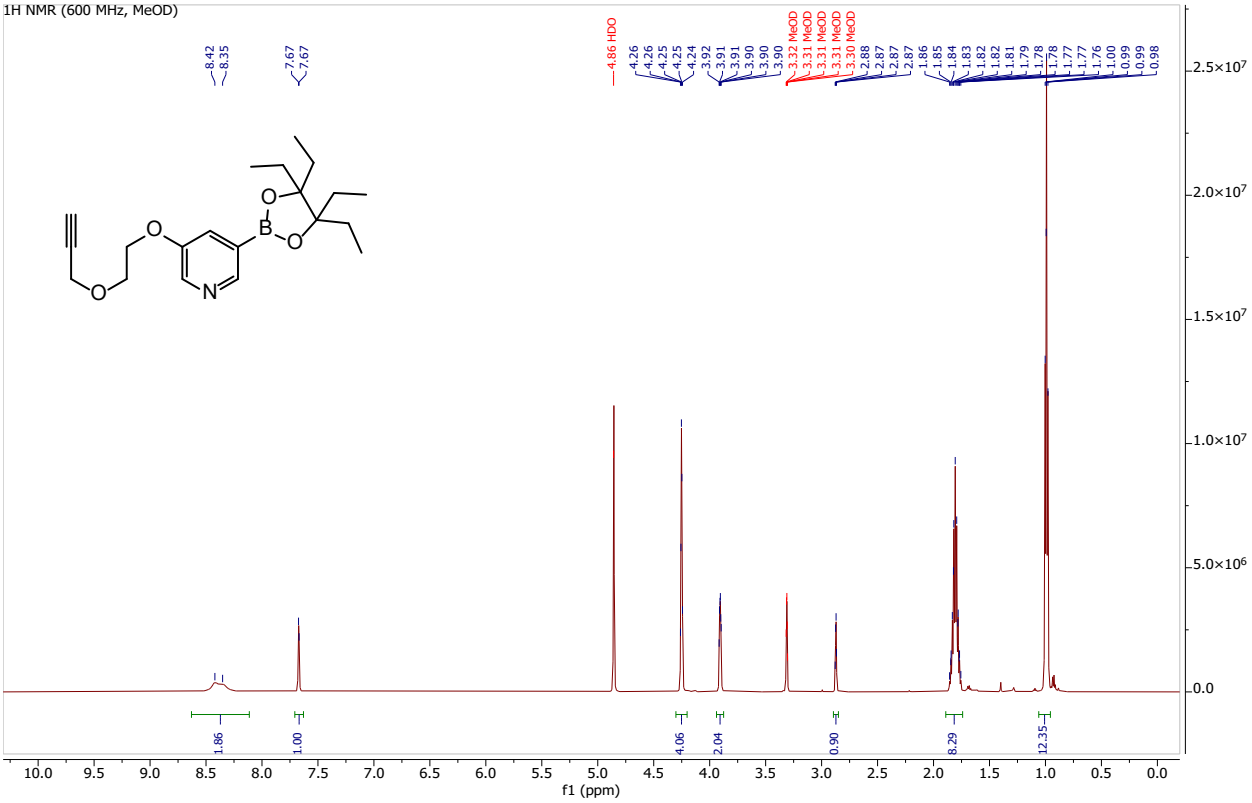

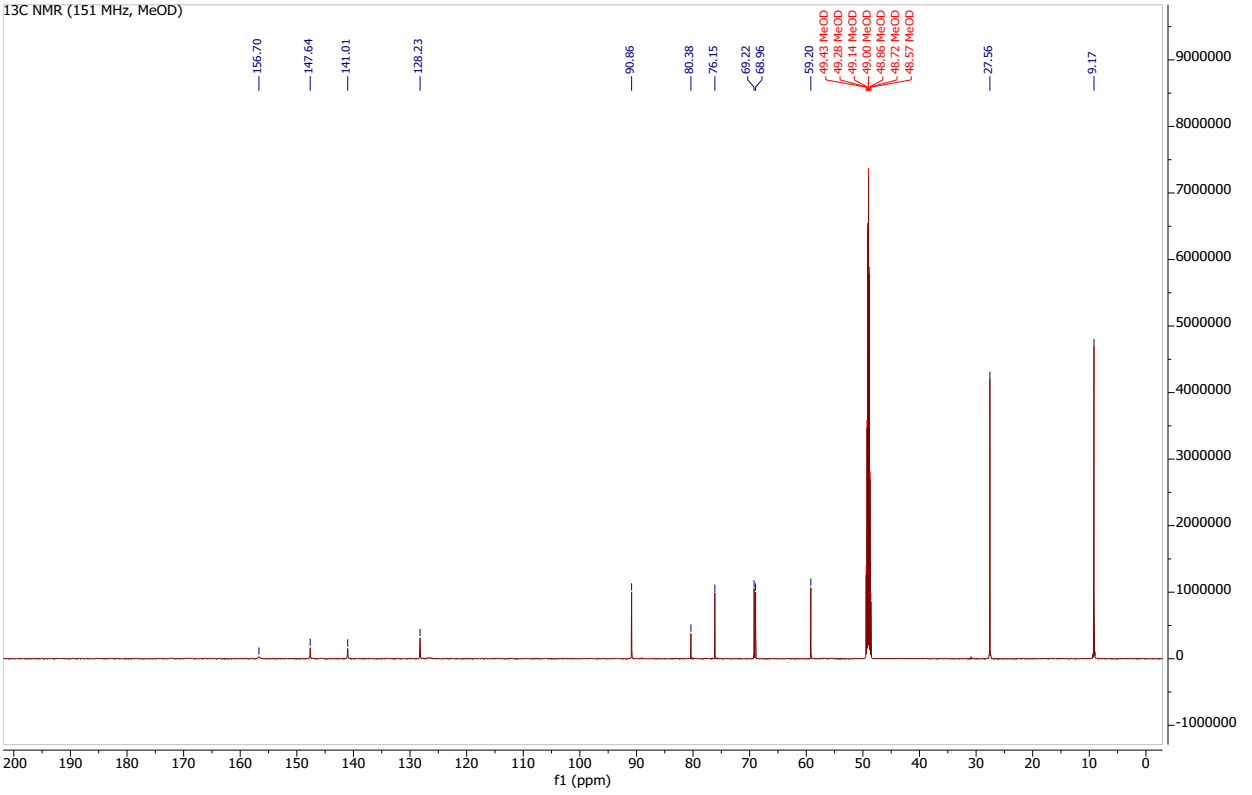

^{1}H and ^{13}CNMR spectra of 25-Gpin

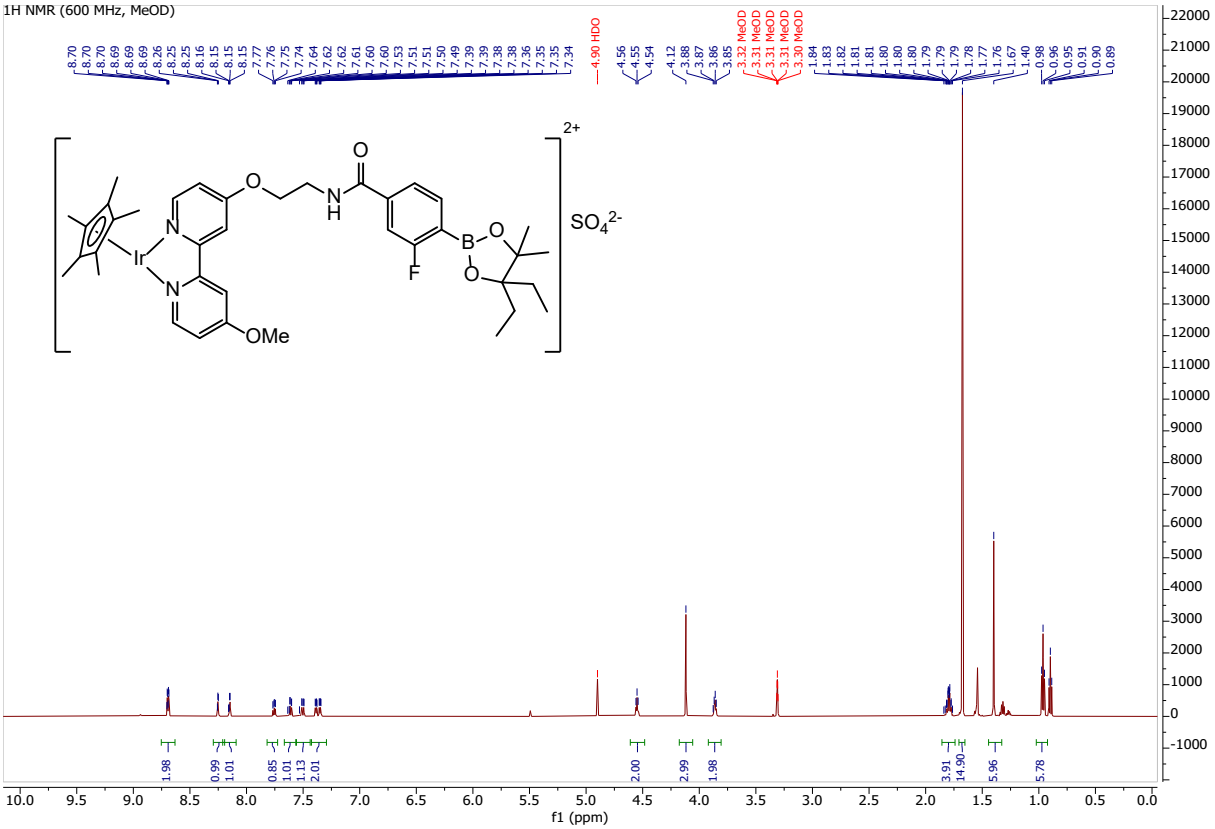

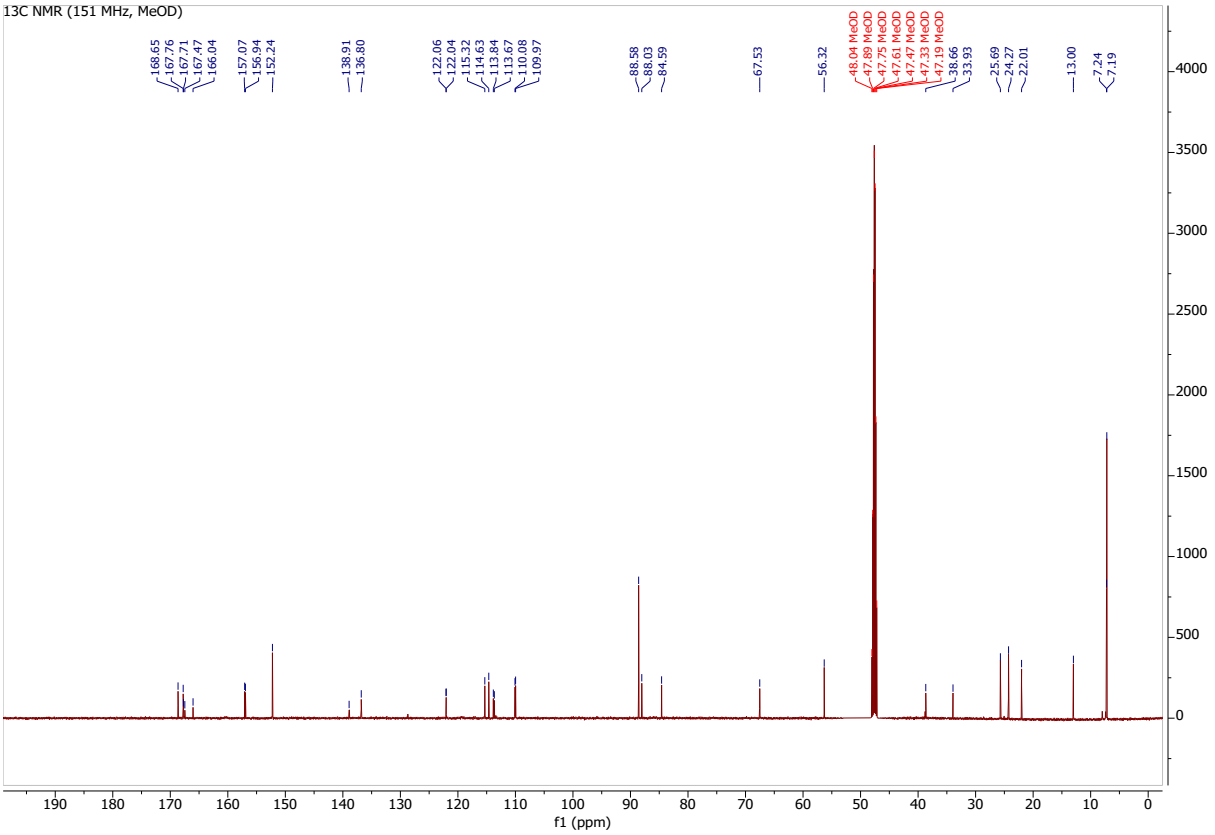

^{1}H and ^{13}CNMR spectra of 27-Epin

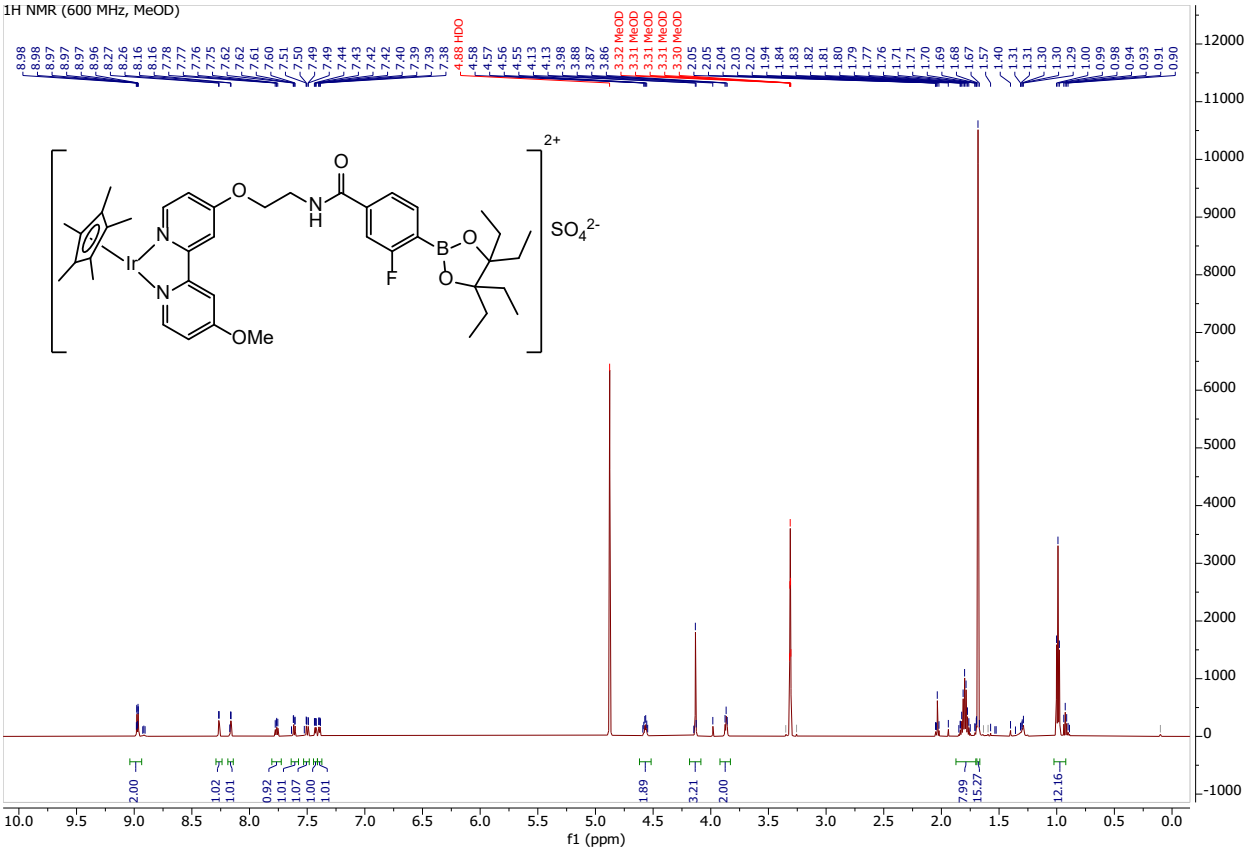

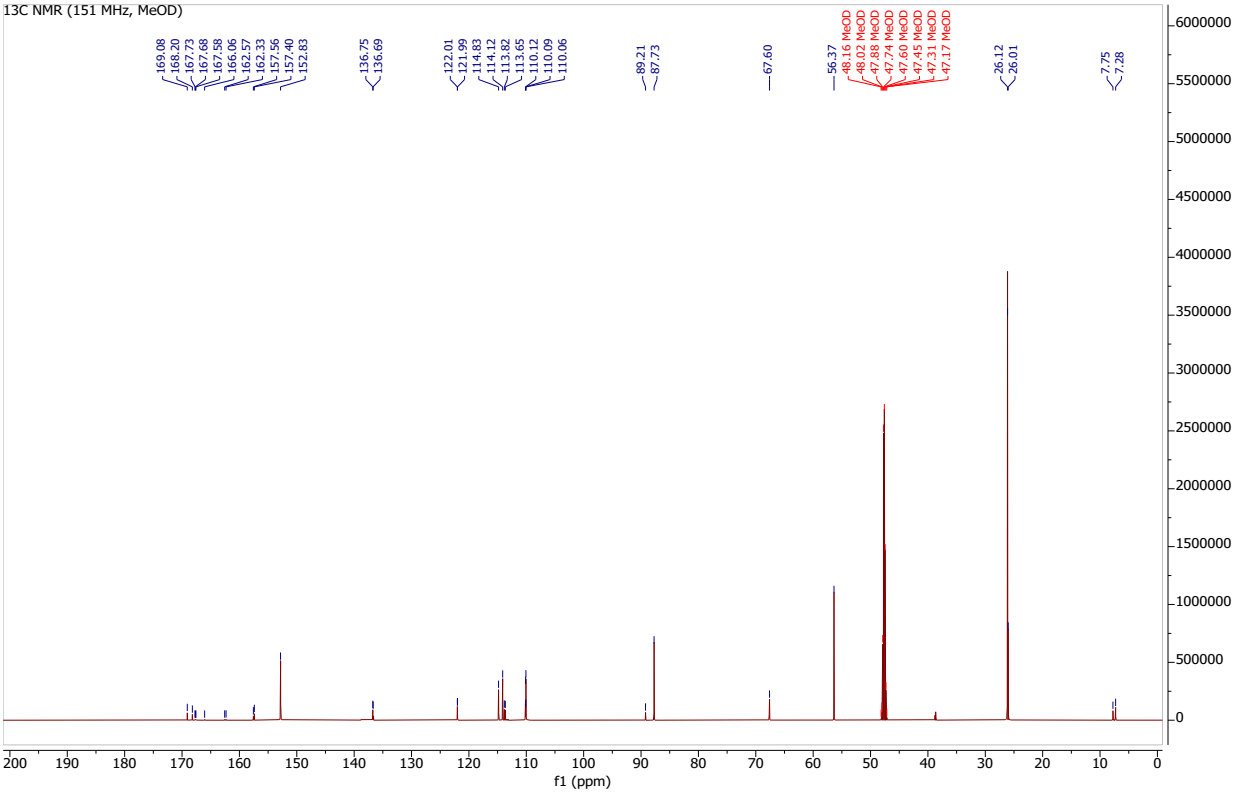

References

(1) Škopić, M. K.; Götte, K.; Gramse, C.; Dieter, M.; Pospich, S.; Raunser, S.; Weberskirch, R.; Brunschweiger, A. Micellar Brønsted Acid Mediated Synthesis of DNA-Tagged Heterocycles. *J. Am. Chem. Soc.* **2019**, *141* (26), 10546–10555. https://doi.org/10.1021/jacs.9b05696.

(2) Zernickel, A.; Du, W.; Ghorpade, S. A.; Sawant, D. N.; Makki, A. A.; Sekar, N.; Eppinger, J. Bedford-Type Palladacycle-Catalyzed Miyaura Borylation of Aryl Halides with Tetrahydroxydiboron in Water. *J. Org. Chem.* **2018**, *83* (4), 1842–1851. https://doi.org/10.1021/acs.joc.7b02771.

(3) Doscher, M. S. [48] Solid-Phase Peptide Synthesis. In *Methods in Enzymology*; Enzyme Structure Part E; Academic Press, 1977; Vol. 47, pp 578–617. https://doi.org/10.1016/0076-6879(77)47050-2.